The Interpretation of Deep Brain Stimulation through Diffusion-Weighted Magnetic Resonance Imaging

Ashley Laurence Bharat Raghu
Pembroke College
University of Oxford

A thesis submitted for the degree of
Doctor of Philosophy
Hilary 2022

Abstract

Advances in neuroimaging, particularly magnetic resonance imaging (MRI), have been fundamental to achieving improvements in clinical outcomes from deep brain stimulation (DBS). These improvements are essentially an increase in the reliability of the procedure as a result of improved accuracy in targeting a neuroanatomic structure of interest. However, many DBS procedures still result in highly variable outcomes between patients, raising the possibility that targeting remains suboptimal in these cases. These procedures may benefit from advanced forms of MRI that can extract unutilised anatomic features for a more individualised approach. Diffusion MRI tractography is a prime candidate for this but has to date mostly been applied to low outcome-variance procedures or with normative data which belies any project of individualisation. This thesis examines three cases of high outcome-variance DBS procedures and interprets them with patient-specific structural connectomes. DBS of the pedunculopontine nucleus in Parkinson's patients with severe gait freezing was interpretable by stimulation-associated connectivity to primary motor cortex (M1), cerebellum, and caudal primary

somatosensory cortex. This suggests connectivity maps of the ventrolateral pontine tegmentum could be useful as an adjunct to targeting. DBS of the ventrocaudal nucleus of thalamus (Vc) in patients with chronic neuropathic pain was interpretable through a homuncular framework superimposed on an individualised connectivity-based parcellation (CBP) of the thalamus aimed at segmenting the Vc. This suggests that CBP may have utility in targeting electrodes to Vc instead of relying on atlas coordinates. Lastly, DBS of the internal pallidum (GPi) for patients with cervical dystonia was interpretable through stimulation associated connectivity to the putamen, specifically the region of putamen characterised by dense input from M1. This was shown to be uncoupled from electrode coordinates, and therefore points to GPi connectivity maps as a promising tool with which to personalise the procedure.

Retrospective data indicates diffusion MRI has promise to improve outcomes in DBS and underscores merit in the future pursuit of prospective work in this field.

I would like to give thanks to several important individuals who have been instrumental in my academic development, arriving at Oxford, and ultimately completing this thesis.

My father, Bharat Raghu, has supported me to get started at each university I have attended. He has been an unfaltering advocate of my academic adventuring, to whom I owe much.

Scotland

David Cole-Hamilton for his mentorship at St Andrews

Mark Hughes and Patrick Statham for their mentorship at Edinburgh

Oxford

Alex Green for inviting me to Oxford, having an insatiable sense of humour, and being an absolutely first-class primary supervisor - and now dear friend

Tipu Aziz for his supervision of my DPhil – a legendary character and giant of the field – it was an honour to work with him at the start of my career in neurosurgery

Stephen Payne for his supervision of my DPhil - perhaps we will revisit cerebral blood flow together one day

Friends

I thank Anna-Katherina Hauperich and Eamonn Molloy for their unshakeable camaraderie during my junior deanship at Pembroke. In what was a difficult year, they were the best colleagues and friends one could ever ask for.

Among my greatest thanks go to Julien Du Vergier. After meeting only a few weeks into Michaelmas 2018 on the squash court, our friendship quickly migrated to premises that sold beer and wine. Our friendship went from strength-to-strength for the duration of our doctorates. In many ways, this is a journey, a mission, a struggle we have succeeded together.

I suspect meeting Tessa Cullen during the third year of my DPhil will turn out to be one of the most formative serendipities in my life. She is exquisite and robust, and already proved a great partner in life. I owe her great thanks for the tedium of proofreading this thesis, and for her very many corrections of it.

CONTENTS

Chapter 1: Neurosurgical Neuroimaging and Stereotaxis

1.1 Introduction 2

1.2 Diffusion-Weighted Magnetic Resonance Imaging 3

1.2.1. Nuclear magnetic resonance 3

1.2.2. Magnetic resonance imaging 4

1.2.3. Diffusion-weighted imaging 5

1.2.4. Diffusion tensor imaging 6

1.2.5. Advanced diffusion imaging 8

1.2.6. Practical considerations 9

1.2.6.1 Image distortions 9

1.2.6.2 Angular resolution 10

1.3 Neuroimaging in Stereotactic Neurosurgery 11

1.3.1 Spatial coordinates 15

1.3.2 Tractography 18

1.3.2.1 Anatomical schema as surgical targets 19

1.3.2.2 Pairing tractography to clinical effects 20

1.3.2.3 Localisation: from coordinates to connectivity contrast 21

1.3.2.4 White versus grey matter 22

1.3.2.5 State of the surgical field 23

1.3.2.6 Methodology 24

1.3.2.7 Normative versus individualised connectomes 26

1.3.2.8 Toward a diffusion MRI personalisation of stereotaxis 28

1.3.3 BOLD-MRI and other advanced neuroimaging 29

1.3.4 Concluding remarks 32

CONTENTS

Chapter 2: Parkinsonian Gait Freezing and Imbalance

2.1 Parkinson's disease and gait freezing 47

2.1.1 Parkinson's disease pathophysiology 47

2.1.2 Gait freezing and postural instability 48

2.2 Deep brain stimulation targeted to the pedunculopontine nucleus 50

2.3 Surgical anatomy of the ventrolateral pontine tegmentum 57

2.4 Neuroimaging of the pedunculopontine nucleus 59

2.5 Experimental work with patient-specific structural connectomes 61

2.5.1 Methods 61

2.5.1.1 Patients and deep brain stimulation 61

2.5.1.2 Questionnaires 62

2.5.1.3 Diffusion imaging acquisition and pre-processing 62

2.5.1.4 Tractography and statistics 63

2.5.1.5 Termination masks 63

2.5.1.6 Cathode and volume of activated tissue 64

2.5.1.7 PPN region 64

2.5.1.8 Electrode locations 65

2.5.1.9 Cortical thickness 65

2.5.2 Results 65

2.5.2.1 Tractography 67

2.5.2.2 Cortical thickness 68

2.5.2.3 Electrode locations 69

2.5.3 Discussion 69

2.5.3.1 Electrode positions and targeting 69

2.5.3.2 Tractography 71

2.5.3.3 Targeting and tractography 75

2.5.3.4 Cortical thickness 76

2.5.3.5 Limitations 77

2.6 Concluding remarks 81

Chapter 3: Chronic Neuropathic Pain

3.1 Anatomical substrates of pain 94

3.2 The thalamus as a putative surgical target for the treatment of chronic pain 100

3.3 Historical review of stereotactic approaches to treat chronic pain 101

3.3.1. Brainstem 101

3.3.1.1. Parabrachial complex 101

3.3.1.2. Mesencephalic tracts 102

3.3.1.3. Periaqueductal grey 102

3.3.2. Diencephalon 105

3.3.2.1. Hypophysis 105

3.3.2.2. Medial lemniscus 106

3.3.2.3. Intralaminar thalamus 106

3.3.2.4. Lateral thalamus 109

3.3.2.5. Pulvinar 111

3.3.3. Internal capsule and cortex 112

3.3.3.1. Posterior limb of internal capsule 112

3.3.3.2. Anterior limb of internal capsule 113

3.3.3.3. Dorsal anterior cingulate 114

3.3.3.4. Dorsal posterior insula 116

3.3.4. Summarising remarks 116

3.4 Neuroimaging of the thalamus 119

3.5 Experimental work with patient-specific structural connectomes 120

3.5.1. Methods 122

3.5.1.1 Patients 122

3.5.1.2 Surgical technique 122

3.5.1.3 Clinical outcomes 123

3.5.1.4 Diffusion imaging acquisition and pre-processing 124

3.5.1.5 Seed and termination masks 124

3.5.1.6 Tractography and parcellation 125

3.5.1.7 Implanted electrode array 125

3.5.1.8 Array – primary somatosensory cortex parcel location analysis 125

3.5.1.9 Stereotactic coordinates 126

3.5.2. Results 126

3.5.2.1 Clinical outcomes 126

3.5.2.2 Array placement in S1 parcel 127

3.5.2.3 Array placement anterior and posterior to S1 parcel 127

3.5.2.4 Medial-lateral quantification 129

3.5.3. Discussion 129

3.5.4.1. Key findings 129

3.5.4.2. Connectivity-based parcellation 130

3.5.4.3. Individualised targeting 130

3.5.4.4. Regional analysis – arm, leg, face, and trunk 132

3.5.4. Limitations 134

3.5.5.1. Generalisability 136

3.6 Conclusions 136

Chapter 4: Cervical Dystonia

4.1 Neuroanatomy 155

4.1.1 Primary somatosensory cortex and somatosensory thalamus 156

4.1.2 Putamen 157

4.1.3 Pedunculopontine nucleus 159

4.1.4 Primary motor and premotor cortex 159

4.1.5 Cortico-basal ganglia anatomic pathways 161

4.1.6 Cerebellum 162

4.2 Stereotactic surgery 163

4.2.1 History and clinical evidence base 163

4.2.2 Mechanisms of high frequency deep brain stimulation 166

4.2.2.1. The role of the globus pallidus interna 166

4.2.2.2. The role of the subthalamic nucleus 172

4.2.2.3. The role of the ventral oralis nuclei 172

4.3 Neuroimaging of the pallidum 173

4.3.1 Structural neuroimaging 173

4.3.2 Diffusion neuroimaging 176

4.4 Experimental work with patient-specific structural connectomes 181

4.4.1 Methods 182

4.2.2.1. Patients 182

4.2.2.2. Clinical rating 183

4.2.2.3. Diffusion imaging acquisition and pre-processing 183

4.2.2.4. Deep brain stimulation 184

4.2.2.5. Termination masks 184

4.2.2.6. Tractography and parcellation 185

4.2.2.7. Statistical analysis 185

4.2.2.8. Coordinate-connectivity relationship 186

4.4.2 Results 187

4.4.2.1. Patient demographics 187

4.4.2.2. DBS connectivity with motor-putamen predicts outcomes 187

4.4.2.3. Connectivity and coordinates are not equivalent 188

4.4.3 Discussion 188

4.4.4 Limitations 192

4.4.4.1. Clinical scores 192

4.4.4.2. Diffusion data 193

4.4.4.3. Diffusion tractography 194

4.4.4.4. Tractography stimulation seed 195

4.4.5 Future work 196

4.5 Conclusions 199

I addicted myself to the opening of heads.

~

Thomas Willis

CHAPTER 1: NEUROSURGICAL NEUROIMAGING AND STEREOTAXIS

ABSTRACT

Magnetic resonance imaging (MRI) is a versatile cross-sectional technique that can identify a large range of anatomic and chemically characteristic features of the brain, including the diffusion of water. This has commended it to broad and varied applications for advancing neurosurgical care, especially stereotaxis. The basis of diffusion-weighted MRI and methods for both interpretation and utilisation are discussed. Practical considerations of acquiring and processing diffusion MRI are reviewed, in the context of acquiring meaning structural connectivity estimates.

The technical considerations of stereotactic neurosurgery are presented, highlighting the combination of stereotactic frame and cranial imaging to target neuroanatomical structures. The project is animated by a 'will to the specific', refining or discarding general anatomic frameworks with progress in imaging. MRI has been crucial to this.

Despite the successes of deep brain stimulation (DBS), targeting remains somewhat crude, and for many indications, clinical outcomes are highly variable. Imaging has facilitated retrospective refinement of the optimal coordinates for procedures. However, this usually relies on generic anatomy and often leaves much variance in outcomes unexplained. Diffusion MRI tractography is a credible technique for revealing additional patient-specific anatomy with potential utility for increasing individualisation of targeting.

This thesis explores an interpretation of DBS using diffusion MRI. The case is made that structural connectivity estimates reveal anatomical information that explains variance in surgical success, thereby highlighting the potential of imaging to further advance neurosurgical treatment.

1.1 INTRODUCTION

The evolution of neurosurgery has been strongly coupled with developments in neuroimaging. Now an indispensable tool to the neurosurgeon, neuroimaging, in hand with advancements in instrumentation, has revealed a broad landscape of meaningful neurosurgical practice that was otherwise hidden in the 'black box' of the calvarium. Likewise, knowledge and understanding of neurosurgical disease has been propelled by neuroimaging, which has had a direct pipeline back into improving practice and surgical care. Now, neuroimaging is essential to localisation, diagnosis, monitoring, planning, operative guidance, follow-up, and surveillance of neurosurgical disease. Before the application of radiation physics to imaging the nervous system, the neurosurgeon was limited to visual inspection of the head, clinical neurological examination, and clinicopathological knowledge to guide high-risk surgeries - correspondingly with a high degree of anatomic uncertainty. Neuroimaging has transformed the balance of risk and benefit in neurosurgery, making procedures viable that otherwise would not have been conceived or attempted.

Leveraging nuclear magnetic resonance (NMR) for brain imaging has proved to be an extraordinarily versatile enterprise, giving rise to a smorgasbord of imaging techniques that continue to grow in range and quality. While X-ray computed tomography (CT), the first cross-sectional imaging technique, had an enormous impact on neurosurgery, a key limitation was tissue differentiation. This meant that localisation was advanced more by CT than diagnosis was. With CT, tissue contrast is determined by the X-ray cross-section of fluid/tissue types, offering little opportunity for manipulation to probe different properties of normal and pathological tissue types. As such, the technique is fundamentally inflexible/non-dynamic.

Unlike with CT, with techniques based on magnetic properties there is not one, but many ways for generating spatial contrast representative of the underlying biology. Indeed, there are as many as the ingenuity and creativity of physicists can conceive. Using these methods, nuanced questions about anatomy and physiology can be addressed non-invasively, to advance understanding of neurosurgical disease.

1.2 DIFFUSION-WEIGHTED MAGNETIC RESONANCE IMAGING

1.2.1 Nuclear magnetic resonance

The phenomenon of NMR was first discovered by Rabi in 1938,[1] and developed into condensed-phase spectroscopy by Bloch and Purcell in 1946.[2,3] This attracted two Nobel prizes in physics to the aforementioned American laureates. NMR spectroscopy was subsequently used for decades to reveal molecular structure before the phenomenon was leveraged for neuroimaging. The technique allows for the probing of nuclear species with spin: those with an uneven number of nucleons (protons and neutrons), most commonly ^{1}H, ^{13}C, ^{31}P. This depends on the phenomenon of the Zeeman effect,[4] where the energy degeneracy of nuclear spin states is lifted in the presence of a magnetic field. This permits NMR to occur, where excited states are stimulated by energy-matched photons and then return to thermodynamic equilibrium by generating photons (at the resonance frequency) on relaxation to the lower energy spin state. As the resonance frequency of any nucleus depends on its chemical environment, and the relative multiplicity of a nucleus within a given environment is conveyed in the signal magnitude, molecular structures can be deduced from spectrographic patterns.

The overwhelming majority of protons in the human body are in essentially the same intra-molecular chemical environment: H_2O - water. This is the species that is probed in almost all clinical magnetic resonance imaging (MRI) studies. Unlike in laboratory spectroscopy, with carefully prepared condensed-phase samples, water protons in the body are in a range of different inter-molecular environments. These depend on the locality of proteins, fats, metals, all with a range of magnetic properties, and which are distributed across the brain depending on tissue type and ongoing physiological and pathological processes. This heterogeneity is conveyed in the resonance signal.

1.2.2 Magnetic resonance imaging

Carr generated the first one-dimensional ^{1}H NMR image at Harvard in 1952.[5] Twenty years later in the USA, Damadian introduced the possibility for using ^{1}H NMR spin-lattice and spin-spin relaxation times for distinguishing biological tissues,[6] and Lauterbur generated two- and three-dimensional images using ^{1}H NMR with magnetic field gradients for spatial localisation.[7] Mansfield, a British mathematician, subsequently developed the mathematics to both dramatically reduce the time for image acquisition and increase image quality. The first human MRI (originally called either NMR zeugmatography or NMR tomography) was performed by FONAR in the US in 1977.[8] The Nobel prize for medicine was shared between Lauterbur and Mansfield in 2003.

Unlike X-ray tomography, tomography based on NMR involves a highly dynamic phenomenon, offering a system open to wide ranging manipulation. This, as well as the technique not involving ionising radiation, gave it the potential to acquire information on neurosurgical biology that CT never could. MR quickly entered neurosurgery shortly after CT,

providing a cross-sectional imaging technique that would completely change the way neurosurgery was practiced in centres wealthy enough to purchase and maintain the equipment. Crucially, the versatility of NMR gave rise to different techniques for acquiring scans, offering a range of tissue contrasts. By conveying different information, the findings of different scans could be combined, thereby increasing the clinical power of the tool to refine differential diagnoses and understand ongoing biology in the brain. Epidemiology, location, morphology, and intensity patterns, all across multiple scan types became a powerful non-invasive diagnostic tool. Due to practical simplicities in imaging the brain (e.g., minimal motion) and global research interest in neurosciences, brain MRI has benefitted from being the space of innovation for many of these techniques. Advanced techniques can now probe chemical characteristics such as pH and neurotransmitters as well as processes such as blood flow and diffusion.

1.2.3 Diffusion-weighted imaging

The technique to generate images where voxels quantify water diffusion was first described in 1985 by Le Bihan and Breton.[9] Diffusion weighting is achieved using a spin echo sequence (90° excitation pulse with a 180° rephasing pulse; long TE, TR) combined with two strong field gradients applied before image acquisition, either side of the rephasing pulse. These large gradients force water molecules to experience different magnetic fields as a function of space, which is expressed in their degree of transverse dephasing. Following the rephasing pulse, the same gradient is applied but in the opposite direction. As such, signal loss at acquisition can be attributed to water proton movement in space, i.e., diffusion over the sequence time. As diffusion over a fixed time is three-dimensional, quantifying this process requires measurement of this signal loss in three planes. For simple diffusion-weighted

imaging (DWI), these three diffusion weighted images are acquired along with a normal T2-weighted image. The three diffusion volumes are averaged to create the (isotropic) DWI, from which the T2-weighted image is subtracted to generate the apparent diffusion coefficient (ADC) image: a map of diffusion coefficients (i.e., how much diffusion is taking place in each voxel).[10]

Due to how water diffusion relates to pathology, DWI/ADC scans have become tools of high utility in neurosurgery. Ischaemia results in restricted diffusion, with scans reporting abnormalities within minutes. Epidermoid tumours and arachnoid cysts are very difficult to differentiate by T1 or T2 image contrast, however DWI/ADC easily reveals their respective solid and liquid constituents. Cerebral abscesses and other pyogenic processes also have a characteristic appearance due their liquid, yet viscous, constituents. The technique also has substantial use in characterisation of a wide range of neuro-oncological disease,[11] probably due mostly to the relationship between diffusion and hypercellularity.[12,13] Most notably, it has proved useful in differentiating paediatric posterior fossa tumours,[14] pineal tumours,[15] and primary CNS lymphoma from malignant gliomas.[16,17]

1.2.4 Diffusion tensor imaging

Diffusion tensor imaging (DTI) is an extension of DWI, first proposed in 1994,[18,19] where an ellipsoid tensor (3x3 matrix) is fitted to each voxel to model its diffusion properties. A key result of this is that fractional anisotropy and principal diffusion direction maps can be reconstructed. Accompanied with the knowledge that diffusion in axonal bundles of white matter is highly directional/anisotropic, this data can be processed to construct whole brain maps of white matter tracts: tractography.[20] Approaches to tracking through the diffusion

parameter field are multiple but are fundamentally either probabilistic[21,22] or deterministic.[23] The benefits and weaknesses of these vary, commending them to different applications.[24,25] While DTI shows enormous clinical promise, it is still undergoing technical and clinical development to improve anatomic fidelity and establish therapeutic utility (i.e. improving clinical outcomes or reducing adverse effects). Nonetheless, it is used routinely by many neurosurgeons in operative planning and navigation, and will likely continue to be used as a matter of surgical preference.[26]

The potential uses are wide ranging. Understanding the relationship of the tumour with key motor and language tracts has appeal for maximising tumour resection and minimising post-operative deficit. With this aim, DTI has been used for glioma resection and showed signs of clinical value.[27–30] Anterior temporal lobectomy for refractory epilepsy is frequently complicated by superior quadrantic visual field defects due to violation of Meyer's loop of the optic radiation. Numerous studies have examined the possible use of DTI in the preservation of this structure and have indicated its use could prevent optic morbidity.[31–33] The upper cranial nerves are visualisable by DTI tractography.[34] Localisation of the facial nerve during surgery for acoustic schwannoma is a key and often challenging step, crucial for its preservation and minimising associated surgical morbidity. DTI tractography appears to reliably identify its location and as such can assist in expediently detecting the facial nerve in the surgical field.[35–37] Stereotactic neurosurgery also has the potential to benefit from tractography. For example, in targeting structures for stimulation in movement disorders,[38–40] major depression,[41,42] and the treatment of arteriovenous malformations (AVM) with stereotactic radiosurgery (SRS).[43] The radiosurgical dosimetric topography can be moulded to avoid identified tracts and appears to result in low morbidity rates. Furthermore,

tractography can be interpreted as a measure of structural connectivity between regions. These tractography-derived structural connectivity estimates are a potentially useful tool to non-invasively understand the human brain, within a network conceptual framework.

1.2.5 Advanced diffusion imaging

The limitations of DTI are important to recognise and provide a motivation to progress beyond it.[44] A key limitation is the modelling of a single fibre bundle at each voxel, which results from the Gaussian diffusion model assumption and is a major anatomical simplification. However, multi-fibre DTI approaches based on compartment models are now available, such as multi-Gaussian tensor modelling and ball-and-stick modelling.[45,46] There are also quasi-model-based multi-fibre methods such as diffusion kurtosis imaging (DKI)[47,48] and reconstructing the diffusion orientation distribution function (ODF) by spherical deconvolution[49,50] from high angular resolution diffusion imaging (HARDI)[51]. In addition, there are model-free approaches to estimating the diffusion profile such as Q-ball imaging (QBI)[52,53] and Q-space imaging (QSI), also often called diffusion spectrum imaging (DSI).[54] In principle these methods are capable of constructing a more anatomically realistic representation by accounting for complex intra-voxel diffusion structure. The benefits of multi-fibre tractography relate to modelling of crossing fibres and increasing sensitivity for detecting non-dominant fibre populations, resulting in constructing more anatomically accurate tracts.[45] However, modelling fanning fibres is highly challenging,[55] and distinguishing crossing and kissing fibres remains an unmet challenge.

New techniques in diffusion MRI are being developed and refined. These include free water elimination,[56] NODDI,[57] multidimensional diffusion MRI,[58] and diffusion-weighted

spectroscopy,[59] all of which provide more information on tissue microstructure and may ultimately result in improved tractography and other clinical applications. This is a fertile area for clinicians to be aware of and leverage for the correct clinical questions.

1.2.6 Practical considerations

1.2.6.1 Image Distortions

Diffusion imaging is typically performed with echo planar imaging (EPI), where k-space is sampled across a single shot. This is key for minimising the impact of motion on the acquired diffusion signal. A consequence of this is that the images are substantively distorted by b0 inhomogeneities, often called susceptibility-induced distortions. The distortions are dependent on the phase-encoding direction and are greatest at the basal frontal lobe and medial temporal lobe, although present throughout the brain. These distortions are of a scale that, if not corrected for, undermine any utility of the images in being helpful for stereotactic analysis. Robust correction of the diffusion-weighted images is achieved by applying the susceptibility-induced off resonance field map, which amounts to a scaled voxel-displacement map. This can be acquired either by direct measurement or calculated from at least two b0 images (i.e. T2-weighted images) which have been affected differently by the field.[60] The latter performs better[61] and usually involves one or more pairs of T2-EPI acquired with opposite phase encoding direction (e.g. anterior-posterior and posterior-anterior). The large magnetic gradients, which are essential for diffusion MRI, also give rise to an important image distortion through the generation of eddy currents. As these large magnetic field gradients are switched on and off, electric current is generated in the brain, which itself has an orthogonal magnetic field that distorts the diffusion signal. As such, eddy current distortions are much larger when higher gradients (e.g. $b < 2000$ s/mm^2) are used. Currently, the most

sophisticated method corrects for these by a Gaussian process which makes predictions of the eddy current-induced field from all diffusion-weighted images (and gradient directions) in an iterative manner.[62,63] Distortions from high gradients are more difficult to correct, but the correction benefits from multi-shell acquisition and denser sampling at the higher gradient (e.g. 32 directions at b = 1000 s/mm^2, 64 directions at b = 2000 s/mm^2).[63] If diffusion MRI is to be used to guide or interpret stereotactic surgeries, it must offer a similar scale of precision to what is considered important in these surgeries. As such, distortion correction must be performed robustly, or the research is not tenable.

1.2.6.2 Angular Resolution

The utility of tractography in neurosurgery will rely on its fidelity to the underlying anatomy. Intravoxel multifibre reconstruction requires dense sampling of the angular dependency of the diffusion-weighted signal, regardless of the method used (e.g multi-tensor or spherical deconvolution etc.). The original publication describing the use of HARDI in this way analysed 3T data with a gradient strength of b = 1077 s/mm^2 obtained from 126 directions and used a multi-Gaussian modelling approach.[51] While there is no strict limit, the approximate lowest parameters for HARDI can be considered a b-value of 1000-1500 s/mm^2 and 60 directions.[64] However, at present, a higher number of directions (e.g. 100) at two shells (e.g. 1000 and 2000 s/mm^2), in a 3T scanner would probably be more representative of HARDI data in the clinical research setting. A good such example in 2017 includes ball-and-stick modelling for tractography of hyperdirect tracts between cortex and the subthalamic nucleus (STN) in stereotactic surgery (3T, b = 1500 s/mm^2, 128 directions) with parameters well-suited for multifibre modelling.[65] Conversely, the example in 2016 of q-ball reconstruction and

tractography of major tracts in presurgical planning for tumour resection (3T, 55 directions, b = 2000 s/mm^2)[29] is technically adequate,[66] yet more tenuous.[67]

Large heterogeneity in tract reconstruction between methods is problematic, and although fibre bundle sensitivity can by high, false-positives bundles are common and often extensive.[68] Importantly, while HARDI data increases sensitivity for detecting non-dominant tracts, this appears to come at the cost of increased false positive tracts.[68] In summary, results must be interpreted within this context when applied clinically, and this represents a challenge for validation in any particular use. Parameters such as signal-to-noise ratio and angular resolution of the data should always be considered with respect to their appropriateness for the tractography intended to be performed. Practically, it must also be recognised that while high-field MRI is increasingly common in clinical settings, the high number of diffusion directions that must be acquired for HARDI is time consuming and therefore more expensive and less practical. Higher b-values generate data with lower signal-to-noise than lower b-values, but with improved angular contrast. As such, combining data from a low and high b-value shell is obviously complementary for estimation of fibre orientations, and results in improved detection of crossing fibres.[69]

1.3 NEUROIMAGING IN STEREOTACTIC NEUROSURGERY

Stereotactic neurosurgery began without the use of neuroimaging in 1908 London, when Horsley and Clarke developed an orthogonal frame that utilised a cartesian coordinate system, with the purpose of studying cerebellar function in monkeys.[70] In 1933, Kirschner performed the first stereotactic surgery in humans, ablating the trigeminal ganglion via the

foramen ovale, assisted by plain radiographs.[71,72] Although a landmark accomplishment, more influential was work by numerous surgeons and engineers in Europe, North America and Japan who both developed their own frames and leveraged the principles of using detailed mapping of human neuroanatomy (i.e. an atlas) and radiographic intra-cerebral landmarks to target a structure with stereotaxis. Among these pioneers, Leksell developed a frame operating on a polar coordinate system (arc-quadrant), which would over time survive as the preferred approach to stereotaxis.[73] Armed with contrast radiographs (pneumoencephalography), Spiegel and Wycis used the ventricular system, namely the foramina of Monro and calcification of the pineal gland, as landmarks. In 1947 they published the first thalamotomy, not for a movement disorder, but for psychiatric disease, as an alternative to the more aggressive lobotomy of the time.[74] Using contrast radiographs (iodo-ventriculography), the third ventricle could be well visualised, allowing tissue forming the ventricular walls to be inferred.[75] Talairach developed a system of anatomical cartography grounded on midline white matter structures at the anterior and posterior walls of the third ventricle: the anterior and posterior commissures (AC and PC).[76,77] As many subcortical structures have reasonably consistent anatomical relationships relative to the intercommissural line and the midsagittal plane, by applying proportional distances to individual brains, this atlas-based system would over time show to be a reasonably reliable system for stereotactic targeting of the diencephalon and other subcortical structures. Following the introduction of CT, Brown developed the N-localizer, three of which incorporated into a stereotactic frame produced three fiducials (radiographic points of reference) in each cross-sectional image.[78] This allowed the CT images to be registered to the stereotactic frame and frame targeting parameters to be calculated based on a location in a CT image. This was deployed in the Brown-Robert-Wells apparatus,[79] which significantly

advanced the principle of targeting deep brain structures using a stereotactic atlas grounded in Talairach coordinates. Cross-sectional imaging was also crucial to advancing stereotactic treatment of lesions throughout the brain (e.g. AVMs and tumours) by radiosurgery.[80]

These same principles were inherited by the age of MRI and were integrated into MRI scanning in the same way. As the resolution, contrast, and range of MRI sequences improved, this enabled a new paradigm of stereotactic targeting: simply visualising the target (sometimes termed 'direct targeting'). This became sufficient to visualise targets such as the STN,[81] while leaving others such as sub-nuclei of the thalamus invisible and reliant on traditional atlas-based methods. Subsequently, targeting of the STN has improved with a shift from T2-weighted images to fluid-attenuated inversion recovery (FLAIR) images.[82] Currently, high-field susceptibility-weighted imaging (SWI)[83,84] and inversion recovery sequences that null white matter (WAIR and FGATIR)[85–87] or both white matter and cerebrospinal fluid (MP2RAGE)[88] can cleanly extract the GPi and have made some progress in extracting the subnuclei of thalamus. The most recent innovation in imaging-guided stereotaxis has been the development of the ClearPoint system by Larson and Starr in San Francisco.[89] They devised an MRI-compatible frame-like system that allows for targeting coordinates to be calculated after the puncture of dura (i.e. on the open brain) thereby avoiding targeting inaccuracies due to brain-shift following egress of cerebrospinal fluid. In brief, this is achieved with a skull-mounted plastic stereotactic delivery system with gadolinium fiducials.

Shortly after the integration of CT and stereotaxis, frameless stereotaxy was invented by Roberts.[90] This technology would be developed, applied to MRI then re-invented, and as neuroimaging manipulation developed, harmonised with multimodal pre-operative and intra-

operative cross-sectional imaging, usually called neuronavigation.[91] Modern neuronavigation apparatus are highly sophisticated, versatile, easy-to-use systems, applicable to general neurosurgery. A typical setup may include a probe that is registered by touch to surface landmarks, such as the nasion, mastoid process, and occipital protuberance, and then co-registered to pre-operative MRI. The probe tip can then be located on the MRI during surgery. Although broadly considered a lower-fidelity process and not preferable for strictly stereotactic procedures, this technique has been of enormous use for anatomical orientation in general neurosurgery and tumour neurosurgery. In fact, its use is so pervasive in the breadth of neurosurgical procedures, it could be considered the most influential legacy of stereotaxis, validating the pioneering men's insights that improving anatomical localisation via mathematical and engineering approaches were the future of improving neurosurgical care.

The provenance of imaging applications in neurosurgery marks the link between developments in neuroimaging and developments in neurosurgery. The former has shaped and driven the latter. It defines the landscape in which neurosurgeons operate and innovate. Acknowledging this coupling, there is a strong argument that MRI has a clear role to play in further advancing the field: increasing what we know about a patient's disease and improving how we can treat it. Nowhere is this more evident than stereotactic neurosurgery, where targeting of specific anatomical structures and circuits with precision is the *sine qua non*. Similarly, the viability of neurosurgical procedures hinges on risk-benefit profile. Following from this, the reliability of a procedure's benefit is critically important for its recommendation, as are avoiding adverse effects such as haemorrhage. The foundational premise of stereotactic surgery is that a functional improvement may be achieved with

minimal adverse effects through the targeting of a particular, very small structure in an individual's brain, thought to be important in their disease. Necessarily, this requires sophisticated mechanical apparatus to reliably target a locus in space and imaging to identify the location of the intended structure in that individual in space. Therefore, MRI has an indispensable role in establishing procedure reliability and safety in stereotactic surgery.

A simple conceptual truth can be appreciated when reflecting on the history of neuroimaging in stereotactic surgery and the appraisal of clinical outcomes: in any controlled study, reliable (or appropriate) targeting is essential for demonstrating efficacy of a treatment and for minimising adverse effects of surgery. For example, if surgeries currently supported by level 1 evidence were conducted with X-ray ventriculography guidance instead of MRI guidance, they would have been unlikely to achieve this (i.e. a 'false' negative trial) and would probably also have had a poorer safety profile due to lower precision and accuracy of implantation (see Figure 1). This would be despite the ground truth that the surgery is, in principle, efficacious. Similarly, where modern stereotactic surgeries are unable to demonstrate significant cohort improvement, yet improvements in individual patients are convincing, the ground truth may well be that the surgery works but that targeting is often inappropriate. Advanced neuroimaging may be able to unveil this ground truth by further optimising targeting of a specific structure, or conversely by revealing precisely how anatomical targeting should actually be different between patients.

1.3.1 Spatial coordinates

Optimised targeting of the appropriate neuroanatomy is essential to deep brain stimulation (DBS) and even more so for permanent stereotactic lesion procedures. DBS has the advantage

of some flexibility, as the multiple electrode contacts on an array can be recruited for stimulation, thereby covering a larger anatomical area. Furthermore, stimulation can be withdrawn, and the lead even revised if necessary. Since 2015, directional leads have been commercially available that offer further flexibility in the plane orthogonal to the lead and have now become standard devices over the past few years. This has made achieving surgical accuracy to an optimal target more forgiving, as after implantation stimulation settings can be chosen to overcome some degree of misplacement. Nonetheless, understanding the optimal target and surgically reaching it are still endeavours of fundamental importance in DBS practice.

Beyond targeting a structure based on prior understanding of functional neuroanatomy and physiology, modern neuroimaging has allowed us to further adduce and optimise the surgical target: essentially retrospective empirical studies in man. Using post-operative MRI of lesion procedures (radiofrequency ablation, radiosurgery, high-intensity focused ultrasound), or post-operative CT registered to a pre-operative MRI for DBS, surgeons have been able to retrospectively identify therapeutic 'sweet-spots'. In its simplest form, this involves correlating the location of the intervention on imaging with clinical outcomes. This requires a spatial transform (either a coordinate system, such as AC-PC, or non-linearly registering the image to a standard space, such as MNI) and referencing to a compatible generic neuroanatomic atlas. In practice, to explain variance in outcomes, analysis requires a form of dimensionality reduction (3D to 1D) such as grounding to a high clinical improvement centroid (continuous method),[92] or allocating electrodes to a small number of specific anatomic structures and the corresponding outcomes compared (discrete method). Alternatively, outcome correlation can be assessed against theoretical stimulation volume using a voxel-

wise t-statistic map and a linear model. An example of this process is the proposition of a territory including the posterolateral ventral globus pallidus interna (GPi) and subpallidal white matter as the 'sweet-volume' for DBS treatment of dystonia.[93] Although such 'sweet-spot/volume' analyses invariably leave much outcome variance unexplained, the results of such experiments already inform the practice of stereotactic surgeons worldwide in movement disorders. Nonetheless, they have also generated controversy, after, in some cases, failing to be replicated consistently[94] and therefore leading to some heterogeneity in clinical practice. For example, such studies have conflicted in their support for the subthalamic nucleus (STN) as the target of choice for non-tremor dominant Parkinson's disease (without significant psychiatric co-morbidity). A spectrum of locations in the subthalamus have been identified, including the dorsal STN,[65,95,96], rostrolateral STN,[94] its border,[97–99] the posterior subthalamic area (PSA),[100,101] and the caudal zona incerta (cZI).[102] Despite this, most surgeons continue to target within the STN (typically dorsolateral), due to support from primate models,[81] overall balance of evidence (particularly regarding bradykinesia and rigidity), and important secondary outcomes like medication reduction.[103]

Discrepancies between studies are likely partly due to methodological limitations of electrode localisation. There is some uncertainty in localisation within an image, and even small systematic discrepancies in neuroimaging (e.g., MRI-CT registration) or defining electrode coordinates would lead to problems due to the relevant anatomical scale. In this regard, post-operative CT appears to be more reliable than post-operative MRI, due to the larger electrode artefact with the latter.[104] Probably more importantly, errors and inconsistencies are possible in the transposition from the individual representation to the common anatomical framework, and there is much disparity in how exactly this is carried out. Importantly, much

variation in human neuroanatomy is not accounted for, despite it being known that this can be quite considerable, for example with the thalamus.[105] Clearly, AC-PC coordinates can only be interpreted as approximations in their correspondence to particular neuroanatomic structures. Non-linear image registrations to an anatomic standard can have straightforward inaccuracies and otherwise are only driven by the available imaging contrast and are further limited by resolution. Ultimately, unless all relevant structures are clearly visible on MRI, inferences must be made on the principle of proportional relationships (distances, sizes, orientations, shapes) during registration. This is crucial to recognise and claims of a particular 'sweet-spot/volume' are seriously undermined when this is not demonstrated in the imaging series it depends on. Ultimately, for validation of specific non-invasive localisation methods, robust post-mortem series are required in parallel, to histologically confirm electrode locations. However, this is rarely done.

Large inter-individual variation is typical of location studies. In other words, one 'location' may work very well for one individual, but very poorly for another. Understanding why this is the case is crucial for advancing practice and is a clear signal that more advanced targeting methods are required. Advanced MRI is a putative tool to examine this. Location methods only concern themselves with 'macroanatomy', whereas functional anatomic organisation (i.e. the network) is also important, likely to vary in disease states, and could be probed with techniques that assess connectivity.[106] In addition to methodological errors in localisation, further heterogeneity could be expected due to variation in pathophysiology and corresponding anatomy between patients, which advanced MRI techniques could probe. It is broadly appreciated that, to improve targeting, a higher degree of personalisation is required than standard structural MRI and a linearly scaled anatomical atlas can provide. Therefore,

progress requires an advanced *a priori* evaluation of an individual's anatomy without the significant assumptions that an atlas overlays.

1.3.2 Tractography

Future practice is likely to see stereotactic surgeons rationalising the surgical target through the results of more complex neuroimaging experiments. The aim, in essence, amounts to replacing either a rigid, linearly scalable atlas or direct targeting of visible nuclei by flexible anatomical concepts pertaining to how the brain is organised. Such an approach is manifestly appealing, as it is recognised that it is the organisation of neural components that is important for function, and their spatial location more of a practicality.

1.3.2.1 Anatomical schema as surgical targets

In keeping with network concepts of brain function, it is recognised that with both DBS and lesioning, treatment effects (improvements and side effects alike) will depend on the connectivity of the target with other brain regions (i.e., connectivity partly defines function).[107] Clearly, lesioning would be expected to cause 'die-back' deafferentation of neurons structurally connected to the lesion. Similarly, the effects of DBS are likely to depend on local white matter tracts and their axonal orientation with respect to the electrical field generated by the system. Indeed, a central element of the rationale in targeting many structures is their participation in known neuroanatomic pathways and circuits which are of particular relevance to the pathophysiology and functional impairment that is hoped to be ameliorated. The historic thinking here has been to disrupt the forward flow of a problematic signal before it is integrated into a higher order representation and manifests as symptoms. Classic examples at the thalamus include the motor ventral intermediate nucleus of thalamus

(VIM) as a target for surgical treatment of tremor, as well as the ventral posterolateral (VPL) and ventral posteromedial (VPM) thalamic nuclei, targeted for limb and head pain respectively. The former is the primary thalamic termination site for the decussating dentatorubrothalamic tract (dDRTT), and the latter are primary termination sites for the medial lemniscus and trigeminothalamic tracts, conveying somatic sensations. Following in this anatomical tradition, with the advent of diffusion MRI tractography, a connectivity-based or 'connectome' approach to optimising neuromodulation surgery is both logical and attractive.[108]

1.3.2.2 Pairing tractography to clinical effects

The above connectomic interpretation of stimulation effects is conceptually broad and appealing in general terms. For example, it subsumes effects on soma connected with distant regions, as well as effects on axons synapsing or passing. As such, it may well capture a meaningful pairing being structural connectivity estimates and clinical effects. However, such applications of tractography that go beyond basic characterisation of stimulation location (i.e. from the general to the more specific) must rely on knowledge (or assumption) of the relevant mechanism of action (e.g. assumptions underpinning size and shape of the stimulation field). Unfortunately, confidence in such knowledge is absent in DBS; indeed, our understanding is particularly murky. Classically, axons and dendrites local to the electrode (particularly large ones) are considered of principle relevance to DBS, as soma have a substantially higher activation threshold.[109] However, DBS may also cause hyperpolarisation of soma and axons/dendrites. Furthermore, as neuronal populations may be excitatory or inhibitory, both these processes could cause inhibition or excitation downstream. Orientation of neural elements to the electric field is also a major determinant of the field's effects. In addition,

beyond ‘simple’ electrical effects, neurochemical effects, neuroglial effects, and effects on plasticity that cause long-term network reorganisation must also be considered as possible major determinants of clinical effects, particularly with chronic stimulation.[110,111]

At the inception of DBS, it was proposed that the high-frequency stimulation that was observed to ameliorate tremor worked via inhibition (of passing fibres rather than ventral thalamic soma), largely due to the clinical comparison with ablative surgery.[112] Although, remarkably, this has partly stood the test of time,[113] across the panoply of DBS surgeries the reality is seemingly much more complex with competing inhibitory and excitatory processes on both inhibitory and excitatory elements, on a background of other biological process. In summary, while much remains unknown, it is clear that; a) mechanisms vary by site (both with respect to specific target, and grey and white matter proximity), b) mechanisms vary by frequency of stimulation, c) mechanisms vary by amplitude of stimulation, and d) mechanisms in any one case of stimulation are likely multiple, of which observed clinical effects are a function.[114]

1.3.2.3 Localisation: from coordinates to connectivity contrast

Anatomical localisation via tractography is a method of leveraging the premise that connectivity patterns define an anatomical locus. By doing this, one shifts the atlas ‘generic neuroanatomy problem’ from small, high heterogeneity, anatomically congested regions (e.g., brain stem) to larger, more homogenous regions (e.g., cortex) where small assignment errors in applying the generic anatomical template to a specific brain are likely to be insignificant. In this way, in theory, tractography could be used to address the previously articulated problem of inaccurate targeting of deep brain structures as a result of applying

generic atlases to individual brains. In keeping with this, it is known that atlas-based targeting delivers considerable target variability with respect to an individual patient's tractography-derived white matter tracts,[115] supporting the appeal of such pre-operative information for surgical planning. As such, analysing an individual patient's white matter pathways using tractography - if attainable with high-fidelity - would appear an attractive method to personalise stereotactic targeting. Tractography derived from diffusion-MRI experiments is indeed proving to be a promising tool in stereotactic neurosurgery, through visualising tracts and by offering a metric of structural connectivity. Although mostly in the realm of neurosurgical science, it is already used by some surgeons.[41,42,116,117]

1.3.2.4 White versus grey matter

Although not exclusively (e.g. anterior internal capsule), surgical targets have historically been mostly nuclei: clusters of cell bodies functioning as integrating-relay hubs where numerous tracts converge, synapse, or pass through. However, white matter tracts are plausible surgical targets in their own right. It is often unclear whether or when it is nuclei (grey matter), or tracts (white matter) that should be targeted for optimal therapy.[93] DBS for essential tremor (ET) serves as a good example. VIM and ZI are the standard targets, yet there is compelling evidence that the key structures for tremor mitigation are fibres of the dDRTT that traverse the PSA and enter the VIM inferiorly.[39,118,119] This would also explain the greater electric efficiency of PSA compared to VIM DBS,[120] through the more orthogonal fibre orientation with respect to a typical lead trajectory. This theory surmises that it is not a particular function of cell bodies in the VIM or ZI that is important or responsible for the therapeutic effect of stimulation on tremor, it is merely their spatial proximity/relationship with the dDRTT axons. As aforementioned, wide ranging spatial coordinates of tremor-therapeutic contacts are

observed (more than might be expected from atlas-error alone), but nonetheless reproducibly localise along the dDRTT, and have a common property of signature structural connectivity.[38,121] Another consideration for targeting white matter is that there is an obvious network selectivity to targeting axons entering/leaving a face of a nuclear subregion than in the subregion grey matter itself, which likely receives input from a range of orientations. The appropriate treatment strategy (white versus grey) will ultimately be determined by the specific electrophysiology and pathophysiology in question.

Notwithstanding these unknowns, the use of tractography to guide stereotactic targeting remains conceptually appealing in two separate but related ways. A) to identify white matter tracts to be targeted in their own right, and B) to rationalise the optimal location (particularly of non-visible subnuclei/regions) based on connectivity profile. Outwith of targeting, tractography research could also be of interest with respect to probing aspects of neuromodulation mechanisms.

1.3.2.5 State of the surgical field

For the above reasons, tractography has been a fertile area of research in surgical movement disorders. This has especially been the case for tremor surgery, as the VIM – the traditional target – cannot be directly visualised on MRI. Instead, its location is inferred with respect to Talairach coordinates and a stereotactic atlas (e.g. Shaltenbrand and Wahren).[122] Tractographic approaches to targeting the VIM have prospectively been shown to be safe and efficacious,[116,117,123] as has targeting of the subcallosal cingulate (SCC) for depression.[42] Yet neither have been robustly validated for improving outcomes compared to the traditional methods, nor have similar methods with any stereotactic surgery. Indeed, prospective work

is sparse, but numerous studies have used retrospective tractography to explore white matter anatomy related to stimulated or lesioned targets, finding support for the theory that structural connectivity is important for surgical outcomes in PD, ET, generalised dystonia, obsessive compulsive disorder (OCD), and Tourette syndrome.[65,121,124–126] As such, one might well consider that due to inter-individual neuroanatomical differences, there is a sound hypothesis that tractography might have value in optimising the targeting of MRI-visible structures, such as the STN, as well as non-visible targets such as the VIM.[38,127] In principle, optimal electrode contacts and stimulation parameters could also be predicted,[128] which might be particularly useful in treating disorders such as dystonia where clinical benefits take months to emerge.

1.3.2.6 Methodology

Tractography is both complicated by, and benefits from, the range of options for how it can be used for targeting. In its simplest conception, known tracts can be visualised (typically by deterministic tractography), and targeted or avoided as deemed appropriate. Analytically, targets can then be assessed by metric distance from or identification within a tract. This strategy stems from a specific white matter structure of interest where the reconstructed anatomy is thought to be key. This approach can be challenging if the tracts are small and cannot be either well visually differentiated from other tracts or otherwise selected by 'seeding' visible structures on a pathway that differentiates it. This can pose a major methodological problem that can result in having to default back to atlas-based inference to some degree.[129] The multiple region of interest (multi-ROI) approach is the standard rejoinder to this problem, using multiple high-sensitivity, low-specificity ROI's to capture a signature anatomical trajectory, and discard other local fibres included in any single ROI.[130,131] More

commonly for analytic research in stereotactic neurosurgery, a probabilistic tractography model is applied, which outputs a metric (e.g. streamlines) of 'structural connectivity' between defined areas (e.g. electrode and gyrus). This strategy engages a connectome concept that structural connectivity metrics attempt to embody. The use of tractography is further complicated by deciding which tracts or 'connections' should be included, excluded, prioritised, avoided; which probabilistic methodology should be used; which diffusion signal modelling to use; and which diffusion MRI acquisition parameters to use. Equally, this versatility is potentially a strength to be leveraged.

The correction of susceptibility-induced distortions, problematic for the echo planar imaging necessary for DTI, and the degree to which the MRI acquisition is capable of encoding crossing fibres are particularly important for high-fidelity tractography. Without the former, accurate anatomical localisation is poor. False positives are an important limitation of tractography,[68] which mandates an essential requirement to only analyse connections that have been established by reliable invasive methods (e.g., tracer studies) in animals, ideally primates. in other words, they should not be used for discovery of 'new' pathways. As sample sizes are typically low in DBS cohort studies, it is important to be selective, carrying out only a small number of *a priori* credible experiments to avoid issues with multiple comparisons if statistical tests are being carried out.

Within the probabilistic 'structural connectome' strategy, approaches to identifying optimal surgical targets adopt one of two conceptual approaches. A) *a priori* parcellation of parent structure (e.g. thalamus) based on voxel-clustered structural connectivity profiles and analysing clinical effects with respect to individual parcels and target's locations;[132–134] or B)

a correlation of clinical outcomes with the target's connectivity to other brain areas[40,65] and backpropagating the optimal connectivity-template pattern for future surgeries (e.g. a connectivity hot-spot as a targeting/implantation reference point). The first method is based on the assumption that the structural connectivity profile of a parent structure should functionally and anatomically segment it. This concept is supported by neuronal tracer experiments, and DTI-based parcellations have produced anatomically plausible results.[135]

1.3.2.7 Normative versus individualised connectomes

Individual's brains are different, including their structural connectivity. Correspondingly, high-field diffusion tractography produces significant differences between individuals in key tracts.[136] Pathology may also manifest in changes of structural connectivity, and this may be variable amongst individuals with the same disease categorisation. This is made concrete by the extensive literature on fractional anisotropy and tract-based spatial statistics experiments analysing neurological and psychiatric conditions against healthy controls. Despite this, numerous studies have used 'normative connectomes':[121,124,125] a spatial average of diffusion parameters, combined from numerous individual subject/patient scans, non-linearly transformed to a common space (i.e. MNI). The benefits of such a method are largely practical: no diffusion scans are required for each individual patient - only the electrode locations - and the diffusion connectome used is typically of a very high-quality (e.g., high signal-to-noise ratio, angular resolution, and spatial resolution) as it did not have to be acquired for specific patients. Obviously, however, any analysis will not reflect any intrinsic differences in connectivity between patients and is instead a form of characterisation of electrode location represented in additional dimensions. Due to this, the application of such results to the improvement of individualised surgical targeting or patient

selection/counselling is, from first principles, arguably very limited. Nonetheless, Wang et al. explore this issue with a study that compares the tractography results of STN DBS within a normative age-matched connectome, a normative young/healthy connectome, and within individual connectomes.[137] Differences between the two approaches (normative and patient-specific) did not reach statistical significance, although there were trends which the authors interpret as the DBS tractography in the individual connectomes explaining more of the variance in outcomes from surgery. The analysis has some limitations, for example, the use of three different diffusion acquisitions among the individual connectome data set. Yet, at least in PD considering STN DBS, it indicates that structural connectomes are more similar than they are different. It should nonetheless be recognised that this may not apply to other pathological cohorts, particularly those that where substantial degeneration or functional reorganisation is characteristic of the disease (e.g., dystonia). This same question has been addressed as a secondary objective in two other studies. Essentially the same conclusion is made in a study of superolateral medial forebrain bundle (slMFB) DBS for depression, although the similarity between normative and individualised connectome analysis is not quantified, and regardless, connectivity failed to show predictive power.[138] However, Baldermann et al. examine anterior limb of internal capsule (ALIC) DBS for OCD, demonstrating clear differences in specific predictive DBS<->cortex connectivity between normative and individualised connectomes (e.g. prominent cingulate and primary motor cortex relationship in the normative analysis but not individualised), although both predicted outcomes with a similar power.[139] Indeed, a closer look at the results of Wang et al. supports a perspective more in line with these findings. We know from Vanegas-Arroyave et al. that STN DBS<->superior frontal gyrus structural connectivity is a major predictor of surgical benefit.[40] Therefore, it is an important region to consider that includes the supplementary

motor area (SMA) and pre-SMA. However, with Wang et al. the Spearman correlation R^2 between individualised and normative DBS<->SMA connectivity was only 0.16-0.18, and for DBS<->pre-SMA connectivity it was only 0.11. One might expect some variation due to differences in diffusion MRI acquisition parameters, but differences of this scale demonstrate that although normative connectomes can predict clinical outcomes, and their connectivity metrics significantly correlate with those from individualised connectomes, the specifics nonetheless actually differ quite substantially. Indeed, despite their conclusions, this is quite clear from the renderings of the respective 'optimal connectivity profiles' for different connectomes presented in their manuscript. If one is aiming to prospectively personalise a surgical procedure using connectivity, the specifics will clearly matter, and by fundamentally ignoring the intrinsic structural connectivity differences between patients the potential for using results to individualise treatment is much more limited. It must be emphasised that analyses based on normative connectomes cannot offer more than normalised electrode coordinates for choosing where to choose as a stereotactic target in an individual patient. All it can do is give a connectomic characterisation of electrode locations, based on an averagely connected brain.

1.3.2.8 Toward a diffusion MRI personalisation of stereotaxis

Research on surgical personalisation using an individual's connectome is currently too limited to make major claims on its potential to upgrade stereotactic surgery. As of yet it has mostly been applied to STN and VIM procedures that have relatively (for the range of DBS indications) low variance in outcomes (i.e. less potential for optimisation).[65,132] Practically, it has the potential to be most germane to surgeries where very large variation in clinical outcomes is routinely observed, and where that variation is currently unexplained. In this

category, there has been some investigation of ALIC DBS for OCD,[140] SCC DBS[42,141,142] and slMFB DBS for depression,[138] and some modest study of anterior cingulate (AC) DBS for pain.[143,144] In summary, AC DBS results are only preliminary and weak, slMFB DBS results were negative, SCC DBS results have showed potential but unfortunately have not clearly improved outcomes in prospective application, and deterministic tractography results in ALIC DBS have showed some promise to guide targeting, explaining ~35% of variance in outcomes. Despite the unimpressive state of the project, the structural connectomic approach to the interpretation of the effects of DBS remains compelling and its exploration still in its infancy. Pedunculopontine nucleus stimulation for PD, thalamic stimulation for pain, and GPi stimulation for dystonia are all prime candidates in which to further examine the prospect of diffusion MRI personalisation of stereotaxis and will be addressed as the corpus of this thesis.

1.3.3 BOLD-MRI and other advanced neuroimaging

In a similar way to diffusion MRI, blood-oxygen-level-dependent (BOLD) imaging, commonly known as functional MRI (fMRI), has also been used in an effort to rationalise variation in clinical outcomes from DBS surgery. Functional connectivity of the stimulated region with other brain areas is calculated, and correlation can be assessed between connectivity patterns and outcomes. This is usually resting state (rs-fMRI) but can be a task/stimulus-based experiment. Often, fMRI data has been combined with diffusion MRI data to generate a bi-modal whole brain connectivity profile associated with surgical success.[121,125,145] In such a study with STN DBS,[145] both connectomes were independent predictors of success. This suggests, at least in principle, that fMRI could be used to refine treatment in addition to diffusion MRI, although as normative connectomes were used this conclusion is somewhat problematic. As a proof of concept, however, individual fMRI data in healthy individuals has

been shown to localise an anatomically plausible thalamic target for tremor,[146] indicating a theoretical use for individualised targeting.

Overall, fMRI appears more suited as a tool for probing mechanistic questions.[147] A rs-fMRI acquisition can be carried out intraoperatively,[148,149] with stimulation on and off, allowing network effects on brain function to be inferred by regional changes in blood oxygenation, under these different conditions.[150–152] There are important non-trivial technical complications relating to electrode artefact in the BOLD signal (particularly with stimulation on), but these can probably be largely overcome.[153] In contrast, it is hard to see how this could ever be possible with diffusion MRI due to the interaction of the metal electrodes with the large magnetic gradients that are used. Furthermore, the experiment itself makes much less sense, as it is not biologically feasible for structural connectivity to change on a time scale of acute on/off stimulation experiments, although the possibility of long-term structural connectivity changes after chronic stimulation would admittedly be interesting to study.[154]

Due to practicalities of image resolution, fMRI has more limited potential to improve stereotactic targeting. At clinically reasonable scanning times, fMRI experiments are typically done at a resolution of around 3 mm^3; 27-times the tissue volume discernible on typical structural MRIs (1 mm^3) and not useful for the relevant anatomical or surgical scales (surgeries are usually accurate to within 1 mm). Comparably, under clinically reasonable scanning times, diffusion MRI is typically acquired at around 2 mm^3 resolution (8-times the tissue volume of a 1 mm^3 structural MRI). Instead, and in addition to mechanistic insight, where fMRI is most likely to improve DBS surgery is in patient selection. In principle, pre-operative fMRI scanning could be performed as part of the clinical assessment of all patients,

but particularly clinically borderline surgical candidates, to see if they have a suitable connectivity profile available to suggest benefit from surgery.[151,155] Indeed, this concept could be developed further, for example in PD, individual patient's fMRI scans might plausibly be used to predict which surgical target to choose (GPi vs. STN vs. VIM vs. ZI) based on what would be clinically optimal for an individual patient. Promising research in this area has been carried out in STN DBS for PD, where it is not the connectivity of the particular electrode locations that is examined, but the connectivity of the STN (pallido-subthalamic)[156] or that between non-STN ROIs.[157] This approach has explained considerable outcome variance. As variance in implant location clearly matters and is intrinsically ignored in such analyses, their demonstrated predictive power points towards a potentially supplemental clinical benefit (via patient selection) to any improvements relating to targeting.

It is unclear what contribution other imaging modalities, such as MR spectroscopy (MRS), could play in improving functional neurosurgery. Neurotransmitter density, such as ɣ-aminobutyric acid (GABA), in key nuclei might be relevant to the efficacy of DBS and could be explored with MRS. MRS can play an important role in stereotactic biopsy, and with increasing indications for stereotactic surgery, MRS may well find a niche. The next-generation of stereotactic procedures are purported to be deep brain drug and vector delivery.[158–160] As their strategy is to rectify cellular and biochemical dysfunction (as opposed to altering network function), patient selection, targeting, or follow-up could, in principle, benefit from metabolic data acquired by MRI.

1.3.4 Concluding remarks

MRI has been fundamental to progress in neurosurgery in general and stereotactic surgery specifically. Advanced forms of MRI are cogent candidate tools for further progress in guiding the right intervention to the right patient. Improvements in targeting from MRI are likely not exhausted, and instead are likely to arise from improved contrast with clinical high-field (7T) structural MRI and high angular resolution diffusion MRI data with multi-fibre modelling. It is possible to conceive of clinical software with automated tract identification and parcellation functionality, allowing for high-fidelity connectivity-based targeting and avoidance of relevant anatomy.[161,162] In addition, organic metabolic (MRS, chemical exchange saturation transfer imaging, amide proton transfer imaging), inorganic metabolic (SWI), structural connectomic (diffusion MRI), and functional connectomic (fMRI) data may provide key insights into patient stratification and precision-diagnosis through granular characterisation of individuals' pathology, and inform the treatment of choice (stereotactic or otherwise). Through an effort to improve care, paired with clinical observations, these techniques can also offer scientific insights into the medical conditions they are applied to, the function of different brain areas, as well as the treatments themselves. Outwith of scientific enquiry, such techniques face many challenges in becoming standard of care in the practice of clinical excellence. The Fryback six level hierarchy can be reformulated to model this challenge: (1) technical feasibility, (2) data relevance, (3) data reliability, (4) therapeutic impact, (5) impact on outcome, and (6) economic acceptability.[163] Satisfying this is a process of discovery, and advanced neuroimaging will be used in the first instance at surgeons preference through pioneering spirit and common sense.

Individualised approaches in stereotactic and functional neurosurgery are most relevant where clinical response is highly variable between patients and their underlying pathology is spatially or physiologically heterogenous. In such cases, information from individualised structural connectomes is likely to be highly relevant. Conversely, where surgeries are quite reliable, such information is less relevant. In this thesis, diffusion MRI will be used to interpret three cases of the former: firstly, DBS treatment of gait freezing and falls, secondly, analgesia, and lastly, cervical dystonia. The thesis will propose that patient-specific structural connectivity parameters, inferred from diffusion MRI, reveal anatomical differences between patients that offer convincing explanations for large variability in clinical effects of DBS, resolving considerable epistemic uncertainty. In each case, the results presented in this thesis inform a possible strategy for using this non-invasive pre-operative technique for personalising surgery to optimise outcomes for patients.

Overall, the arc of progress in stereotactic neurosurgery has taken a trajectory from cruder approaches based on generalised neuroanatomy to being an increasingly personalised project, tailored to an individual's neuroanatomy. One can expect this journey to continue.

REFERENCES

1. Rabi II, Zacharias JR, Millman S, Kusch P. A New Method of Measuring Nuclear Magnetic Moment. Phys Rev 1938;53(4):318–318.
2. Bloch F, Hansen WW, Packard M. Nuclear Induction. Phys Rev 1946;69(3–4):127–127.
3. Bloch F, Hansen WW, Packard M. The Nuclear Induction Experiment. Phys Rev 1946;70(7–8):474–85.
4. Zeeman P. The Effect of Magnetisation on the Nature of Light Emitted by a Substance. Nature 1897;55(1424):347–347.

5. Carr H. Free precession techniques in nuclear magnetic resonance. 1952;

6. Damadian R. Tumor Detection by Nuclear Magnetic Resonance. Science 1971;171(3976):1151–3.

7. Lauterbur PC. Image Formation by Induced Local Interactions: Examples Employing Nuclear Magnetic Resonance. Nature 1973;242(5394):190–1.

8. Damadian R, Goldsmith M, Minkoff L. NMR in cancer: XVI. FONAR image of the live human body. Physiol Chem Phys 1977;9(1):97–100, 108.

9. Le Bihan D, Breton E. Imagerie de diffusion in vivo par résonance magnétique nucléaire. C R Acad Sci Paris 1985;Série II:1109–12.

10. Le Bihan D, Breton E, Lallemand D, Grenier P, Cabanis E, Laval-Jeantet M. MR imaging of intravoxel incoherent motions: application to diffusion and perfusion in neurologic disorders. Radiology 1986;161(2):401–7.

11. Yamasaki F, Kurisu K, Satoh K, et al. Apparent Diffusion Coefficient of Human Brain Tumors at MR Imaging. Radiology 2005;235(3):985–91.

12. Hayashida Y, Hirai T, Morishita S, et al. Diffusion-weighted Imaging of Metastatic Brain Tumors: Comparison with Histologic Type and Tumor Cellularity. Am J Neuroradiol 2006;27(7):1419.

13. Sugahara T, Korogi Y, Kochi M, et al. Usefulness of diffusion-weighted MRI with echo-planar technique in the evaluation of cellularity in gliomas. J Magn Reson Imaging 1999;9(1):53–60.

14. Rumboldt Z, Camacho DLA, Lake D, Welsh CT, Castillo M. Apparent Diffusion Coefficients for Differentiation of Cerebellar Tumors in Children. Am J Neuroradiol 2006;27(6):1362.

15. Dumrongpisutikul N, Intrapiromkul J, Yousem DM. Distinguishing between Germinomas and Pineal Cell Tumors on MR Imaging. Am J Neuroradiol 2012;33(3):550–5.

16. Toh C-H, Castillo M, Wong AM-C, et al. Primary Cerebral Lymphoma and Glioblastoma Multiforme: Differences in Diffusion Characteristics Evaluated with Diffusion Tensor Imaging. Am J Neuroradiol 2008;29(3):471–5.

17. Guo AC, Cummings TJ, Dash RC, Provenzale JM. Lymphomas and High-Grade Astrocytomas: Comparison of Water Diffusibility and Histologic Characteristics. Radiology 2002;224(1):177–83.

18. Basser PJ, Mattiello J, Lebihan D. Estimation of the Effective Self-Diffusion Tensor from the NMR Spin Echo. J Magn Reson B 1994;103(3):247–54.

19. Basser PJ, Mattiello J, LeBihan D. MR diffusion tensor spectroscopy and imaging. Biophys J 1994;66(1):259–67.

20. Conturo TE, Lori NF, Cull TS, et al. Tracking neuronal fiber pathways in the living human brain. Proc Natl Acad Sci 1999;96(18):10422–7.

21. Girard G, Whittingstall K, Deriche R, Descoteaux M. Towards quantitative connectivity analysis: reducing tractography biases. NeuroImage 2014;98:266–78.

22. Behrens TEJ, Woolrich MW, Jenkinson M, et al. Characterization and propagation of uncertainty in diffusion-weighted MR imaging. Magn Reson Med 2003;50(5):1077–88.

23. Basser PJ, Pajevic S, Pierpaoli C, Duda J, Aldroubi A. In vivo fiber tractography using DT-MRI data. Magn Reson Med 2000;44(4):625–32.

24. Petersen MV, Lund TE, Sunde N, et al. Probabilistic versus deterministic tractography for delineation of the cortico-subthalamic hyperdirect pathway in patients with Parkinson disease selected for deep brain stimulation. J Neurosurg 2017;126(5):1657–68.

25. Sarwar T, Ramamohanarao K, Zalesky A. Mapping connectomes with diffusion MRI: deterministic or probabilistic tractography? Magn Reson Med 2019;81(2):1368–84.

26. Essayed WI, Zhang F, Unadkat P, Cosgrove GR, Golby AJ, O'Donnell LJ. White matter tractography for neurosurgical planning: A topography-based review of the current state of the art. NeuroImage Clin 2017;15:659–72.

27. Abhinav K, Yeh F-C, Mansouri A, Zadeh G, Fernandez-Miranda JC. High-definition fiber tractography for the evaluation of perilesional white matter tracts in high-grade glioma surgery. Neuro-Oncol 2015;17(9):1199–209.

28. Castellano A, Bello L, Michelozzi C, et al. Role of diffusion tensor magnetic resonance tractography in predicting the extent of resection in glioma surgery. Neuro-Oncol 2012;14(2):192–202.

29. Caverzasi E, Hervey-Jumper SL, Jordan KM, et al. Identifying preoperative language tracts and predicting postoperative functional recovery using HARDI q-ball fiber tractography in patients with gliomas. J Neurosurg 2016;125(1):33–45.

30. Kuhnt D, Bauer MHA, Becker A, et al. Intraoperative Visualization of Fiber Tracking Based Reconstruction of Language Pathways in Glioma Surgery. Neurosurgery 2012;70(4):911–20.

31. Chen X, Weigel D, Ganslandt O, Buchfelder M, Nimsky C. Prediction of visual field deficits by diffusion tensor imaging in temporal lobe epilepsy surgery. NeuroImage 2009;45(2):286–97.

32. Winston GP, Daga P, Stretton J, et al. Optic radiation tractography and vision in anterior temporal lobe resection. Ann Neurol 2012;71(3):334–41.

33. Yogarajah M, Focke NK, Bonelli S, et al. Defining Meyer's loop-temporal lobe resections, visual field deficits and diffusion tensor tractography. Brain 2009;132(6):1656–68.

34. Hodaie M, Quan J, Chen DQ. In Vivo Visualization of Cranial Nerve Pathways in Humans Using Diffusion-Based Tractography. Neurosurgery 2010;66(4):788–96.

35. Taoka T, Hirabayashi H, Nakagawa H, et al. Displacement of the facial nerve course by vestibular schwannoma: Preoperative visualization using diffusion tensor tractography. J Magn Reson Imaging 2006;24(5):1005–10.

36. Gerganov VM, Giordano M, Samii M, Samii A. Diffusion tensor imaging–based fiber tracking for prediction of the position of the facial nerve in relation to large vestibular schwannomas. J Neurosurg 2011;115(6):1087–93.

37. Song F, Hou Y, Sun G, et al. In vivo visualization of the facial nerve in patients with acoustic neuroma using diffusion tensor imaging–based fiber tracking. J Neurosurg 2016;125(4):787–94.

38. Klein JC, Barbe MT, Seifried C, et al. The tremor network targeted by successful VIM deep brain stimulation in humans. Neurology 2012;78(11):787–95.

39. Coenen VA, Allert N, Paus S, Kronenbu¨rger M, Urbach H, Ma¨dler B. Modulation of the Cerebello-Thalamo-Cortical Network in Thalamic Deep Brain Stimulation for Tremor. Neurosurgery 2014;75(6):657–70.

40. Vanegas-Arroyave N, Lauro PM, Huang L, et al. Tractography patterns of subthalamic nucleus deep brain stimulation. Brain 2016;139(4):1200–10.

41. Schlaepfer TE, Bewernick BH, Kayser S, Mädler B, Coenen VA. Rapid Effects of Deep Brain Stimulation for Treatment-Resistant Major Depression. Biol Psychiatry 2013;73(12):1204–12.

42. Riva-Posse P, Choi KS, Holtzheimer PE, et al. A connectomic approach for subcallosal cingulate deep brain stimulation surgery: prospective targeting in treatment-resistant depression. Mol Psychiatry 2018;23(4):843–9.

43. Koga T, Maruyama K, Kamada K, et al. Outcomes of Diffusion Tensor Tractography–Integrated Stereotactic Radiosurgery. Int J Radiat Oncol 2012;82(2):799–802.

44. Farquharson S, Tournier J-D, Calamante F, et al. White matter fiber tractography: why we need to move beyond DTI. J Neurosurg 2013;118(6):1367–77.

45. Behrens TEJ, Berg HJ, Jbabdi S, Rushworth MFS, Woolrich MW. Probabilistic diffusion tractography with multiple fibre orientations: What can we gain? NeuroImage 2007;34(1):144–55.

46. Peled S, Friman O, Jolesz F, Westin C-F. Geometrically constrained two-tensor model for crossing tracts in DWI. Magn Reson Imaging 2006;24(9):1263–70.

47. Glenn GR, Helpern JA, Tabesh A, Jensen JH. Optimization of white matter fiber tractography with diffusional kurtosis imaging: DKI Tractography. NMR Biomed 2015;28(10):1245–56.

48. Glenn GR, Kuo L-W, Chao Y-P, Lee C-Y, Helpern JA, Jensen JH. Mapping the Orientation of White Matter Fiber Bundles: A Comparative Study of Diffusion Tensor Imaging, Diffusional Kurtosis Imaging, and Diffusion Spectrum Imaging. Am J Neuroradiol 2016;37(7):1216–22.

49. Tournier J-D, Calamante F, Connelly A. Robust determination of the fibre orientation distribution in diffusion MRI: Non-negativity constrained super-resolved spherical deconvolution. 2007;35(4):1459–72.

50. Tournier J-D, Calamante F, Gadian DG, Connelly A. Direct estimation of the fiber orientation density function from diffusion-weighted MRI data using spherical deconvolution. NeuroImage 2004;23(3):1176–85.

51. Tuch DS, Reese TG, Wiegell MR, Makris N, Belliveau JW, Wedeen VJ. High angular resolution diffusion imaging reveals intravoxel white matter fiber heterogeneity. Magn Reson Med 2002;48(4):577–82.

52. Tuch DS, Reese TG, Wiegell MR, Van J. Wedeen. Diffusion MRI of Complex Neural Architecture. Neuron 2003;40(5):885–95.

53. Tuch DS. Q-ball imaging. Magn Reson Med 2004;52(6):1358–72.

54. Wedeen VJ, Wang RP, Schmahmann JD, et al. Diffusion spectrum magnetic resonance imaging (DSI) tractography of crossing fibers. NeuroImage 2008;41(4):1267–77.

55. Sotiropoulos SN, Behrens TEJ, Jbabdi S. Ball and rackets: Inferring fiber fanning from diffusion-weighted MRI. NeuroImage 2012;60(2):1412–25.

56. Pasternak O, Sochen N, Gur Y, Intrator N, Assaf Y. Free water elimination and mapping from diffusion MRI. Magn Reson Med 2009;62(3):717–30.

57. Zhang H, Schneider T, Wheeler-Kingshott CA, Alexander DC. NODDI: Practical in vivo neurite orientation dispersion and density imaging of the human brain. NeuroImage 2012;61(4):1000–16.

58. Topgaard D. Multidimensional diffusion MRI. J Magn Reson 2017;275:98–113.

59. Palombo M, Shemesh N, Ronen I, Valette J. Insights into brain microstructure from in vivo DW-MRS. NeuroImage 2018;182:97–116.

60. Andersson JLR, Skare S, Ashburner J. How to correct susceptibility distortions in spin-echo echo-planar images: application to diffusion tensor imaging. NeuroImage 2003;20(2):870–88.

61. Graham MS, Drobnjak I, Jenkinson M, Zhang H. Quantitative assessment of the susceptibility artefact and its interaction with motion in diffusion MRI. PLOS ONE 2017;12(10):e0185647.

62. Andersson JLR, Sotiropoulos SN. An integrated approach to correction for off-resonance effects and subject movement in diffusion MR imaging. NeuroImage 2016;125:1063–78.

63. Graham MS, Drobnjak I, Zhang H. Realistic simulation of artefacts in diffusion MRI for validating post-processing correction techniques. NeuroImage 2016;125:1079–94.

64. Descoteaux M. High Angular Resolution Diffusion Imaging (HARDI) [Internet]. In: Wiley Encyclopedia of Electrical and Electronics Engineering. John Wiley & Sons, Ltd; 2015. p. 1–25.Available from: https://onlinelibrary.wiley.com/doi/abs/10.1002/047134608X.W8258

65. Akram H, Sotiropoulos SN, Jbabdi S, et al. Subthalamic deep brain stimulation sweet spots and hyperdirect cortical connectivity in Parkinson's disease. NeuroImage 2017;158:332–45.

66. Tournier J-D, Calamante F, Connelly A. Determination of the appropriate *b* value and number of gradient directions for high-angular-resolution diffusion-weighted imaging. NMR Biomed 2013;26(12):1775–86.

67. Schilling KG, Nath V, Blaber J, et al. Effects of b-value and number of gradient directions on diffusion MRI measures obtained with Q-ball imaging [Internet]. 2017. Available from: https://doi.org/10.1117/12.2254545

68. Maier-Hein KH, Neher PF, Houde J-C, et al. The challenge of mapping the human connectome based on diffusion tractography. Nat Commun 2017;8(1):1349.

69. Jbabdi S, Sotiropoulos SN, Savio AM, Graña M, Behrens TEJ. Model-based analysis of multishell diffusion MR data for tractography: How to get over fitting problems. Magn Reson Med 2012;68(6):1846–55.

70. Horsley V, Clarke RH. The structure and functions of the cerebellum examined by a new method. Brain 1908;31(1):45–124.

71. Kirschner M. Zur elektrochirurgie. Arch Klin Chir 1931;167:761–8.

72. Kirschner M. Die Punktionstechnik und die Elektrokoagulation des Ganglion Gasseri. Über gezielte Operationen. Arch Klin Chir 1933;176:581–620.

73. Leksell L. A Stereotaxic Apparatus For Intracerebral Surgery. Acta Chir Scand 1949;99:229–223.

74. Spiegel EA, Wycis HT, Marks M, Lee AJ. Stereotaxic Apparatus for Operations on the Human Brain. Science 1947;106(2754):349–50.

75. Mazoyer B. Jean Talairach (1911–2007): A life in stereotaxy. Hum Brain Mapp 2008;29(2):250–2.

76. Talairach J, Hecaen H, David M, Monnier M, De Ajuriaguerra J. Recherches sur la coagulation thérapeutique des structures sous-corticales chez l'homme. Rev Neurol (81):4–24.

77. Talairach J, David M, Tournoux P, Corredor H, Kvasina T. Atlas d'anatomie stéréotaxique. Repérage radiologique indirect des noyaux gris centraux des régions mésencephalo-sous-optique et hypothalamique de l'homme. Paris: Masson & Cie; 1957.

78. Brown RA. A computerized tomography-computer graphics approach to stereotaxic localization. J Neurosurg 1979;50(6):715–20.

79. Brown RA, Roberts TS, Osborn AG. Stereotaxic Frame and Computer Software for CT-directed Neurosurgical Localization. Invest Radiol 1980;15(4):308–12.

80. Leksell L. Stereotactic radiosurgery. J Neurol Neurosurg Psychiatry 1983;46(9):797–803.

81. Aziz TZ, Nandi D, Parkin S, et al. Targeting the Subthalamic Nucleus. Stereotact Funct Neurosurg 2001;77(1–4):87–90.

82. Senova S, Hosomi K, Gurruchaga J-M, et al. Three-dimensional SPACE fluid-attenuated inversion recovery at 3 T to improve subthalamic nucleus lead placement for deep brain stimulation in Parkinson's disease: from preclinical to clinical studies. J Neurosurg 2016;125(2):472–80.

83. Abosch A, Yacoub E, Ugurbil K, Harel N. An Assessment of Current Brain Targets for Deep Brain Stimulation Surgery With Susceptibility-Weighted Imaging at 7 Tesla. Neurosurgery 2010;67(6):1745–56.

84. Li J, Li Y, Gutierrez L, et al. Imaging the Centromedian Thalamic Nucleus Using Quantitative Susceptibility Mapping. Front Hum Neurosci 2020;13:447.

85. Vassal F, Coste J, Derost P, et al. Direct stereotactic targeting of the ventrointermediate nucleus of the thalamus based on anatomic 1.5-T MRI mapping with a white matter attenuated inversion recovery (WAIR) sequence. Brain Stimulat 2012;5(4):625–33.

86. Neudorfer C, Kroneberg D, Al-Fatly B, et al. Personalizing deep brain stimulation using advanced imaging sequences. medRxiv 2021;2021.10.04.21264488.

87. Grewal SS, Middlebrooks EH, Kaufmann TJ, et al. Fast gray matter acquisition T1 inversion recovery MRI to delineate the mammillothalamic tract for preoperative direct targeting of the anterior nucleus of the thalamus for deep brain stimulation in epilepsy. Neurosurg Focus 2018;45(2):E6.

88. Tanner M, Gambarota G, Kober T, et al. Fluid and white matter suppression with the MP2RAGE sequence. J Magn Reson Imaging 2012;35(5):1063–70.

89. Larson PS, Starr PA, Bates G, Tansey L, Richardson RM, Martin AJ. An Optimized System for Interventional Magnetic Resonance Imaging-Guided Stereotactic Surgery: Preliminary Evaluation of Targeting Accuracy. Oper Neurosurg 2012;70(suppl_1):ons95–103.

90. Roberts DW, Strohbehn JW, Hatch JF, Murray W, Kettenberger H. A frameless stereotaxic integration of computerized tomographic imaging and the operating microscope. J Neurosurg 1986;65(4):545–9.

91. Enchev Y. Neuronavigation: geneology, reality, and prospects. Neurosurg Focus 2009;27(3):E11.

92. Schönecker T, Gruber D, Kivi A, et al. Postoperative MRI localisation of electrodes and clinical efficacy of pallidal deep brain stimulation in cervical dystonia. J Neurol Neurosurg Psychiatry 2015;86(8):833–9.

93. Reich MM, Horn A, Lange F, et al. Probabilistic mapping of the antidystonic effect of pallidal neurostimulation: a multicentre imaging study. Brain 2019;142(5):1386–98.

94. Garcia-Garcia D, Guridi J, Toledo JB, Alegre M, Obeso JA, Rodríguez-Oroz MC. Stimulation sites in the subthalamic nucleus and clinical improvement in Parkinson's disease: a new approach for active contact localization. J Neurosurg 2016;125(5):1068–79.

95. Hamel W. Deep brain stimulation of the subthalamic nucleus in Parkinson's disease: evaluation of active electrode contacts. J Neurol Neurosurg Psychiatry 2003;74(8):1036–46.

96. Welter M-L, Schupbach M, Czernecki V, et al. Optimal target localization for subthalamic stimulation in patients with Parkinson disease. Neurology 2014;82(15):1352–61.

97. Lanotte MM. Deep brain stimulation of the subthalamic nucleus: anatomical, neurophysiological, and outcome correlations with the effects of stimulation. J Neurol Neurosurg Psychiatry 2002;72(1):53–8.

98. Yokoyama T, Sugiyama K, Nishizawa S, et al. The Optimal Stimulation Site for Chronic Stimulation of the Subthalamic Nucleus in Parkinson's Disease. Stereotact Funct Neurosurg 2001;77(1–4):61–7.

99. Herzog J, Fietzek U, Hamel W, et al. Most effective stimulation site in subthalamic deep brain stimulation for Parkinson's disease. Mov Disord 2004;19(9):1050–4.

100. Maks CB, Butson CR, Walter BL, Vitek JL, McIntyre CC. Deep brain stimulation activation volumes and their association with neurophysiological mapping and therapeutic outcomes. J Neurol Neurosurg Psychiatry 2009;80(6):659–66.

101. Voges J, Volkmann J, Allert N, et al. Bilateral high-frequency stimulation in the subthalamic nucleus for the treatment of Parkinson disease: correlation of

therapeutic effect with anatomical electrode position. J Neurosurg 2002;96(2):269–79.

102. Plaha P. Stimulation of the caudal zona incerta is superior to stimulation of the subthalamic nucleus in improving contralateral parkinsonism. Brain 2006;129(7):1732–47.

103. Blomstedt P, Stenmark Persson R, Hariz G-M, et al. Deep brain stimulation in the caudal zona incerta versus best medical treatment in patients with Parkinson's disease: a randomised blinded evaluation. J Neurol Neurosurg Psychiatry 2018;89(7):710–6.

104. Mirzadeh Z, Chapple K, Lambert M, Dhall R, Ponce FA. Validation of CT-MRI fusion for intraoperative assessment of stereotactic accuracy in DBS surgery. Mov Disord 2014;29(14):1788–95.

105. Morel A, Magnin M, Jeanmonod D. Multiarchitectonic and stereotactic atlas of the human thalamus. J Comp Neurol 1997;387(4):588–630.

106. Middlebrooks EH, Domingo RA, Vivas-Buitrago T, et al. Neuroimaging Advances in Deep Brain Stimulation: Review of Indications, Anatomy, and Brain Connectomics. Am J Neuroradiol 2020;41(9):1558–68.

107. Alhourani A, McDowell MM, Randazzo MJ, et al. Network effects of deep brain stimulation. J Neurophysiol 2015;114(4):2105–17.

108. Horn A, Fox MD. Opportunities of connectomic neuromodulation. NeuroImage 2020;221:117180.

109. Herrington TM, Cheng JJ, Eskandar EN. Mechanisms of deep brain stimulation. J Neurophysiol 2016;115(1):19–38.

110. Ashkan K, Rogers P, Bergman H, Ughratdar I. Insights into the mechanisms of deep brain stimulation. Nat Rev Neurol 2017;13(9):548–54.

111. Bekar L, Libionka W, Tian G-F, et al. Adenosine is crucial for deep brain stimulation–mediated attenuation of tremor. Nat Med 2008;14(1):75–80.

112. Benabid AL, Pollak P, Gao D, et al. Chronic electrical stimulation of the ventralis intermedius nucleus of the thalamus as a treatment of movement disorders. J Neurosurg 1996;84(2):203–14.

113. Anderson TR, Hu B, Iremonger K, Kiss ZHT. Selective Attenuation of Afferent Synaptic Transmission as a Mechanism of Thalamic Deep Brain Stimulation-Induced Tremor Arrest. J Neurosci 2006;26(3):841.

114. Mohan UR, Watrous AJ, Miller JF, et al. The effects of direct brain stimulation in humans depend on frequency, amplitude, and white-matter proximity. Brain Stimulat 2020;13(5):1183–95.

115. Anthofer J, Steib K, Fellner C, Lange M, Brawanski A, Schlaier J. The variability of atlas-based targets in relation to surrounding major fibre tracts in thalamic deep brain stimulation. Acta Neurochir (Wien) 2014;156(8):1497–504.

116. Fenoy AJ, Schiess MC. Comparison of tractography-assisted to atlas-based targeting for deep brain stimulation in essential tremor. Mov Disord 2018;33(12):1895–901.

117. Muller J, Alizadeh M, Matias CM, et al. Use of probabilistic tractography to provide reliable distinction of the motor and sensory thalamus for prospective targeting during asleep deep brain stimulation. J Neurosurg 2022;136(5):1371–80.

118. Groppa S, Herzog J, Falk D, Riedel C, Deuschl G, Volkmann J. Physiological and anatomical decomposition of subthalamic neurostimulation effects in essential tremor. Brain 2014;137(1):109–21.

119. Elble RJ. Mechanisms of deep brain stimulation for essential tremor. Brain 2014;137(1):4–6.

120. Barbe MT, Reker P, Hamacher S, et al. DBS of the PSA and the VIM in essential tremor: A randomized, double-blind, crossover trial. Neurology 2018;91(6):e543–50.

121. Al-Fatly B, Ewert S, Kübler D, Kroneberg D, Horn A, Kühn AA. Connectivity profile of thalamic deep brain stimulation to effectively treat essential tremor. Brain 2019;142(10):3086–98.

122. Schaltenbrand G, Wahren W, Hassler RG. Atlas for stereotaxy of the human brain. 2nd rev. and enl. Stuttgart: Thieme; 1977.

123. Krishna V, Sammartino F, Agrawal P, et al. Prospective Tractography-Based Targeting for Improved Safety of Focused Ultrasound Thalamotomy. Neurosurgery 2018;84(1):160–8.

124. Johnson KA, Duffley G, Anderson DN, et al. Structural connectivity predicts clinical outcomes of deep brain stimulation for Tourette syndrome. Brain 2020;143(8):2607–23.

125. Okromelidze L, Tsuboi T, Eisinger RS, et al. Functional and Structural Connectivity Patterns Associated with Clinical Outcomes in Deep Brain Stimulation of the Globus Pallidus Internus for Generalized Dystonia. Am J Neuroradiol 2020;41(3):508–14.

126. Li N, Baldermann JC, Kibleur A, et al. A unified connectomic target for deep brain stimulation in obsessive-compulsive disorder. Nat Commun 2020;11(1):3364.

127. Tian Q, Wintermark M, Jeffrey Elias W, et al. Diffusion MRI tractography for improved transcranial MRI-guided focused ultrasound thalamotomy targeting for essential tremor. NeuroImage Clin 2018;19:572–80.

128. Krishna V, Sammartino F, Rabbani Q, et al. Connectivity-based selection of optimal deep brain stimulation contacts: A feasibility study. Ann Clin Transl Neurol 2019;6(7):1142–50.

129. Hong JH, Son SM, Jang SH. Identification of spinothalamic tract and its related thalamocortical fibers in human brain. Neurosci Lett 2010;468(2):102–5.

130. Huang H, Zhang J, van Zijl PCM, Mori S. Analysis of noise effects on DTI-based tractography using the brute-force and multi-ROI approach. Magn Reson Med 2004;52(3):559–65.

131. Wakana S, Caprihan A, Panzenboeck MM, et al. Reproducibility of quantitative tractography methods applied to cerebral white matter. NeuroImage 2007;36(3):630–44.

132. Akram H, Dayal V, Mahlknecht P, et al. Connectivity derived thalamic segmentation in deep brain stimulation for tremor. NeuroImage Clin 2018;18:130–42.

133. Patriat R, Cooper SE, Duchin Y, et al. Individualized tractography-based parcellation of the globus pallidus pars interna using 7T MRI in movement disorder patients prior to DBS surgery. NeuroImage 2018;178:198–209.

134. Middlebrooks EH, Tuna IS, Almeida L, et al. Structural connectivity–based segmentation of the thalamus and prediction of tremor improvement following thalamic deep brain stimulation of the ventral intermediate nucleus. NeuroImage Clin 2018;20:1266–73.

135. Behrens TEJ, Johansen-Berg H, Woolrich MW, et al. Non-invasive mapping of connections between human thalamus and cortex using diffusion imaging. Nat Neurosci 2003;6(7):750–7.

136. Lenglet C, Abosch A, Yacoub E, De Martino F, Sapiro G, Harel N. Comprehensive in vivo Mapping of the Human Basal Ganglia and Thalamic Connectome in Individuals Using 7T MRI. PLoS ONE 2012;7(1):e29153.

137. Wang Q, Akram H, Muthuraman M, et al. Normative vs. patient-specific brain connectivity in deep brain stimulation. NeuroImage 2021;224:117307.

138. Coenen VA, Schlaepfer TE, Bewernick B, et al. Frontal white matter architecture predicts efficacy of deep brain stimulation in major depression. Transl Psychiatry 2019;9(1):197.

139. Baldermann JC, Melzer C, Zapf A, et al. Connectivity Profile Predictive of Effective Deep Brain Stimulation in Obsessive-Compulsive Disorder. Biol Psychiatry 2019;85(9):735–43.

140. Liebrand LC, Caan MWA, Schuurman PR, et al. Individual white matter bundle trajectories are associated with deep brain stimulation response in obsessive-compulsive disorder. Brain Stimulat 2019;12(2):353–60.

141. Choi KS, Riva-Posse P, Gross RE, Mayberg HS. Mapping the “Depression Switch” During Intraoperative Testing of Subcallosal Cingulate Deep Brain Stimulation. JAMA Neurol 2015;72(11):1252.

142. Riva-Posse P, Choi KS, Holtzheimer PE, et al. Defining Critical White Matter Pathways Mediating Successful Subcallosal Cingulate Deep Brain Stimulation for Treatment-Resistant Depression. Biol Psychiatry 2014;76(12):963–9.

143. Boccard SGJ, Fernandes HM, Jbabdi S, et al. Tractography Study of Deep Brain Stimulation of the Anterior Cingulate Cortex in Chronic Pain: Key to Improve the Targeting. World Neurosurg 2016;86:361-370.e3.

144. Fernandes HM, Van Hartevelt TJ, Boccard SGJ, et al. Novel fingerprinting method characterises the necessary and sufficient structural connectivity from deep brain stimulation electrodes for a successful outcome. New J Phys 2015;17(1):015001.

145. Horn A, Reich M, Vorwerk J, et al. Connectivity Predicts deep brain stimulation outcome in Parkinson disease: DBS Outcome in PD. Ann Neurol 2017;82(1):67–78.

146. Anderson JS, Dhatt HS, Ferguson MA, et al. Functional Connectivity Targeting for Deep Brain Stimulation in Essential Tremor. Am J Neuroradiol 2011;32(10):1963–8.

147. Saenger VM, Kahan J, Foltynie T, et al. Uncovering the underlying mechanisms and whole-brain dynamics of deep brain stimulation for Parkinson's disease. Sci Rep 2017;7(1):9882.

148. Knight EJ, Testini P, Min H-K, et al. Motor and Nonmotor Circuitry Activation Induced by Subthalamic Nucleus Deep Brain Stimulation in Patients With Parkinson Disease. Mayo Clin Proc 2015;90(6):773–85.

149. Gibson WS, Jo HJ, Testini P, et al. Functional correlates of the therapeutic and adverse effects evoked by thalamic stimulation for essential tremor. Brain 2016;139(8):2198–210.

150. Horn A, Wenzel G, Irmen F, et al. Deep brain stimulation induced normalization of the human functional connectome in Parkinson's disease. Brain 2019;142(10):3129–43.

151. Kahan J, Urner M, Moran R, et al. Resting state functional MRI in Parkinson's disease: the impact of deep brain stimulation on 'effective' connectivity. Brain 2014;137(4):1130–44.

152. Mueller K, Jech R, Růžička F, et al. Brain connectivity changes when comparing effects of subthalamic deep brain stimulation with levodopa treatment in Parkinson's disease. NeuroImage Clin 2018;19:1025–35.

153. In M-H, Cho S, Shu Y, et al. Correction of metal-induced susceptibility artifacts for functional MRI during deep brain stimulation. NeuroImage 2017;158:26–36.

154. van Hartevelt TJ, Cabral J, Deco G, et al. Neural Plasticity in Human Brain Connectivity: The Effects of Long Term Deep Brain Stimulation of the Subthalamic Nucleus in Parkinson's Disease. PLoS ONE 2014;9(1):e86496.

155. Albano L, Agosta F, Basaia S, et al. Functional connectivity in Parkinson's disease candidates for deep brain stimulation. Npj Park Dis 2022;8(1):4.

156. Younce JR, Campbell MC, Hershey T, et al. Resting-State Functional Connectivity Predicts STN DBS Clinical Response. Mov Disord 2021;36(3):662–71.

157. Shang R, He L, Ma X, Ma Y, Li X. Connectome-Based Model Predicts Deep Brain Stimulation Outcome in Parkinson's Disease. Front Comput Neurosci 2020;14:571527.

158. Whone A, Luz M, Boca M, et al. Randomized trial of intermittent intraputamenal glial cell line-derived neurotrophic factor in Parkinson's disease. Brain 2019;142(3):512–25.

159. Christine CW, Bankiewicz KS, Van Laar AD, et al. Magnetic resonance imaging–guided phase 1 trial of putaminal *AADC* gene therapy for Parkinson's disease. Ann Neurol 2019;85(5):704–14.

160. Nutt JG, Curtze C, Hiller A, et al. Aromatic L-Amino Acid Decarboxylase Gene Therapy Enhances Levodopa Response in Parkinson's Disease. Mov Disord 2020;35(5):851–8.

161. O'Donnell LJ, Suter Y, Rigolo L, et al. Automated white matter fiber tract identification in patients with brain tumors. NeuroImage Clin 2017;13:138–53.

162. Zhang W, Olivi A, Hertig SJ, van Zijl P, Mori S. Automated fiber tracking of human brain white matter using diffusion tensor imaging. NeuroImage 2008;42(2):771–7.

163. Fryback DG, Thornbury JR. The Efficacy of Diagnostic Imaging. Med Decis Making 1991;11(2):88–94.

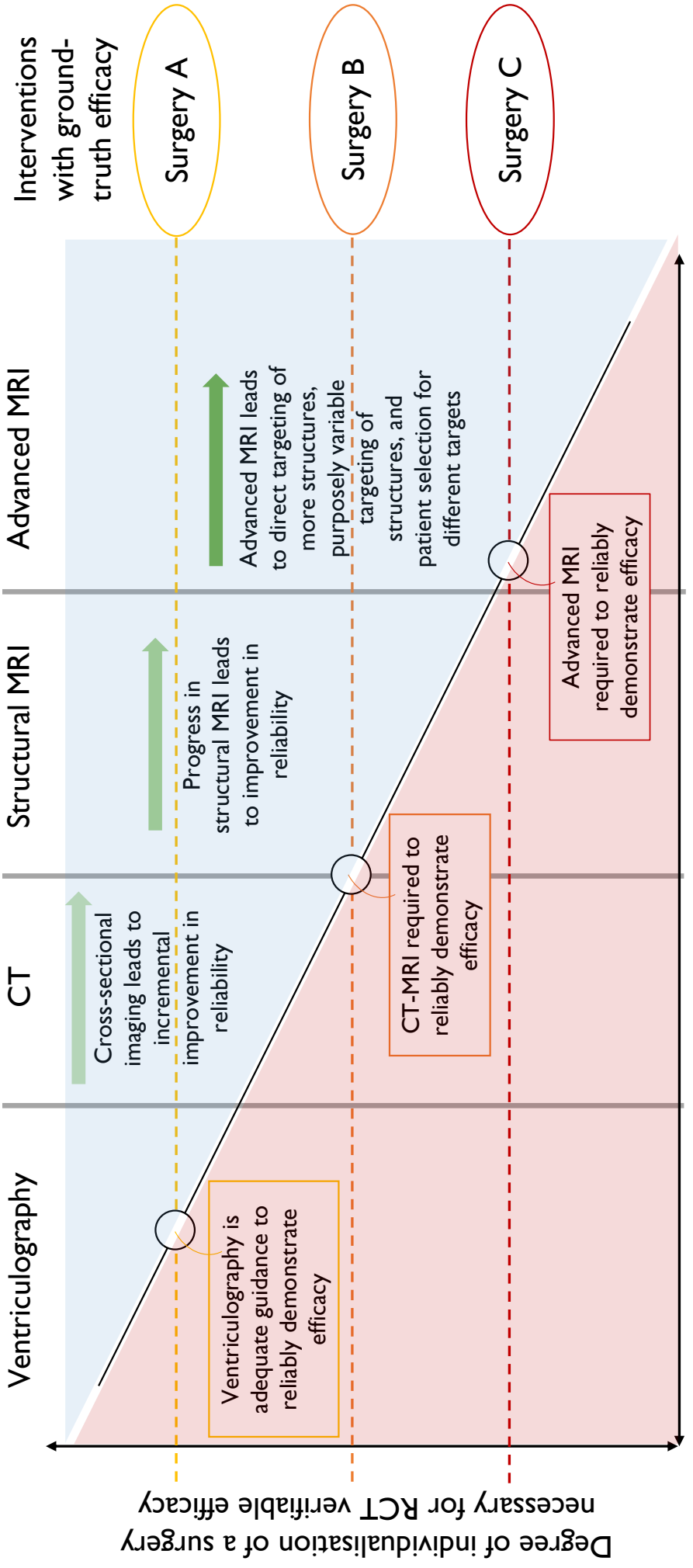

Figure I. **Proposed relationship between advances in neuroimaging and the ability to demonstrate efficacy of stereotactic surgeries by group analysis.** Diagonal line is a simplistic representation of the improvements in targeting afforded by new imaging modalities and their refinement. Randomised controlled trials (RCTs) carried out prematurely under inappropriate imaging guidance (y-value below diagonal – in the red) leads to Type II error, despite improvements in individual patients which may be demonstrable by N-of-1 studies.

I had pulled my mask up to cover my nose and mouth. His covered mouth only.

~

Wilder G. Penfield

CHAPTER 2: PARKINSONIAN GAIT FREEZING AND IMBALANCE

ABSTRACT

Parkinson's disease (PD) dominated by gait freezing and associated falls is rare, but severely debilitating and resistant to standard treatments. Studies in a macaque model of PD identified deep brain stimulation of the pedunculopontine nucleus as a promising surgical procedure for the treatment of Parkinsonian gait and balance dysfunction. It has, however, produced mixed clinical results that are poorly understood. I used tractography with the aim to rationalise this heterogeneity. A cohort of eight patients with postural instability and gait disturbance (PD subtype) underwent pre-operative structural and diffusion MRI, then progressed to deep brain stimulation targeting the pedunculopontine nucleus. Pre-operative and follow-up assessments were carried out using the Gait and Falls Questionnaire and Freezing of Gait Questionnaire. Probabilistic diffusion tensor tractography was carried out between the stimulating electrodes and both cortical and cerebellar regions of a priori interest. Structural connectivity between stimulating electrode and precentral gyrus ($r = 0.81$, $p = 0.01$), Brodmann areas 1 ($r = 0.78$, $p = 0.02$) and 2 ($r = 0.76$, $p = 0.03$) were correlated with clinical improvement. A negative correlation was also observed for the superior cerebellar peduncle ($r = -0.76$, $p = 0.03$). Both motor and sensory structural connectivity of the stimulated surgical target characterises the clinical benefit, or lack thereof, from surgery. In what is a challenging region of brainstem to effectively target, these results provide insights into how this can be better achieved. The mechanisms of action are likely to have both motor and sensory components, commensurate with the probable nature of the underlying dysfunction.

2.1 PARKINSON'S DISEASE AND GAIT FREEZING

2.1.1 Parkinson's disease pathophysiology

Parkinson's disease (PD) describes a neurodegenerative process that encompasses a broad spectrum of patient symptomatology, with shared underlying features. While the cardinal symptoms are tremor, rigidity, akinesia, and postural instability, the symptom profile individuals are burdened with varies widely beyond this description. In addition, the underlying proteopathy (synucleinopathy) is shared with other disorders, namely PD dementia, Lewy body dementia and multiple system atrophy. PD is twice as common in men than women. It is most commonly diagnosed in the seventh decade preceded by a symptomatic prodrome and asymptomatic pathology, likely spanning many decades. Early symptoms typically include hyponosmia, sleep disturbance (typically 'rapid eye movement sleep disorder'), depression, and constipation. The pathological hallmark is dopaminergic cell loss in the substantia nigra pars compacta (SNpc), and the corresponding characteristic motor and non-motor symptoms that arise due to the loss of this input to the corpus striatum. However, PD is not solely a mesencephalic dopamine disease: pathological survey reveals a diffuse, neurodegenerative illness, bilateral and asymmetric.[1,2] A range of neurotransmitter systems are compromised, including serotonergic, noradrenergic, and cholinergic, among others. Pathology is progressive, selective, and widespread in both the central and peripheral nervous systems, where the enteric nervous system, olfactory bulb, and the medulla oblongata are thought to be damaged first.[3] Reflecting this observation, the retrograde prion-like spread of alpha-synuclein from the gut is established as a credible theory in the pathogenesis of PD.[4] More recently, a cortico-striatal pathogenic mechanism has emerged as a parallel process or adjunct to this theory.[5] Lewy bodies occur centrally and peripherally in both parasympathetic and sympathetic arms of the autonomic nervous system.[6]

Corresponding autonomic dysfunction is common (particularly cardiac sympathetic denervation), may present early, and can become severe as the disease progresses.[4] Although a classic 'movement disorder', non-motor symptoms in PD can contribute most to disability, particularly late in the disease course.[7] Cognitive decline usually manifests late, with dementia characteristic of end-stage disease.[8] The manifestation of different clinical phenotypes is plausibly attributed to different patterns of Lewy pathology and neuronal degeneration in individuals, although robust evidence of this is often lacking.

2.1.2 Gait freezing and postural instability

Freezing of gait (FoG) is a mysterious and heterogenous phenomenon, broadly defined as "brief, episodic absence or marked reduction of forward progression of the feet despite the intention to walk."[9] It remains poorly understood and may be a manifestation of different underlying dysfunctional processes. FoG can arise as part of a secondary movement disorder resulting from cortical, basal ganglia, or brain stem lesions.[10] In PD, FoG is common in advanced disease but, rarely, can be a principally morbid motor symptom in early disease. Clinically, it may involve the feeling of feet being stuck to the floor, trembling of the legs in place, and precipitation or relief by a range of curious cues and cognitive circumstances. Most notable of these are the relationship of FoG with spaces such as doorways[11] and emotion/excitement, the former which acts as a precipitant, the latter as a reliever. In PD, FoG is associated with disease severity,[12] does not correlate with classically dopamine responsive cardinal symptoms (tremor, bradykinesia, rigidity) but does correlate with midline symptoms such as postural instability.[13] Furthermore, while FOG is usually improved by L-DOPA, and further improved by MAO-B inhibitors, it is more resistant than other motor symptoms and in some patients FoG is not improved or even elicited by dopamine

replacement.[14] As such, the profile of this symptom stimulates the possibility that non-dopaminergic signalling plays an important role, which would necessarily implicate nuclei other than the SNc. Five main hypotheses are available to explain FoG, although they are not necessarily exclusive and may not be universal between patients. These include abnormal gait pattern generation, a problem with central drive and automaticity of movement, frontal and executive dysfunction, perceptual malfunction, and abnormal coupling of posture with gait.[9]

Achieving bipedal balance is profoundly non-trivial, requiring integration of multiple afferent signals including vestibular, visual, somatosensory, and proprioceptive information. Complicated and appropriate efferent motor programs must then be delivered to effective musculoskeletal apparatus, and repeatedly updated based on new sensory information to place the body's centre of mass over its support base during movement (dynamic balance) or when stationary (static balance). Central imbalance has a range of aetiologies, for example, cerebellar, vestibular, and general cognitive impairment. Imbalance leading to falls in PD is certainly heterogeneous with different neurological and mechanical factors playing important roles in different patients. For example, simple biomechanical factors such as stooped posture and musculoskeletal deterioration will be detrimental to balance. Bradykinesia and rigidity can cause balance impairment, for example, by inhibiting appropriate automated postural responses to externally applied perturbations to the body. It prevents the dynamic coordination of synergistic muscles required to maintain balance from postural perturbations, with co-contraction of muscles across joints. In late disease, impaired proprioception, executive dysfunction, limited postural set, and lack of automaticity predominate. On this complicated backdrop, FoG is recognised as the most common proximal

cause of falls.[15] Such falls are commonly injurious and can result in fractures with potentially major sequelae.

Recognition of the large clinical spectrum of PD has led to the attribution of subtypes. In 1990 two contrasting subtypes emerged from a baseline analysis of the American DATATOP cohort: tremor dominant (TD) PD and postural instability and gait disturbance (PIGD) PD.[16] The development of gait freezing and balance problems (and also speech problems) are strongly associated,[13] from which clinical validity for the PIGD subtype is drawn. Nonetheless, its legitimacy has been challenged.[17] The concept has been destabilised by the finding that freezing of gait and balance problems have different demographic, non-motor, and genetic predictors,[18] alluding to an important distinction. In addition, data driven cluster analyses fail to locate the PIGD subtype.[19] Instead early onset, rapidly progressive, TD, and non-TD (NTD) subtypes are found. The NTD subtype is associated with a greater cortical burden of Lewy bodies,[20] which would likely include PIGD patients, if they were so classified. This is commensurate with the higher level of cognitive impairment that has been observed in NTD and PIGD. Similarly, the PIGD subtype has been associated with greater cortical atrophy. Regardless of the distinction between NTD and PIGD, there are a small subgroup of patients whose motor morbidity is dominated by severe gait freezing and imbalance leading to falls.

2.2 DEEP BRAIN STIMULATION TARGETED TO THE PEDUNCULOPONTINE NUCLEUS

The results of deep brain stimulation (DBS) of the subthalamic nucleus (STN) or the internal pallidum (GPi) have demonstrated less dramatic effects on FoG than cardinal motor symptoms. Specifically, STN DBS typically leads to modest improvement in L-DOPA responsive

FoG,[21] and can alleviate L-DOPA induced FoG. However, it may also generate new FoG in a non-trivial proportion of patients.[22] More specifically, it appears that benefits are greater with middle frequency (60 Hz) stimulation, whereas the benefits are attenuated and then reversed with increasing voltage of the high frequency (130 Hz) stimulation typically used in STN DBS for PD.[23] Further important observations regarding the role of the STN include the characterisation of FoG by low-frequency (4-13 Hz) STN-cortical decoupling in the less striatal-dopamine replete hemisphere,[24] and the improvement of FoG with dopamine and noradrenaline reuptake inhibition via methylphenidate in patients receiving STN DBS.[25] The effect of GPi DBS on FoG has not been explicitly studied. While it does typically lead to a modest improvement in PIGD symptom scores,[26] this is unlikely to be due to improvement in FoG, and indeed FoG may emerge following stimulation.[27] As such, STN or GPi DBS are unsuitable for both the ~5% of patients with early and severe gait freezing refractory to medications and the dominant source of motor disability,[13] and the patients where refractory gait disorders predominate in advanced disease.[12] Stimulation of the brainstem has attracted considerable interest in attempts to meet this problem, as well as when FoG emerges following GPi or STN DBS.

Numerous lines of evidence point to a region in the upper brainstem that is involved in gait initiation and FoG. During the 20th century, the mesencephalic locomotor region (MLR) was identified and explored following the observation that locomotion could be induced through stimulation of the ventrolateral upper brainstem in the decerebrate, precollicular cat.[28–30] This region corresponds to the pedunculopontine nucleus (PPN) and its environs. In man, lesions of this region have also implicated it in gait. A rare case of small bilateral infarcts of the pons, restricted to the PPN region, was reported as presenting with FoG.[31] Also, a rare

case of unilateral pontomesencephalic haemorrhage involving the PPN region is reported as presenting with a failure to initiate gait, particularly contralateral to the lesion.[32] Indeed, the majority of published lesions causing FoG are in the upper ventral brainstem.[10] Severity of balance and gait symptoms correlate with cholinergic deficits,[33,34] signalling that degenerating cholinergic nuclei, such as the PPN, may have a role.[1,35,36] Ultimately, the possibility of targeting the PPN for PD treatment was propelled by the demonstration of akinesia improvement in the 1-methyl 4-phenyl 1,2,3,6-tetrahydropyridine (MPTP) monkey model of PD through a) microinjection of the GABA antagonist bicuculine,[37] and b) low frequency electrical stimulation,[38] both independent of dopaminergic mechanisms.[39] Subsequently, both neurophysiological and functional imaging experiments have confirmed the crucial role of the PPN in control of locomotion, with different regions of the PPN involved in different aspects.[40–42] However, its environs, most notably the cuneiform nucleus (Cnf), also facilitate aspects of gait,[40] complicating the functional interpretation of this region and interventions targeted there.

Despite the primate research being carried out in Oxford, DBS of the PPN in man was first reported in 2005 by the Bristol (lone bilateral PPN) and Toronto (dual bilateral PPN-STN) groups.[43,44] Subsequently, neurosurgery centres have reported mixed and complicated clinical results from DBS targeting the PPN in PD (see Table 1),[45–48] which are difficult to parse and synthesise into a comprehensive understanding. Ultimately, the clinical results have been modest and disappointing overall, and have not led to a clinically impactfully procedure in the same way as, for example, DBS to the STN has. The reasons for this are likely multiple, with the clinical experience of this procedure highlighting a number of surgical and academic challenges. Nonetheless, it is clear at least that stimulation of the PPN region (ventrolateral

pontine tegmentum) can alter aspects of gait and balance in some patients.[49,50] While PPN DBS was originally proposed as a treatment in PD for gait ignition failure and FoG,[38] the indications for surgery and subsequent primary clinical assessment usually includes the full gamut of PD gait and balance symptoms (or otherwise termed axial symptoms). These are typically assessed under the gait, balance, and freezing elements of the Unified Parkinson's Disease Rating Scale (UPDRS) II and the gait and postural instability elements of UPDRS III.[51] These are all ordinal scales with five ranks, which as metrics lack detail and sensitivity to change (authors that use them acknowledge their weakness in assessing PD gait and FoG)[48], but may be appropriate to capture clinically relevant differences. The Rating Scale for Gait Evaluation (RSGE) is sometimes used and offers a broad evaluation of gait disturbance in PD but without in depth attention to FoG.[52] FoG itself is difficult to measure objectively in the clinic, partly due to its fluctuating nature. The best practical metric is probably the FoG component (6 questions, 24 points) of the Gait and Falling Questionnaire (GFQ).[53] Many other aspects of gait and balance can be measured, such as aspects of postural sway[54] and biomechanical parameters of gait initiation.[50] It is likely that numerous brainstem regions coordinate this range of gait and balance functions, and the PPN is unlikely to be the crucial dysfunctional node in all cases where some form of axial dysfunction is present. Indeed, authors have suggested that patients with predominant FoG in the absence of other major gait and balance disturbance may be the most appropriate candidates for PPN DBS.[45]

The ventrolateral pontine tegmentum up to the mesopontine junction, where the PPN resides, is anatomically compact and difficult to target. Large lateral ventricles, typical of the atrophied brain seen in these patients, can make viable trajectories quite limited, and there remains no consensus on where to identify and target the PPN from MRI scans,[55] despite

pronouncements from some authors.[56] It would also seem inevitable that DBS macroelectrodes targeted towards the PPN will, in some cases, end up primarily in other nuclei, and also that stimulation will spread to other areas of putative importance in gait. When a stereotactic surgery is performed, directed at a particular target, the question can always be asked "where did the electrode end up?". What naturally follows from this are the questions: "What are the limits of certainty on attribution of anatomical nomenclature?", and "By what parameters can such an attribution be made?". Indeed, authors often acknowledge this uncertainty in reporting their results, finding it hard to honestly report that therapeutic electrodes are in the PPN or other nuclei.[45] All this uncertainty provides context for interpreting the highly mixed clinical results of PPN DBS; some studies report improvement in FoG,[46,57] others report improvement in falls,[48] other groups report improvement in balance,[54] and individual patients within cohorts have shown convincing improvements in different parameters under double-blinded assessment.[45,48] Of note, these reports do indeed highlight different therapeutic locations (e.g. caudal PPN versus rostral PPN/cuneiform), which would unsurprisingly point to stimulation in different locations of the ventrolateral pontine tegmentum giving different effects.

Returning to FoG, the caudal PPN appears to be the target of choice[46] and seems to act by relieving a block to pre-prepared movement.[58] Although, due to uncertainty in localisation, the proximity of the caudal PPN to the locus coeruleus raises the possibility that effects could be attributed to the latter, in view of the noradrenergic hypothesis of FoG espoused by some.[25,59,60] Nonetheless, FoG is an episodic phenomenon and as such it would make sense for treatment to be delivered in an adaptive (otherwise termed closed-loop) fashion, delivering stimulation on freezing, reminiscent of initiating locomotion in the decerebrate

cats through stimulation of the MLR. Indeed, this was proposed by Beudel and Brown in 2016[61] following the observation of low frequency (5-12Hz) PPN region activity as a putative signature of FoG.[62,63] Themselves believing this signal was at 1-8Hz,[64] this was later attempted in Florida by Molina et al. where standard bilateral GPi stimulation was supplemented by closed-loop bilateral PPN stimulation, regulated by detection of increased 1-8Hz power at the site of implantation.[65] Their results were promising, in so far that three of five patients had very significant improvement in FoG, however, two patients deteriorated. Such an approach requires further investigation, as well as the possibility of kinematically driven closed-loop stimulation. Standard PPN DBS alongside DBS at other nuclei has also been explored in order to improve FoG, as an otherwise resistant symptom to treatment. This includes concomitant stimulation of the STN,[47] the zona incerta,[66,67] and the GPi.[68] Although the possibility of counteracting or confounding therapeutic effects of PPN DBS with this strategy should be considered, all these studies reported additive improvement through dual stimulation, highlighting this as a serious clinical option for patients with the appropriate motor symptom profile. An alternative approach to accessing the PPN is to modulate an important input nucleus to the PPN. The major subcortical input to the PPN arises from the GPi and the substantia nigra pars reticulata (SNpr),[69] with the effect of GPi DBS already having been commented on. The PPN is under direct inhibitory GABA-ergic tone from the SNpr,[70–73] and with SNpr overactivity being characteristic of PD, it would seem reasonable that SNpr stimulation at the appropriate frequency would be able to drive or reduce this tone on the PPN, with the possibility of reducing FoG. This was first explored by Chastan et al. who revealed that SNpr DBS improves axial motor symptoms (assessed globally) as well as some aspects of gait initiation, although FoG was not examined explicitly.[74] Weiss et al., acknowledging the evidence for the role of the PPN in FoG, also pursued this

neuromodulation strategy of targeting SNpr with the aim of modulating descending nigropontine neurons.[75] They used bilateral dual nigral-STN DBS with a 'two-birds-one-stone' technique, the SNpr lying caudally adjacent to the STN. They used interleaved high frequency (125Hz) pulses and specifically demonstrated additional improvement in FoG with combined stimulation, whereas postural control and axial motor function more globally were unchanged compared to lone STN stimulation.

In summary, it remains unknown why the PIGD symptoms, and FoG specifically, of some patients improve with treatment, and with others it does not. There is a lack of consensus on where and how to target the PPN, with a range of anatomical and imaging factors as well as variability of the brain stem between different patients compounding the challenge. This problem of uncertainty and inconsistency in electrode location likely contributes to observed variability in outcomes. Although stimulation of the PPN region may improve a range of axial symptoms, indication for PPN DBS per se, and therefore patient candidacy, should probably be restricted to severe FoG and associated falls (not associated with dopamine withdrawal) and in the absence of other major refractory gait abnormalities. The scoring systems for FoG are used inconsistently between studies, and their weaknesses in capturing changes in FoG may explain some negative findings. There is no consensus on whether unilateral or bilateral implantation should be the preferred approach. Although studies have been performed across a wide low-to-middle frequency range, stimulation at lower frequencies has become preferred,[76,77] with the prospect of closed-loop stimulation in its infancy. A comprehensive clinical review can be found by the Movement Disorders Society PPN DBS Working Group.[78]

Table 1. Freezing of gait outcomes from DBS to the pedunculopontine nucleus in Parkinson's Disease.

Authors	Year	Centre	Uni or bilateral	Hz	N	Outcomes	Metrics
Plaha et al.[44]	2005	Bristol	Bilateral	20-25	2	Both improved in short term.	UPDRS-PIGD, Tinetti
Mazzone et al.[77]	2009	Rome	Mixed	25	12	Significant improvement.	UPDRS-PIGD
Moro et al.[48]	2010	Toronto	Unilateral	50-70	6	No significant difference under double blind assessment	UPDRS-PIGD
Ferraye et al.[45]	2010	Grenoble	Bilateral	15-25	6	Small significant improvement in off-drug, not on-drug condition under double blind assessment	UPDRS-PIGD, GFQ
Thevathasan et al.[46]	2011	Brisbane	Bilateral	35	5	Significant improvement. All patients improved.	UPDRS-PIGD, GFQ
Welter et al.[50]	2015	Paris	Bilateral	20-40	4	All improved	UPDRS-PIGD, RSGE
Mestre et al.[79]	2016	Toronto	Unilateral	60-70	6	Significant improvement in off-drug, not on-drug condition under double blind assessment at 2 years but not 4 years.	UPDRS-PIGD

2.3 SURGICAL ANATOMY OF THE VENTROLATERAL PONTINE TEGMENTUM

The ventrolateral pontine tegmentum is a cytoarchitecturally and functionally complex region, leading to varying accounts of parcellation and nomenclature. The PPN[80,81] or pedunculopontine tegmental nucleus (PPTg)[82] divided into compacta and dissipata subnuclei has more recently been revised to three nuclei: the pedunculotegmental nucleus (PTg),

isthmic reticular formation (isRt) and the retroisthmic nucleus (RIs).[83] At the caudal pole of this complex, the thin ventrolateral tegmental area (VLTg) separates the RIs from the medial lemniscus, and continues caudally as a larger structure than previously described.[82,83] The PPN itself is not a traditional nucleus per se, but is a diffuse reticular nucleus with indistinct boundaries. The relevant atlases describing it use cytoarchitectural features that may underestimate its size. Immunohistochemical approaches suggest it may indeed be better defined with greater caudal extension.[84,85]

The SCP is found closely adjacent, essentially medial to the PPN; this relationship is reflected in the naming of the PPN. It is medioventral rostrally and transitions to mediodorsal caudally, with cells of the pars dissipata (rostral) intermingled with SCP fibres. While the caudal portion of the PPN is medially bounded exclusively by the SCP, at its rostral end, it is medially bordered by the central tegmental tract (CTgT), with close proximity to the mamillotegmental tract, para/trochlear nuclei, and medial longitudinal fasciculus. The spinothalamic tract (STT) is found laterally to the PPN, the lateral lemniscus (LL) is found dorsolaterally, and the ML is found ventrolaterally, where it separates the PPN from the SN at its rostral pole. The rostral portion of the PPN is bounded dorsally and dorsomedially by the CnF, and ventrally by the retrorubral fields. The caudal pole of the PPN is in close proximity to the lateral parabrachial nuclei.

The relationships described above demonstrate how anatomically congested this region is, and how stereotactic targeting is destined to be challenging. It also points to side effects of stimulation that are to be expected with increasing voltage of stimulation or slight misplacement. These include paraesthesias (ML, STT), buzzing (LL), oscillopsia (ocular nuclei),

autonomic dysfunction (CTgT), as examples. Acknowledging the distance from the PPN from the bicommissural plane and large non-linear inter-individual variation in brain stem anatomy, achieving accurate a reliable targeting of this region is a daunting prospect. This difficulty likely contributes to variation in outcomes between centres and within centres. Our group implants and stimulate more caudally than most groups,[46] simply on the empirical grounds of our own experience that such stimulation is more effective. However, the lack of consensus on what to target in the PPN region (e.g. rostral versus caudal versus CnF) and how such targeting should be both defined and appraised, is important to acknowledge.

2.4 NEUROIMAGING OF THE PEDUNCULOPONTINE NUCLEUS

Neuroimaging of the PPN is challenging due to anatomical features described above, such as cell density, which manifest as low grey-white matter contrast in the region. Imaging of the PPN, like other deep brain nuclei, is also somewhat technically handicapped due to the relatively longer distances from the MR receiver array, compared to cortex. A method was proposed by Zrinzo et al. where the possibility of using a 1.5T proton density acquisition for visualising the PPN was investigated. Despite claims that direct localisation of PPN was possible in all cases, the method has not been taken up widely and needs further validation to establish whether what is ascribed as the PPN is indeed the PPN and the PPN alone, and not another nucleus in the region. High field MP2RAGE acquisitions, known for generating good grey-white matter contrasts, have also been used,[86] and are probably superior to low field proton density if they are available.

Unique features of the PPN's location are open to exploitation in order to indirectly target the nucleus. These are primarily the PPN's proximity to major white matter tracts, which are easily discernible with diffusion MRI due to their high fractional anisotropy (FA). The application of the diffusion tensor model and visualising the principle diffusion directions delineates the SCP clearly, and has been proposed as an anatomical landmark from which the location of the PPN could be estimated.[87] Similarly, FA contrast has been proposed as useful for locating the PPN, with its feasibility demonstrated and validated in a post-mortem human brain.[88] Another alternative leveraging diffusion MRI is a deterministic tractography-based approach. This involves reconstructing the SCP, spinothalamic tract, and medial lemniscus, in order to help triangulate the PPN and demarcate a viable surgical corridor.[86] This process could be feasibly automated. Bianciardi et al. have developed and validated a probabilistic atlas of the mesopontine tegmentum.[89] This is publicly available and based on the combination of 7T diffusion MRI-derived FA contrast and T2-weighted MRI contrast. The template delineates five nuclei in the region: CnF, PTg, oral pontine reticular, paramedian raphe, and caudal linear raphe. This is designed for co-registration to standard structural MRI scans, which could be helpful in targeting the PPN. Alternatively, if comparable high resolution MRI data was required, the same semi-automated process they used to generate the atlas could be used in individual PPN DBS patients. In summary, while the ventrolateral pontine tegmentum is a challenging brain region to image, the high spatial contrast in its diffusion properties indicate that individualised diffusion tractography data may have utility in surgical targeting and assessing surgery to the PPN.

2.5 EXPERIMENTAL WORK WITH PATIENT-SPECIFIC STRUCTURAL CONNECTOMES - see

***Journal of Neural Transmission*, Volume 128, Issue 5, 2021, Pages 659-70 for associated published manuscript**

The reasoning for the employment of diffusion MRI in DBS is three-fold, a) stimulation is likely to modulate the functioning of regions with which it is structurally connected, b) regional anatomy can be 'fingerprinted' by its connectivity profile, giving an individualised (non-atlas based) approach to identifying targets not readily discernible from imaging contrast, and c) connectivity estimates between known regions can give insights into individual pathology and evolution of disease. Given the current uncertainties concerning PPN DBS, connectomic data is therefore highly relevant. Current data are limited to PPN tractography in healthy individuals,[90] and single DBS cases,[91] leaving questions relating to clinical outcomes unaddressed. I have therefore used structural and diffusion MRI in a series of PIGD-PD patients who underwent DBS targeting the PPN in order to understand the relationship between tractography-based structural connectivity estimates of stimulation in the ventrolateral pontine tegmentum, and clinical outcomes following surgery. I followed up implications of the results by analysing relevant regions of cortical thickness with respect to pre-operative symptom severity, as an indicator of atrophy.

2.5.1 Methods

2.5.1.1 Patients and deep brain stimulation

Between 2010 and 2012, eight consecutive patients (all male) with severe, medically refractory PIGD-PD were scheduled for implantation of bilateral electrodes (Medtronic 3887/89) in the PPN, undergoing surgery as described elsewhere[46] at the John Radcliffe Hospital. Briefly, we aim just lateral to the horizontal superior cerebellar decussating fibres in the pons. Respecting the lateral ventricles, as vertical as possible a trajectory is taken with

the purpose of passing the electrode through this point along the long axis of the PPN. All patients were referred to Oxford Functional Neurosurgery, met UK PD Brain Bank criteria, and underwent assessment by a consultant neurologist, neurosurgeon, and neuropsychologist, all with expertise in movement disorders, before being offered surgical treatment.

Patients were programmed by a neuromodulation nurse experienced in movement disorders. Briefly, stimulation from all contacts was systematically explored, beginning with monopolar screening at 35 Hz, 60 μs and amplitude titrated with ceilings established by side effects (e.g. oscillopsia). Bipolar stimulation was explored for additional benefit/tolerability.

2.5.1.2 Questionnaires

The GFQ (score/64) was completed by patients pre-operatively and at 1-2 year follow-up.[53] The GFQ, and the Freezing of Gait Questionnaire (FOGQ; score/24), a component of the GFQ, were both analysed. UPDRS data were not analysed, as the corresponding PIGD metrics were deemed too insensitive.[46,50]

2.5.1.3 Diffusion imaging acquisition and pre-processing

Pre-operative MRI was performed on a 1.5T Phillips Achieva using a modified spin echo sequence with SENSE parallel imaging. In plane resolution was 1.818 by 1.818 mm^2, and 64 2-mm thick slices were acquired in an interleaved fashion. Diffusion weighting (b = 1200 s/mm^2) was applied along 32 non-colinear gradient directions, with one non-diffusion weighted volume (b = 0). Correction for distortions and subject movement was carried out using the *FMRIB Software Library* (FSL; Oxford, UK).[92] The susceptibility-induced off-resonance field was estimated using *topup.*[92,93] Instead of using two b=0 spin-echo EPI with opposing PE-

direction, the field was estimated from a b=0 volume and a structural T2-weighted scan, without any distortions. Motion and eddy currents were corrected for using *eddy*,[94,95] with outlier detection and replacement.[96] Single shell ball and stick modelling of local diffusion parameters was carried out using BEDPOSTX, with up to two crossing fibres per voxel.[97,98]

2.5.1.4 Tractography and statistics

Probabilistic tractography was carried out using PROBTRACX with distance correction.[97,98] For each of the streamlines generated by PROBTRACX, I counted the number of seeds that reached each of the regions described below (*2.5.1.6 Termination masks*). Those counts were explored for linear relationships with clinical GFQ and FOGQ improvement (absolute) by calculating both Pearson and Spearman's rho correlations (two-tailed) in SPSS (IBM, New York). Both stimulation cathode and 'volume of activated tissue' (VAT) connectivity were averaged over left and right for each patient, then compared with the difference between pre-operative and follow-up questionnaire scores. Statistically significant relationships were assessed further by substituting relative (%) clinical improvement as the dependent variable.

2.5.1.5 Termination masks

A T1-weighted preoperative image was used to generate parcellated anatomic surfaces using Freesurfer (Harvard, USA).[99,100] T2 fluid-attenuated inversion recovery (FLAIR) images were used for pial surface optimisation. Parcellations of the white-grey matter boundary surface were utilised as masks, including the precentral gyrus and postcentral gyrus from the Desikan Kelliany Atlas,[101] as well as BA 1, 2, 3a, 3b and 6. As no supplementary motor area (SMA) parcellation was available, the Harvard-Oxford cortical atlas was used to generate a mask of the SMA, which was then registered to MRI scans using FLIRT.[102–104] The ICBM-DTI-81 white

matter labels atlas was used to generate a mask of the superior cerebellar peduncle (SCP), which was cropped to the cerebellar portion only and registered to MRI scans using FLIRT and FNIRT.[102–105]

2.5.1.6 Cathode and volume of activated tissue

Post-operative computed tomography (CT) images were registered to MRI using FLIRT.[102–104] Lead contacts were identified based on CT artefacts and array dimensions. VAT around the cathode was approximated as a sphere, calculated based on a finite element model, utilising impedance and voltage data from the DBS system acquired at follow-up.[106] VAT is based on axonal activation. However, the precise mechanisms of DBS in the PPN region are unknown. As such, the cathode contact for each lead was represented as a single diffusion voxel; single-voxel seed analysis has value as the centroid of any other effects, and for possible targeting implications. VAT masks were seeded and tracked to each termination mask. Stimulation cathode masks were seeded and tracked to precentral gyrus, BA6, SMA and SCP termination masks only. '<->' is used to denote streamlines between seed and termination mask.

2.5.1.7 PPN region

To assess whether our cathode<->SMA results were driven by the cathode's precise location, tractography from the larger PPN region was carried out. An 8 mm column (four diffusion voxels), descending from the mid-inferior collicular level, was used to represent the PPN region. Placement was reviewed and agreed on by stereotactic surgeons (doctoral supervisors: T. Aziz and A. Green). PPN region masks were seeded and tracked to the SMA termination mask only.

2.5.1.8 Electrode locations

The vertical distance between stimulating cathode and the obex was calculated from fused CT-FLAIR, then plotted against associated clinical outcomes. Leads were plotted in MNI ICBM 2009b NLIN ASYM space using Lead-DBS v2.3.[107] Coregistration was performed with FLIRT, normalisation with ANT,[108] electrode reconstruction with PaCER,[109] and plotted with nuclei from the Harvard AAN atlas[110] in Lead Group.

2.5.1.9 Cortical Thickness

Respecting both somatosensory and motor aspects of the tractography results, cortical thickness of respective functional domains were analysed as an atrophy surrogate. Mean thickness values were extracted from Freesurfer's statistical output for BA 1, 2, 3a, 3b, and 6, precentral gyrus, postcentral gyrus, supramarginal gyrus, and superior and inferior parietal regions.[111] These were subjected to correlational analysis, both unilaterally and bilaterally, with the severity of pre-operative symptoms (GFQ).[112]

2.5.2 Results

Seven of eight patients were successfully implanted with DBS electrodes bilaterally. In one patient, one electrode took an errant trajectory, was not revised or utilised, and was therefore not included due to its unsatisfactory position. Three of eight patients showed deterioration at follow up (Table 2, median = 12 mts, Q_1-Q_3: 12-16 mts). Adverse outcomes from surgery included a small subdural haematoma in patient C, post-operative confusion (Salmonella) in patient E, and a post-operative diplopia on left lateral gaze in patient F, that resolved by discharge. Side effects of stimulation that bounded stimulation parameters included oscillopsia, buzzing in head/eye/nose, tightness around head, tightening of jaw,

contralateral arm tremor, and pulling in the eye. Patient H developed a mild dysarthria associated with deep breathing, which may have been related to stimulation.

Table 2: Clinical data

Patient	Age at Surgery	Qu	Pre-op	Improvement		Follow up / mts	Long term outcome
				Absolute	%		
A	55	GFQ	55	14	25	12	Still uses at 10 years
		FOGQ	22	7	32		
B	77	GFQ	39	5	13	12	Dead 4 years after surgery
		FOGQ	22	5	23		
C	74	GFQ	22	1	5	12	Dead 3 years after surgery
		FOGQ	15	6	40		
D	56	GFQ	40	2	5	12	Dead 8 years after surgery
		FOGQ	15	2	13		
E	67	GFQ	30	-14	-47	18	Dead 4 years after surgery
		FOGQ	11	-9	-82		
F	71	GFQ	30	-8	-27	29*	Dead 4 years after surgery
		FOGQ	11	-3	-27		
G	68	GFQ	43	-3	-7	16	Revision at 18 mts, no benefit. Doesn't use.
		FOGQ	21	0	0		
H	71	GFQ	36	12	33	12	Dead 6 years after surgery
		FOGQ	13	-1	-8		

Qu = questionnaire. Pre-op = preoperative. Mts = months *Follow up delayed due to patient illness

Table 3. Stimulation parameters

Patient	Side	Frequency / Hz	Amplitude / V	Pulse width / μs
A	Left	35	2	60
	Right	35	2	60
B	Left	NA	NA	NA
	Right	35	2	60
C	Left	35	3.5	60
	Right	35	3.5	60
D	Left	35	3.5	70
	Right	35	2.8	90
E	Left	35	4	90
	Right	35	4	90
F	Left	25	4.3	70
	Right	25	4.3	70
G	Left	35	2.5	90
	Right	35	2.5	90
H	Left	35	3.8	60
	Right	35	4	60

2.5.2.1 Tractography

Under parametric analysis, VAT connectivity with four regions (precentral gyrus, SCP, BA1, BA2) demonstrated significant ($p<0.05$) relationships with clinical GFQ outcomes (Fig.1). VAT<->precentral gyrus connectivity alone demonstrated significant relationships with both GFQ and FOGQ improvement. All these survived non-parametric assessment (Fig.1). Cathode connectivity with two regions demonstrated significant parametric relationships with clinical outcomes (SCP: GFQ and FOGQ, SMA: FOGQ only), but neither FOGQ correlation reached significance under non-parametric assessment (Fig.1). The negative correlation of cathode/VAT<->SCP connectivity with GFQ improvement was not mediated by a correlation

with either SCP fractional anisotropy (FA) (r=0.01, n.s) or mean diffusivity (r=0.28, n.s). Connectivity with BA6 did not demonstrate any significant relationships with clinical improvement (GFQ. VAT: r=0.47, n.s; cathode: r=0.53, n.s), likewise between VAT and postcentral gyrus, BA3b (Fig.1), or 3a (r=0.22, n.s).

Most significant findings for absolute change in clinical outcome remained significant when assessed against relative (%) change (VAT-GFQ: precentral r=0.77, SCP r= -0.78, BA1 r=0.75, BA2 r=0.72; Cathode-GFQ: SCP r=-0.87; Cathode-FOGQ: SCP r=-0.83, SMA r=-0.90). Correlation of relative FOGQ improvement and VAT<->precentral gyrus connectivity became insignificant (r=0.69, p=0.056).

2.5.2.2 Cortical thickness

Under parametric analysis, assessed bilaterally, BA6, BA1 and the postcentral gyrus demonstrated significant ($p<0.05$) negative correlations with preoperative GFQ (Fig.2). BA2 trended to significance (p=0.06). Assessed unilaterally, on the right, only BA6 trended to significance in this regard (p=0.053). On the left, BA1, BA2, postcentral and supramarginal gyri, inferior and superior parietal regions demonstrated significant ($p<0.05$) negative correlations with preoperative GFQ (Fig.2). BA2 (p=0.06) and BA6 (p=0.07) trended to significance. No regions, assessed bilaterally, survived non-parametric testing. Left BA1, BA2, left postcentral, supramarginal, inferior parietal remained significant under non-parametric assessment, and BA3b trended to significance (p=0.07).

2.5.2.3 Electrode locations

A trend was observed for deeper stimulation being more efficacious (Fig.3). Based on exploratory 3-D reconstruction (the limitations of which should be appreciated in its interpretation), the patient having the largest benefit (Patient A) from surgery had the PPN speared along its long-axis bilaterally (Fig.4). This patient was maintained on monopolar stimulation caudal to what is considered the PPN on this atlas, and notably could be consistent with proximity to the locus coeruleus or the parabrachial nuclei. Patient B improving substantially in gait freezing and falls, had cathodic stimulation close to that of patient A, but more anterior. Patient C also improving substantially, speared the PPN along its long-axis, with stimulation delivered to the mid-rostral PPN. For patients E, F and H for whom stimulation clearly did not improve their freezing of gait, their electrodes did not track the long-axis of the PPN bilaterally and cathodic stimulation avoided the PPN and the region in continuity-caudal to it. Patient G delivered stimulation in the rostral PPN, patient F had unused contacts available in rostral to mid PPN, and patients E and H had no contacts in the PPN. The reconstruction indicated that DBS lead trajectories were less oblique for patients whose FOGQ scores had not improved at follow up (Fig.4).

2.5.3 Discussion

2.5.3.1 Electrode positions and targeting

One patient stood out amongst our small series for overt clinical improvement and patient satisfaction, maintained for many years (Patient A). On reconstruction of the electrodes, it may not be coincidental that, despite acknowledging limitations in image registration and atlas methodologies, his two leads speared the long axes of the PPN bilaterally (delivering stimulation caudally), particularly considering the spread of leads in general (Fig.4). Similar to

Mazzone et al.[113], a trend was observed for deeper stimulation being better (Fig.3). Clinically successful stimulation is, at least in our experience, delivered at the caudal PPN, or indeed caudal to what is sometimes considered to be the PPN. This raises important questions as to whether the PPN is indeed the relevant structure (e.g. in deference to VLTg), whether afferent/efferent fibres entering the caudal PPN could be the optimal target, and whether the PPN would be better considered as a longer nucleus. Mazzone et al. have identified the VLTg / RIs (ventral-caudal PPN) as a likely common location of therapeutic stimulation in their patients.[113] When considering the original lesional and stimulation primate research implicating the PPN, it is difficult to exclude the possibility that caudal structures were involved. The PPN is a diffuse reticular nucleus with indistinct boundaries, and the relevant atlases describing it use cytoarchitectural features that may underestimate its size. Immunohistochemical approaches suggest it may indeed be better defined with greater caudal extension.[84,85] In addition, the somatosensory and cerebellar tractography results (Fig.1) are suggestive of a ventrolateral tendency of effective stimulation as the PPN is bounded in that respect by the ML and spinothalamic tract, which both project strongly to the postcentral gyrus. That the caudal and rostral PPN should be distinguished is now clear. There are major chemical and structural differences, for example, GABAergic neurons are much more populous in the caudal PPN,[114] and structural connectivity with motor cortices is weaker there.[115] There is also clinical [45,46] and pre-clinical support for the caudal PPN as the preferable target for ameliorating gait disorders.[116]

In a larger series than ours, it was demonstrated that lead location within the pons did not appear to explain variance in clinical outcomes.[117] This is difficult to explain, but variation in brainstem anatomy likely plays a role. In our series, while precise location of therapeutic

cathodes differed substantively, it would appear that patients with robust improvement in their gait freezing had lead implants following more anterior-posterior oblique trajectories, consistent with the PPN long-axis (Fig.4). The other trajectories only offered the opportunity to stimulate the rostral PPN. In addition, there was a trend towards deeper stimulation being better (Fig.3).

DBS lead implantation alone can be considered a microlesion intervention along its trajectory, with accompanying peri-lead gliosis.[118,119] Step length and speed have been observed to improve after surgery, in the absence of stimulation, and so has been attributed to a lesioning effect.[50] As such, disruption of the PPN by implantation through its length could be a critical feature of successful surgery to improve gait freezing. Clearly rostral implantation/stimulation would not achieve this. As a practical consideration, when large lateral ventricles are present, as is often the case in these patients due to atrophy, trajectories to access the pontine tegmentum can be very limited.

2.5.3.2 Tractography

I had good *a priori* reasons to justify investigating structural connectivity with the regions of interest in our study. Neuronal tracer studies have identified frontal cortical projections to the PPN, in particular from primary motor and premotor cortices.[115,120,121] Considering the motor phenomenology of falls and gait disturbance, examining the precentral gyrus and BA6 is clearly justified. Cerebellar connectivity was also assessed, namely the SCP, as both afferent and efferent connections have been established by neuronal tracing,[122,123] and the well-established importance of the cerebellum in motor control and balance. The PPN is located between three ascending sensory pathways: the spinothalamic tracts, the SCP, and perhaps

most importantly, the medial lemniscus (ML). Considering both the proximity of the PPN to the ML, and the typical VAT (radius ≈ 3-4 mm), this implies that when an electrode is placed in the PPN, capture of the ascending lemniscal system in the tractography seed is highly likely (see Paxinos *et al.*, 2012 for anatomical distances).[83] Postcentral gyrus connectivity merited investigation, a) as a marker of accurate placement in the PPN, and b) the possibility that incidental ML stimulation may contribute to clinical improvement. Indeed, the latter has been speculatively postulated by both Moro et al.[48] and Mazzone et al.[113] Some of our patients reported somatosensory paraesthesias with increasing amplitude of low frequency stimulation, and there is credible neurophysiological evidence that chronic PPN DBS does reversibly neuromodulate the ML.[113] Furthermore, evidence is accumulating that suggests dorsal column stimulation improves Parkinsonian gait dysfunction and falls.[124–127] Therefore, although direct anatomical connections between the parietal lobe and PPN have not been established, and neurophysiological evidence for such connections is weak,[128] I examined connectivity between the VAT (but not the cathode) and the postcentral gyrus, as well as its functionally distinct divisions (BA 3a, 3b, 1, 2).

Connectivity of the crown (BA1) and posterior bank (BA2) of the postcentral gyrus had a stronger correlation with improvement than the anterior bank (BA3a/b). If one posits a causal relationship between ML modulation and clinical improvement, one might expect that BA2 connectivity would be highly correlated. BA2 projects to primary motor cortex,[129] but also receives proprioceptive input, which it combines with tactile information.[130] Left and right BA2 also have dense reciprocal callosal projections,[131] indicating a function in sided coordination. The alternative interpretation is that the positive correlation *only* represents a marker of the PPN lead being located correctly or otherwise. Explicitly, this suggests optimal

implantation in the ventral PPN (or the VLTg), i.e. adjacent to the ML, a region that other experienced authors with some of the best clinical results have commonly located their electrodes.[113] The clinical results of PPN DBS have varied substantially between centres, which is at least partly attributable to different targeting strategies. One centre reporting some of the best results (Rome, Italy), utilises somatosensory evoked potentials (SEPs), and by so doing defines or 'grounds' the appropriate lead location by its proximity to the ML.[132] Our somatosensory tractography results support the clinical logic and relevance of this targeting methodology.

The correlation of VAT<->precentral gyrus connectivity with clinical improvement was robust. High connectivity is likely to be a feature of successful PPN-DBS, which emphasises the importance of precentral gyrus input to the PPN. Stimulation of the PPN region can elicit locomotion in decerebrate animals, *ipso facto*, without cortical input,[133] and in PIGD-PD there is a block to the release of pre-programmed ballistic movements, which can be relieved by PPN stimulation.[58] It is possible cortical modulation of the diseased PPN may function as a block to subcortically and spinally located locomotor programmes, which low frequency stimulation can release. Chronic dopamine depletion in a rodent model of PD demonstrated the development of strengthened, abnormal low frequency functional connectivity between primary motor cortex and the PPN, led by the cortex.[134] This in principle demonstrates a pathological neurophysiological substrate that PPN DBS could ameliorate, which is consistent with our tractography results. Conversely, in PD, low frequency functional connectivity between the PPN region and the SMA arises during movement preparation on dopaminergic medications but not off them.[135] Additionally, during motor performance, blood flow to the SMA is increased when PD akinesia is treated with dopamine agonists.[136] This describes an

opposing valence of precentral gyrus- and SMA-PPN interaction that mirrors the motor cortex tractography correlations I found for gait freezing. A PET study of three patients implicated SMA activation from DBS targeting the PPN, however, as the clinical benefits were both mixed and minimal, they are difficult to relate clearly to our SMA tractography findings.[137]

The SMA correlation with gait freezing I observed was driven by three patients (E, F, H) who deteriorated following surgery and had much higher cathode<->SMA connectivity (Fig.1). While impossible to exclude, it is difficult to ascribe their high SMA connectivity to placement in regions outwith the PPN with potentially higher SMA connectivity, for example, the cuneiform nucleus or retrorubral field. Supporting this, all three patients had high PPN region<->SMA connectivity (Fig.1), i.e. not just high SMA connectivity with the smaller locus where the cathode ended up. Furthermore, these patients also had the lowest pre-operative gait freezing severity (Fig.1, Table 2), lending support to the notion that they have a different phenotype. Recognising that PD gait freezing can likely arise from different pathophysiological processes, it is plausible that when high connectivity between SMA and the PPN is present, that this is protective against gait freezing and DBS is liable to disrupt it or otherwise leave the principal cause of freezing unchecked. Physiological top-down modulation of PPN output will depend on parallel, differential input from the SMA (e.g. posture preparation) and precentral gyrus (e.g. step initiation). It is possible that when this becomes uncoordinated or unbalanced, that the PPNs role in gait initiation is best served purely by subcortical circuits. This is perhaps consistent with findings that PPN DBS does not eliminate gait freezing but can improve it in some patients.

While VAT modelling is derived from principles of axonal activation, results from 'cathode analysis' may best represent other mechanisms, such as lesioning, whilst also offering a more precise connectivity mapping of the stereotactic target. Regarding the SCP results, high connectivity could derive from electrodes being placed too medially, in the SCP. Irrespective of any true PPN<->SCP connectivity variance, a negative correlation would be observed if electrodes were so positioned. If this is not responsible, it may be that beneficial cerebellar outflow (likely excitatory) to the PPN is disrupted by stimulation. However, as the SCP did not show signs of degeneration that explained differences in connectivity estimates, the former explanation seems most likely.

Overall, our results are consistent with the concept that gait dysfunction in PD has sensory and motor components: perhaps even implying a disorder of sensorimotor integration. Indeed, some authors have concluded that the PPN is best considered as a nucleus of sensorimotor integration.[138]

2.5.3.3 Targeting and tractography

Targeting the PPN remains challenging and controversial.[139] It is not clearly visible on typical MRI scans, and combined with its distance from the bicommissural plane and large non-linear inter-individual variation in brain stem anatomy, a consensus on targeting strategy remains to be reached.[55] Recognising both the difficulty and uncertainties in targeting the PPN region, and the limitations in applying atlases, diffusion tractography-based structural connectivity estimates offer an objective, 'clinical outcome grounded' approach to locating the optimum target in this region of the brainstem in an individual patient. This may have the potential to supplant or operate as a modifier to targeting based on atlas-based anatomical relations. As

described in *2.4. Neuroimaging of the pedunculopontine nucleus*, other ways of using diffusion MRI for targeting the PPN are also promising.

2.5.3.4 Cortical thickness

Neuroimaging-derived cortical thickness measurements are well established as correlates of cognitive and sensorimotor function. Despite methodological challenges in acquiring accurate measurements, rational relationships have been observed between this metric and normal cognitive aging,[140] as well as a range of neuropathologic processes.[141,142]Similarly, gait dysfunction appears to be reflected in patterned loss of cortical thickness.[143,144] It is intuitive that depopulation of the cortex via normal or pathological degeneration will lead to a decrease in cortical thickness, and that the functional domains pertaining to the involved cortical regions will be compromised to some degree.

In this study, since both motor and somatosensory cortices appeared relevant to clinical improvement with stimulation; appealing to treatment-disease homology, it seemed plausible that atrophy of caudal-frontal and parietal lobes may relate to pre-operative symptom severity, measured by GFQ. Although I lacked longitudinal data, as cortical thickness in healthy brains has low variance in a given area, I supposed that cross-sectional analysis may nonetheless have some value. My results suggest that left parietal lobe, bilateral postcentral gyrus, and bilateral premotor cortex atrophy may partly account for the PIGD-PD phenotype severity. This adds further support to the concept of gait dysfunction as both a motor and sensory failure. Remarkably, when considering divisions of the postcentral gyrus, the same pattern of correlation strength (BA3a<BA3b<BA1/2) was observed (Fig.2), as it was with tractography (Fig.1). This reinforces suspicion around the role of the posterior part of this

gyrus in the dynamics of this disease. Cortical atrophy in PD has been previously studied, using both voxel-based morphometry and cortical thickness analyses.[145–147] Although specific results are mixed, both parietal lobe atrophy, and regions of BA6 (mostly medial) have been implicated in PIGD-PD. Loci of hypometabolism in the left postcentral gyrus and left inferior parietal lobule, detected by PET, have been observed to characterise PIGD-PD, relative to tremor-dominant PD.[148]

2.5.3.6 Limitations

The key limitations of the study are primarily those intrinsic to tractography, our acquisition, and those related to cohort size. The latter puts large constraints on the power to detect relationships, and high likelihood of type II error. For example, I did not find that premotor cortex connectivity was important, although I suspected that it would be, given its well-established involvement in posture and gait.[149] Nonetheless, that statistically significant relationships were found following investigation of a small number of *a priori* relevant structures, could be a testament to the importance of our findings. On the other hand, one must accept that while statistically significant, these results could also have come about by chance. As such, they require replication. However, this study nonetheless represents substantive progress in tractography analysis of PPN DBS patients with PIGD-PD, and highlights prospects for both targeting and re-evaluation of concepts of DBS in the ventrolateral pontine tegmentum.

Diffusion MRI tractography benefits from high numbers of gradient directions and high angular resolution available from multi-shell acquisitions. Our diffusion data were acquired with a single shell formulation with a relatively low number of gradient directions, which

lowers the quality of structural information encoded in the data. Nonetheless, it is accepted that such a diffusion study can be used to produce meaningful tractography with meaningful clinical results.[150] These results now need to be challenged with replication. This would ideally be carried out with a brainstem optimised acquisition (see Ezra et al.)[151], both with higher quality angular and spatial resolution (e.g. <1.5 mm isotropic), and in a larger cohort (e.g. 15 patients).

Isolating the interpretation of the results of studies such as this requires disambiguating electrode location-associated connectivity differences from intrinsic connectivity differences. The small number of patients in the study made this impractical and is methodologically quite challenging in the first instance due to anatomical features of the brain region in question. If replication of this study is attempted, a prospective assessment of how this could be achieved should be carried out.

Although the VAT model is widely used, it is extrinsically flawed beyond the internal flaw of failing to account for theoretically important features, such as local fibre orientation. Indeed, its broad application is plainly criticised by its creator (see Stimulating Brains podcast. #10 Cameron McIntyre, and the same author in personal communications to myself). There are some tractography studies where I believe the individualised stimulation field modelling is certainly the right approach. A great example of this is published by Vanegas-Arroyave et al.[150] Monopolar stimulation was explicitly used in all patients, with impedances, voltage and clinical/side effects all measured in an experiment on the same day. Therefore, there is a tight connection between parameters and effects, and validated monopolar models of VAT are well established.[106,152] This matching/relationship breaks down in the clinical scenarios of

many studies. In the simplest case, patients are programmed with a given voltage of stimulation and an upper and lower bound. Subsequently, within this range, voltage is patient directed and changes while they are in the community. The electrode impedance also changes over time, as observed at follow-up. The VAT models depend fundamentally on the voltage and impedance values that are inputted, and therefore this uncertainty generates error – enough which may well undermine the project. Furthermore, to my knowledge, there are no validated models for bipolar stimulation in DBS (although one is available in the Lead-DBS package). Experts in and associated with our group think it is questionable to attempt a very specific, individualised approach to the VAT that makes the approximation of a monopolar model to bipolar stimulation. Another issue that I think may arise in attempting the individualised VAT approach is a 'self-fulfilling prophecy' effect, which could, theoretically, generate spurious connectivity-outcome correlations. Clinically, in our general DBS experience, some patients who do not receive benefit from stimulation, will run their voltage low (perhaps to avoid side-effects) whereas patients receiving good benefit may tend to raise their voltage to the higher bound of what is tolerable/programmed. As larger tractography seeds necessarily generate larger connectivity estimates, it is easy to see how this individualised VAT approach could generate a bias in a correlation, and results that can be misinterpreted. As such, on balance, the elegance and simplicity of performing the same tractography experiment for every patient may be favourable in some studies. Nonetheless, in this study the VAT model was employed, as patients were maintained on monopolar stimulation, and the variability in settings over follow-up was thought to be quite limited.

Cortical parcellations generated by Freesurfer are anatomic estimations, not direct functional or cytoarchitectonic measures. Therefore, it must be appreciated that some degree of inaccuracy will occur.

Our field of view only included the brain and did not extend down into the cervical spinal cord. In considering projections from the PPN, rodent data indicate that rostral connectivity is much larger than caudal connectivity.[153] Nonetheless, diffusion data including the cervical spinal cord that could make a meaningful assessment of PPN-spinal cord connectivity would be attractive, as these circuits are thought to be important for the PPNs locomotor functions.[40,133,154]

Appropriate patient selection for any surgery is crucial. With regards to PPN DBS, patients who suffer severe gait disturbances are highly heterogeneous. Indeed, as aforementioned (*2.2 Deep brain stimulation targeted to the pedunculopontine nucleus*) selection criteria for PPN DBS have often included a range of severe gait disorders, not just FoG.[45,48] Even among patients with severe FoG, there are a range of phenotypes that are likely to be pathologically quite different. This includes younger patients who have early, severe, medication resistant FoG as the dominant source of motor disability. It also includes more elderly patients who develop FoG later in their disease, and patients who develop FoG following DBS of the STN or GPi. Improvement of FoG should probably be the aim of surgery, and younger patients are probably the best candidates for PPN DBS.[78] The cohort in this study had a degree of heterogeneity, and notably the patient who benefitted most from surgery (Patient A) was significantly younger than most of the others (55 years, mean = 67 years). This might also

have had some bearing on the clinical outcome-based correlations, and as such is an important limitation to consider in interpreting the results.

2.6 CONCLUDING REMARKS

DBS in the ventrolateral pontine tegmentum targeting the PPN is characterised by higher structural connectivity to the precentral gyrus and BA1/2 of the postcentral gyrus when it is effective in improving gait and balance symptoms of PIGD-PD. The converse can be said of connectivity to the SCP. Stimulating the most caudal and lateral part of the PPN may offer the best chance of relieving symptoms, whereas stimulating the SCP medially may worsen them. Low cortical thickness of the left parietal lobe and bilateral premotor cortices is associated with higher severity of PIGD-PD disease. Together, this points to a sensorimotor mechanism of action and underlying dysfunction.

While constituting an advance in the field, results should be viewed as preliminary. This is primarily due to small patient numbers and the use of diffusion data not optimised for the brainstem. These results should initiate a line of clinical neuroimaging research to evaluate and optimise PPN DBS for FoG and falls.

REFERENCES

1. Braak H, Tredici KD, Rüb U, de Vos RAI, Jansen Steur ENH, Braak E. Staging of brain pathology related to sporadic Parkinson's disease. Neurobiol Aging 2003;24(2):197–211.

2. Braak H, Bohl JR, Müller CM, Rüb U, de Vos RAI, Del Tredici K. Stanley Fahn Lecture 2005: The staging procedure for the inclusion body pathology associated with sporadic Parkinson's disease reconsidered. Mov Disord 2006;21(12):2042–51.

3. Del Tredici K, Rüb U, de Vos RAI, Bohl JRE, Braak H. Where Does Parkinson Disease Pathology Begin in the Brain? J Neuropathol Exp Neurol 2002;61(5):413–26.

4. Schapira AHV, Chaudhuri KR, Jenner P. Non-motor features of Parkinson disease. Nat Rev Neurosci 2017;18(7):435–50.

5. Foffani G, Obeso JA. A Cortical Pathogenic Theory of Parkinson's Disease. Neuron 2018;99(6):1116–28.

6. Wakabayashi K, Takahashi H. Neuropathology of Autonomic Nervous System in Parkinson's Disease. Eur Neurol 1997;38 Suppl 2:2–7.

7. Schrag A, Dodel R, Spottke A, Bornschein B, Siebert U, Quinn NP. Rate of clinical progression in Parkinson's disease. A prospective study. Mov Disord 2007;22(7):938–45.

8. Hely MA, Reid WGJ, Adena MA, Halliday GM, Morris JGL. The Sydney multicenter study of Parkinson's disease: The inevitability of dementia at 20 years: Twenty Year Sydney Parkinson's Study. Mov Disord 2008;23(6):837–44.

9. Nutt JG, Bloem BR, Giladi N, Hallett M, Horak FB, Nieuwboer A. Freezing of gait: moving forward on a mysterious clinical phenomenon. Lancet Neurol 2011;10(8):734–44.

10. Fasano A, Laganiere SE, Lam S, Fox MD. Lesions causing freezing of gait localize to a cerebellar functional network: Lesion Network Mapping and FOG. Ann Neurol 2017;81(1):129–41.

11. Almeida QJ, Lebold CA. Freezing of gait in Parkinson's disease: a perceptual cause for a motor impairment? J Neurol Neurosurg Psychiatry 2010;81(5):513–8.

12. Giladi N, Treves TA, Simon ES, et al. Freezing of gait in patients with advanced Parkinson's disease. J Neural Transm 2001;108(1):53–61.

13. Giladi N, McDermott MP, Fahn S, et al. Freezing of gait in PD: Prospective assessment in the DATATOP cohort. Neurology 2001;56(12):1712–21.

14. Giladi N. Medical treatment of freezing of gait. Mov Disord 2008;23(S2):S482–8.

15. Latt MD, Lord SR, Morris JGL, Fung VSC. Clinical and physiological assessments for elucidating falls risk in Parkinson's disease: Predictors of Falls in Parkinson's Disease. Mov Disord 2009;24(9):1280–9.

16. Jankovic J, McDermott M, Carter J, et al. Variable expression of Parkinson's disease: A base-line analysis of the DAT ATOP cohort. Neurology 1990;40(10):1529–1529.

17. Kotagal V. Is PIGD a legitimate motor subtype in Parkinson disease? Ann Clin Transl Neurol 2016;3(6):473–7.

18. Factor SA, Steenland NK, Higgins DS, et al. Postural instability/gait disturbance in Parkinson's disease has distinct subtypes: an exploratory analysis. J Neurol Neurosurg Psychiatry 2011;82(5):564–8.

19. Lewis SJG. Heterogeneity of Parkinson's disease in the early clinical stages using a data driven approach. J Neurol Neurosurg Psychiatry 2005;76(3):343–8.

20. Selikhova M, Williams DR, Kempster PA, Holton JL, Revesz T, Lees AJ. A clinico-pathological study of subtypes in Parkinson's disease. Brain 2009;132(11):2947–57.

21. Vercruysse S, Vandenberghe W, Munks L, Nuttin B, Devos H, Nieuwboer A. Effects of deep brain stimulation of the subthalamic nucleus on freezing of gait in Parkinson's disease: a prospective controlled study. J Neurol Neurosurg Psychiatry 2014;85(8):871–7.

22. Ferraye MU, Debu B, Fraix V, et al. Effects of subthalamic nucleus stimulation and levodopa on freezing of gait in Parkinson disease. Neurology 2008;70(16 Pt 2):1431–7.

23. Moreau C, Defebvre L, Destee A, et al. STN-DBS frequency effects on freezing of gait in advanced Parkinson disease. Neurology 2008;71(2):80–4.

24. Pozzi NG, Canessa A, Palmisano C, et al. Freezing of gait in Parkinson's disease reflects a sudden derangement of locomotor network dynamics. Brain 2019;142(7):2037–50.

25. Moreau C, Delval A, Defebvre L, et al. Methylphenidate for gait hypokinesia and freezing in patients with Parkinson's disease undergoing subthalamic stimulation: a multicentre, parallel, randomised, placebo-controlled trial. Lancet Neurol 2012;11(7):589–96.

26. Bakker M, Esselink RAJ, Munneke M, Limousin-Dowsey P, Speelman HD, Bloem BR. Effects of stereotactic neurosurgery on postural instability and gait in Parkinson's disease. Mov Disord 2004;19(9):1092–9.

27. Ghika J, Villemure J-G, Fankhauser H, Favre J, Assal G, Ghika-Schmid F. Efficiency and safety of bilateral contemporaneous pallidal stimulation (deep brain stimulation) in levodopa-responsive patients with Parkinson's disease with severe motor fluctuations: a 2-year follow-up review. J Neurosurg 1998;89(5):713–8.

28. Hinsey JC, Ranson SW, McNattin RF. The rôle of the hypothalamus and mesencephalon in locomotion. Arch Neurol Psychiatry 1930;23(1):1–43.

29. Grillner S, Shik ML. On the Descending Control of the Lumbosacral Spinal Cord from the "Mesencephalic Locomotor Region." Acta Physiol Scand 1973;87(3):320–33.

30. Garcia-Rill E, Skinner RD, Fitzgerald JA. Activity in the mesencephalic locomotor region during locomotion. Exp Neurol 1983;82(3):609–22.

31. Kuo S-H, Kenney C, Jankovic J. Bilateral pedunculopontine nuclei strokes presenting as freezing of gait. Mov Disord 2008;23(4):616–9.

32. Masdeu JC, Alampur U, Cavaliere R, Tavoulareas G. Astasia and gait failure with damage of the pontomesencephalic locomotor region. Ann Neurol 1994;35(5):619–21.

33. Gilman S, Koeppe RA, Nan B, et al. Cerebral cortical and subcortical cholinergic deficits in parkinsonian syndromes. Neurology 2010;74(18):1416–23.

34. Bohnen NI, Muller MLTM, Koeppe RA, et al. History of falls in Parkinson disease is associated with reduced cholinergic activity. Neurology 2009;73(20):1670–6.

35. Dautan D, Huerta-Ocampo I, Witten IB, et al. A Major External Source of Cholinergic Innervation of the Striatum and Nucleus Accumbens Originates in the Brainstem. J Neurosci 2014;34(13):4509–18.

36. Rinne JO, Ma SY, Lee MS, Collan Y, Röyttä M. Loss of cholinergic neurons in the pedunculopontine nucleus in Parkinson's disease is related to disability of the patients. Parkinsonism Relat Disord 2008;14(7):553–7.

37. Nandi D, Aziz TZ, Giladi N, Winter J, Stein JF. Reversal of akinesia in experimental parkinsonism by GABA antagonist microinjections in the pedunculopontine nucleus. Brain 2002;125(11):2418–30.

38. Jenkinson N, Nandi D, Miall RC, Stein JF, Aziz TZ. Pedunculopontine nucleus stimulation improves akinesia in a Parkinsonian monkey: NeuroReport 2004;15(17):2621–4.

39. Jenkinson N, Nandi D, Oram R, Stein JF, Aziz TZ. Pedunculopontine nucleus electric stimulation alleviates akinesia independently of dopaminergic mechanisms: NeuroReport 2006;17(6):639–41.

40. Caggiano V, Leiras R, Goñi-Erro H, et al. Midbrain circuits that set locomotor speed and gait selection. Nature 2018;553(7689):455–60.

41. Tattersall TL, Stratton PG, Coyne TJ, et al. Imagined gait modulates neuronal network dynamics in the human pedunculopontine nucleus. Nat Neurosci 2014;17(3):449–54.

42. Karachi C, Andre A, Bertasi E, Bardinet E, Lehericy S, Bernard FA. Functional Parcellation of the Lateral Mesencephalus. J Neurosci 2012;32(27):9396–401.

43. Mazzone P, Lozano A, Stanzione P, et al. Implantation of human pedunculopontine nucleus: a safe and clinically relevant target in Parkinson's disease: NeuroReport 2005;16(17):1877–81.

44. Plaha P, Gill SS. Bilateral deep brain stimulation of the pedunculopontine nucleus for Parkinson's disease. NeuroReport 2005;16(17):1883–7.

45. Ferraye MU, Debu B, Fraix V, et al. Effects of pedunculopontine nucleus area stimulation on gait disorders in Parkinson's disease. Brain 2010;133(1):205–14.

46. Thevathasan W, Coyne TJ, Hyam JA, et al. Pedunculopontine Nucleus Stimulation Improves Gait Freezing in Parkinson Disease. Neurosurgery 2011;69(6):1248–54.

47. Stefani A, Lozano AM, Peppe A, et al. Bilateral deep brain stimulation of the pedunculopontine and subthalamic nuclei in severe Parkinson's disease. Brain 2007;130(6):1596–607.

48. Moro E, Hamani C, Poon Y-Y, et al. Unilateral pedunculopontine stimulation improves falls in Parkinson's disease. Brain 2010;133(1):215–24.

49. Mazzone P, Paoloni M, Mangone M, et al. Unilateral deep brain stimulation of the pedunculopontine tegmental nucleus in idiopathic Parkinson's disease: Effects on gait initiation and performance. Gait Posture 2014;40(3):357–62.

50. Welter M-L, Demain A, Ewenczyk C, et al. PPNa-DBS for gait and balance disorders in Parkinson's disease: a double-blind, randomised study. J Neurol 2015;262(6):1515–25.

51. Fahn S, Elton RL. UPDRS program members. Unified Parkinsons disease rating scale. Recent Dev Park Dis 1987;2:153–63.

52. Martínez-Martín P, Urra DG, Quijano T del S, et al. A New Clinical Tool for Gait Evaluation in Parkinson's Disease. Clin Neuropharmacol 1997;20(3).

53. Giladi N, Shabtai H, Simon ES, Biran S, Tal J, Korczyn AD. Construction of freezing of gait questionnaire for patients with Parkinsonism. Parkinsonism Relat Disord 2000;6(3):165–70.

54. Perera T, Tan JL, Cole MH, et al. Balance control systems in Parkinson's disease and the impact of pedunculopontine area stimulation. Brain 2018;141(10):3009–22.

55. Hamani C, Aziz T, Bloem BR, et al. Pedunculopontine Nucleus Region Deep Brain Stimulation in Parkinson Disease: Surgical Anatomy and Terminology. Stereotact Funct Neurosurg 2016;94(5):298–306.

56. Zrinzo L, Zrinzo LV, Tisch S, et al. Stereotactic localization of the human pedunculopontine nucleus: atlas-based coordinates and validation of a magnetic resonance imaging protocol for direct localization. Brain 2008;131(6):1588–98.

57. Thevathasan W, Cole MH, Graepel CL, et al. A spatiotemporal analysis of gait freezing and the impact of pedunculopontine nucleus stimulation. Brain 2012;135(5):1446–54.

58. Thevathasan W, Pogosyan A, Hyam JA, et al. A block to pre-prepared movement in gait freezing, relieved by pedunculopontine nucleus stimulation. Brain 2011;134(7):2085–95.

59. Morgante F, Fasano A. Improvement with Duloxetine in Primary Progressive Freezing Gait. Neurology 2010;75(23):2130.

60. Grimbergen YA, Langston JW, Roos RA, Bloem BR. Postural instability in Parkinson's disease: the adrenergic hypothesis and the locus coeruleus. Expert Rev Neurother 2009;9(2):279–90.

61. Beudel M, Brown P. Adaptive deep brain stimulation in Parkinson's disease. Parkinsonism Relat Disord 2016;22:S123–6.

62. Fraix V, Bastin J, David O, et al. Pedunculopontine Nucleus Area Oscillations during Stance, Stepping and Freezing in Parkinson's Disease. PLoS ONE 2013;8(12):e83919.

63. Androulidakis AG, Mazzone P, Litvak V, et al. Oscillatory activity in the pedunculopontine area of patients with Parkinson's disease. Exp Neurol 2008;211(1):59–66.

64. Molina R, Hass CJ, Sowalsky K, et al. Neurophysiological Correlates of Gait in the Human Basal Ganglia and the PPN Region in Parkinson's Disease. Front Hum Neurosci 2020;14:194.

65. Molina R, Hass CJ, Cernera S, et al. Closed-Loop Deep Brain Stimulation to Treat Medication-Refractory Freezing of Gait in Parkinson's Disease. Front Hum Neurosci 2021;15:633655.

66. Khan S, Javed S, Mooney L, et al. Clinical outcomes from bilateral versus unilateral stimulation of the pedunculopontine nucleus with and without concomitant caudal zona incerta region stimulation in Parkinson's disease. Br J Neurosurg 2012;26(5):722–5.

67. Khan S, Mooney L, Plaha P, et al. Outcomes from stimulation of the caudal zona incerta and pedunculopontine nucleus in patients with Parkinson's disease. Br J Neurosurg 2011;25(2):273–80.

68. Schrader C, Seehaus F, Capelle HH, Windhagen A, Windhagen H, Krauss JK. Effects of Pedunculopontine Area and Pallidal DBS on Gait Ignition in Parkinson's Disease. Brain Stimulat 2013;6(6):856–9.

69. Carpenter MB, Carleton SC, Keller JT, Conte P. Connections of the subthalamic nucleus in the monkey. Brain Res 1981;224(1):1–29.

70. Granata AR, Kitai ST. Inhibitory substantia nigra inputs to the pedunculopontine neurons. Exp Brain Res 1991;86(3):459–66.

71. Nakamura Y, Tokuno H, Moriizumi T, Kitao Y, Kudo M. Monosynaptic nigral inputs to the pedunculopontine tegmental nucleus neurons which send their axons to the medial reticular formation in the medulla oblongata. An electron microscopic study in the cat. Neurosci Lett 1989;103(2):145–50.

72. Noda T, Oka H. Distribution and morphology of tegmental neurons receiving nigral inhibitory inputs in the cat: An intracellular HRP study. J Comp Neurol 1986;244(2):254–66.

73. Kang Y, Kitai ST. Electrophysiological properties of pedunculopontine neurons and their postsynaptic responses following stimulation of substantia nigra reticulata. Brain Res 1990;535(1):79–95.

74. Chastan N, Westby GWM, Yelnik J, et al. Effects of nigral stimulation on locomotion and postural stability in patients with Parkinson's disease. Brain 2008;132(1):172–84.

75. Weiss D, Walach M, Meisner C, et al. Nigral stimulation for resistant axial motor impairment in Parkinson's disease? A randomized controlled trial. Brain 2013;136(7):2098–108.

76. Nosko D, Ferraye MU, Fraix V, et al. Low-frequency versus high-frequency stimulation of the pedunculopontine nucleus area in Parkinson's disease: a randomised controlled trial. J Neurol Neurosurg Psychiatry 2015;86(6):674–9.

77. Mazzone P, Insola A, Sposato S, Scarnati E. The Deep Brain Stimulation of the Pedunculopontine Tegmental Nucleus. Neuromodulation Technol Neural Interface 2009;12(3):191–204.

78. Thevathasan W, Debu B, Aziz T, et al. Pedunculopontine nucleus deep brain stimulation in Parkinson's disease: A clinical review: Clinical Review of PPN DBS. Mov Disord 2018;33(1):10–20.

79. Mestre TA, Sidiropoulos C, Hamani C, et al. Long-term double-blinded unilateral pedunculopontine area stimulation in Parkinson's disease: A 4-Year Blinded Assessment of PPN Stimulation for PD. Mov Disord 2016;31(10):1570–4.

80. Lavoie B, Parent A. Pedunculopontine nucleus in the squirrel monkey: Cholinergic and glutamatergic projections to the substantia nigra. J Comp Neurol 1994;344(2):232–41.

81. Lavoie B, Parent A. Pedunculopontine nucleus in the squirrel monkey: Projections to the basal ganglia as revealed by anterograde tract-tracing methods. J Comp Neurol 1994;344(2):210–31.

82. Paxinos G, Huang X. Atlas of the human brainstem. San Diego: Academic Press; 1995.

83. Paxinos G, Xu-Feng H, Sengul G, Watson C. Chapter 8 - Organization of Brainstem Nuclei. In: Mai JK, Paxinos G, editors. The Human Nervous System (Third Edition). San Diego: Academic Press; 2012. p. 260–327.

84. Mesulam M-M, Geula C, Bothwell MA, Hersh LB. Human reticular formation: Cholinergic neurons of the pedunculopontine and laterodorsal tegmental nuclei and some cytochemical comparisons to forebrain cholinergic neurons. J Comp Neurol 1989;283(4):611–33.

85. Manaye KF, Zweig R, Wu D, et al. Quantification of cholinergic and select non-cholinergic mesopontine neuronal populations in the human brain. Neuroscience 1999;89(3):759–70.

86. Cong F, Wang J-W, Wang B, et al. Direct localisation of the human pedunculopontine nucleus using MRI: a coordinate and fibre-tracking study. Eur Radiol 2018;28(9):3882–92.

87. Aravamuthan BR, Muthusamy KA, Stein JF, Aziz TZ, Johansen-Berg H. Topography of cortical and subcortical connections of the human pedunculopontine and subthalamic nuclei. NeuroImage 2007;37(3):694–705.

88. Henssen DJHA, Kuppens D, Meijer FJA, van Cappellen van Walsum AM, Temel Y, Kurt E. Identification of the pedunculopontine nucleus and surrounding white matter tracts on 7T diffusion tensor imaging, combined with histological validation. Surg Radiol Anat 2019;41(2):187–96.

89. Bianciardi M, Strong C, Toschi N, et al. A probabilistic template of human mesopontine tegmental nuclei from in vivo 7 T MRI. NeuroImage 2018;170:222–30.

90. Muthusamy KA, Aravamuthan BR, Kringelbach ML, et al. Connectivity of the human pedunculopontine nucleus region and diffusion tensor imaging in surgical targeting. J Neurosurg 2007;107(4):814–20.

91. Schweder PM, Hansen PC, Green AL, Quaghebeur G, Stein J, Aziz TZ. Connectivity of the pedunculopontine nucleus in parkinsonian freezing of gait: NeuroReport 2010;21(14):914–6.

92. Smith SM, Jenkinson M, Woolrich MW, et al. Advances in functional and structural MR image analysis and implementation as FSL. NeuroImage 2004;23:S208–19.

93. Andersson JLR, Skare S, Ashburner J. How to correct susceptibility distortions in spin-echo echo-planar images: application to diffusion tensor imaging. NeuroImage 2003;20(2):870–88.

94. Andersson JLR, Sotiropoulos SN. An integrated approach to correction for off-resonance effects and subject movement in diffusion MR imaging. NeuroImage 2016;125:1063–78.

95. Andersson JLR, Sotiropoulos SN. Non-parametric representation and prediction of single- and multi-shell diffusion-weighted MRI data using Gaussian processes. NeuroImage 2015;122:166–76.

96. Andersson JLR, Graham MS, Zsoldos E, Sotiropoulos SN. Incorporating outlier detection and replacement into a non-parametric framework for movement and distortion correction of diffusion MR images. NeuroImage 2016;141:556–72.

97. Behrens TEJ, Woolrich MW, Jenkinson M, et al. Characterization and propagation of uncertainty in diffusion-weighted MR imaging. Magn Reson Med 2003;50(5):1077–88.

98. Behrens TEJ, Berg HJ, Jbabdi S, Rushworth MFS, Woolrich MW. Probabilistic diffusion tractography with multiple fibre orientations: What can we gain? NeuroImage 2007;34(1):144–55.

99. Dale AM, Fischl B, Sereno MI. Cortical Surface-Based Analysis. 1999;9(2):179–94.

100. Fischl B. FreeSurfer. NeuroImage 2012;62(2):774–81.

101. Desikan RS, Ségonne F, Fischl B, et al. An automated labeling system for subdividing the human cerebral cortex on MRI scans into gyral based regions of interest. NeuroImage 2006;31(3):968–80.

102. Jenkinson M, Smith S. A global optimisation method for robust affine registration of brain images. Med Image Anal 2001;5(2):143–56.

103. Jenkinson M, Bannister P, Brady M, Smith S. Improved Optimization for the Robust and Accurate Linear Registration and Motion Correction of Brain Images. NeuroImage 2002;17(2):825–41.

104. Greve DN, Fischl B. Accurate and robust brain image alignment using boundary-based registration. NeuroImage 2009;48(1):63–72.

105. Andersson JL, Jenkinson M, Smith S. Non-linear registration aka Spatial normalisation FMRIB Technical Report TR07JA2. FMRIB Anal Group Univ Oxf 2007;1–22.

106. Mädler B, Coenen VA. Explaining Clinical Effects of Deep Brain Stimulation through Simplified Target-Specific Modeling of the Volume of Activated Tissue. Am J Neuroradiol 2012;33(6):1072–80.

107. Horn A, Li N, Dembek TA, et al. Lead-DBS v2: Towards a comprehensive pipeline for deep brain stimulation imaging. NeuroImage 2019;184:293–316.

108. Avants B, Epstein C, Grossman M, Gee J. Symmetric diffeomorphic image registration with cross-correlation: Evaluating automated labeling of elderly and neurodegenerative brain. Med Image Anal 2008;12(1):26–41.

109. Husch A, V. Petersen M, Gemmar P, Goncalves J, Hertel F. PaCER - A fully automated method for electrode trajectory and contact reconstruction in deep brain stimulation. NeuroImage Clin 2018;17:80–9.

110. Edlow BL, Takahashi E, Wu O, et al. Neuroanatomic Connectivity of the Human Ascending Arousal System Critical to Consciousness and Its Disorders. J Neuropathol Exp Neurol 2012;71(6):531–46.

111. Winkler AM, Kochunov P, Blangero J, et al. Cortical thickness or grey matter volume? The importance of selecting the phenotype for imaging genetics studies. NeuroImage 2010;53(3):1135–46.

112. Fischl B, Dale AM. Measuring the thickness of the human cerebral cortex from magnetic resonance images. Proc Natl Acad Sci 2000;97(20):11050–5.

113. Mazzone P, Vilela Filho O, Viselli F, et al. Our first decade of experience in deep brain stimulation of the brainstem: elucidating the mechanism of action of stimulation of the ventrolateral pontine tegmentum. J Neural Transm 2016;123(7):751–67.

114. Martinez-Gonzalez C, Bolam JP, Mena-Segovia J. Topographical Organization of the Pedunculopontine Nucleus. Front Neuroanat 2011;5:22.

115. Matsumura M, Nambu A, Yamaji Y, et al. Organization of somatic motor inputs from the frontal lobe to the pedunculopontine tegmental nucleus in the macaque monkey. Neuroscience 2000;98(1):97–110.

116. Gut NK, Winn P. Deep Brain Stimulation of Different Pedunculopontine Targets in a Novel Rodent Model of Parkinsonism. J Neurosci 2015;35(12):4792–803.

117. Mazzone P, Sposato S, Insola A, Scarnati E. The Clinical Effects of Deep Brain Stimulation of the Pedunculopontine Tegmental Nucleus in Movement Disorders May Not Be Related to the Anatomical Target, Leads Location, and Setup of Electrical Stimulation. Neurosurgery 2013;73(5):894–906.

118. Nielsen MS, Bjarkam CR, Sørensen JC, Bojsen-Møller M, Sunde NAa, Østergaard K. Chronic subthalamic high-frequency deep brain stimulation in Parkinson's disease ? a histopathological study. Eur J Neurol 2007;14(2):132–8.

119. Orlowski D, Michalis A, Glud AN, et al. Brain Tissue Reaction to Deep Brain Stimulation-A Longitudinal Study of DBS in the Goettingen Minipig. Neuromodulation Technol Neural Interface 2017;20(5):417–23.

120. von Monakow KH, Akert K, Künzle H. Projections of precentral and premotor cortex to the red nucleus and other midbrain areas in macaca fascicularis. Exp Brain Res 1979;34(1):91–105.

121. Edley SM, Graybiel AM. The afferent and efferent connections of the feline nucleus tegmenti pedunculopontinus, pars compacta. J Comp Neurol 1983;217(2):187–215.

122. Hazrati L-N, Parent A. Projection from the deep cerebellar nuclei to the pedunculopontine nucleus in the squirrel monkey. Brain Res 1992;585(1–2):267–71.

123. Ruggiero DA, Anwar M, Golanov EV, Reis DJ. The pedunculopontine tegmental nucleus issues collaterals to the fastigial nucleus and rostral ventrolateral reticular nucleus in the rat. Brain Res 1997;760(1–2):272–6.

124. Samotus O, Parrent A, Jog M. Spinal Cord Stimulation Therapy for Gait Dysfunction in Advanced Parkinson's Disease Patients: Spinal Cord Stimulation for Gait in PD. Mov Disord 2018;33(5):783–92.

125. de Lima-Pardini AC, Coelho DB, Souza CP, et al. Effects of spinal cord stimulation on postural control in Parkinson's disease patients with freezing of gait. eLife 2018;7:e37727.

126. Fonoff ET, de Lima-Pardini AC, Coelho DB, et al. Spinal Cord Stimulation for Freezing of Gait: From Bench to Bedside. Front Neurol 2019;10:905.

127. Pinto de Souza C, Hamani C, Oliveira Souza C, et al. Spinal cord stimulation improves gait in patients with Parkinson's disease previously treated with deep brain stimulation: Spinal Cord Stimulation in PD. Mov Disord 2017;32(2):278–82.

128. Insola A, Padua L, Scarnati E, Valeriani M. Where are the somatosensory evoked potentials recorded from DBS leads implanted in the human pedunculopontine tegmental nucleus generated? Mov Disord 2011;26(8):1572–3.

129. Porter LL. Patterns of projections from area 2 of the sensory cortex to area 3a and to the motor cortex in cats. Exp Brain Res 1992;91(1):85–93.

130. Keysers C, Kaas JH, Gazzola V. Somatosensation in social perception. Nat Rev Neurosci 2010;11(6):417–28.

131. Killackey HP, Gould HJ, Cusick CG, Pons TP, Kaas JH. The relation of corpus callosum connections to architectonic fields and body surface maps in sensorimotor cortex of new and old world monkeys. J Comp Neurol 1983;219(4):384–419.

132. Insola A, Valeriani M, Mazzone P. Targeting the Pedunculopontine Nucleus. Oper Neurosurg 2012;71(suppl_1):ons96–103.

133. Garcia-Rill E, Houser CR, Skinner RD, Smith W, Woodward DJ. Locomotion-inducing sites in the vicinity of the pedunculopontine nucleus. Brain Res Bull 1987;18(6):731–8.

134. Valencia M, Chavez M, Artieda J, Bolam JP, Mena-Segovia J. Abnormal functional connectivity between motor cortex and pedunculopontine nucleus following chronic dopamine depletion. J Neurophysiol 2014;111(2):434–40.

135. Tsang EW, Hamani C, Moro E, et al. Involvement of the human pedunculopontine nucleus region in voluntary movements. Neurology 2010;75(11):950–9.

136. Jenkins IH, Fernandez W, Playford ED, et al. Impaired activation of the supplementary motor area in Parkinson's disease is reversed when akinesia is treated with apomorphine. Ann Neurol 1992;32(6):749–57.

137. Ballanger B, Lozano AM, Moro E, et al. Cerebral blood flow changes induced by pedunculopontine nucleus stimulation in patients with advanced Parkinson's disease: A [15O] H2O PET study. Hum Brain Mapp 2009;30(12):3901–9.

138. Winn P. Experimental studies of pedunculopontine functions: Are they motor, sensory or integrative? Parkinsonism Relat Disord 2008;14:S194–8.

139. Mazzone P, Sposato S, Insola A, Scarnati E. The deep brain stimulation of the pedunculopontine tegmental nucleus: towards a new stereotactic neurosurgery. J Neural Transm 2011;118(10):1431–51.

140. Fjell AM, Walhovd KB, Reinvang I, et al. Selective increase of cortical thickness in high-performing elderly—structural indices of optimal cognitive aging. NeuroImage 2006;29(3):984–94.

141. Thompson PM, Hayashi KM, Sowell ER, et al. Mapping cortical change in Alzheimer's disease, brain development, and schizophrenia. NeuroImage 2004;23:S2–18.

142. Sailer M, Fischl B, Salat D, et al. Focal thinning of the cerebral cortex in multiple sclerosis. Brain 2003;126(8):1734–44.

143. Maidan I, Mirelman A, Hausdorff JM, Stern Y, Habeck CG. Distinct cortical thickness patterns link disparate cerebral cortex regions to select mobility domains. Sci Rep 2021;11(1):6600.

144. Ezzati A, Katz MJ, Lipton ML, Lipton RB, Verghese J. The association of brain structure with gait velocity in older adults: a quantitative volumetric analysis of brain MRI. Neuroradiology 2015;57(8):851–61.

145. Rosenberg-Katz K, Herman T, Jacob Y, Giladi N, Hendler T, Hausdorff JM. Gray matter atrophy distinguishes between Parkinson disease motor subtypes. Neurology 2013;80(16):1476–84.

146. Herman T, Rosenberg-Katz K, Jacob Y, Giladi N, Hausdorff JM. Gray matter atrophy and freezing of gait in Parkinson's disease: Is the evidence black-on-white?: Gray Matter Atrophy and Freezing of Gait in PD. Mov Disord 2014;29(1):134–9.

147. Uribe C, Segura B, Baggio HC, et al. Cortical atrophy patterns in early Parkinson's disease patients using hierarchical cluster analysis. Parkinsonism Relat Disord 2018;50:3–9.

148. Zhang L, Li T-N, Yuan Y-S, et al. The Neural Basis of Postural Instability Gait Disorder Subtype of Parkinson's Disease: A PET and fMRI Study. CNS Neurosci Ther 2016;22(5):360–7.

149. Takakusaki K. Functional Neuroanatomy for Posture and Gait Control. J Mov Disord 2017;10(1):1–17.

150. Vanegas-Arroyave N, Lauro PM, Huang L, et al. Tractography patterns of subthalamic nucleus deep brain stimulation. Brain 2016;139(4):1200–10.

151. Ezra M, Faull OK, Jbabdi S, Pattinson KT. Connectivity-based segmentation of the periaqueductal gray matter in human with brainstem optimized diffusion MRI: Segmentation of the PAG with Diffusion MRI. Hum Brain Mapp 2015;36(9):3459–71.

152. Butson CR, Cooper SE, Henderson JM, McIntyre CC. Patient-specific analysis of the volume of tissue activated during deep brain stimulation. NeuroImage 2007;34(2):661–70.

153. Spann BM, Grofova I. Origin of ascending and spinal pathways from the nucleus tegmenti pedunculopontinus in the rat. J Comp Neurol 1989;283(1):13–27.

154. Skinner RD, Kinjo N, Henderson V, Garcia-Rill E. Locomotor projections from the pedunculopontine nucleus to the spinal cord. NeuroReport 1990;1(3):183–6.

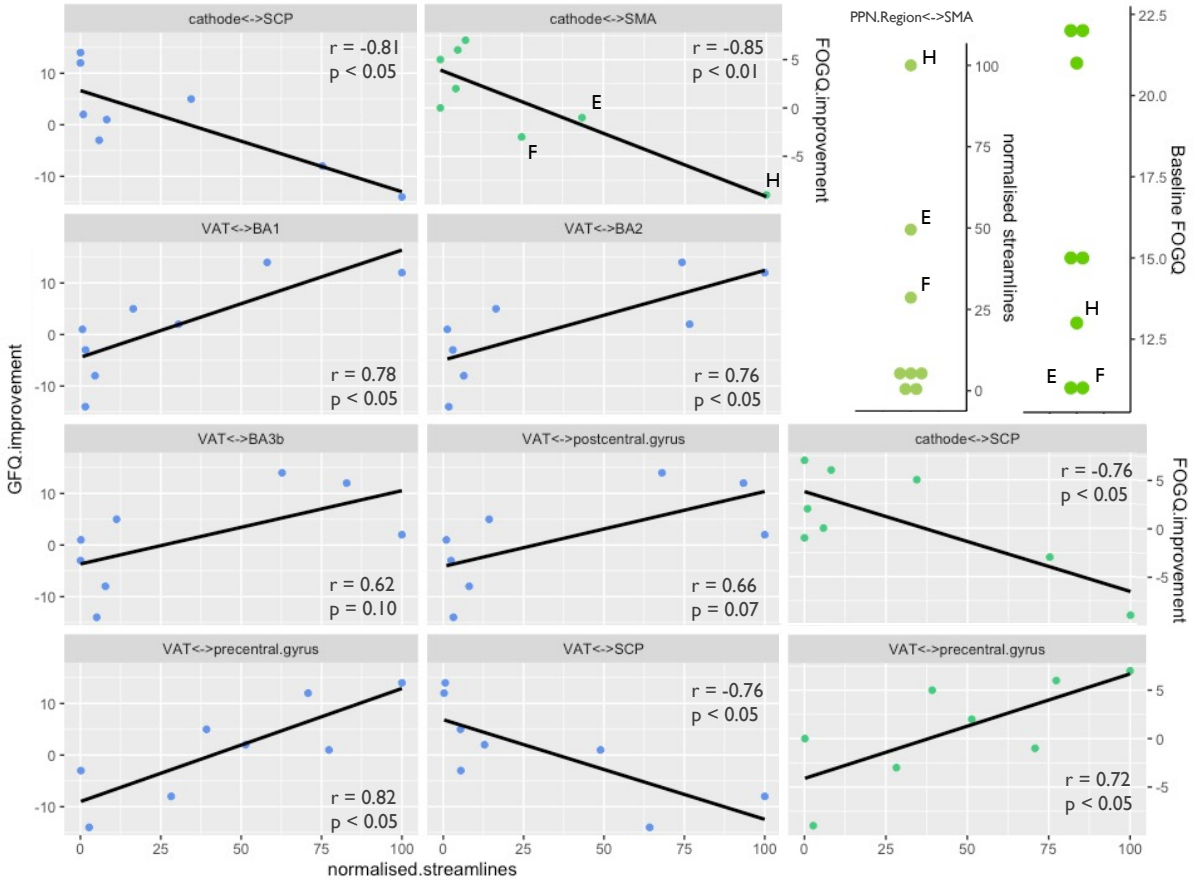

Fig 1. **Tractography.** Correlation of clinical improvement with structural connectivity between DBS leads and cortical/cerebellar regions of interest. *Pearson:* see panels. GFQ Spearman's: Cathode<->SCP: r = -0.81, p < 0.05. VAT<->BA1: r = 0.79, p < 0.05 . VAT<->BA2: r = 0.71, p < 0.05. VAT<->BA3b: r = 0.64, p = 0.09. VAT<->postcentral gyrus: r = 0.62, p = 0.10. VAT<->precentral gyrus: r = 0.76, p < 0.05. VAT<->SCP: r = -0.88, p < 0.01. FOGQ Spearman's: Cathode<->SMA: r = -0.55, n.s. Cathode<->SCP: r = -0.45, n.s. VAT<->precentral gyrus: r = 0.71, p < 0.05. Top right: Patients E,F and H PPN Region<->SMA connectivity and baseline FOGQ.

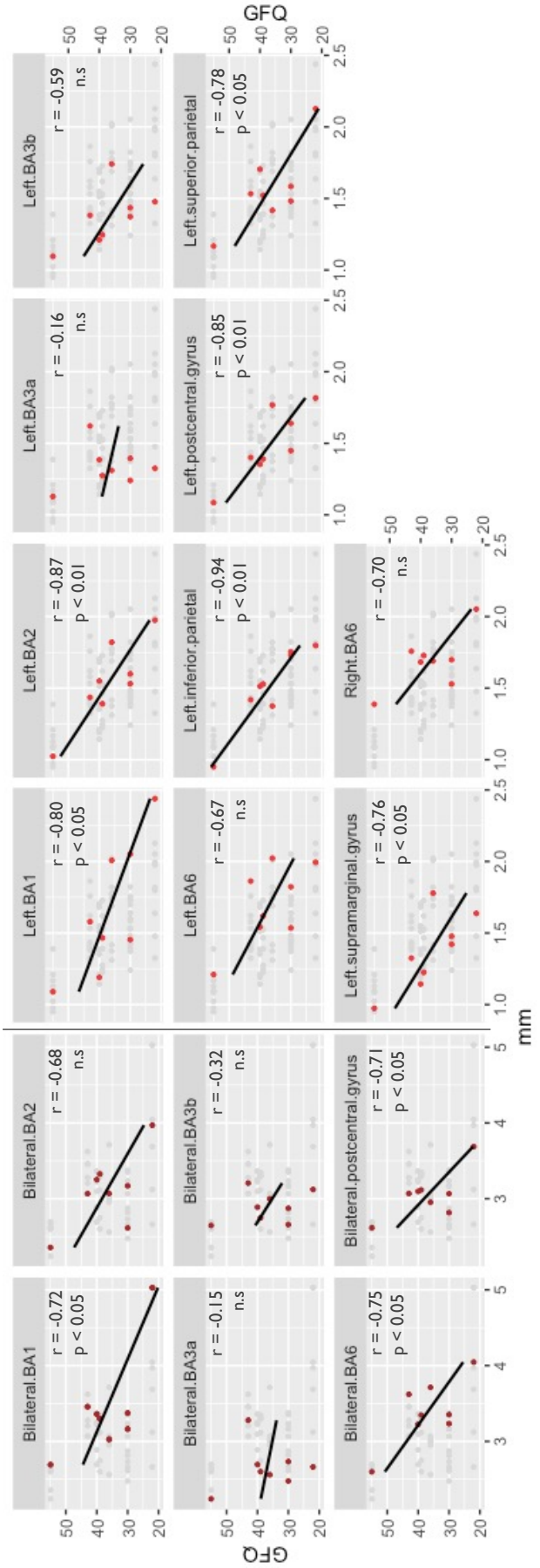

Fig 2. **Cortical thickness.** Correlation of mean cortical thickness with pre-operative symptom severity (GFQ). *Pearson*: see panels. *Spearman's*: *Bilateral:* BA1: r = -0.40, n.s. BA2: r = -0.49, n.s. BA3a: r = -0.06, n.s. BA3b: r = -0.17, n.s. BA6: r = -0.58, n.s. postcentral gyrus: r = -0.31, n.s. *Left:* BA1: r = -0.72, p<0.05. BA2: r = -0.77, p<0.05. BA3a: r = -0.08, n.s. BA3b: r = -0.67, n.s. BA6: r = -0.58, n.s. inferior parietal: r = -0.85, p < 0.01 . postcentral gyrus: r = -0.85, p < 0.01. superior parietal: r = -0.44, n.s. supramarginal: r = -0.78, p < 0.05. *Right:* BA6: r=-0.37, n.s.

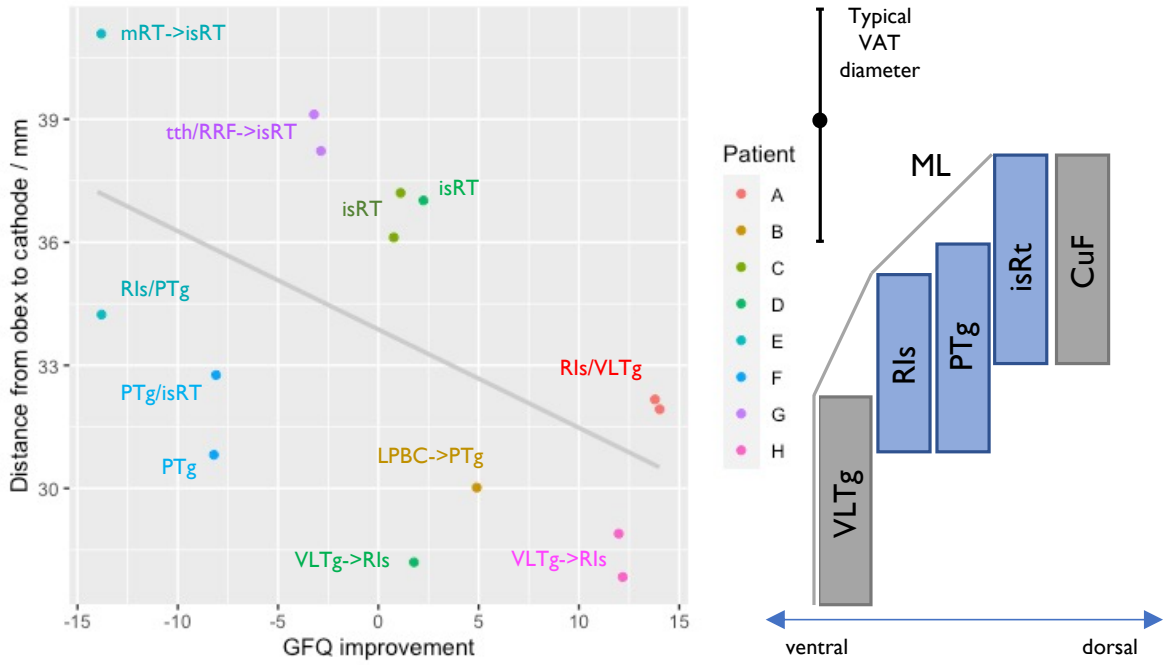

Fig 3. **Cathode depth**. Plot of depth vs. clinical improvement, contextualised relative to nuclei of the ventrolateral pontine tegmentum by Paxinos et al 2012 brainstem atlas, and grounded in distance to the obex. Cathodes are labelled with the most likely location within the PPN based on the same atlas. When distance from the obex precludes atlas-based assignment to the PPN, '->' denotes most likely PPN location to be stimulated. VLTg = ventrolateral tegmental area; Ris = retroisthmic nucleus; PTg = pedunculotegmental nucleus; isRt = isthmic reticular formation; CuF = cuneiform nucleus; ML = medial lemniscus; mRT = mesencephalic reticular formation; tth = trigeminal lemniscus; RRF = retrorubral field; LPBC = lateral parabrachial complex.

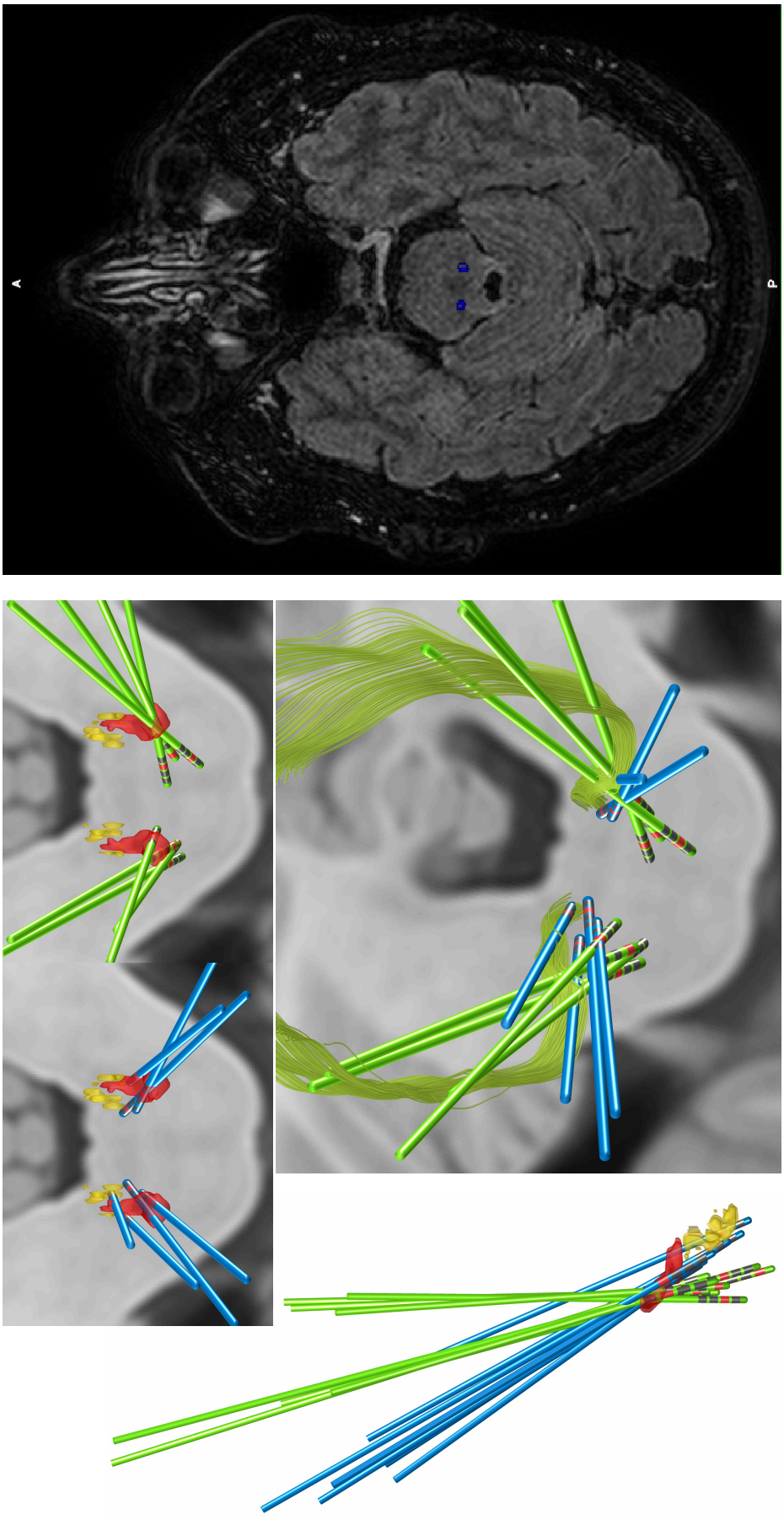

Fig. 4. **Stimulation electrodes**. Left and centre: Reconstruction of DBS electrodes. Blue = Improved gait freezing. Green = No improvement. Red = PPN. Yellow = Parabrachial nuclei. Green fibres = medial lemniscus. Right: Fused CT-FLAIR showing stimulating cathode locations of Patient A.

How can I possibly work without any yellow paper?

~

Hugh W. B. Cairns

CHAPTER 3. CHRONIC NEUROPATHIC PAIN

ABSTRACT

Surgery to the thalamus has a long history for treating pain and despite failures remains physiologically attractive. Success depends on sophisticated patient selection and accurate targeting. Anatomy of the posterolateral thalamus varies substantially between individuals, presenting a challenge for surgical targeting. Patient specific, connectivity-based parcellation of the thalamus may effectively approximate the ventrocaudal nucleus (Vc). This remains to be robustly validated or assessed as a method to guide surgical targeting. A cohort of nineteen patients with regional, chronic neuropathic pain underwent pre-operative structural and diffusion MRI, then progressed to deep brain stimulation (DBS) targeting the Vc based on traditional atlas coordinates. Retrospectively, surgical thalami were segmented then parcellated based on tractography estimates of thalamo-cortical connectivity. The location of each patient's electrode array was analysed with respect to their somatosensory (S1) parcel and compared across patients with reference to the thalamic homunculus. Ten patients achieved long-term pain relief. An average-array was 61% located in the S1 parcel (Q_1-Q_3: 42-74%). In patients who achieved long-term benefit from surgery, array location in the individually generated S1 parcels was medial for face pain, centro-medial for arm pain, and centro-lateral for leg pain. Patients who did not benefit from surgery did not follow this pattern. Standard stereotactic coordinates of electrode locations diverged from the individualised pattern, signalling the potential of diffusion MRI for improving clinical outcomes in pain surgery. Connectivity-based parcellation of the thalamus appears to be a reliable method for segmenting Vc. Identifying the Vc in this way and targeting medio-laterally as appropriate for the region of pain, merits exploration in an effort to increase the yield of successful surgeries.

3.1 ANATOMICAL SUBSTRATES OF PAIN

A neural system conveying a signal of noxious stimuli is present in taxa of distant phylogeny, with many anatomical and biochemical features highly conserved. Reflexive response to and volitional motivation by noxious stimuli is of clear adaptive value. In humans, this is demonstrated with most clarity in the misfortune of individuals who lack this signal (e.g. congenital insensitivity to pain +/- anhidrosis: CIP/A). Contrasting with the concrete, objective concept of noxious stimuli, the experience of pain itself is harder to define: a higher order, subjective, multi-dimensional (sensory-discriminative, affective-motivational, cognitive-evaluative) phenomenon that likely requires a more complicated neural architecture than many species possess, or at least phenomenologically differs between species. Indeed, despite pain being the prototypic and most common complaint for seeing a doctor, and despite efforts of generations of physicians and scientists, patients might be surprised to know that the neurological basis for their symptoms are so inconclusively understood. This is particularly true of maladaptive chronic pathological pain, in comparison with adaptive acute physiological pain.

In this evolutionary context, in humans, the ascending nociceptive pathways can be considered based on incremental phylogenetic antiquity, as described by Mehler in 1957,[1] and developed by Bishop in 1959.[2] This framework appeals through the protopathic complement present in species sharing increasingly distant common ancestors to man and acknowledging the respective development or lack thereof of the forebrain. In order, this terminology includes the archispinothalamic, paleospinothalamic, and neospinothalamic tracts. The former involves unmyelinated fibres that take more complex, diffuse, and bilateral

routes, mostly to the brain stem, and to a lesser extent the medial thalamus and hypothalamus, whereas the latter involves myelinated fibres that take a simpler, more unilateral projection with retained somatotopy aimed to the lateral thalamus.

Taking an evolutionary perspective, each pathway in turn can be interpreted to 'add something' to the collection, transmission, and integration of nociceptive information, and in man, also to his pain experience. This must also have provided a significant adaptative advantage. For example, the sensory-discriminative pain system may be more advanced in primates as we have the manual dexterity and cognition to better target our actions to relieving the external cause, whereas in comparison, the relevance of such a precise system in an amphibian is less obvious. Chronic neuropathic pain, resulting from injury or disease, is conversely not adaptive and can be attributed to some aspect of this pain architecture not working properly. As such, the aim of neurosurgery in treating chronic pain has been to understand the relevant anatomy and physiology of pain and intervene at a relevant structure to produce analgesia.

An excellent review of the anatomical substrates of pain can be found in work by Lenz and colleagues, and from which much of the following summary is inspired.[3] Afferent nociceptive signals are transmitted from the periphery by small, thinly myelinated Aδ and small, unmyelinated C fibres: pseudounipolar neurons with soma in the dorsal root ganglia.[4,5] These fibres enter the spinal cord via the lateral division of the dorsal root, entering through Lissauer's tract before synapsing in the dorsal grey horn.[6] A similar schema exists for head, facial, and intraoral structures, with soma in cranial ganglia (Meckel's ganglion: V, geniculate

ganglion: VII, petrosal ganglion: IX, and jugular ganglion: X) synapsing in the spinal trigeminal nucleus, a long structure spanning the pons to the upper cervical cord.

Aδ fibres predominantly synapse in Rexed lamina I,[7,8] with a minority synapsing in lamina V,[9] whereas C fibers also synapse in lamina I but mostly synapse in lamina II:[10] the substantia gelatinosa.[11,12] Some C-fibre pathways ascend and descend in a multi-synaptic route through the cord via laminae IV to VIII, before ascending to more rostral targets. Lamina II is notable for its receipt of descending modulation from the somatosensory cortex travelling in the corticospinal tract,[13] as well as from brain stem nuclei travelling in the dorsal lateral funiculus.[14] Indeed, nociceptive cells in dorsal horn are in receipt of descending modulation from a range of brainstem nuclei, including projections from the hypothalamus,[15] periaqueductal grey,[16] locus coeruleus,[17] and raphe magnus,[18] among others.

Two major spinal cord funiculi transmit nociceptive fibres: the dorsolateral funiculus and the anterolateral funiculus. The post-synaptic dorsal column system is a minor pathway involved in visceral pain signalling, arising from deep Rexed laminae and ascending in the medial aspect of the dorsal columns.[19,20] Predominantly arising from laminae III and IV, these neurons synapse in gracile and cuneate nuclei of the cervico-medullary junction, as a relay to the thalamus. The former is notably recognised as signalling pelvic visceral sensations. The dorsolateral funiculus transmits the myelinated spinocervicothalamic system, which ascends ipsilaterally to the lateral cervical nucleus, after which approximately one third of post-synaptic neurons decussate and join the medial lemniscus to terminate in the region of the thalamic ventral posterior nucleus, and two thirds of post-synaptic neurons are directed to the midbrain.[21] Lamina I neurons projecting to the midbrain also travel in the dorsolateral

funiculus.[22,23] The anterolateral funiculus is dominated by neurons that ascend to the brainstem: loosely grouped as the spinoreticular and spinomesencephalic tracts (arising from deep laminae in this fasciculus).[24] Targets include the tectum, periaqueductal grey, parabrachial complex,[25] and throughout the medial ponto-medullary reticular formation.[26,27] Distribution is bilateral but denser ipsilateral to the side of assent. A minority of neurons in these funiculi comprise the spinothalamic tract. The spinothalamic tract is mostly a contralateral system, having decussated in the anterior commissure, except in the caudal cord where ipsilateral projections are dominant.[28] The spinothalamic system has two divisions: medial and lateral. Laminae I and V characteristically supply the lateral thalamic targets, and laminae VI-VII the medial thalamic targets.[29–31] Notably, there is a substantial lamina I input to a region at the caudal pole of VPL.[32,33]

Thalamic anatomy has been famously confused through the numerous atlantean terminologies employed, with their broad but not completely corresponding homology. Major systems of nomenclature includes those of Hassler, Feremutsch and Simma, Hirai and Jones, Percheron, and Morel, although there are many others.[34] As results of neuronal tracing and physiological studies are reported with such different thalamic terminology, the project of comparing and integrating these results faces that added challenge. In considering the lateral thalamus, there is general agreement on a ventral caudal (Vc) or ventral posterior (VP) mass, with external (or lateral: VPL), and internal (or medial: VPM) subdivisions, themselves distinctly divided by the arcuate lamina (lamella arcuata). The lateral mass may be justifiably further subdivided based on cell density into anterior and posterior components (e.g. VPLa - low, VPLp – high, by both Hirai and Morel).[35,36] The medial inferior margin of the VP mass is sometimes given special designation (e.g. VPI and parvocellular VPM by Morel), and of

relevance to spinothalamic terminations in the thalamus an inconsistently named and divided set of nuclei are found posterior and posteroinferior to the medial VP mass. For example, within Morel's framework this territory includes the anterior pulvinar (APul), the posterior nucleus (Po), and the limitans-suprageniculate (SG),[35] whereas within Hassler's framework these are described within the ventrocaudal terminological tree.[37]

The VPI, nestled between the ventral aspects of VPL and VPM, is traversed by lemniscal fibres destined for these nuclei. The medial lemniscal and spinal trigeminolemniscal neurons terminate densely in the VPL and VPM, observed as parvalbumin-positive staining. The Po and SG also function as the inferior portal to the thalamus (collectively, Hassler's nucleus limitans portae), particularly for spinothalamic fibres, and in contrast to lemniscal fibres, there is also a dense focus of terminations there (the Po/Sg).[38,39] Dorsal to this, the APul, mostly corresponding to Hassler's ventrocaudalis portae, also has an anatomic portal function in passing fibres anteriorly to VPL and VPM. Terminations also occur there (the APul), within the VPL and VPM, and continue further anteriorly to the posterior ventrolateral nucleus (VLp),[40] commonly known as Hassler's ventral intermediate nucleus (VIm): the cerebellothalamic relay. Conversely, lemniscal termini are constrained to the VP,[40,41] where they exhibit exquisite somatotopy. Fibre bundles enter posteriorly and run anteriorly, forming laterally convex parasagittal sheets. These are stacked mediolaterally, with receptive fields progressing from intraoral, face, thumb, fingers (radial to ulnar), arm, and leg.[42] On this background of parvalbumin-rich, cytochrome oxidase-rich lemniscal neurons, calbindin-rich, cytochrome oxidase-weak spinothalamic (VPL) and trigeminospinothalmic (VPM) neurons terminate in burst-like or archipelago-like clusters throughout the complex.[43] The principal cortical target of VP is the primary somatosensory cortex, and is thought to be crucial to the

sensory-discriminative component of pain. Although notably, the lemniscal fibres arrive at layers III and IV of the cortex, whereas spinothalamic fibres arrive more superficially at layers I and II.[40,41,44]

The caudal pole of VP has become a region of increasing interest with respect to pain. Craig's posterior ventral medial nucleus (Vmpo), characterised by high insula and cingulate connectivity, was immediately controversial,[45] and has ultimately not survived critical examination regarding claims as an exclusive focus of lamina I, high-threshold, calbindin-positive, thermo- and nociceptive specific neurons.[46] Nonetheless, there clearly is a region medial of the caudal pole of VP that is particularly calbindin-rich, and probably corresponds to the APul and/or possibly Po. Indeed, this thalamic neighbourhood principally projects cortically to parasylvian territories. In the monkey, Po and APul project strongly to retroinsular cortex, and SG to posterior (granular) insula.[47,48] A recent study of 42 patients with thalamic vascular injury, 31 of whom developed thalamic pain (Déjerine-Roussy syndrome), identified APul as the region of maximal lesion convergence (97%) in those with central pain, contrasting with only 40% in those without pain.[49] Recent human invasive neurophysiology also supports APul having an important role in nociceptive processing.[50]

The medial thalamus is also in receipt of spinothalamic and spinotrigeminothalamic fibres, mostly arising from deep Rexed laminae,[28,51] and is thought to mediate suffering or the affective-motivational dimension of pain. They enter through the internal medullary lamina, which divides medial and lateral thalamus, traverse the centre median nucleus (CM), principally entering the caudal pole of the central lateral nucleus (CL), and mostly terminate in the posterior region of that nucleus.[52] A minority terminate more anteriorly in CL, as well

as in the parafasicular nucleus (Pf) and paralaminar regions of the mediodorsal nucleus. The intralaminar nuclei characteristically project diffusely across cortex, mostly terminating at layer I but also III and VI, however, projections are most dense to the cingulate, insula, and parasylvian regions.[53–55] In addition, these nuclei give rise to extensive ipsilateral thalamostriate projections.[56,57]

3.2 THE THALAMUS AS A PUTATIVE SURGICAL TARGET TO TREAT CHRONIC PAIN

The overwhelming majority of nociceptive fibres ascending in the anterolateral system terminate in the brain stem, with only a minority reaching the thalamus. As such, this could argue against the thalamus as a prime surgical target to treat recalcitrant chronic pain. Four arguments arise against this (see Fig.1). A fifth point of context is that the brainstem is deep and highly anatomically congested, which is problematic for targeting and stimulation induced side effects. As a deeper structure, it is surgically/stereotactically more difficult to reach than the thalamus.

Head and Holmes postulated in the early 20th century that thalamic imbalance in protopathic and epicritic functioning was important for neurogenic pain.[58] While they highlighted a thalamic inhibitory process involving cortico-thalamic transmission, in the mid-20th century, Kendall postulated a similar thalamic process but arising from spino-thalamic transmission.[59] At the end of the 20th century the observation of thalamocortical dysrhythmia (increased coherence of low-frequency gamma oscillations) through magnetoencephalography (MEG) implicated dysfunctional thalamocortical loops in the neurogenic pain state.[60] At a similar time, Craig postulated that central pain arises when integration of pain and temperature

fails,[61] a form of thermoregulatory dysfunction, inspired through results from the thermal grill illusion experiment.[62] Anatomically, this was grounded in a specific thalamic nucleus mediating spinal afferents and cortical projections.[63,64] Ultimately, most theories finesse a theme of central disinhibition or sensitisation with concomitant hyperexcitability and activity of spinal and/or supra-spinal neurons. However, the thalamus recurs as a fundamentally important node, which advocates for the thalamus as a putative surgical target in ameliorating chronic pain.

3.3 HISTORICAL REVIEW OF STEREOTACTIC APPROACHES TO TREATMENT OF PAIN

The surgical approach to pain has been rooted in understanding of functional anatomy and physiology built up from scientific results in a range of disciplines. The rationale has been that interruption or modulation of neural pathways than convey, supress, amplify, or integrate the pain experience could result in therapeutic benefit. Below, the clinical experience of brainstem, thalamic, and cortical targets are summarised.

3.3.1 Brainstem

3.3.1.1 Parabrachial complex

The parabrachial complex both receives ascending nociceptive inputs and also play a role in descending pain modulation via the rostroventral medulla.[65] Animal studies demonstrated evidence of stimulation induced analgesia,[66] precipitating investigation in humans with success in two patients with morphine-resistant malignant pain.[67] Similarly, stimulation of the subparabrachial nucleus (the Kölliker-Fuse) specifically, induced inhibition of dorsal horn

neurons to noxious stimuli in cats.[68] Young et al. targeted this nucleus in humans with some success, along with some undesired effects (compulsive stimulation with social withdrawal).[69]

3.3.1.2 Mesencephalic tracts

Open mesencephalic tractotomy was advanced by Walker (Chicago) in 1942,[70] and the stereotactic procedure (SMT) by Mazars et al. (Paris) in 1960.[71] The logic of the procedure is to interrupt the ascending coalesced spinothalamic and trigeminal spinothalamic tracts as they traverse the midbrain, with the aim of treating unilateral, contralateral pain. As a lesioning procedure in an anatomically congested area, neurological complications are of considerable concern.[72] Idiosyncratic to this procedure, patients can develop a severe dysaesthesia.[73] Some surgeons augmented the procedure medially in order to target the mesencephalic reticular formation.[74] Nonetheless, SMT has survived in the surgical armamentarium as an option for treating unilateral head and neck cancer pain.

3.3.1.3 Periaqueductal grey

Following lesioning procedures, pain often returns after a period of relief. As a therapeutic modality, deep brain stimulation (DBS) gives the opportunity to change stimulation settings over time, in a hope to combat such recurrence when longer-term pain relief is required. As such, DBS for pain became an attractive concept in the treatment of non-malignant pain. DBS of the periaqueductal grey (PAG) followed from experiments in mammals demonstrating analgesic effects.[75] Hoshobuchi in San Francisco[76] and Richardson in New Orleans[77,78] both found similar effects in 1977 with malignant and non-malignant pain in man, with the former utilising a placebo (dummy battery) to validate the acute analgesia observed. Naloxone reversibility of the effect was demonstrated, and increased beta-endorphin and enkephalins

were found in ventricular cerebrospinal fluid (CSF) following stimulation, thus implicating an opioid based mechanism.[76,79,80] Naloxone reversibility was later questioned by Young,[81] who would nonetheless confirm raised levels of CSF beta-endorphin and enkephalins that were elicited by stimulation.[82] The involvement of the opioid system would remain a contentious issue, particularly when the methodology used to determine CSF opiate reactivity was shown to be flawed.[83] More recently, opioid radioligand positron emission tomography (PET) has been used to demonstrate that rostral dorsal PAG DBS results in endogenous opioid release in the caudal dorsal PAG.[84] However, as this observation was not correlated with analgesia, which in this study was not naloxone reversible, its importance remains unclear. A comparison of dorsal and ventral electrodes suggests that the naloxone question may be partly explainable by placement, with dorsal DBS analgesia being opioid driven.[85] Since the PAG is known to function as part of a descending modulatory system via the serotonergic raphe nuclei, a serotonergic mechanism has also been considered. There is some evidence that tolerance to PAG DBS can be augmented with serotonin precursor supplementation.[86]

Clear and well-articulated pre-clinical support, combined with promising clinical results, led PAG DBS to gain popularity and to being used extensively, particularly in combination with thalamic stimulation (Table 1). This popularity quickly faded following the failure of two multi-centre, industry-funded, open-label, non-controlled trials to meet primary endpoints for efficacy.[87] In addition, common early indications, such as failed back surgery syndrome and chronic lower back/leg pain, later proved to be well catered for by spinal cord stimulation.[88,89] Despite these trials, PAG DBS continues to be used off-label,[90] with surgeons typically favouring the more rostral PAG (usually termed the periventricular grey: PVG) due to the side effects (e.g. oscillopsia, gaze palsies) often experienced at the more caudal and anatomically

congested midbrain level. The PAG appears to possess somatotopy, which can guide electrode placement intra-operatively.[91,92] While well supported indications for PAG DBS are unclear, with post-stroke central pain notoriously difficult to treat medically, PAG appears to be the surgical target of choice, with clinically meaningful benefit maintained at two years in up to 70% of patients.[93] Benefits are in the sensory dimension of pain (not affective or evaluative), and this typically requires decreasing frequency and voltage overtime as tolerance develops.[94] Currently, a randomised controlled trial (RCT) is planned at Oxford for the assessment of dual central grey/lateral thalamus DBS for post-stroke pain.

Table 1. Illustrative papers on deep brain stimulation of the PAG/PVG and VPL/VPM

Author	Year	Place	Number (bilateral)	Diagnoses	Success %	Follow up
PAG/PVG						
Plotkin [95]	1982	Johannesburg	48 (0)	S, P, N	79%	3 yrs
Hosobuchi	1986	San Francisco	16 (16)	S, P, T, N	69%	2-14 yrs
Kumar [96]	1997	Saskatchewan	49 (3)	S, P	71%	Avg 7 yrs
VPL/VPM						
Hosobuchi	198	San Francisco	76	B, S, P, T	58%	2-14 yrs
Siegfried [97]	1987	Zurich	89 (4)	B, S, P, T	79%	6 mts – 6 yrs
Gybels [98]	1993	Leuven	36 (0)	B, S, P, T	31%	Avg 4 yrs
Kumar [96]	1997	Saskatchewan	16 (0)	B, P, S, T	44%	Avg 4 yrs
Yamamoto [99]	2006	Tokyo	18 (0)	P	78%	1 yr

Pereira [100]	2007	Porto	12 (0)	P	75%	1 yr
Mixed PAG/PVG - VPL/VPM						
Levy [101]	1987	San Francisco	141	B, S, P, T, N	30%	Avg 6 yrs
Hamani [102]	2006	Toronto	20	B, S, P, T, N	25%	Avg 5 yrs
Rasche [103]	2006	Heidelberg	56	B, S, P, T, N	36%	Avg 3 yrs

B = Brain lesion, S = Spinal cord lesion, P = Peripheral lesion, T = Trigeminal distribution, N = Neoplasia

3.3.2 Diencephalon

3.3.2.1 Hypophysis

Reduction in malignant pain following hypophysectomy was first observed in 1953 by Luft and Olivecrona working in Stockholm.[104] The operation was performed for advanced prostatic and breast malignancies, with the rationale that tumours appeared to be hormonally driven, based on observations with hormone drugs, castration, and adrenalectomy.[105] Also in Stockholm, stereotactic radiosurgery (SRS) to the pituitary was introduced in 1972,[106] with stereotactic chemical hypophysectomy following in 1977.[107]

Indication broadened to other malignancies, and pathological examination after successful chemical hypophysectomy demonstrated destruction of the pituitary stalk and loss of the median eminence and supraoptic and paraventricular nuclei, leading the authors to speculate that posterior pituitary hormones or related peptides were involved in central pain processing.[108] Initial results in post-stroke central pain (SRS and invasive ablation) were promising,[109,110] but longer-term results (1-year) were disappointing.[111] Some interest in hypophysectomy for malignant pain has been maintained, based on historic success rates of

75%.[112] Similar response rates have been achieved, although for most, pain recurs over months.[113] Nonetheless, an SRS RCT is planned for opioid-refractory pain secondary to a terminal malignancy (any origin), to help establish any possible role for the treatment in modern end-of-life care.[114] The mechanism of action remains largely a mystery, although notably, the dorsal horn is modulated by the anterior pituitary. Thyroid-releasing hormone is concentrated in laminae II and III inhibitory interneurons,[115] and corticotropin-releasing factor (CRF) is similarly concentrated in ascending lamina I neurons, as well as deeper Rexed laminae where CRF increases following hypophysectomy.[116] Indeed CRF has probably been neglected with respect to possible functions in pain modulation.[117]

3.3.2.2 Medial lemniscus

The lemniscal fibres entering the ventral margin of thalamus have been targeted as a variation on stimulating somatosensory thalamus, particularly in hemi-body pain. The aim of this is to broaden somatotopic coverage but with a similar effect to stimulating VP thalamus.[102]

3.3.2.3 Intralaminar thalamus

Targeting the nuclei of the intralaminar group, namely the centrolateral (CL), centromedian (CM), and parafasicular (PF) nuclei, originates with Talaraich in 1949.[118] Subsequently, over many decades these nuclei have been tackled with invasive ablation and radiosurgery in an attempt to relieve pain due to malignant and non-malignant causes (Table 2.). Indeed, a range of operations have been described including thalamic tractotomy (syn. thalamolaminotomy), medial thalamotomy, CL thalamotomy, CM thalamotomy, and CM-Pf stimulation. The most significant contributions come from Jeanmonod and colleagues in Zurich, using invasive radiofrequency thermoablation. Their experience across a wide range of conditions, and at

long-term follow up, is that approximately 50% of patients have greater than 50% relief, with approximately 20% having complete relief and 30% no benefit.[119] They also observed that bilateral treatment was more successful, probably reflecting the more bilateral projection of spinothalamic fibres to the intralaminar thalamus, compared to VP thalamus. Essentially identical results have been produced by Young and colleagues in Seattle but instead by using stereotactic radiosurgery.[120,121] Young et al. target CM-PF and the lateral margin of the medial dorsal nucleus, whereas Jeanmonod et al. emphasise targeting the CL. The former was animated by attribution of a focus of spontaneous neuronal hyperactivity in deafferentation pain,[122] the latter appealing as the dominant locus of spinothalamic intralaminar terminations.

The technique of high intensity focused-ultrasound ablation (FUS) for stereotactic brain lesioning was pioneered in Zurich, and originally applied to pain in targeting the posterior part of CL.[123] This non-invasive technique has demonstrated similar efficacy to the equivalent invasive procedure across a range of neuropathic pain conditions.[124] Interestingly, applied to classical, idiopathic, and secondary trigeminal neuralgia in a small series, 100% of patients had surgical success,[125] perhaps signifying the need to homogenise regional pain in patient selection for future clinical trials. The excellent safety profile of FUS,[126] and good cognitive morbidity profile of CL lesions,[127] suggests it is likely to feature in future treatment pathways for trigeminal neuralgia. DBS in this region has received little attention but, nonetheless, may have similar efficacy.[128,129] Dual PAG/CM-PF DBS has also been attempted successfully,[130] including with a single-lead technique (a long medial array, spearing both nuclei).[131]

Table 2. Key papers on surgery to the medial thalamus

Author	Year	Place	Number (bilateral)	Diagnoses	Success %	Follow up
Invasive Ablation						
Sano [132]	1965	Tokyo	10 (7)	B, S, P, N	80	1mt -2.5yrs
Fairman [133]	1972	B. Aires	165 (0)	N	70	death
Hitchcock [134]	1981	Edinburgh	19 (8)	B, S, T, N	90	Avg 15 mt
Niizuma [135]	1982	Sendai	15 (0)	B, P	33	2 mts
Jeanmonod [119]	2001	Zurich	96 (41)	B, S, P, T, N	53	Avg 3.5 yrs
Radiosurgery						
Steiner [136]	1980	Stockholm	50 (18)	N	52	death
Young [121]	2001	Seattle	61(3)	B, S, P, T	53	Avg 6 yrs
Urgosik [137]	2018	Prague	30 (0)	B, T, P	37	Avg 24 mts
Lovo [138]	2019	S. Salvador	10 (0)	T, P	60	Avg 1 yr
Deep Brain Stimulation						
Hariz [128]	1995	London	4 (0)	B, P, T	50	Avg 16 mts
Krauss [129]	2002	Mannheim	3 (0)	B, P	66	1-2 yrs
Focused-Ultrasound						
Jeanmonod [124]	2012	Zurich	11 (6)	B, S, P, T	55	3 mts
Gallay [125]	2020	Zurich	8 (8)	T	100	Avg 2 yrs

3.3.2.4 Lateral thalamus

Thalamotomy of the ventrocaudal nucleus (Vc) was conceptually unpopular due to the likelihood of epicritic deficits and concern over eliciting the thalamic syndrome. Nonetheless, the procedure was explored by some surgeons, notably Mark at Harvard in 1960, guided by contrast ventriculograms.[139] Epicritic deficits were indeed common but not universal, while painful dysaesthesia was rare and then treatable with enlargement of the lesion. Pain relief was achieved for less than six months, suitable for many of their cancer patients but not a wider chronic pain cohort, and therefore attracted interest for DBS. Stimulation of the lateral thalamus, namely the VPL and VPM nuclei, was first published by Hoschobuchi in San Francisco in 1973, although it is claimed to have been performed prior to this in France during the early 1960s. The Vc (VPL-VPM complex) is targeted medio-laterally with the aim of mirroring the homuncular somatotopy of the nucleus with the patient's distribution of symptoms. As such, the procedure is most logical for regional pain. Findings in chronic pain among amputees with and without phantoms limbs led to a particular interest in Vc DBS for deafferentation pain. Key among these were the enlarged thalamic-stump representation in patients with stump pain (suggesting the stump representation had supplanted that of the amputated limb), and the evoking of sensations in phantom limbs through Vc stimulation (demonstrating a functioning thalamic representation of the amputated limb).[140] Consistent with this, peripheral deafferentation appears to respond well to this treatment, in particular phantom limb or stump pain, for which success is in the region of 70-90%.[90,99,101]

The therapeutic mechanism of the surgery remains unclear. A placebo-analgesic effect (related to placebo-paraesthesia effect) is established, at least with short term use,[141] casting doubt on the legitimacy of reported efficacy. While this remains unresolved, PET has

demonstrated modulation of both the anterior cingulate and insula through therapeutic stimulation, key cortical regions involved in pain processing.[142,143]

Observations from opioid system experiments led to the view that PAG and Vc DBS had different but potentially complementary mechanisms of action; the former being indicated for nociceptive pain, and the later for neuropathic pain. On this basis, Hosobuchi pioneered dual stimulation for 'mixed' pain syndromes in 1983,[144] which subsequently became a standard surgical approach to chronic pain. Ultimately, the utility and validity of this framework would not bear critical analysis, and in retrospect was far too simplistic. Nonetheless, this approach of modulating (or having the option to modulate) two nodes in the pain network remained attractive, as a strategy to increase the yield of successful pain relief. Typically, evidence of insertional effect and trial stimulation is appraised to inform internalisation of either a single or dual channel system, or none at all. The Oxford experience in this found approximately 15% not progressing to full implantation, and 45% reporting less pain than in their pre-operative state in the long term.[90] Clinically meaningful long-term success of this approach, as it currently stands, can be expected to be 25-35%.[101–103] While the PAG can be the medial target with this strategy, often the more rostral PVG is chosen due to oscillopsia and other side effects from stimulation at the level of the aqueduct. However, the PVG and the CM-Pf of thalamus are spatially so close that it would be hard to anatomically disambiguate a DBS electrode targeted to either as stimulating one and not the other, depending on which contact is being used. Acknowledging this clinical reality (see Commentary to Boccard et al.)[90], Krauss in Hannover has published a series of 40 patients receiving dual CM-Pf/Vc DBS for chronic neuropathic pain,[145] with similar results to the dual PVG/Vc stimulation by Aziz.[90]

3.3.2.5 Pulvinar

The possibility of a surgically relevant pain region lying posterior to Vc has long been recognised, notably by Mehler in 1966.[146] Indeed, in 1960 Hassler noted stimulation and lesioning of limitans portae (syn. Po) eliciting and alleviating pain respectively.[147] Targeting the pulvinar was explored in the 1970s, but never gained wide popularity. Through targeting CM, experience led Mayanagi to drift posteriorly into PuA, ultimately concluding that lesions involving the pulvinar were more effective for alleviating pain.[148] Both anterior and medial pulvinotomy have been performed for control of both malignant and non-malignant pain (30% pain free, n=60, 1-2 yrs),[149,150] with stimulation before lesioning eliminating or reducing pain in some patients.[77,151] A case of chronic DBS followed, where pain secondary to brachial plexus avulsion was relieved for three years before recurring.[152] Although anteromedial pulvinotomy remained in the surgical armamentarium of some neurosurgeons as late as the mid-90s,[153] to my knowledge it is no longer practiced as a treatment for pain.

Nonetheless, a number of modern findings have shed new light on this historic operation and point to a region of surgical interest posterior to Vc. Thalamic pain can occur after a posterior circulation stroke in the geniculo-thalamic artery distribution, which includes Vc, CM, CL, Po, PuA, among other nuclei, implying a crucial role for compromised regions of thalamus in chronic central pain. Recent retrospective analyses, using MRI and stereotactic thalamic atlases, implicate the PuA (essentially synonymous with both ventrocaudalis portae and oral pulvinar),[154–157] even as the most critical structure of interest.[49] Conversely, these studies signify lesions of Craig's VmPo are much less relevant, if at all. In animals, it has long been appreciated that activity in the pulvinar is generated from noxious stimuli transmitted via the anterolateral system.[158,159] This has more recently been confirmed through local field

potentials (LFPs) in humans, indeed demonstrating larger amplitude responses there to nociceptive stimuli (nociceptive-specific laser stimulation) than other putative 'pain nuclei' (VPL, CL).[50] Spinothalamic afferents have been traced to PuA,[31,40] and stimulation of PuA can generate thermo- and noci-sensory experiences.[160]

Despite its putative role as a key thalamic nucleus in pain, in receipt of nociceptive and thermoceptive lamina 1 projections, VmPo has not been formally targeted to treat pain. This is likely due to the controversy of its nature or existence. However, due to the proposed proximity of VmPo to CM, VPM, and anterior pulvinar, errors in targeting these and inter-individual thalamic variation allow it to be assumed that VmPo has been inadvertently treated with stimulation and lesioning. The spatial similarities between VmPo, anterior pulvinar, and the posterior margin of Vc (particularly the medial portion) should be noted. Empirical surgical experiences have often trended posteriorly towards the pulvinar. It has long been appreciated that in targeting VPL or VPM the posterior region is preferable.[161] This necessarily raises the issue of whether the posterior margin of Vc or a specific posterior nucleus is indeed the salient lateral thalamic pain target.

3.3.3 Internal capsule and cortex

3.3.3.1 Posterior limb of internal capsule

The internal capsule is a white matter highway carrying information to and from the cortex. The posterior limb (PLIC), known to carry somatosensory fibres to the cortex, was first targeted in 1974 by Adams in San Francisco.[162,163] The principle of targeting pain fibres leaving the thalamus for the cortex has not been favoured, with surgeons preferring to target thalamic somaesthetic subnuclei. While primarily seen as a variant of somatosensory

thalamus stimulation, PLIC stimulation has been used specifically following thalamic stroke when little viable thalamic tissue remains.[96,101] Nonetheless, benefits from PLIC stimulation over VC have been recorded in their own right through intra-operative exploration,[164] with some authors targeting it specifically. Most notably, Naamba reported five of eight patients with post-stroke pain having good or excellent results,[165] and Hunsche had success in three of four patients with thalamic pain at one year using DTI-tractography in an attempt to target spinothalamocortical tract fibres within the PLIC.[166]

3.3.3.2 Anterior limb of internal capsule

Lempka et al. carried out a double-blinded RCT at the Cleveland Clinic for treatment of post-stroke hemi body pain with anaesthesia dolorosa (n = 9) by anterior limb (ALIC) and nucleus accumbens (NA) stimulation.[167] Aiming to modulate the affective-motivational sphere of pain, the trial failed to meet primary and secondary endpoints set by the investigators. However, improvements in outcomes measuring affective and cognitive components of pain were observed. There was a non-trivial risk of seizures (20%) associated with the procedure. The sensory aspects of pain were, as expected, unchanged by treatment. Beginning at the modern multi-dimensional conception of pain (sensory-discriminative, affective-motivational, cognitive-evaluative), the authors argue that analgesia, per se, may not be an appropriate treatment goal in some patients, and decreasing pain-related suffering and disability is more appropriate. This trial represents a major step forward in stereotactic pain research in several ways, despite the small number of patients. It was a double-blind RCT and was not funded by industry. Biomarkers of investigational use were systematically collected (MEG, MRI, fMRI) with both the patient population clinically refined and the trial outcomes set by modern pain research/ideas.

3.3.3.3 Dorsal anterior cingulate

The cingulum white matter bundle connects ventral paleocortex (uncus and parahippocampal gyrus) to the subcallosal gyrus and constitutes the core of white matter supplying the cingulate cortex. The continuum of these cortical structures has often been classified as 'the limbic lobe'. The anterior cingulate (AC) is considered to be important in pain,[168,169] particularly the cognitive and affective aspects of pain,[170] as well as part of the descending pain modulation system in conjunction with brainstem structures such as the PAG and raphe magnus.

Cingulotomy was first explored by Foltz in 1961, borne out of observations from the more extensive frontal lobotomy, in the attempt to modify the emotional aspects of patients suffering with a less invasive procedure.[171] Patients were selected with prominent emotional components to their pain syndrome, and good or excellent results were achieved in 12 of 16 patients, with better results from bilateral lesions. Notably, patients with the pre-operative psychiatric diagnosis of 'inadequate personality' responded least well. Prior to the establishment of the multi-dimensional theory of pain, the results are described as pain 'relief', alluding to the non-sensori-discriminative effects.

Bilateral cingulotomy subsequently became popular for pain control (Table 3.), particularly with terminal malignant disease, where concerns relating to cognitive and personality changes are less pertinent.[172] Spooner et al. pioneered DBS of the AC at Vanderbilt in 2007, aiming to create a 'virtual lesion' with effects similar to cingulotomy.[173] In Oxford, Aziz took up the mantle, exploring the technique with a substantive series of patients with non-malignant pain, many of whom had failed previous DBS.[174,175] Similar effects on the affective

sphere of pain were demonstrated in some patients. Others failed trial stimulation, suffered from broken leads or infections, or otherwise did not benefit. In addition, induction of seizures was a non-trivial problem from treatment,[175] not dissimilarly to cingulotomy.[176] Although, notably, with cingulotomy different surgeons report widely varying rates of seizures among their patients (e.g. 39%[176] versus 0%[177,178]) implying that specific lesion location/size may be of critical importance. Overall, in the Oxford cohort, these complications left a minority of patients using DBS in the long term, albeit some with remarkable relief. Circumvention of seizure induction and kindling appears to be achievable through a sensing-enabled system through ramp-up ramp-down cycling.[179] Ultimately, when AC DBS is effective, painful sensations are still present, but they do not bother the patient. In other words, the salience/valence of sensations has been modulated.

Table 3. Illustrative papers on surgery to the anterior cingulate

Author	Year	Place	Number (bilateral)	Diagnoses	Success %	Follow up
Invasive Ablation						
Foltz [180]	1968	San Francisco	35 (29)	B, S, P, T, N	77%	1-9 yrs
Wilkinson [176]	1999	Massachusetts	23 (23)	S, P, T, N	43%	2-9 yrs
Yen [177]	2005	Taiwan	22 (22)	S, P, T, N	41%	1-12 mts
Strauss [178]	2017	Tel Aviv	13 (13)	N	62%	1-10 mts
Deep Brain Stimulation						
Boccard [175]	2015	Oxford	24 (24)	B, S, P, T	33%	Avg 2 yrs
Levi [181]	2019	Milan	5 (5)	B	40%	18 mts

3.3.3.4 Dorsal posterior insula

The insula cortex is postulated as key to interoception: internal awareness of bodily states.[64,182] As such, it's potential relevance to chronic pain is clear, where an aberration in the normal sense of bodily self is a characteristic, if not the primary complaint, of many sufferers. Craig's VmPo,[63] (or otherwise a medio-caudal region within or outwith VP, such as APul) is purported to project strongly and topographically to the dorsal posterior insula (DPIns).[183] Functional imaging support for a role of DPIns in pain followed,[184–186] and stereotactic stimulation has also revealed somatotopic organisation of pain responses.[187] Furthermore, lesions in this region can lead to a specific central pain syndrome: parasylvian pain.[188] As a modern development in the anatomical basis of pain, the DPIns is a plausible modern target for stereotactic targeting. First-in-man DPIns DBS took place in Oxford 2020 (currently unpublished), in a patient previously having failed PVG, VPL, and AC DBS. During simulation programming, paraesthesias (pleasant and unpleasant depending on settings) were reproducibly elicited, specifically in the painful area.

3.3.4 Summarising remarks

Perhaps the most striking impression from reviewing the history of stereotactic treatments for chronic pain is the breadth and sheer multiplicity of anatomical targets that have been approached. Second, is that despite this, none have survived or otherwise been proven to work. As such, to quote Coffey, "Investigators should accept the possibility that the treatment under study may have no benefits compared with a control group."[87] Nonetheless, the long-term pain relief reported by a large number of patients who were otherwise highly refractory to treatment remains unexplained, and naturally animates the interest of involved surgeons and maintains interest in the procedures.

The Medtronic 3380 and 3387 level 3 evidence trials were instigated in the late-1980s/early-1990s as a response to a US Food and Drug Administration ruling for this requirement. The results were subsequently buried by Medtronic, and approval was not applied for. Prior to this event, pain was a major indication for DBS. Subsequently, it was reversed to an uncommon and investigational procedure. Coffey deserves considerable credit for unearthing the data, and bringing it to public scrutiny.[87] While these trials did not reach primary endpoints for efficacy, scrutiny reveals these were not 'truly negative' trials. The prospectively defined criteria for success were arguably too ambitious, beyond what is often reported in other case series but still meaningful to many patients with nowhere else to go. Also problematic are the very high number of centres involved, introducing heterogeneity in clinical and surgical practice and technique. Many indications are also outdated from today's lens as they respond well to spinal cord stimulation or recognised to respond poorly to DBS. Lastly, less robust surgical equipment was available at the time; most importantly neuroimaging was much less advanced than it is now, and correspondingly the ability to target brain structures accurately is now much improved - implantation can even be MRI-verified.[189] As such, the firm brake applied to DBS for pain was probably not justified, or otherwise premature. However, in a way the results of the Medtronic non-controlled cohort study are somewhat moot, as large series have subsequently been published, and the appropriate modern evidential standard is the double-blind RCT.

Unfortunately, the Cleveland Clinic VS/ALIC DBS trial was negative. Nonetheless, it showed important effects in metrics that arguably should have been chosen as the primary endpoint. This perhaps reflects prematurity of the trial, informed with very limited prior experience of the procedure. Oxford is about to begin recruitment for a PAG/Vc RCT, also for post-stroke

pain. This trial has less ambitious secondary endpoints for pain improvement that reflects their long clinical experience with the procedure, and a primary endpoint capturing quality of life. One approach to improve our clinical understanding is to systematically collect multiplatform data in such trials, including advanced imaging, electrophysiology, and quantitative sensory testing (QST), and then to use observed patterns of clinical outcome correlations to inform subsequent more individualised trials. An alternative approach for explaining and developing the evidence base would be 'N-of-1 trials', where clinically successful patients are studied under controlled and blinded conditions. Ultimately, this would confirm or refute the efficacy of the treatment, informing the need for future research efforts. The results could still be generalised and fed-back through patient selection to prospective work, through detailed physiological profiling of proven therapeutic cases. In practice, however, blinding patients can often be difficult due to stimulation induced paraesthesias.

Ultimately, chronic pain is phenomenologically heterogeneous, both in symptomatology and pathophysiology, which makes treating it in a unified way unattractive. In a limited example, this point is made well in syringomyelia patients with and without pain; Ducreux et al. comprehensively demonstrate the folly of considering pain as a single entity with respect to the underlying pathologic neurophysiology.[190] They used QST and neuroimaging to map spontaneous pain, cold-allodynia, and tactile-allodynia to sensory deficit and functional imaging features. For example, they show that tactile- and cold-allodynia have different signature profiles on fMRI, and through comparisons with controls indicate that they are likely underpinned by distinct mechanisms. They also show that in spontaneous pain, the degree of thermosensory deficits (and assumed deafferentation) is high and linked to intensity of

burning pain, whereas comparatively, patients with allodynia were less thermosensory deficient. The corresponding pattern of deafferentation was later confirmed with spinal cord DTI.[191] One might conclude from this that when evoked pain is present, sensory deafferentation of thalamus is not primarily involved in pain generation. Residual spinothalamic tract neurons are postulated to function as spinal pain generator following spinal cord injury,[192] suggesting that neuromodulation at the DRG or the cord may be more sensible with evoked pain, rather than at a minimally deafferented thalamus without hyperexcitability. These studies show that features of pain such as this are likely to matter greatly when it comes to neuromodulation therapeutics aimed at converting pathologic neurophysiology. Indeed, the best results for individual patients may require a highly individualised approach more suited to adaptive or closed-loop DBS with multiple implanted electrodes.[193,194]

3.4 NEUROIMAGING OF THE THALAMUS

The thalamus has a complex architecture and is comprised of functionally and structurally distinct subnuclei. However, their bio-magnetic properties are not sufficiently different for subnuclei to be clearly distinguished with standard structural MRI contrast. 7T imaging can generate some intra-thalamic contrast, with the best published attempts using susceptibility-weighted imaging (SWI),[195] and white matter-nulled magnetisation-prepared rapid gradient echo (WMn-MP-RAGE).[196] Nonetheless, it is appreciated that different subnuclei are characterised by, in some cases, very different cortical and subcortical connectivity patterns. As such, the strategy of using diffusion MRI tractography structural connectivity estimates to inform inferential division of the nucleus into parcels has an obvious attraction. This was first

performed in Oxford in 2003, specifically using thalamo-cortical structural connectivity to parcellate the thalamus, and rendering a plausible demarcation of large subnuclear divisions, including the motor ventral lateral nucleus and the somatosensory Vc.[197,198] Since then, higher quality diffusion data has been used to generate more detailed thalamic parcellations.[199] Crucially, these non-invasive parcellations are inferential estimates with respect to nuclear subdivisions, and require invasive direct validation. To that end, DBS surgery has been leveraged to explore the resultant motor subnucleus segmentation of the Oxford algorithm, which was resultantly biologically validated.[200,201] In principle, these non-interventional studies demonstrate the real possibility of individualising targeting with this technique improving DBS outcomes for essential tremor, although this remains to be demonstrated with prospective interventional and controlled research. Segmentation of the somatosensory subnucleus has not been validated in this way, although there is some limited preliminary support from stereotactic electrophysiology in two thalami (two epileptic patients, one thalamus each).[202]

3.5 EXPERIMENTAL WORK WITH PATIENT-SPECIFIC STRUCTURAL CONNECTOMES - see *Journal of Neurosurgery*, Volume 137, Issue 1, July 2022, Pages 209-16 for associated published manuscript

As discussed in *3.2.3 Diencephalon*, surgical targeting of the thalamus for the treatment of chronic neuropathic pain has been explored since the early years of stereotactic surgery,[118] with the somatosensory Vc attracting the most investigation with DBS.[99–101,203] Results have varied widely among patients, the reasons for which are poorly understood and have held back proliferation of the treatment. While neurophysiological heterogeneity is assumed to be the major contributor to this variance,[204] an important component may well be inaccurate surgical targeting.

The Vc is not readily distinguished by modern structural T1- or T2-weighted MRI, although intra-thalamic contrast from high-field SWI merits further clinical research.[195,205,206] As such, stereotactic targeting currently relies on a generalised atlas-based approach from stereotactic coordinates grounded in the mid-commissural point (MCP). The simplicity and elegance of this approach contrasts with the complexity of individualised approaches to targeting and the numerous technical assumptions they necessarily make.[196,200,201] Nonetheless, individualised approaches, and improving them, remain appealing as non-linear three-dimensional individual differences in thalamic anatomy are recognised.[35] These are noted to be particularly significant in the posterolateral region, where the Vc is located. As such, the possible gains in targeting accuracy in lateral thalamic surgery for pain through an individualised approach are of heightened salience.

The use of individual patient diffusion MRI acquisitions to construct thalamo-cortical structural connectivity-based parcellations is an attractive strategy for achieving this, with a putative Vc being characterised by high primary somatosensory cortex connectivity. Exploring this possibility essentially requires two steps. Firstly, it requires an adequate invasive validation that the neuroimaging Vc segmentation approximates the biological Vc. Using DBS, this validation could grow from two observations: A) a reliable degree of congruence between electrodes that were stereotactically targeted towards Vc based on atlas coordinates (i.e. a traditional approach) and the diffusion MRI derived Vc parcel; and B) that electrical stimulation from these electrodes generated responses consistent with placement in the Vc (i.e. pain relief and/or paraesthesia). Secondly, it requires assessment of clinical outcomes with reference to stimulation location within both the individualised framework and within the standardised framework. The somatosensory homunculus of the Vc is surgically highly

relevant, with medio-lateral adjustments to targeting applied commensurate with the body part requiring sensory modulation.[42] Therefore, evidence for utility of individual diffusion MRI for optimising therapeutic targeting in this surgery, is best interpreted and rationalised through frameworks that take this into account. The hypothesis then follows that electrode locations classified within the individualised homuncular framework would be more coherent with clinical outcomes than when classified within the standardised homuncular framework, if indeed the diffusion data could inform improved targeting to individual patient's neuroanatomy.

3.5.1 Methods

3.5.1.1 Patients

Nineteen patients (fourteen male) with severe, regional, unilateral, medically refractory, chronic neuropathic pain (not arising from brain lesions) were scheduled for implantation of unilateral electrodes (Medtronic 3387) in the Vc, with or without a second electrode in the central grey matter. Referred by the chronic pain management service, all patients underwent assessment by a multidisciplinary team, including consultant neurosurgeon, neuropsychologist, and pain surgery advanced nurse practitioners, before being offered surgical treatment.

3.5.1.2 Surgical technique

All patients had pre-operative planning structural MRI within three months before surgery. Patients then underwent standard stereotactic implantation of DBS electrodes at the John Radcliffe Hospital.[90] A Cosman-Roberts-Wells stereotactic frame (Radionics, MA, USA) was fixed to the skull under sedation and local anaesthetic. A pre-operative computed

tomography (CT) scan was performed and fused with the preoperative MRI using Radionics Imaging Fusion and Stereoplan software (Radionics, MA, USA). Targets were then defined from coordinates grounded in the MCP using the Schaltenbrand-Wahren Atlas. In general, coordinates were chosen as AP: - 8-10 mm, vertical: 0 mm, lateral: 10-14 mm (depending on body part and with minor lateral adjustments if there was a large third ventricle).

Surgery was performed awake under local anaesthesia, using a 2.7mm twist drill craniostomy. After durotomy, CSF egress was minimised, and impedance was measured whilst passing (~30° to vertical) a Radionics electrode to the target. The DBS electrode was then passed down the same track. Final electrode position was guided by clinical assessment with intra-operative stimulation and subjective reporting by an awake patient. Patients underwent an in-patient trial using an external pulse generator for 7-14 days, followed by implantation of a permanent pulse generator or explanation, depending on the clinical result. Diffusion MRI-based analysis was carried out retrospectively.

3.5.1.3 Clinical outcomes

Patient records were reviewed to establish whether patients had achieved substantial long-term pain relief. This was defined as maintained regular use of the thalamic lead at last follow-up (a minimum of 12 months) with greater than 30% relief or a consistent description of equivalent life-improving surgical outcome. When records were insufficient, patients were contacted for evaluation. Patients were divided into 'benefit' or 'no benefit'. All patients were categorised before neuroimaging analysis was carried out.

3.5.1.4 Diffusion imaging acquisition and pre-processing

Pre-operative MRI was performed on a 1.5T Phillips Achieva using a modified spin echo sequence with SENSE parallel imaging. In plane resolution was 1.818 by 1.818 mm^2, and 64 2 mm thick slices were acquired in an interleaved fashion. Diffusion weighting (b = 1200 s/mm^2) was applied along 32 non-colinear gradient directions, with one non-diffusion weighted volume (b = 0). Correction for distortions and subject movement was carried out using the *FMRIB Software Library* (FSL; Oxford, UK).[207] The susceptibility-induced off-resonance field was estimated using *topup*.[207,208] Instead of using two b=0 spin-echo EPI with opposing PE-direction, the field was estimated from a b=0 volume and a same session structural T2-weighted scan, without any distortions. Motion and eddy currents were corrected for using *eddy*,[209,210] with outlier detection and replacement.[211] Single shell ball and stick modelling of local diffusion parameters was carried out using BEDPOSTX, with up to two crossing fibres per voxel.[212,213]

3.5.1.5 Seed and termination masks

FIRST,[214] a Bayesian model-based segmentation/registration tool in FSL,[207] was applied to same session T1-weighted MRI scans to extract thalamus masks for each patient, with boundary voxels included. The Harvard-Oxford cortical atlas was used to generate masks of the frontal pole, premotor cortex, primary motor cortex, primary somatosensory cortex, parietal cortex, and occipital pole, which were then registered to T1-weighted MRI scans using FLIRT and FNIRT.[215–218]

3.5.1.6 Tractography and parcellation

Connectivity-based hard parcellation of the operative thalamus was carried out using the '*find the biggest*' algorithm in FSL with the above cortical classifiers (Fig.2).[197] Probabilistic tractography was carried out using PROBTRACX.[212,213]

3.5.1.7 Implanted electrode array

Post-operative CT images were registered to 1 mm isotropic T1-weighted MRI using FLIRT.[215–217] The electrode array was estimated based on CT artefacts and known dimensions: assessed in the transverse plane, the most inferior artefact was discarded as the lead tip, and the array assigned to the superior 10 slices. The array was modelled as a 2x2 mask in each transverse slice, placed at the artefact centre: overall, a 40-voxel array mask. This is an overestimate due to voxel dimensions and to ensure capture of the array, accounting for uncertainty in artefact-lead localisation.

3.5.1.8 Array - primary somatosensory cortex parcel location analysis

The array mask was overlaid on the S1 parcel and the thalamus, then assessed. Each of the 40 voxels of the array was classified as either in the S1 parcel, anterior to it, posterior to it, or not in the thalamus. Array depth was grounded to the inferior margin of thalamus at the S1 parcel and compared across patients (Fig.3).

The medial-lateral position of the array with respect to the S1 parcel was quantified. This was carried out in the transverse plane at every slice where the array mask included S1 parcel voxels, was directly adjacent to the S1 parcel anteriorly or posteriorly, or was medial or lateral to the S1 parcel. The distance (M) between medial voxels and the medial margin, and the

distance (L) between lateral voxels and the lateral margin were calculated. At each level (L-M)/(L+M) was calculated: i.e. generating a scale where 0 = central, 1 = medial margin, -1 = lateral margin (Fig.4). Following this, the average of every valid level was calculated for each patient.

I observed that in all patients treated with thalamic stimulation for arm pain, the S1-thalamic connectivity density map demonstrated a clear medial-lateral connectivity gradient (see Fig.2A for example). In order to validate the above medial-lateral quantification method, I utilised this feature. The number of streamlines ('density') at each array voxel was normalised by dividing by the mean of all non-zero thalamic voxels in that patient's map. This was performed so that array-S1 connectivity could be assessed relative to the thalamic topography. These normalised streamlines were summed across the whole array, compared across arrays, and compared to the results of the above medial-lateral quantification (Fig.5).

3.5.1.9 Stereotactic coordinates

Retrospectively, anterior commissure - posterior commissure (AC-PC) coordinates of the electrode array were calculated from fused post-operative CT - pre-operative MRI, using Neuroinspire software (Renishaw, UK).

3.5.2 Results

3.5.2.1 Clinical outcomes

Ten of nineteen patients achieved long-term pain relief attributed to thalamic stimulation (Table 4). Patients without benefit included three patients with arm pain (all explanted due to lack of benefit), one patient with leg pain (explanted due to lack of benefit), one patient

with trunk pain (explanted for lack of benefit), and four patients with face pain (two explanted for lack of benefit, including one with tongue pain). Of the two who were not explanted, one reported minimal benefit, and the other received excellent long-term improvement from PAG stimulation, but never benefitted from, or established use of, the thalamic lead.

3.5.2.2 Array placement in S1 parcel

A median of 24.5 of the 40 array voxels (61%, Q_1-Q_3: 17-30) were allocated to the S1 parcel. This was 28 voxels for arm pain, 24 voxels for leg pain, and 17.5 voxels for face pain.

3.5.2.3 Array placement anterior and posterior to S1 parcel

A median of 0 of the 40 array voxels (0%, Q_1-Q_3: 0-6) were allocated anterior to the S1 parcel. This was 0.5 voxels for arm pain, 4.5 voxels for leg pain, and 0 voxels for face pain. A median of 5 of the 40 array voxels (12.5%, Q_1-Q_3:1.5-15.5) were allocated posterior to the S1 parcel. This was 11 voxels for arm pain, 3.5 voxels for leg pain, and 6 voxels for face pain. Anterior and posterior allocations were found dorsally and ventrally respectively, consistent with the typical rostro-caudal surgical trajectory. On average, arrays associated with long-term benefit had higher coverage posterior to the S1 parcel (13 voxels) than those not associated with benefit (5 voxels), with correspondingly less, on average, in the S1 parcel (19 vs 30 voxels). For patients with long-term benefit, the contacts of the most used electrode configurations had, on average, a ratio of 1:1 for S1 parcel and posterior voxels.

Table 4. Clinical data

Patient	Pathology	Region	Pre-op	Clinical outcome	Benefit Classification
A	Brachial plexus injury (avulsion)	Arm - L	2 good, 6 average, 9 NRS bad day	More than 50% pain relief at 18 mts. Uses all day.	Yes
B	Spinal cord injury (compression)	Arm > Leg - R	10 NRS	At 5 yrs 4/10 on good days, 7/10 on bad days. Continues to help him cope with pain. Still uses at 8yrs, 24/7, reporting benefit.	Yes
C	Ulnar nerve crush injury	Arm - R	10 NRS	At 6 mts 0 NRS. Delighted with the results. At 1 yr, excellent pain relief. At 2yrs stimulator working well controlling his pain. Explanted at 5 yrs due to infection.	Yes
D	Brachial plexus injury (Phantom)	Arm - R	Background 3, exacerbated to 8 NRS.	40% reduction in background pain at 1 year, with exacerbations no longer occurring. Uses all day. 70% pain relief at 8 yr follow up. Left with background pain, nothing compared to what he had before surgery.	Yes
E	Brachial plexus injury (Avulsion)	Arm - R	10 NRS, “at the end of coping”	At 3 years “cannot live without it”. At 5yrs, uses 24/7, 3 NRS and improved QOL. Uses 24/7 at 9 yrs, 5 NRS.	Yes
F	Brachial plexus injury	Arm - L	Intractable burning, severe	Initial good response, lasting less that 1 mt. Then no pain relief, and explanted at 14mts.	No
G	Brachial plexus injury	Arm - R	10 NRS	Initially good response (NRS 3) but minimal at 2yrs (NRS 9). Explanted at 4 years when NRS 10.	No
H	Phantom limb (Brachial plexus injury + amputation)	Arm - L	Excruciating, agonizing, severe	Stimulation felt in right place, but no pain relief achieved, so explanted at 6 mts.	No
I	Spinal cord injury (AVM)	Leg - R	7 NRS	40-50% relief at 3yrs	Yes
J	Spinal cord injury (syrinx)	Leg > Face - L	7-8 NRS	At 5 yrs NRS 0 at baseline and uses 24/7, but still has dysaesthesia. GIC: much better.	Yes
K	Idiopathic (possible spine injury)	Leg - R	7 NRS	At 7 yrs more than 50% pain reduction maintained with 100% coverage. Uses all day.	Yes
L	Complex limb trauma + surgeries	Leg - R	Intractable	No benefit. Leads explanted within trial.	No
M	Facial trauma	Face - R	3 good, 7 average, 10 NRS bad day	Still using 3 yrs later, but reports minimal benefit.	No
N	Trigeminal neuralgia	Face - L	10 NRS	Pain free at 15 mts. At 4yrs "stimulation has changed his life". 100% "normal pain" gone, but has occasional paroxysms of 4 NRS.	Yes
O	Trigeminal neuralgia	Face - L	5 good, 6 average, 10 NRS bad day	Painful area covered, but no pain relief. Explanted after a year due to lack of efficacy.	No
P	Trigeminal neuralgia (tooth extraction)	Face - L	7 NRS	No pain relief from thalamic lead, therefore never uses. Has very significant pain relief from PAG lead. At 4yr follow up his pain is 0 on good and 2 NRS on bad days. Same at 6 yrs.	No
Q	Trigeminal neuralgia	Face - L	10 NRS	100% pain relief post-op. Pain has steadily got worse over the years. Still uses at 9 years, 7.5 NRS. Describes surgery as a success and best surgical Tx he has had (prior MVDs).	Yes
R	Tongue pain	Face - R	Severity of pain destroyed her life, and was unable to work	No benefit. Could exacerbate pain. Leads explanted within trial.	No
S	Idiopathic	Trunk - L	9 NRS	No benefit. Leads explanted within trial.	No

NRS = 0-10 numerical rating scale, AVM = arteriovenous malformation, GIC = global impression of change scale, PAG = periaqueductal gray, Tx = treatment, MVD = microvascular decompression

3.5.2.4 Medial-lateral quantification

The median position of arrays revealed somatotopic topography for patients who benefitted from surgery, which was not evident for those who did not (Fig.3). This was not evident from AC-PC coordinates (Fig.6). The alternative method replicated the same pattern for medial-lateral quantification (Fig.5), supporting its validity. Aiming for homuncular congruence within parameters of beneficial arrays (Fig.4) and following this diffusion MRI-based individualised approach to targeting, patients F, H, M, O, P, R, S would have had their electrodes targeted more medially, and patient L more laterally, compared to following the atlas-based approach.

3.5.3 Discussion

3.5.3.1 Key findings

I validate a connectivity-based parcellation method for approximating individual patient's Vc of thalamus. The principal finding supporting this is that in the large majority of patients there was substantial overlap between estimates of electrode array location and the S1 parcel, the array having been targeted towards the Vc based on atlas coordinates. In many cases pain relief was achieved, and in others non-analgesic sensory paraesthesia occurred with stimulation. Second, the individualised Vc segmentation demonstrated potential utility for guiding stereotactic targeting to increase the yield of responders to surgery. When considered with respect to the S1 parcel, I found the medio-lateral position of the arrays generated a pattern that a) distinguished itself from atlas coordinates, and b) where congruency (as surgically intended) between painful-region and thalamic homunculus matched with long-term benefit. This invites speculation that had electrode targeting been guided by the individualised diffusion MRI-derived thalamic parcellation, more patients would have achieved long-term analgesia. Lastly, which thalamic nucleus to surgically target to treat

chronic pain remains an unresolved question, although Vc has been most popular. The seemingly non-random, homuncular-congruent locations of beneficial electrodes (and vice versa) found in this study adds support to the Vc as a legitimate target for pain modulation, and not just stimulation spread to another regional nucleus.

3.5.3.2 Connectivity-based parcellation

Substantive structural neuroanatomical information can be encoded in diffusion MRI data, and its use to reconstruct white matter tracts has been broadly validated.[219–221] Parcellation of the thalamus into subnuclei, however, while driven by diffusion MRI-derived structural connectivity estimates, hinges on classification algorithms and therefore presents a different validation issue. Such a project makes anatomic sense, results match well with anatomical atlases and known thalamo-cortical connectivity of individual parcels/subnuclei,[197,199] and results are highly reproducible within- and between-subjects.[222] However, biological validation of these inferential results is highly problematic in humans due to the unacceptable invasiveness that would be required. In addition, numerous criticisms and caveats have been applied to parcellation methodology.[223,224] DBS offers a unique opportunity to explore this technique in humans and has previously been used to give some biological validation to segmentation of the motor thalamus.[200,201] Here I extend validation of this technique to the somatosensory thalamus.

3.5.3.3 Individualised targeting

Both probabilistic [200,201] and deterministic [225,226] tractography-based methods have proved valid non-invasive individualised approaches to locating the motor thalamus, as an alternative to standard coordinates, and with the potential to optimise clinical outcomes. Deterministic

tractography has also been used to attempt imaging reconstruction of the spinothalamic tract, followed by prospective integration into target planning for PLIC stimulation in four patients with thalamic pain.[166] Their decent clinical results suggest that diffusion MRI could offer a credible data source for non-invasive identification of a patient's somatosensory thalamus, for the purpose of targeting for regional chronic pain. Connectivity-based parcellation using probabilistic tractography is the principal way to divide up each patients' thalamus to assess that.

Pursuing individualised targeting of the Vc is particularly germane given its variability[35] and possible pathological changes.[140] The prevailing assumption is that in most cases where thalamic stimulation fails to significantly reduce neuropathic pain, the major factor is a mismatch of suitability between the treatment and the individual's neuropathophysiology. Nonetheless, it is notable that all ten patients who benefitted from thalamic stimulation long-term had electrode arrays placed appropriately with respect to a homuncular interpretation of the S1 parcel. Conversely, under the same system of interpretation, there is a case to be made that eight patients had electrodes inappropriately or sub-optimally placed and did not benefit from surgery. This leaves only one patient (G) without long-term benefit with an appropriately placed electrode. However, he actually had a moderately beneficial surgical course before being explanted at four years, which may bear on this result. As such, my analysis of this case series challenges the aforementioned assumption, raising the possibility that surgical targeting may account for a majority of variance in clinical outcomes.

A credible surgical strategy follows from my results. First, pre-operative imaging is collected and processed to obtain the patient's S1 parcel, as an estimate of Vc. Secondly, based on the

region of the patient's pain, a parasagittal plane on their S1 parcel is identified to match the homunculus (Fig.4). Lastly, the electrode is aimed toward the S1 parcel in that plane, probably to the posterior margin, expecting to reach the spinal afferents that enter the Vc nucleus posteriorly.[227] Finding that therapeutic electrodes are, on average, half in, half posterior to the S1 parcel is commensurate with targeting the posterior margin, as well as long-recognised empirical surgical experience favouring more posterior placement.[161]

3.5.3.4 Regional analysis - arm

Three patients did not achieve long-term benefit (F, G, H). Patient F's array appears placed lateral, and H's very laterally within the parcel, not centrally as appropriate for arm pain. Patient G's array had similar characteristics to C and E, and although explanted at four years for lack of benefit, initial response was substantial (Table 4) with some benefit maintained for over a year. All patients who had substantial long-term benefit had electrodes passing through the central ($\Delta \approx 0$) or centro-medial ($\Delta \approx 0.5$) S1 parcel (Fig.4), matching up well with the intended Vc target for arm pain. Highest streamline counts were observed at the lateral margin of the S1 parcel in all these patients (see example in Fig.2A). As such, high relative connectivity suggests lateral placement. Indeed, this indicator (Fig.5) corroborated my quantification of the array positions in the S1 parcels (Fig.4), supporting its validity.

Regional analysis - leg

Patient J's array was positioned largely lateral to the thalamus. Given that the segmentation was generous (i.e. included boundary voxels), it is likely very little of this array was placed in the thalamus, and instead adjacent to it in the PLIC. Paraesthesias and pain relief in his leg may have been due to PLIC stimulation. Nonetheless, as a conservative radius estimate of

'activated' tissue from the electrode is 2-3 mm,[228] it is clear the most lateral cells in Vc (i.e. leg cells) would also be targeted. Patient L's array was positioned centro-medially ($\Delta > 0$) within the S1 parcel. This is likely to be more appropriate for targeting trunk or arm pain, not leg pain, and suggests an explanation for why the patient never received any benefit from stimulation and was explanted within the trial period. Both patient I's and K's arrays were arguably appropriately placed ($\Delta < 0$) within the S1 parcel (Fig.4), with major portions of their arrays in the centro-lateral or lateral parcel.

Regional analysis - face

Both patients with substantial long-term benefit from surgery had electrodes that were positioned more dorsally and medially in the thalamus, with very similar spatial relationships with respect to the S1 parcel (Fig.3). While this may be consistent with correct placement within the VPM or a nearby nucleus such as the anterior pulvinar, the dorsal position indicates it could be more consistent with placement in intralaminar nuclei (e.g. centrolateral nucleus) that are targeted by some surgeons for treatment of pain.[124] The tongue is represented most medially within the thalamic homunculus, consistent with $\Delta \approx 1$. However, patient R's array was placed centromedially ($\Delta = 0.3$), perhaps explaining her unsuccessful surgical course, with explanation after in-patient trial.

Regional analysis - trunk

Only one patient was implanted for trunk pain, unfortunately not achieving any pain relief. My analysis revealed that the electrode was placed antero-lateral in the S1 parcel, more consistent with a location for targeting leg pain. Although highly speculative without trunk

pain patients with clinical benefit to analyse, the homunculus principle would give the expected optimal location as central within the Vc, perhaps -0.1< Δ < 0.1.

3.5.4 Limitations

The estimated overlap between array and S1 parcel was not 100% or even 75% in the overwhelming majority of patients (Q_3=74%). However, total containment of the quadripolar array in Vc would not be expected by a surgeon given the typical planned stereotactic trajectory. I also recognise that "how much" of the array in the S1 parcel being labelled as "substantial" is arbitrary. Nonetheless, my judgement is that an average greater than 50% of a 10 mm array, in parallel with the clinical effects observed, is adequate for validation.

My suggestion that the 'homuncular analysis' reveals some potential utility of connectivity-based parcellation in individualised targeting within Vc relies on the distinction between patients with 'benefit' and 'no benefit'. Classification inevitably contains some arbitrariness. The assessed information had both qualitative (e.g. failed trial) and quantitative (e.g. numerical pain scores) components, and was retrospectively classified. My classification criteria were made on grounds which I believed were clinically most meaningful, so that any results would be so framed. While classification was trivial in most patients, in two patients (G, M) different plausible criteria could have led to different classification.

Despite the above discussion of clinical benefit classification, the lack of a multidimensional pain assessment, such as the McGill Pain Questionnaire or the Brief Pain Inventory (BPI), is a significant limitation. If the study had been prospective in nature, a much more detailed protocol of psychometric data collection would have been prudent. This could have included

the BPI at specified time points of follow up. In addition, this could be supplemented by self-reporting of unidimensional pain and quality of life ratings on a daily or weekly basis via a smart phone. This is desirable as pain is highly subjective, multidimensional, and challenging to measure. It is modulated by a range of biological and psychosocial states and can change considerably day-to-day. Arguably the best foil to this is the approach outlined above, which can capture trends, reveal regression to the mean, and pick up on how different people report their pain experience. While the data in this study was retrospectively acquired, the study was designed to minimise the relevance of the limited psychometric pain outcome data available. Principally, this was achieved by segregating two groups that were convincingly discernible on clinical grounds, instead of designing a study based on continuous outcome variables. An alternative design based on the latter would arguably have been preferable but would have required the more robust multidimensional pain outcome data detailed above.

In many patients, stimulation was felt in the correct body region but did not give pain relief. By my evaluation these electrodes were sub-optimally located. This paraesthesia could be understood as local electric influence of stimulation perhaps up to 4mm radius from the electrode. However, as the relevant electro-therapeutic effects of Vc stimulation are unknown, it is difficult to interpret or predict whether pain relief should be expected from this. My analysis and interpretation rely upon the precise array location being most relevant. Precise location may be particularly relevant for non-axonal surgical effects, such as those related to adenosine[229] and astroglia.[230]

We do not perform microelectrode recordings (MERs) due to the additional operative risk, but nonetheless such data may have provided an interesting comparison with my results.

There is uncertainty regarding the clinical benefit that MERs may or may not confer; at present this is essentially speculative for Vc surgery for pain. Comparatively, here, an MR-guided individualised approach to optimising electrode location signals potential benefit, and being non-invasive, is ultimately preferable to MERs.

Different methods, algorithms, and processes of statistical inference used for rationalising a thalamic parcellation are available.[199,224] Results are likely to vary depending on these parameters, as well as the diffusion acquisition and cortical classifiers. As such, the external validity of my results to other methodologies is unknown. I did attempt some different permutations of cortical classifiers with the same algorithm, which did not yield notably different S1 parcel results.

Both the retrospective nature of this research and case series structure make conclusions about the potential surgical utility of this method inconclusive. The value of my findings is limited to highlighting the real possibility that such methods may have value in improving surgical practice, and merit broader prospective study.

3.5.4.1 Generalisability

It is likely that in all the patients studied here, there was deafferentation of primary sensory neuron input to secondary sensory neurons (with cell bodies in the Vc). As such, these results should not be extrapolated to pathology (e.g. thalamic or parasylvian pain syndromes) where this is clearly not the case.

3.6 CONCLUSIONS

Chronic neuropathic pain is phenomenologically heterogeneous and characterised by variable neurophysiological features. Nonetheless, surgical intervention at the thalamus remains an attractive treatment. Stereotactic surgery targeted to a large number of brain regions has been attempted, but only with limited success. A modern approach to surgical treatment of pain will require increasingly individualised sophisticated methods, in order to match the intervention to the pathology of the patient. Part of this will be improved targeting of specific subnuclei. With respect to Vc, while atlas-based targeting is likely adequate in many patients, an individualised approach is likely to benefit patients with thalamic anatomy deviating more from atlas standards. This experimental work presents a validation of connectivity-based parcellation as an individualised approach to the Vc. Specifically, a Bayesian model-based segmentation coupled with a diffusion tractography-based parcellation appears robust for approximating the Vc. A homuncular framework embedded in this individualised segmentation was evaluated to interpret clinical outcomes. This segmentation/parcellation, combined with an interpretation based on the thalamic homunculus, may have utility as an adjunct for stereotactic targeting of the Vc for unilateral regional neuropathic pain.

REFERENCES

1. Mehler WR. The mammalian “Pain tract” in phylogeny. Anat Rec 1957;127(2):332.
2. Bishop GH. The relation between nerve fiber size and sensory modality: phylogenetic implications of the afferent innervation of cortex. J Nerv Ment Dis 1959;128(2):89–114.
3. Lenz FA, Casey KL, Jones EG, Willis WD. The Human Pain System: Experimental and Clinical Perspectives. Cambridge: Cambridge University Press; 2010.

4. Burgess PR, Perl ER. Myelinated afferent fibres responding specifically to noxious stimulation of the skin. J Physiol 1967;190(3):541–62.

5. Georgopoulos AP. Functional properties of primary afferent units probably related to pain mechanisms in primate glabrous skin. J Neurophysiol 1976;39(1):71–83.

6. Ranson SW. The course within the spinal cord of the non-medullated fibers of the dorsal roots: A study of Lissauer's tract in the cat. J Comp Neurol 1913;23(4):259–81.

7. Kumazawa T, Perl ER. Excitation of marginal and substantia gelatinosa neurons in the primate spinal cord: Indications of their place in dorsal horn functional organization. J Comp Neurol 1978;177(3):417–34.

8. Kumazawa T, Perl ER, Burgess PR, Whitehorn D. Ascending projections from marginal zone (Lamina I) neurons of the spinal dorsal horn. J Comp Neurol 1975;162(1):1–11.

9. Light AR, Perl ER. Spinal termination of functionally identified primary afferent neurons with slowly conducting myelinated fibers. J Comp Neurol 1979;186(2):133–50.

10. Kumazawa T, Perl ER. Primate cutaneous sensory units with unmyelinated (C) afferent fibers. J Neurophysiol 1977;40(6):1325–38.

11. Ralston HJ, Ralston DD. The distribution of dorsal root axons in laminae I, II and III of the macaque spinal cord: A quantitative electron microscope study. J Comp Neurol 1979;184(4):643–83.

12. Ralston HJ. The fine structure of laminae I, II and III of the macaque spinal cord. J Comp Neurol 1979;184(4):619–41.

13. Cheema SS, Rustioni A, Whitsel BL. Light and electron microscopic evidence for a direct corticospinal projection to superficial laminae of the dorsal horn in cats and monkeys. J Comp Neurol 1984;225(2):276–90.

14. Basbaum AI, Fields HL. Endogenous pain control mechanisms: Review and hypothesis. Ann Neurol 1978;4(5):451–62.

15. Swanson LW, McKellar S. The distribution of oxytocin- and neurophysin-stained fibers in the spinal cord of the rat and monkey. J Comp Neurol 1979;188(1):87–106.

16. Mantyh PW. Connections of midbrain periaqueductal gray in the monkey. II. Descending efferent projections. J Neurophysiol 1983;49(3):582–94.

17. Hentall ID, Mesigil R, Pinzon A, Noga BR. Temporal and Spatial Profiles of Pontine-Evoked Monoamine Release in the Rat's Spinal Cord. J Neurophysiol 2003;89(6):2943–51.

18. Fields HL, Basbaum AI, Clanton CH, Anderson SD. Nucleus raphe magnus inhibition of spinal cord dorsal horn neurons. Brain Res 1977;126(3):441–53.

19. Gildenberg PL, Hirshberg RM. Limited myelotomy for the treatment of intractable cancer pain. J Neurol Neurosurg Psychiatry 1984;47(1):94–6.

20. Willis WD, Al-Chaer ED, Quast MJ, Westlund KN. A visceral pain pathway in the dorsal column of the spinal cord. Proc Natl Acad Sci 1999;96(14):7675–9.

21. Brown AG. The spinocervical tract. Prog Neurobiol 1981;17(1–2):59–96.

22. McMahon SB, Wall PD. A system of rat spinal cord lamina 1 cells projecting through the contralateral dorsolateral funiculus. J Comp Neurol 1983;214(2):217–23.

23. Menétrey D, Chaouch A, Binder D, Besson JM. The origin of the spinomesencephalic tract in the rat: an anatomical study using the retrograde transport of horseradish peroxidase. J Comp Neurol 1982;206(2):193–207.

24. Mehler WR, Feferman ME, Nauta WJH. Ascending axon degeneration following anterolateral cordotomy. An experimental study in the monkey. Brain 1960;83(4):718–50.

25. Wiberg M, Westman J, Blomqvist A. Somatosensory projection to the mesencephalon: An anatomical study in the monkey. J Comp Neurol 1987;264(1):92–117.

26. Haber LH, Moore BD, Willis WD. Electrophysiological response properties of spinoreticular neurons in the monkey. J Comp Neurol 1982;207(1):75–84.

27. Kevetter GA, Haber LH, Yezierski RP, Chung JM, Martin RF, Willis WD. Cells of origin of the spinoreticular tract in the monkey. J Comp Neurol 1982;207(1):61–74.

28. Willis WD, Kenshalo DR, Leonard RB. The cells of origin of the primate spinothalamic tract. J Comp Neurol 1979;188(4):543–73.

29. Apkarian AV, Hodge CJ. Primate spinothalamic pathways: I. A quantitative study of the cells of origin of the spinothalamic pathway. J Comp Neurol 1989;288(3):447–73.

30. Apkarian AV, Hodge CJ. Primate spinothalamic pathways: II. The cells of origin of the dorsolateral and ventral spinothalamic pathways. J Comp Neurol 1989;288(3):474–92.

31. Apkarian AV, Hodge CJ. Primate spinothalamic pathways: III. Thalamic terminations of the dorsolateral and ventral spinothalamic pathways. J Comp Neurol 1989;288(3):493–511.

32. Craig AD (Bud). Retrograde analyses of spinothalamic projections in the macaque monkey: Input to ventral posterior nuclei. J Comp Neurol 2006;499(6):965–78.

33. Craig AD (Bud), Zhang E-T. Retrograde analyses of spinothalamic projections in the macaque monkey: Input to posterolateral thalamus. J Comp Neurol 2006;499(6):953–64.

34. Mai JK, Majtanik M. Toward a Common Terminology for the Thalamus. Front Neuroanat 2019;12:114.

35. Morel A, Magnin M, Jeanmonod D. Multiarchitectonic and stereotactic atlas of the human thalamus. J Comp Neurol 1997;387(4):588–630.

36. Hirai T, Jones EG. A new parcellation of the human thalamus on the basis of histochemical staining. Brain Res Rev 1989;14(1):1–34.

37. Hassler RG. Architectonic organization of the thalamic nuclei. In: Schaltenbrand G, Walker AE, editors. Stereotaxy of the Human Brain. New York: Georg Thieme; 1982. p. 140–80.

38. Ralston HJ, Ralston DD. The primate dorsal spinothalamic tract: evidence for a specific termination in the posterior nuclei (Po/SG) of the thalamus. Pain 1992;48(1):107–18.

39. Jones EG, Lensky KM, Chan VH. Delineation of thalamic nuclei immunoreactive for calcium-binding proteins in and around the posterior pole of the ventral posterior complex. Thalamus Relat Syst 2001;1(3):213–24.

40. Rausell E, Bae C, Vinuela A, Huntley G, Jones E. Calbindin and parvalbumin cells in monkey VPL thalamic nucleus: distribution, laminar cortical projections, and relations to spinothalamic terminations. J Neurosci 1992;12(10):4088–111.

41. Rausell E, Jones E. Chemically distinct compartments of the thalamic VPM nucleus in monkeys relay principal and spinal trigeminal pathways to different layers of the somatosensory cortex. J Neurosci 1991;11(1):226–37.

42. Lenz FA, Dostrovsky JO, Tasker RR, Yamashiro K, Kwan HC, Murphy JT. Single-unit analysis of the human ventral thalamic nuclear group: somatosensory responses. J Neurophysiol 1988;59(2):299–316.

43. Boivie J. An anatomical reinvestigation of the termination of the spinothalamic tract in the monkey. J Comp Neurol 1979;186(3):343–69.

44. Jones EG. The thalamic matrix and thalamocortical synchrony. Trends Neurosci 2001;24(10):595–601.

45. Willis WD, Zhang X, Honda CN, Giesler GJ. A critical review of the role of the proposed VMpo nucleus in pain. J Pain 2002;3(2):79–94.

46. Graziano A. Widespread Thalamic Terminations of Fibers Arising in the Superficial Medullary Dorsal Horn of Monkeys and Their Relation to Calbindin Immunoreactivity. J Neurosci 2004;24(1):248–56.

47. Mufson EJ, Mesulam MM. Thalamic connections of the insula in the rhesus monkey and comments on the paralimbic connectivity of the medial pulvinar nucleus. J Comp Neurol 1984;227(1):109–20.

48. Burton H, Jones EG. The posterior thalamic region and its cortical projection in new world and old world monkeys. J Comp Neurol 1976;168(2):249–301.

49. Vartiainen N, Perchet C, Magnin M, et al. Thalamic pain: anatomical and physiological indices of prediction. Brain 2016;139(3):708–22.

50. Bastuji H, Frot M, Mazza S, Perchet C, Magnin M, Garcia-Larrea L. Thalamic Responses to Nociceptive-Specific Input in Humans: Functional Dichotomies and Thalamo-Cortical Connectivity. Cereb Cortex 2016;26(6):2663–76.

51. Stevens RT, Hodge CJ, Apkarian AV. Medial, Intralaminar, and Lateral Terminations of Lumbar Spinothalamic Tract Neurons: A Fluorescent Double-Label Study. Somatosens Mot Res 1989;6(3):285–308.

52. Jones EG, Lenz FA, Casey KL, Willis WD, editors. Terminations within the thalamus: Organization of the central pain pathways. In: The Human Pain System: Experimental and Clinical Perspectives. Cambridge: Cambridge University Press; 2010. p. 64–195.

53. Royce GJ, Bromley S, Gracco C, Beckstead RM. Thalamocortical connections of the rostral intralaminar nuclei: An autoradiographic analysis in the cat. J Comp Neurol 1989;288(4):555–82.

54. Royce GJ, Mourey RJ. Efferent connections of the centromedian and parafascicular thalamic nuclei: An autoradiographic investigation in the cat. J Comp Neurol 1985;235(3):277–300.

55. Kaufman EFS, Rosenquist AC. Efferent projections of the thalamic intralaminar nuclei in the cat. Brain Res 1985;335(2):257–79.

56. Fenelon G, Francois C, Percheron G, Yelnik J. Topographic distribution of the neurons of the central complex (centre médian-parafascicular complex) and of other thalamic neurons projecting to the striatum in macaques. Neuroscience 1991;45(2):495–510.

57. Jones EG, Leavitt RY. Retrograde axonal transport and the demonstration of non-specific projections to the cerebral cortex and striatum from thalamic intralaminar nuclei in the rat, cat and monkey. J Comp Neurol 1974;154(4):349–77.

58. Head H, Holmes G. Sensory disturbances from cerebral lesions. Brain 1911;34(2–3):102–254.

59. Kendall D. Some observations on central pain. Brain 1939;62(3):253–73.

60. Llinas RR, Ribary U, Jeanmonod D, Kronberg E, Mitra PP. Thalamocortical dysrhythmia: A neurological and neuropsychiatric syndrome characterized by magnetoencephalography. Proc Natl Acad Sci 1999;96(26):15222–7.

61. Craig AD (Bud). Pain Mechanisms: Labeled Lines Versus Convergence in Central Processing. Annu Rev Neurosci 2003;26(1):1–30.

62. Craig A, Bushnell M. The thermal grill illusion: unmasking the burn of cold pain. Science 1994;265(5169):252–5.

63. Craig AD, Bushnell MC, Zhang E-T, Blomqvist A. A thalamic nucleus specific for pain and temperature sensation. Nature 1994;372(6508):770–3.

64. Craig AD. How do you feel? Interoception: the sense of the physiological condition of the body. Nat Rev Neurosci 2002;3:655–66.

65. Roeder Z, Chen Q, Davis S, Carlson JD, Tupone D, Heinricher MM. Parabrachial complex links pain transmission to descending pain modulation: PAIN 2016;157(12):2697–708.

66. DeSalles AAF, Katayama Y, Becker DP, Hayes RL. Pain suppression induced by electrical stimulation of the pontine parabrachial region. J Neurosurg 1985;62(3):397–407.

67. Katayama Y, Tsubokawa T, Hirayama T, Yamamoto T. Pain Relief following Stimulation of the Pontomesencephalic Parabrachial Region in Humans: Brain Sites for Nonopiate-Mediated Pain Control. Stereotact Funct Neurosurg 1985;48(1–6):195–200.

68. Hodge CJ, Apkarian AV. Inhibition of dorsal-horn cell responses by stimulation of the Kölliker-Fuse nucleus. J Neurosurg 1986;65(6):825–33.

69. Young RF, Tronnier VM, Rinaldi PC. Chronic stimulation of the Kölliker-Fuse nucleus region for relief of intractable pain in humans. J Neurosurg 1992;76(6):979–85.

70. Walker AE. Mesencephalic tractotomy: a method for the relief of unilateral intractable pain. Arch Surg 1942;44(5):953.

71. Mazars G, Pansini A, Chiarelli J. Coagulation du faisceau spino-thalamique et du faisceau quinto-thalamique par stéréotaxie — Indications — Résultats. Acta Neurochir (Wien) 1960;8(2):324–6.

72. Shieff C, Nashold BS. Stereotactic Mesencephalic Tractotomy for the Relief of Thalamic Pain. Br J Neurosurg 1987;1(3):305–10.

73. Drake CG, McKenzie KG. Mesencephalic Tractotomy for Pain: Experience with Six Cases. J Neurosurg 1953;10(5):457–62.

74. Amano K, Iseki H, Notani M, et al. Rostral Mesencephalic Reticulotomy for Pain Relief Report of 15 Cases. In: Gillingham FJ, Gybels J, Hitchcock E, Rossi GF, Szikla G, editors. Advances in Stereotactic and Functional Neurosurgery 4. Vienna: Springer Vienna; 1980. p. 391–3.

75. Reynolds DV. Surgery in the Rat during Electrical Analgesia Induced by Focal Brain Stimulation. Science 1969;164(3878):444–5.

76. Hosobuchi, Y, Adams JE, Linchitz R. Pain Relief by Electrical Stimulation of the Central Gray Matter in Humans and Its Reversal by Naloxone. Science 1977;197(4299):5.

77. Richardson DE, Akil H. Pain reduction by electrical brain stimulation in man. Part 1: Acute administration in periaqueductal and periventricular sites. J Neurosurg 1977;47(2):178–83.

78. Richardson DE, Akil H. Pain reduction by electrical brain stimulation in man. Part 2: Chronic self-administration in the periventricular gray matter. J Neurosurg 1977;47(2):184–94.

79. Hosobuchi Y, Rossier J, Bloom F, Guillemin R. Stimulation of human periaqueductal gray for pain relief increases immunoreactive beta-endorphin in ventricular fluid. Science 1979;203(4377):279–81.

80. Akil H, Richardson D, Hughes J, Barchas J. Enkephalin-like material elevated in ventricular cerebrospinal fluid of pain patients after analgetic focal stimulation. Science 1978;201(4354):463–5.

81. Young RF, Chambi VI. Pain relief by electrical stimulation of the periaqueductal and periventricular gray matter. J Neurosurg 1987;66(3):364–71.

82. Young RF, Bach FW, Van Norman AS, Yaksh TL. Release of /3-endorphin and methionine-enkephalin into cerebrospinal fluid during deep brain stimulation for chronic pain. J Neurosurg 1993;79(6):816–25.

83. Fessler R, Brown F, Rachlin, Mullan S, Fang V. Elevated beta-endorphin in cerebrospinal fluid after electrical brain stimulation: artifact of contrast infusion? Science 1984;224(4652):1017–9.

84. Sims-Williams H, Matthews JC, Talbot PS, et al. Deep brain stimulation of the periaqueductal gray releases endogenous opioids in humans. NeuroImage 2017;146:833–42.

85. Pereira EAC, Wang S, Peachey T, et al. Elevated gamma band power in humans receiving naloxone suggests dorsal periaqueductal and periventricular gray deep brain stimulation produced analgesia is opioid mediated. Exp Neurol 2013;239:248–55.

86. Hosobuchi Y. Tryptophan reversal of tolerance to analgesia induced by central grey stimulation. The Lancet 1978;312(8079):47.

87. Coffey RJ. Deep Brain Stimulation for Chronic Pain: Results of Two Multicenter Trials and a Structured Review. Pain Med 2001;2(3):183–92.

88. Kapural L, Peterson E, Provenzano DA, Staats P. Clinical Evidence for Spinal Cord Stimulation for Failed Back Surgery Syndrome (FBSS): Systematic Review. Spine Phila Pa 1976 2017;42(Suppl 14):S61–6.

89. Al-Kaisy A, Palmisani S, Smith TE, et al. Long-Term Improvements in Chronic Axial Low Back Pain Patients Without Previous Spinal Surgery: A Cohort Analysis of 10-kHz High-Frequency Spinal Cord Stimulation over 36 Months. Pain Med 2018;19(6):1219–26.

90. Boccard SGJ, Pereira EAC, Moir L, Aziz TZ, Green AL. Long-term Outcomes of Deep Brain Stimulation for Neuropathic Pain: Neurosurgery 2013;72(2):221–31.

91. Bittar RG, Nandi D, Carter H, Aziz TZ. Somatotopic organization of the human periventricular gray matter. J Clin Neurosci 2005;12(3):240–1.

92. Pereira EAC, Wang S, Owen SLF, Aziz TZ, Green AL. Human Periventricular Grey Somatosensory Evoked Potentials Suggest Rostrocaudally Inverted Somatotopy. Stereotact Funct Neurosurg 2013;91(5):290–7.

93. Owen SLF, Green AL, Stein JF, Aziz TZ. Deep brain stimulation for the alleviation of post-stroke neuropathic pain: Pain 2006;120(1–2):202–6.

94. Pereira EAC, Moir L, McIntyre CC, Green AL, Aziz TZ. Deep brain stimulation for central post-stroke pain: relating outcomes and stimulation parameters in 21 patients. Acta Neurochir (Wien) 2008;150(9):968.

95. Plotkin R. Results in 60 Cases of Deep Brain Stimulation for Chronic Intractable Pain. Appl Neurophysiol 1982;45(1–2):173–8.

96. Kumar K, Toth C, Nath RK. Deep Brain Stimulation for Intractable Pain: A 15-Year Experience. Neurosurgery 1997;40(4):736–47.

97. Siegfried J. Sensory Thalamic Neurostimulation for Chronic Pain. Pacing Clin Electrophysiol 1987;10(1):209–12.

98. Gybels J, Kupers R, Nuttin B. Therapeutic stereotactic procedures on the thalamus for pain. Acta Neurochir (Wien) 1993;124(1):19–22.

99. Yamamoto T, Katayama Y, Obuchi T, et al. Thalamic Sensory Relay Nucleus Stimulation for the Treatment of Peripheral Deafferentation Pain. Stereotact Funct Neurosurg 2006;84(4):180–3.

100. Pereira EAC, Boccard SG, Linhares P, et al. Thalamic deep brain stimulation for neuropathic pain after amputation or brachial plexus avulsion. Neurosurg Focus 2013;35(3):E7.

101. Levy RM, Lamb S, Adams JE. Treatment of Chronic Pain by Deep Brain Stimulation: Long Term Follow-up and Review of the Literature. Neurosurgery 1987;21(6):885–93.

102. Hamani C, Schwalb JM, Rezai AR, Dostrovsky JO, Davis KD, Lozano AM. Deep brain stimulation for chronic neuropathic pain: Long-term outcome and the incidence of insertional effect: Pain 2006;125(1):188–96.

103. Rasche D, Rinaldi PC, Young RF, Tronnier VM. Deep brain stimulation for the treatment of various chronic pain syndromes. Neurosurg Focus 2006;21(6):1–8.

104. Luft R, Olivecrona H. Experiences With Hypophysectomy in Man. J Neurosurg 1953;10(3):301–16.

105. Luft R, Olivecrona H. Hypophysectomy in the treatment of malignant tumors. Cancer 1957;10(4):789–94.

106. Backlund EO, Rähn T, Sarby B, Schryver A de, Wennerstrand J. Closed Stereotaxic Hypophysectomy by Means of 60Co Gamma Radiation. Acta Radiol Ther Phys Biol 1972;11(6):545–55.

107. Katz J MD, Levin AB MD. Treatment of Diffuse Metastatic Cancer Pain by Instillation of Alcohol into the Sella Turcica. Anesthesiol J Am Soc Anesthesiol 1977;46(2):115–20.

108. Levin AB, Katz J, Benson RC, Jones AG. Treatment of Pain of Diffuse Metastatic Cancer by Stereotactic Chemical Hypophysectomy: Long Term Results and Observations on Mechanism of Action. Neurosurgery 1980;6(3):258–62.

109. Hayashi M, Chernov M, Kouyama N, Tokumaru O, Kawakami Y. Gamma knife surgery of the pituitary: new treatment for thalamic pain syndrome. J Neurosurg 2005;102(Special Supplement):38–41.

110. Levin AB, Ramirez LF, Katz J. The use of stereotaxic chemical hypophysectomy in the treatment of thalamic pain syndrome. J Neurosurg 1983;59(6):1002–6.

111. Hayashi M, Chernov MF, Taira T, et al. Outcome After Pituitary Radiosurgery for Thalamic Pain Syndrome. Int J Radiat Oncol 2007;69(3):852–7.

112. Ramirez LF, Levin AB. Pain Relief after Hypophysectomy. Neurosurgery 1984;14(4):499–504.

113. Lovo EE, Campos F, Caceros VE, et al. Automated Stereotactic Gamma Ray Radiosurgery to the Pituitary Gland in Terminally Ill Cancer Patients with Opioid Refractory Pain. Cureus 2019;11(6):e4811.

114. Borius P-Y, Garnier SR, Baumstarck K, et al. An Open-Label, Analgesic Efficacy and Safety of Pituitary Radiosurgery for Patients With Opioid-Refractory Pain: Study Protocol for a Randomized Controlled Trial. Neurosurgery 2018;83(1):146–53.

115. Fleming AA, Todd AJ. Thyrotropin-releasing hormone- and GABA-Iike immunoreactivity coexist in neurons in the dorsal horn of the rat spinal cord. Brain Res 1994;638(1–2):347–51.

116. Merchenthaler I, Hynes MA, Vigh S, Shally AV, Petrusz P. Immunocytochemical localization of corticotropin releasing factor (CRF) in the rat spinal cord. Brain Res 1983;275(2):373–7.

117. Zheng H, Lim JY, Seong JY, Hwang SW. The Role of Corticotropin-Releasing Hormone at Peripheral Nociceptors: Implications for Pain Modulation. Biomedicines 2020;8(12):623.

118. Hécaen H, Talairach J, David M, Dell M. Coagulations limitées du thalamus dans les algies du syndrome thalamique - résultats thérapeutiques et physiologiques. Rev Neurol (Paris) 1949;81(11):917–31.

119. Jeanmonod D, Magnin M, Morel A, Siegemund M. Surgical control of the human thalamocortical dysrhythmia: I. Central lateral thalamotomy in neurogenic pain. Thalamus Relat Syst 2001;1(1):71–9.

120. Young RF, Vermeulen SS, Grimm P, et al. Gamma Knife Thalamotomy for the Treatment of Persistent Pain. Stereotact Funct Neurosurg 1995;64(Suppl. 1):172–81.

121. Young RF, Jacques DB, Mark R, Copcutt B. 794 Gamma Knife Medial Thalamotomy for Treatment of Chronic Pain: Long-term Results. Neurosurgery 2001;49(2):534–534.

122. Rinaldi PC, Young RF, Albe-Fessard D, Chodakiewitz J. Spontaneous neuronal hyperactivity in the medial and intralaminar thalamic nuclei of patients with deafferentation pain. J Neurosurg 1991;74(3):415–21.

123. Martin E, Jeanmonod D, Morel A, Zadicario E, Werner B. High-intensity focused ultrasound for noninvasive functional neurosurgery. Ann Neurol 2009;66(6):858–61.

124. Jeanmonod D, Werner B, Morel A, et al. Transcranial magnetic resonance imaging–guided focused ultrasound: noninvasive central lateral thalamotomy for chronic neuropathic pain. Neurosurg Focus 2012;32(1):E1.

125. Gallay MN, Moser D, Jeanmonod D. MR-Guided Focused Ultrasound Central Lateral Thalamotomy for Trigeminal Neuralgia. Single Center Experience. Front Neurol 2020;11:271.

126. Gallay MN, Moser D, Jeanmonod D. Safety and accuracy of incisionless transcranial MR-guided focused ultrasound functional neurosurgery: single-center experience with 253 targets in 180 treatments. J Neurosurg 2019;130(4):1234–43.

127. Pirrotta R, Jeanmonod D, McAleese S, et al. Cognitive Functioning, Emotional Processing, Mood, and Personality Variables Before and After Stereotactic Surgery. Neurosurgery 2013;73(1):121–8.

128. Hariz MI, Bergenheim AT. Thalamic Stereotaxis for Chronic Pain: Ablative Lesion or Stimulation? Stereotact Funct Neurosurg 1995;64(1):47–55.

129. Krauss JK, Pohle T, Weigel R, Burgunder J-M. Deep brain stimulation of the centre median-parafascicular complex in patients with movement disorders. J Neurol Neurosurg Psychiatry 2002;72(4):546–8.

130. Sims-Williams HP, Javed S, Pickering AE, Patel NK. Characterising the Analgesic Effect of Different Targets for Deep Brain Stimulation in Trigeminal Anaesthesia Dolorosa. Stereotact Funct Neurosurg 2016;94(3):174–81.

131. Hollingworth M, Sims-Williams H, Pickering A, Barua N, Patel N. Single Electrode Deep Brain Stimulation with Dual Targeting at Dual Frequency for the Treatment of Chronic Pain: A Case Series and Review of the Literature. Brain Sci 2017;7(12):9.

132. Sano K, Yoshioka M, Ogashiwa M, Ishijima B, Ohye C. Thalamolaminotomy. Stereotact Funct Neurosurg 1966;27(1–3):63–6.

133. Fairman D, Llavallol MA. Thalamic tractotomy for the alleviation of intractable pain in cancer. Cancer 1973;31(3):700–7.

134. Hitchcock ER, Teixeira MJ. A comparison of results from center-median and basal thalamotomies for pain. Surg Neurol 1981;15(5):341–51.

135. Niizuma H, Kwak R, Hideki SI, Suzuki J, Saso S. Follow-Up Results of Centromedian Thalamotomy for Central Pain. Appl Neurophysiol 1982;45(3):324–5.

136. Steiner L, Forster D, Leksell L, Meyerson BA, Boëthius J. Gammathalamotomy in intractable pain. Acta Neurochir (Wien) 1980;52(3–4):173–84.

137. Urgosik D, Liscak R. Medial Gamma Knife thalamotomy for intractable pain. J Neurosurg 2018;129(Suppl1):72–6.

138. Lovo EE, Torres B, Campos F, et al. Stereotactic Gamma Ray Radiosurgery to the Centromedian and Parafascicular Complex of the Thalamus for Trigeminal Neuralgia and Other Complex Pain Syndromes. Cureus 2019;11(12):e6421.

139. Mark VH. Clinical Aspects of Stereotactic Thalamotomy in the Human: Part I. The Treatment of Chronic Severe Pain. Arch Neurol 1960;3(4):351–67.

140. Davis KD, Kiss ZHT, Luo L, Tasker RR, Lozano AM, Dostrovsky JO. Phantom sensations generated by thalamic microstimulation. Nature 1998;391(6665):385–7.

141. Marchand S, Kupers RC, Bushnell CM, Duncan GH. Analgesic and placebo effects of thalamic stimulation: Pain 2003;105(3):481–8.

142. Duncan GH, Kupers RC, Marchand S, Villemure J-G, Gybels JM, Bushnell MC. Stimulation of Human Thalamus for Pain Relief: Possible Modulatory Circuits Revealed by Positron Emission Tomography. J Neurophysiol 1998;80(6):3326–30.

143. Davis KD, Taub E, Duffner F, et al. Activation of the anterior cingulate cortex by thalamic stimulation in patients with chronic pain: a positron emission tomography study. J Neurosurg 2000;92(1):64–9.

144. Hosobuchi Y. Combined Electrical Stimulation of the Periaqueductal Gray Matter and Sensory Thalamus. Stereotact Funct Neurosurg 1983;46(1–4):112–5.

145. Abdallat M, Saryyeva A, Blahak C, et al. Centromedian–Parafascicular and Somatosensory Thalamic Deep Brain Stimulation for Treatment of Chronic Neuropathic Pain: A Contemporary Series of 40 Patients. Biomedicines 2021;9(7):731.

146. Mehler WR. The Posterior Thalamic Region in Man. Confin Neurol 1966;27(1–3):18–29.

147. Hassler R. Die zentralen Systeme des Schmerzes. Acta Neurochir (Wien) 1960;8(4):353–423.

148. Mayanagi Y, Bouchard G. Evaluation of Stereotactic Thalamotomies for Pain Relief with Reference to Pulvinar Intervention. Stereotact Funct Neurosurg 1976;39(3–4):154–7.

149. Laitinen L. Anterior Pulvinotomy in the Treatment of Intractable Pain. In: Gillingham FJ, Hitchcock ER, editors. Advances in Stereotactic and Functional Neurosurgery 2. Vienna: Springer Vienna; 1977. p. 223–5.

150. Yoshii N, Mizokami T, Ushikubo T, Kuramitsu T, Fukuda S. Long-Term Follow-Up Study after Pulvinotomy for Intractable Pain. Stereotact Funct Neurosurg 1980;43(3–5):128–32.

151. Yoshii N, Fukuda S. Several Clinical Aspects of Thalamic Pulvinotomy. Stereotact Funct Neurosurg 1976;39(3–4):162–4.

152. Heimburger RF. Electrical Stimulation Across the Midline and Between Basal Ganglion Nuclei. Stereotact Funct Neurosurg 1989;52(2–4):227–33.

153. Whittle IR, Jenkinson JL. CT-guided stereotactic antero-medial pulvinotomy and centromedian-parafascicular thalamotomy for intractable malignant pain. Br J Neurosurg 1995;9(2):195–200.

154. Sprenger T, Seifert CL, Valet M, et al. Assessing the risk of central post-stroke pain of thalamic origin by lesion mapping. Brain 2012;135(8):2536–45.

155. Montes C, Magnin M, Maarrawi J, et al. Thalamic thermo-algesic transmission: ventral posterior (VP) complex versus VMpo in the light of a thalamic infarct with central pain: Pain 2005;113(1):223–32.

156. Kim JH, Greenspan JD, Coghill RC, Ohara S, Lenz FA. Lesions Limited to the Human Thalamic Principal Somatosensory Nucleus (Ventral Caudal) Are Associated with Loss of Cold Sensations and Central Pain. J Neurosci 2007;27(18):4995–5004.

157. Krause T, Brunecker P, Pittl S, et al. Thalamic sensory strokes with and without pain: differences in lesion patterns in the ventral posterior thalamus. J Neurol Neurosurg Psychiatry 2012;83(8):776–84.

158. Richardson DE, Zorub DS. Sensory Function of the Pulvinar. Stereotact Funct Neurosurg 1970;32(2–5):165–73.

159. Yoshii N, Adachi K, Kudo T. Further Studies on the Stereotaxic Thalamotomy for Pain Relief. Tohoku J Exp Med 1970;102:225–32.

160. Lenz FA, Seike M, Richardson RT, et al. Thermal and pain sensations evoked by microstimulation in the area of human ventrocaudal nucleus. J Neurophysiol 1993;70(1):200–12.

161. Mazars GJ. Intermittent stimulation of nucleus ventralis posterolateralis for intractable pain. Surg Neurol 1975;4(1):93–5.

162. Adams JE, Hosobuchi Y, Fields HL. Stimulation of internal capsule for relief of chronic pain. J Neurosurg 1974;41(6):740–4.

163. Fields HL, Adams JE. Pain after cortical injury relieved by electrical stimulation of the internal capsule. Brain 1974;97(1):169–78.

164. Hosobuchi Y, Adams JE, Rutkin B. Chronic thalamic and internal capsule stimulation for the control of central pain. Surg Neurol 1975;4(1):91–2.

165. Namba S, Wani T, Shimizu Y, et al. Sensory and motor responses to deep brain stimulation Correlation with anatomical structures. J Neurosurg 1985;63(2):224–34.

166. Hunsche S, Sauner D, Runge MJR, et al. Tractography-Guided Stimulation of Somatosensory Fibers for Thalamic Pain Relief. Stereotact Funct Neurosurg 2013;91(5):328–34.

167. Lempka SF, Malone DA, Hu B, et al. Randomized clinical trial of deep brain stimulation for poststroke pain: DBS for Pain. Ann Neurol 2017;81(5):653–63.

168. Talbot J, Marrett S, Evans A, Meyer E, Bushnell M, Duncan G. Multiple representations of pain in human cerebral cortex. Science 1991;251(4999):1355–8.

169. Lieberman MD, Eisenberger NI. The dorsal anterior cingulate cortex is selective for pain: Results from large-scale reverse inference. Proc Natl Acad Sci 2015;112(49):15250–5.

170. Rainville P. Pain Affect Encoded in Human Anterior Cingulate But Not Somatosensory Cortex. Science 1997;277(5328):968–71.

171. Foltz L, White LE. Pain “relief” by frontal cingulotomy. J Neurosurg 1962;19(2):89–100.

172. Viswanathan A, Harsh V, Pereira EAC, Aziz TZ. Cingulotomy for medically refractory cancer pain. Neurosurg Focus 2013;35(3):E1.

173. Spooner J, Yu H, Kao C, Sillay K, Konrad P. Neuromodulation of the cingulum for neuropathic pain after spinal cord injury. J Neurosurg 2007;107(1):169–72.

174. Boccard SGJ, Fitzgerald JJ, Pereira EAC, et al. Targeting the Affective Component of Chronic Pain: A Case Series of Deep Brain Stimulation of the Anterior Cingulate Cortex. Neurosurgery 2014;74(6):628–37.

175. Boccard SGJ, Prangnell SJ, Pycroft L, et al. Long-Term Results of Deep Brain Stimulation of the Anterior Cingulate Cortex for Neuropathic Pain. World Neurosurg 2017;106:625–37.

176. Wilkinson HA, Davidson KM, Davidson RI. Bilateral Anterior Cingulotomy for Chronic Noncancer Pain. Neurosurgery 1999;45(5):1129–36.

177. Yen CP, Kung SS, Su YF, Lin WC, Howng SL, Kwan AL. Stereotactic bilateral anterior cingulotomy for intractable pain. J Clin Neurosci 2005;12(8):886–90.

178. Strauss I, Berger A, Ben Moshe S, et al. Double Anterior Stereotactic Cingulotomy for Intractable Oncological Pain. Stereotact Funct Neurosurg 2017;95(6):400–8.

179. Huang Y, Cheeran B, Green AL, Denison TJ, Aziz TZ. Applying a Sensing-Enabled System for Ensuring Safe Anterior Cingulate Deep Brain Stimulation for Pain. Brain Sci 2019;9(7):150.

180. Foltz EL, White LE. The role of rostral cingulumotomy in “pain” relief. Int J Neurol 1968;6(3–4):353–73.

181. Levi V, Cordella R, D’Ammando A, et al. Dorsal anterior cingulate cortex (ACC) deep brain stimulation (DBS): a promising surgical option for the treatment of refractory thalamic pain syndrome (TPS). Acta Neurochir (Wien) 2019;161(8):1579–88.

182. Craig AD. How do you feel — now? The anterior insula and human awareness. Nat Rev Neurosci 2009;10(1):59–70.

183. Bud Craig AD. Topographically organized projection to posterior insular cortex from the posterior portion of the ventral medial nucleus in the long-tailed macaque monkey: VMpo input to posterior insula. J Comp Neurol 2014;522(1):36–63.

184. Segerdahl AR, Mezue M, Okell TW, Farrar JT, Tracey I. The dorsal posterior insula subserves a fundamental role in human pain. Nat Neurosci 2015;18(4):499–500.

185. Craig AD, Chen K, Bandy D, Reiman EM. Thermosensory activation of insular cortex. Nat Neurosci 2000;3(2):184–90.

186. Brooks JCW, Zambreanu L, Godinez A, Craig AD (Bud), Tracey I. Somatotopic organisation of the human insula to painful heat studied with high resolution functional imaging. NeuroImage 2005;27(1):201–9.

187. Mazzola L, Isnard J, Peyron R, Guénot M, Mauguière F. Somatotopic organization of pain responses to direct electrical stimulation of the human insular cortex: Pain 2009;146(1):99–104.

188. Garcia-Larrea L, Perchet C, Creac’h C, et al. Operculo-insular pain (parasylvian pain): a distinct central pain syndrome. Brain 2010;133(9):2528–39.

189. Starr PA, Christine CW, Theodosopoulos PV, et al. Implantation of deep brain stimulators into the subthalamic nucleus: technical approach and magnetic resonance imaging–verified lead locations. J Neurosurg 2002;97(2):370–87.

190. Ducreux D, Attal N, Parker F, Bouhassira D. Mechanisms of central neuropathic pain: a combined psychophysical and fMRI study in syringomyelia. Brain 2006;129(4):963–76.

191. Hatem SM, Attal N, Ducreux D, et al. Clinical, functional and structural determinants of central pain in syringomyelia. Brain 2010;133(11):3409–22.

192. Wasner G, Lee BB, Engel S, McLachlan E. Residual spinothalamic tract pathways predict development of central pain after spinal cord injury. Brain 2008;131(9):2387–400.

193. Shirvalkar P, Sellers KK, Schmitgen A, et al. A Deep Brain Stimulation Trial Period for Treating Chronic Pain. J Clin Med 2020;9(10):3155.

194. Shirvalkar P, Veuthey TL, Dawes HE, Chang EF. Closed-Loop Deep Brain Stimulation for Refractory Chronic Pain. Front Comput Neurosci 2018;12:18.

195. Abosch A, Yacoub E, Ugurbil K, Harel N. An Assessment of Current Brain Targets for Deep Brain Stimulation Surgery With Susceptibility-Weighted Imaging at 7 Tesla. Neurosurgery 2010;67(6):1745–56.

196. Su JH, Thomas FT, Kasoff WS, et al. Thalamus Optimized Multi Atlas Segmentation (THOMAS): fast, fully automated segmentation of thalamic nuclei from structural MRI. NeuroImage 2019;194:272–82.

197. Behrens TEJ, Johansen-Berg H, Woolrich MW, et al. Non-invasive mapping of connections between human thalamus and cortex using diffusion imaging. Nat Neurosci 2003;6(7):750–7.

198. Johansen-Berg H, Behrens TEJ, Sillery E, et al. Functional–Anatomical Validation and Individual Variation of Diffusion Tractography-based Segmentation of the Human Thalamus. Cereb Cortex 2005;15(1):31–9.

199. Lambert C, Simon H, Colman J, Barrick TR. Defining thalamic nuclei and topographic connectivity gradients in vivo. NeuroImage 2017;158:466–79.

200. Akram H, Dayal V, Mahlknecht P, et al. Connectivity derived thalamic segmentation in deep brain stimulation for tremor. NeuroImage Clin 2018;18:130–42.

201. Middlebrooks EH, Tuna IS, Almeida L, et al. Structural connectivity–based segmentation of the thalamus and prediction of tremor improvement following thalamic deep brain stimulation of the ventral intermediate nucleus. NeuroImage Clin 2018;20:1266–73.

202. Elias WJ, Zheng ZA, Domer P, Quigg M, Pouratian N. Validation of connectivity-based thalamic segmentation with direct electrophysiologic recordings from human sensory thalamus. NeuroImage 2012;59(3):2025–34.

203. Hosobuchi Y, Adams JE, Rutkin B. Chronic Thalamic Stimulation for the Control of Facial Anesthesia Dolorosa. Arch Neurol 1973;29(3):158–61.

204. Hirato M, Miyagishima T, Gouda T, Takahashi A, Yoshimoto Y. Electrical Thalamic Stimulation in the Anterior Part of the Ventral Posterolateral Nucleus for the Treatment of Patients With Central Poststroke Pain. Neuromodulation 2021;24(2):361–72.

205. Xiao Y, Zitella LM, Duchin Y, et al. Multimodal 7T Imaging of Thalamic Nuclei for Preclinical Deep Brain Stimulation Applications. Front Neurosci 2016;10:264.

206. Jorge J, Gretsch F, Najdenovska E, et al. Improved susceptibility-weighted imaging for high contrast and resolution thalamic nuclei mapping at 7T. Magn Reson Med 2020;84(3):1218–34.

207. Smith SM, Jenkinson M, Woolrich MW, et al. Advances in functional and structural MR image analysis and implementation as FSL. NeuroImage 2004;23:S208–19.

208. Andersson JLR, Skare S, Ashburner J. How to correct susceptibility distortions in spin-echo echo-planar images: application to diffusion tensor imaging. NeuroImage 2003;20(2):870–88.

209. Andersson JLR, Sotiropoulos SN. An integrated approach to correction for off-resonance effects and subject movement in diffusion MR imaging. NeuroImage 2016;125:1063–78.

210. Andersson JLR, Sotiropoulos SN. Non-parametric representation and prediction of single- and multi-shell diffusion-weighted MRI data using Gaussian processes. NeuroImage 2015;122:166–76.

211. Andersson JLR, Graham MS, Zsoldos E, Sotiropoulos SN. Incorporating outlier detection and replacement into a non-parametric framework for movement and distortion correction of diffusion MR images. NeuroImage 2016;141:556–72.

212. Behrens TEJ, Woolrich MW, Jenkinson M, et al. Characterization and propagation of uncertainty in diffusion-weighted MR imaging. Magn Reson Med 2003;50(5):1077–88.

213. Behrens TEJ, Berg HJ, Jbabdi S, Rushworth MFS, Woolrich MW. Probabilistic diffusion tractography with multiple fibre orientations: What can we gain? NeuroImage 2007;34(1):144–55.

214. Patenaude B, Smith SM, Kennedy DN, Jenkinson M. A Bayesian model of shape and appearance for subcortical brain segmentation. NeuroImage 2011;56(3):907–22.

215. Jenkinson M, Smith S. A global optimisation method for robust affine registration of brain images. Med Image Anal 2001;5(2):143–56.

216. Jenkinson M, Bannister P, Brady M, Smith S. Improved Optimization for the Robust and Accurate Linear Registration and Motion Correction of Brain Images. NeuroImage 2002;17(2):825–41.

217. Greve DN, Fischl B. Accurate and robust brain image alignment using boundary-based registration. NeuroImage 2009;48(1):63–72.

218. Andersson JL, Jenkinson M, Smith S. Non-linear registration aka Spatial normalisation FMRIB Technical Report TR07JA2. FMRIB Anal Group Univ Oxf 2007;1–22.

219. Conturo TE, Lori NF, Cull TS, et al. Tracking neuronal fiber pathways in the living human brain. Proc Natl Acad Sci 1999;96(18):10422–7.

220. Lawes INC, Barrick TR, Murugam V, et al. Atlas-based segmentation of white matter tracts of the human brain using diffusion tensor tractography and comparison with classical dissection. NeuroImage 2008;39(1):62–79.

221. Schilling KG, Petit L, Rheault F, et al. Brain connections derived from diffusion MRI tractography can be highly anatomically accurate—if we know where white matter pathways start, where they end, and where they do not go. Brain Struct Funct 2020;225(8):2387–402.

222. Traynor C, Heckemann RA, Hammers A, et al. Reproducibility of thalamic segmentation based on probabilistic tractography. NeuroImage 2010;52(1):69–85.

223. Clayden JD, Thomas DL, Kraskov A. Tractography-based parcellation does not provide strong evidence of anatomical organisation within the thalamus. NeuroImage 2019;199:418–26.

224. Eickhoff SB, Thirion B, Varoquaux G, Bzdok D. Connectivity-based parcellation: Critique and implications. Hum Brain Mapp 2015;36(12):4771–92.

225. Sammartino F, Krishna V, King NKK, et al. Tractography-Based Ventral Intermediate Nucleus Targeting: Novel Methodology and Intraoperative Validation. Mov Disord 2016;31(8):1217–25.

226. King NKK, Krishna V, Basha D, et al. Microelectrode recording findings within the tractography-defined ventral intermediate nucleus. J Neurosurg 2017;126(5):1669–75.

227. Lenz FA. The ventral posterior nucleus of thalamus is involved in the generation of central pain syndromes. APS J 1992;1(1):42–51.

228. Mädler B, Coenen VA. Explaining Clinical Effects of Deep Brain Stimulation through Simplified Target-Specific Modeling of the Volume of Activated Tissue. Am J Neuroradiol 2012;33(6):1072–80.

229. Bekar L, Libionka W, Tian G-F, et al. Adenosine is crucial for deep brain stimulation–mediated attenuation of tremor. Nat Med 2008;14(1):75–80.

230. Vedam-Mai V. Deep brain stimulation and the role of astrocytes. Mol Psychiatry 2012;17:124–31.

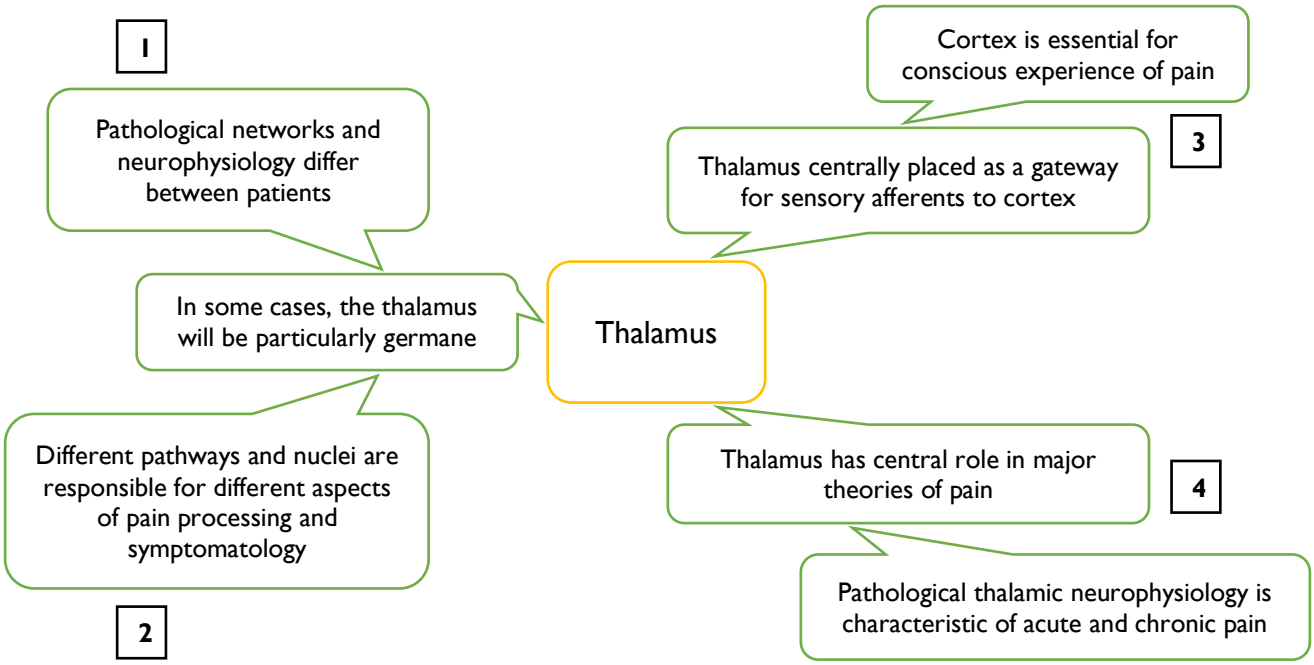

Figure 1**. Structure of arguments for continued interest in thalamic surgery to treat neuropathic pain**.

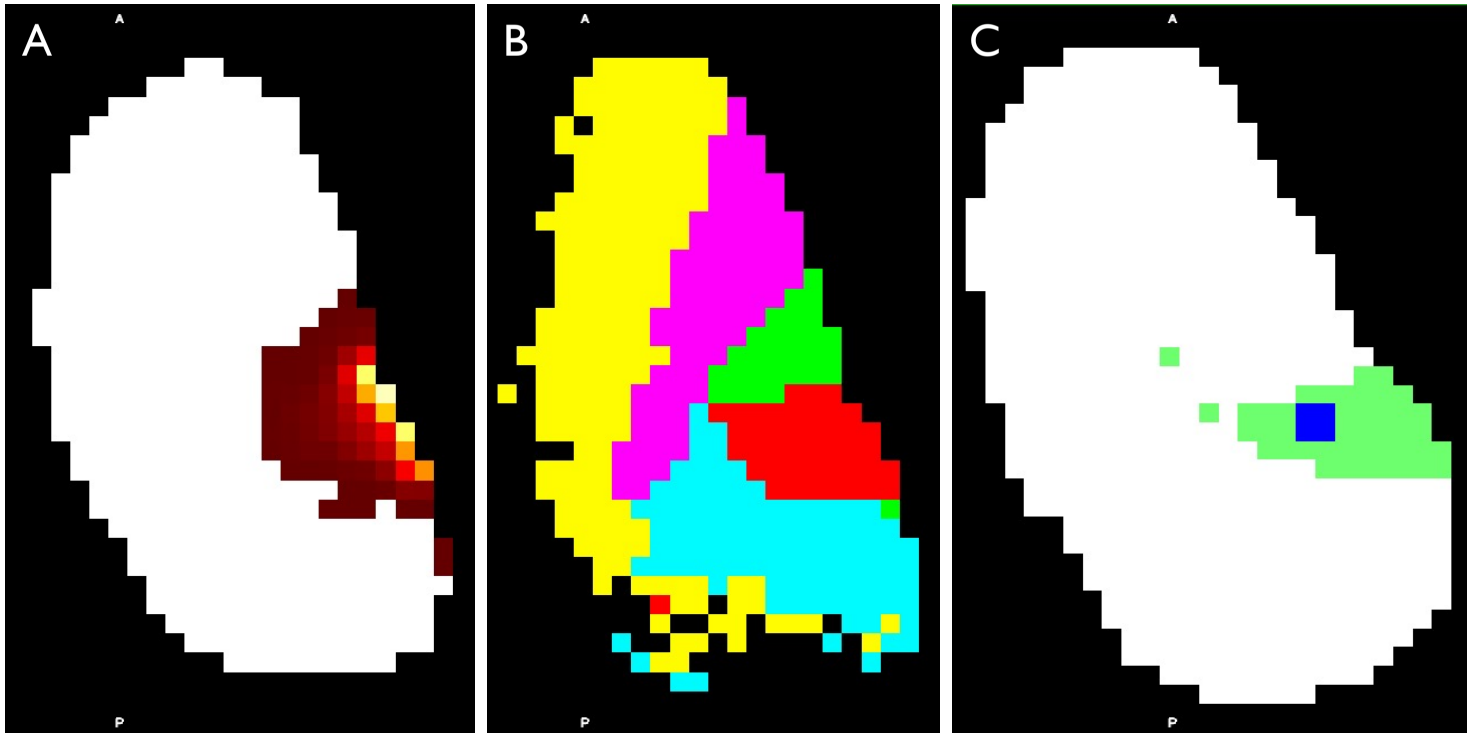

Figure 2. **Thalamic tractography and parcellation**. Examples of transverse slices of segmented left thalamus in a patient are shown. A: S1 connectivity density (*yellow* indicates high density, and *brown* indicates low). B: Parcellation (*red* indicates S1). C: S1 parcel (*green*) with an estimate of the implanted electrode array (*blue*), which was targeted on the basis of traditional coordinates.

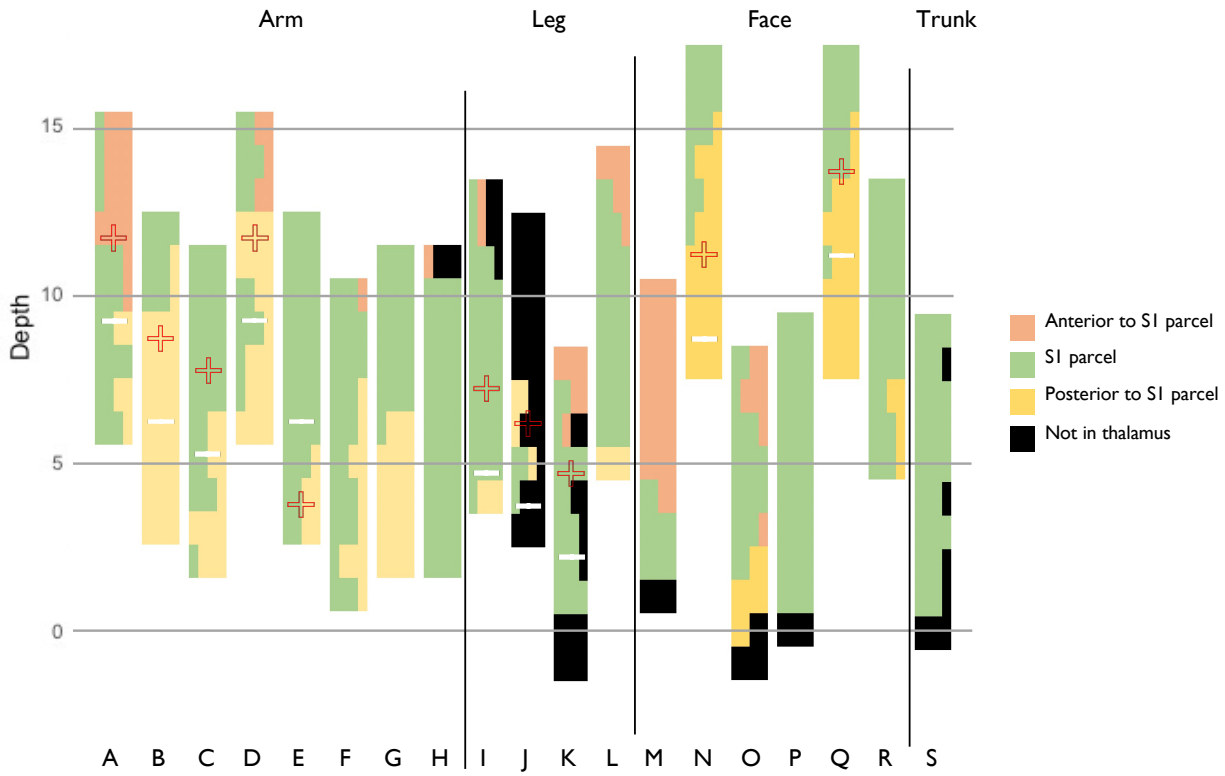

Figure 3. **Electrode array locations relative to S1 parcels**. The arrays of patients A–S are plotted according to depth (in millimetres) (0 mm = S1 parcel base), with the proportion of the array in the S1 parcel, or otherwise, indicated at each level according to colour. For patients whose thalamic array was attributed to long-term benefit, the typically active cathode (*plus sign*) and anode (*minus sign*) locations are marked.

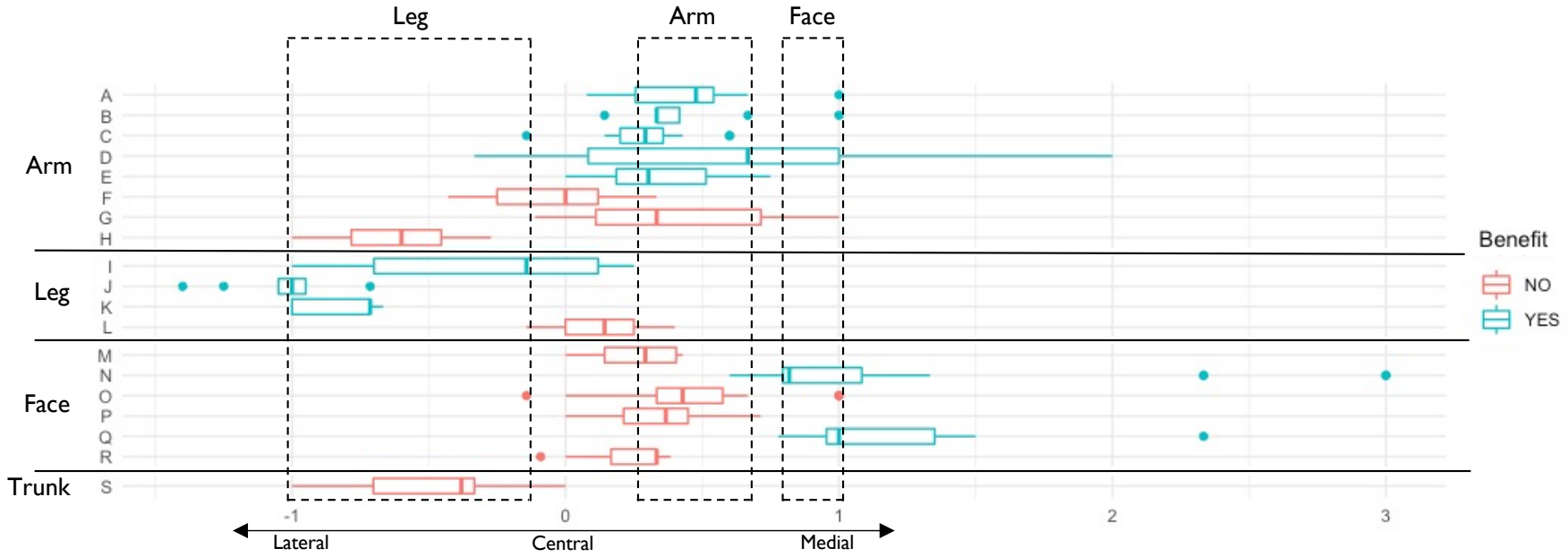

Figure 4. **Quantified mediolateral relationship of the electrode arrays with S1 parcels**. Box-and-whisker plots for patients A–S summarise the array positions (lateral [-1] to medial [1] margin of parcel) with respect to their S1 parcels, along their length. *Dots* indicate outliers. *Dotted lines* bound the maximum-minimum range for median mediolateral values of the beneficial arrays in specified regional pain. Compared across patients, a coherent homuncular pattern is demonstrated for patients with long-term benefit.

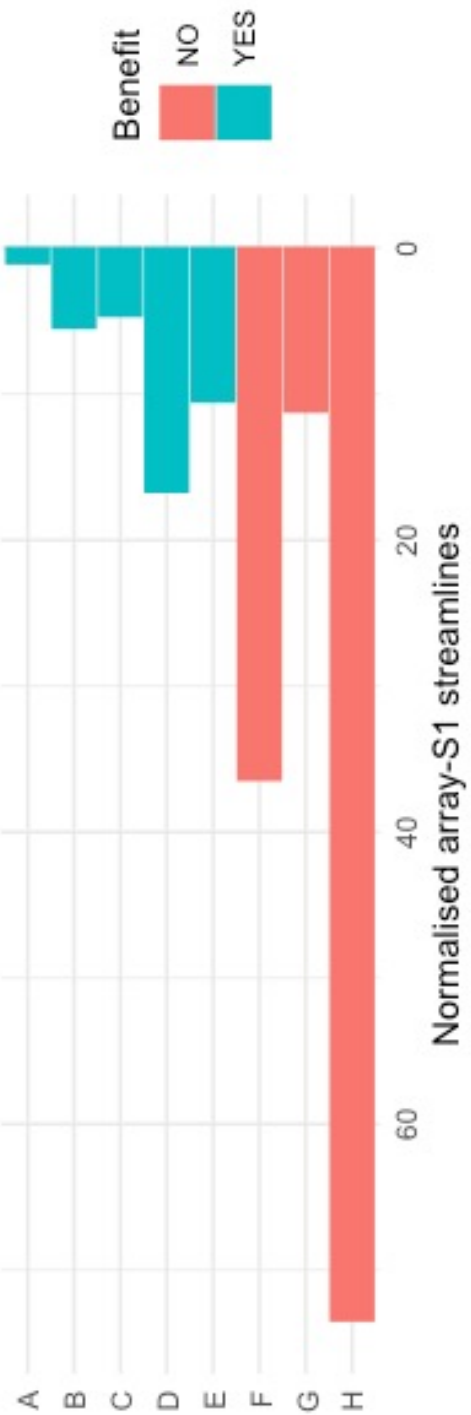

Figure 5. **Normalised total electrode array–S1 connectivity**. The second method for quantifying the mediolateral relationship of an array with the corresponding S1 parcel relies on the observed mediolateral strength gradient of S1 connectivity (high-lateral, low- medial) in patients A–H. The similar pattern to that shown in Fig. 4. supports the validity of the quantification methodology used for Fig. 4.

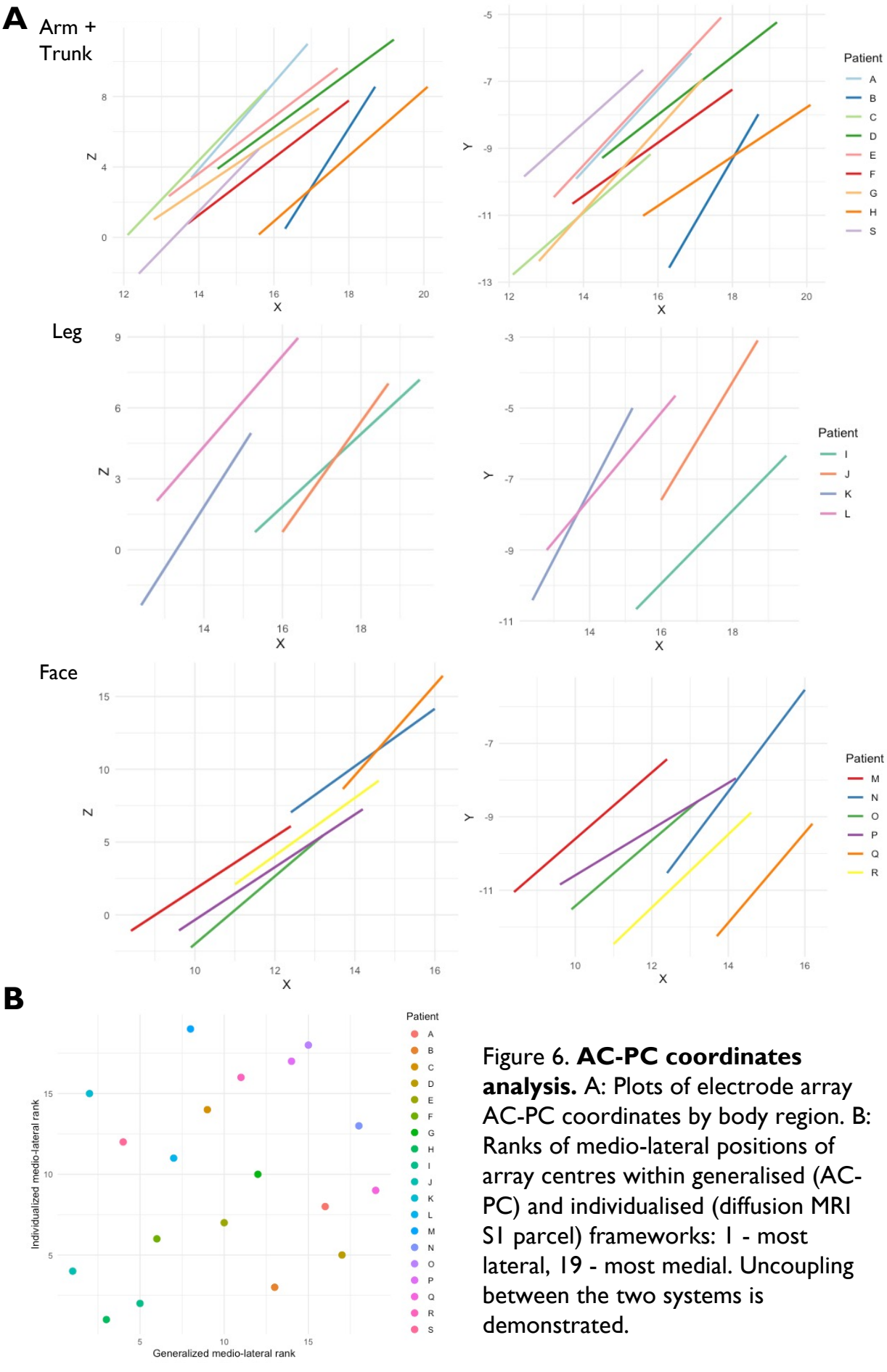

Figure 6. **AC-PC coordinates analysis.** A: Plots of electrode array AC-PC coordinates by body region. B: Ranks of medio-lateral positions of array centres within generalised (AC-PC) and individualised (diffusion MRI S1 parcel) frameworks: 1 - most lateral, 19 - most medial. Uncoupling between the two systems is demonstrated.

Reminds me of college…

~

Tipu Z. Aziz

CHAPTER 4: CERVICAL DYSTONIA

ABSTRACT

Cervical dystonia is a non-degenerative movement disorder characterised by dysfunction of both motor and sensory cortico-basal ganglia networks. Deep brain stimulation targeted to the internal pallidum (GPi) is an established treatment, but its' specific mechanisms remain elusive, and response to therapy is highly variable. Modulation of key dysfunctional networks via axonal connections is likely important. Fifteen patients underwent pre-operative diffusion-MRI acquisitions and then progressed to bilateral DBS targeting the posterior GPi. Severity of disease was assessed pre-operatively and later at follow-up. Scans were used to generate tractography-derived connectivity estimates between the bilateral regions of stimulation and relevant structures. Connectivity to the putamen correlated with clinical improvement and a series of cortical connectivity-based putaminal parcellations identified the primary motor (M1) putamen as the key node (r=0.70, p=0.004). A regression model with this connectivity and electrode coordinates explained 68% of variance in outcomes (r= 0.83, p=0.001), with both being significant explanatory variables. I conclude that modulation of the M1 putamen – posterior GPi limb of the cortico-basal ganglia loop is characteristic of successful DBS treatment of cervical dystonia. Pre-operative diffusion imaging contains additional information that predicts outcomes, implying utility for patient selection and/or individualised targeting.

4.1 NEUROANATOMY

Cervical dystonia (CD) is a rare chronic neurological disorder, characterised by involuntary contractions of the neck musculature that result in abnormal head movements and posture. It has an incidence of 1.2 per 100,000 person-years and a prevalence of 0.4%, with a female proclivity of around 80%.[1,2] While conceptualised as a focal movement disorder, less conspicuous sensory abnormalities[3] and cognitive abnormalities are also recognised,[4,5] the former of which may be an endophenotypic trait.[6]

CD is only intelligible as a network disorder (syn. circuit disorder), in so far that it is hard to reconcile what is known about the neuroanatomy and pathophysiology of dystonia without recognising the coordination and co-functioning of a number of anatomical structures. Perhaps this is illustrated most clearly from the observation of lesions across a range of different brain areas that can produce the same clinical picture: a secondary cervical dystonia.[7] Common lesion locations resulting in CD include the pons, midbrain, cerebellum, striatum, and pallidum.[7] Furthermore, lesion network mapping demonstrates there is a common functional brain network that connects these lesion regions, and this network demonstrates abnormal resting state functional connectivity in idiopathic cervical dystonia.[8] This essentially confirms a functionally-connected CD network, although it's specificity to CD has not been examined. Complementary to this, dual magnetoencephalography (MEG) and local field potentials (LFPs) have revealed sensorimotor cortico-pallidal beta coherence, pallido-temporal 4-8 Hz coherence, pallido-cerebellar 7-13 Hz coherence, with the latter inversely correlating with dystonia severity.[9]

Focal hand dystonia (FHD) and writer's cramp (WC) are both clinically common and practical for study, leading to a dystonia literature most populated by these patients. It is difficult to know what can be related to CD from findings in other focal dystonias, generalised dystonia, and dystonias where a specific genetic cause has been identified, as very little has been established regarding what neuroanatomically and neurophysiologically distinguishes them. However, it is usually assumed that these disorders are very similar, or at least that they have more in common than they are different. Acknowledging this limitation, I discuss aberrations in a number of brain regions that have been observed in dystonia.

4.1.1 Primary somatosensory cortex and somatosensory thalamus

A landmark study in dystonia, utilising a primate model of FHD, found complex changes in the primary somatosensory cortex (S1).[10] They can be summarised as dedifferentiation of cortical somatic representations, with decrease in specificity and abnormal topography. These results were subsequently supported by electroencephalography (EEG) mapping experiments in humans with FHD,[11] and by functional magnetic resonance imaging (fMRI) mapping experiments in humans with a range of focal hand and arm dystonias.[12] The latter also indicated a possible decrease in activation of the secondary somatosensory cortex. Other neuroimaging studies have found additional abnormalities, namely a decrease in left S1 grey matter in right-sided WC,[13] and an increase in the fractional anisotropy of the posterior limb of the internal capsule (PLIC) bilaterally.[14] This PLIC region was structurally connected to S1, therefore implying connection also to the somatosensory relay nucleus of thalamus (ventrocaudal nucleus, Vc). Indeed, invasive neurophysiological experiments in dystonia patients undergoing stereotactic surgery point to a reorganised mapping in the somatosensory thalamus analogous to that found in S1,[15] and that these altered

somatosensory maps have implications for the somatosensory input to motor thalamus.[16] Evidence for this same concept of a mismatched focusing of somatosensory afferents on the motor system was later generated from non-invasive electrophysiology experiments in CD and FHD.[17] Finally, the case for a pivotal role of the somatosensory system in CD is made clinically concrete by the sensory trick (or *geste antagoniste*), which is a classic, characteristic feature of CD.[18,19] Although successful sensory tricks do give rise to widespread cortical activation changes, including in frontal, parietal, and occipital lobes,[20] this process is clearly led by the somatosensory system.

4.1.2 Putamen

The putamen is the most common lesion site for secondary dystonia[21–23] and among the most common in secondary CD.[8] The previously mentioned reorganisation observed in S1 and Vc raises the question whether other regions in the common network previously discussed may feature similar anatomic and physiological pathology. To my knowledge, this has not been directly examined for the putamen, however, fMRI experiments with right-sided FHD patients have demonstrated altered left putamen somatic topography and reduced distances between some putamen body region representations bilaterally.[24] While not definitive, it suggests that pathologic dedifferentiation and topographic changes may be more widespread in the 'common network'. This has obvious implications for deep brain stimulation (DBS), as such changes are unlikely to be identical between patients, and a more individualised approach to treatment may be required. The putamen sits between the cortex (from which it is under glutamatergic excitatory control) and the pallidum (to which it sends inhibitory GABAergic projections). Cholinergic interneurons of the putamen are of disputed importance in CD. Single-photon emission computed tomography (SPECT) experiments suggest a deficit in

cholinergic nerve terminals in the putamen;[25] however, post-mortem analyses have not found a decreased number of these neurons.[26] Conversely, rodent forebrain deletion of DYT1/torsin1 leads to a selective degeneration of large cholinergic interneurons in the putamen, with corollary findings found at post-mortem in human DYT1+ dystonia patients.[27] In addition, some people with Alzheimer's disease, who are susceptible, can develop a reversible secondary CD from taking acetylcholinesterase inhibitors,[28] indicating the cholinergic system is likely to have some role in CD.

The putamen may be larger in patients with focal (cranial or hand) dystonia.[29] In particular, the middle putamen may be expanded in musicians dystonia.[30] However, voxel-based morphometry (VBM) experiments in CD have produced conflicting results by demonstrating smaller putamina.[31,32] In DYT1+ dystonia, a VBM experiment found a negative correlation between size and dystonia severity for both left and right putamina, although the same study suggested that CD putamina were larger than both controls' and DYT1+ dystonia patients'.[33] In CD, the fractional anisotropy is higher in the putamen bilaterally.[34,35] Taken together, a coherent narrative has not emerged regarding degeneration or hypertrophy of the putamen in CD.

PET experiments in CD have shown higher glucose metabolism bilaterally in the lentiform nucleus.[36,37] In right-sided FHD, fMRI data indicate decreased activation in the left posterior putamen but with increased connectivity with primary sensorimotor cortex.[38] In parallel with this, increased connectivity of the anterior putamen with the premotor cortex was observed. In CD, resting state fMRI has indicated enhanced functional connectivity between bilateral anterior putamen and the sensorimotor network.[39]

4.1.3 Pedunculopontine nucleus

The pedunculopontine nucleus (PPN) is found in the upper brainstem, bridging the midbrain and the rostral ventrolateral pontine tegmentum. Although spatially separated from the structures classically grouped as the basal ganglia, functionally the PPN is considered by many authors to be worthy of membership. GPi neurons (presumably GABA-ergic inhibitory) project to the non-cholinergic (pars dissipata) PPN,[40] and the PPN provides major ascending cholinergic and glutamatergic output to the substantia nigra.[41] The PPN also has a large output (most likely cholinergic) to the STN, and a smaller output to the pallidum,[42] in addition to descending output regulating the spinal cord.[43] Post-mortem analysis of DYT1+ dystonia patients reveal inclusion bodies in the PPN,[44] and profoundly sparse or absent choline acetylcholinesterase staining in CD patients, thereby indicating a functional cholinergic deficit in CD.[26] An experiment in the 1-methyl-4-phenyl-1,2,3,6-tetrahydropyridine (MPTP) primate model of PD demonstrated that therapeutic DBS of the GPi resulted in inhibition of the PPN.[45] This was attributed to DBS driving the nucleus, increasing inhibitory tone from the GPi on the PPN, but nonetheless, demonstrates that possible influences of GPi DBS in dystonia on the PPN should be taken seriously.

4.1.4 Primary motor and premotor cortex

It has been recognised for decades from initial work in focal task specific dystonias that there is a shift in the balance of excitation and inhibition in local circuits of M1, which ultimately result in a net increase in M1 output.[46] $GABA_B$-mediated intracortical inhibition of corticomotor cells via M1 inhibitory interneurons is a reproducible finding in primary focal dystonia, including CD.[47] In addition, $GABA_A$-mediated afferent-induced inhibition of M1, a measure of sensorimotor integration, is also reliably reduced.[47] PET imaging of $GABA_A$

receptor availability in M1 using ^{11}C-flumenazil has yielded mixed results. In a mixed dystonia cohort (dominated by DYT1+ patients), a reduction was observed at M1, premotor, S1, and secondary somatosensory (S2) cortices.[48] A reduction was observed in a right-handed FHD cohort at the left M1 and S1,[49] whereas in a CD cohort an increase was observed at the right M1, plausibly a compensatory response to loss of afferent-induced inhibition.[50] Transcranial magnetic stimulation (TMS) experiments in a mixed primary dystonia cohort indicate there is abnormal premovement M1 excitability.[51] TMS has also been used to demonstrate that motor cortex has excessive plasticity in CD.[52] Indeed, abnormal motor cortex associative plasticity is a core, replicable finding in dystonia,[53] distinguishing it from psychogenic dystonia, [54] with both LTP- and LTD-like plasticity, abnormal with respect to both gain and spatial organisation.[55] Interestingly, while increased M1 plasticity is common to CD and DYT1 dystonias, it distinguishes these patients from non-manifesting DYT1 carriers.[56] A pilot trial of repetitive TMS for CD across a range of brain areas identified M1 and dorsal premotor cortex (PMd) as targets with the greatest potential for therapeutic benefit.[57] PMd likely also plays a pathophysiologic role in CD. For example, the relationship between premotor cortex and M1 is abnormal in both CD and FHD, namely that there is enhanced PMd inhibition of M1.[58,59] VBM experiments are conflicted in their findings with respect to M1 in CD.[31,60] There is some evidence that M1 undergoes somatic topographic reorganisation in CD, similar to that observed in other brain regions.[61] It follows from these observations that excitatory output from M1, for example via the putamen through the cortical-basal ganglia pathways, will be abnormally regulated and excessive. Nambu et al. demonstrate in a patient with CD that stimulation of M1 evokes long-lasting inhibition in the pallidum, which presumably would result in decreased pallidal inhibition of the thalamus and increased thalamocortical signalling as a consequence.

4.1.5 Cortico-basal ganglia anatomic connectivity

Major anatomical connections unite the cortex, the basal ganglia, and the thalamus in descending and ascending loops.[62] These exist in parallel, partially overlapping, and functionally distinct pathways that respect cortical and topographical domains.[63] Among pathways that originate in limbic, oculomotor, and other prefrontal cortical regions, the motor, or otherwise termed sensorimotor loop, is a network of principal interest in dystonia, including CD. The motor loop largely pivots on the putamen, receiving inputs from premotor, primary motor, and somatosensory cortices.[64–66] The majority of the rostro-caudal axis of the putamen is supplied by motor and somatosensory cortical projections, with somatotopic organisation retained from the cortex,[67,68] and with individual body parts represented over a long anteroposterior extent of the nucleus.[69] The putamen sends topographically organised projections that terminate in the ventrolateral GPi,[70–73] where a form of gross somatotopy is ultimately retained.[74] Somatotopy is further maintained in the ascending loop through the thalamus to the cortex.[75] Movements related to cervical musculature appear to be represented more caudally and ventrally in the GPi, but span a considerable area. However, recognising that somatotopic disorganisation is a feature of dystonia, it is possible that this gain in anatomical entropy occurs with spatial or functional variation between individuals, throughout the basal ganglia. In other words, the gain in disorder is common, but the specific state occupied is not shared. If this were so, and matching between disordered state and surgery was relevant to the mechanism of GPi surgery, one would expect an optimum DBS target that was not generic but substantively individualised.

4.1.6 Cerebellum

While historically the cortical-subcortical circuits pertaining to cerebellum and basal ganglia were considered segregate, strong arguments now support their synthesis as parts of a unified functional anatomic schema.[76] However, irrespective of this conceptual framework, the cerebellum and the basal ganglia certainly participate intimately, particularly in the control of movement.[77] Indeed, fMRI analyses in humans indicate this relationship dysfunctions or fails in CD.[78] This is supported by pre-clinical animal research.[79] However, whether conceptually the basal ganglia or cerebellum should be considered of privileged importance in dystonia is controversial.[80,81] Lesions of the cerebellum are amongst the most common of those that result in secondary CD.[7] Interestingly, posterior fossa tumours have long been associated with new abnormal head position[82,83] and CD can even resolve following treatment of a cerebellar tumour.[84] Macroscopic atrophy is present, with or without cerebellar signs, in a minority of patients with sporadic CD.[85] However, micropathological analysis in a small cohort of CD patients ubiquitously demonstrated patchy Purkinje cell loss, with areas of focal gliosis and torpedo bodies.[86] The cerebellum is also implicated in other dystonias, particularly DYT1 dystonia. TorsinA is distributed widely through cerebellar cortex, cerebellar nuclei, Purkinje cells, and cerebellar glia;[87] and in knock-out mice, cerebellar synaptogenesis is highly susceptible to loss of TorsinA function.[88] Indeed, it is loss of function in the cerebellum, not basal ganglia, that appears to be crucial for the development of dystonia.[89] Structural cerebellothalamocortical connectivity appears to be compromised in DYT1 and DYT6 dystonia patients, whereas in non-manifesting carriers this is more preserved.[90] The motor sequency learning deficits that are found in human DYT1 dystonia, but not DYT6 dystonia, appear to be related to the integrity of this pathway, and which themselves are associated with different patterns of cerebellar activation.[91] In contrast with

these generalised dystonias, it has been suggested that focal dystonias may arise from more restricted cerebellar damage or dysfunction in a particular area.[92] The precise role of the cerebellum in CD has not been elucidated, but preliminary clinical research suggests it could be driving abnormal head rotation,[93] and electrophysiology utilising pallidal DBS electrodes demonstrates that pallido-cerebellar alpha band coherence is negatively correlated with dystonia severity.[9] Considered to be a measure of functional connectivity, this suggests that the breakdown of cerebello-basal ganglia signalling is part of the pathphysiology of CD. Lastly, the functional connectivity of therapeutic GPi DBS locations indicate that modulation of the cerebellum is highly likely.[8]

4.2 STEREOTACTIC SURGERY

Surgical targeting of the pallidum for the treatment of dystonia emerged from clinical observations in Parkinson's disease, namely improvement in dystonic features following pallidotomy.[94] Prior to this, surgical options were limited to intra- and extra-dural peripheral denervations and myomectomies.[95] DBS to the medial pallidum (GPi) for CD was first investigated in 1999 by Krauss in Bern, Switzerland [96] shortly followed in 2001 by Aziz in Oxford, England.[97] Subsequently, a number of groups reported observational data with similar results, supporting the efficacy of this surgery in CD (see Table 1), and with blinded assessments indicating this benefit is maintained long-term (52.6 % +/- 26.4 improvement in severity at five years follow-up).[98] Level 1 evidence for this surgery was established in 2005 for the treatment of primary generalised dystonia,[99] and in 2006 for primary segmental dystonia,[100] with comprehensive observational data indicating substantial long-term benefit.[101] In CD, level 1 evidence was established much later, in 2014, from a multicentre

Table 1. Summary of DBS outcomes in cervical dystonia

Author	Year	Group	Number	Target	TWSTRS severity improvement %
Kiss et al.[102]	2007	Calgary	10	GPi	42.9 +/- 29.9
Hamani et al.[103]	2008	Toronto	13	GPi	53.0 +/- 22.6
Sadnicka et al.[104]	2013	Queen's Square	11	GPi	58.4 +/- 20.8
Witt et al.[105]	2013	San Francisco / Toronto	28	GPi	50.8 +/- 27.6
Volkmann et al.[106]	2014	Multicentre RCT – Austria, Germany, Norway	62	GPi	47.0 +/- 27.1
Huebl et al.[107]	2015	Berlin / Mannheim	22	GPi	49.3 +/- 27.1
Ostrem et al.[108]	2011	San Francisco	9	STN	62.9 +/- 30.8

randomised controlled trial (RCT), the findings of which supported high frequency (HF) DBS to the GPi.[106] As such, HF-DBS to the posterior region of the GPi has become established as the treatment of choice for severe, medically refractory dystonia.[109] This CD trial randomised patients to implantation and sham stimulation or implantation and true stimulation with a 1-to-1 ratio. Toronto Western Spasmodic Torticollis Rating Scale of severity (TWSTRS-s) scores reduced by 5.1 points (SD = 5.1) in the stimulation arm and reduced by 1.3 points (SD = 2.4) in the sham arm at three months follow-up. The mean between group difference was 3.8 points (95% CI, 1.8 to 5.8), with a mean baseline of 20.4 points. This amounts to ~20% average

improvement in dystonia severity at three months, which is likely to increase over the first year of treatment but probably peaking at less than the ~50% typically measured in observational studies (see Table 1). However, clinical improvement is highly variable, with typical series recording a spread of patients from those who suffer a small deterioration and those whose dystonia is almost completely resolved. The reasons for this are not understood,[105] but their elucidation is crucial for improving both patient selection and the surgical procedure (e.g. individualised targeting). These unknowns animate the experimental work of this chapter.

Not dissimilarly to the inception of GPi DBS for dystonia, the targeting of the STN was arrived at from observations in PD.[110,111] Promising results were observed with STN DBS in generalised and segmental dystonia,[112,113] with three main arguments advanced by its advocates: a) effects of DBS are observed immediately, allowing better stimulation parameter-symptom matching; b) some patients are GPi DBS refractory or poorly responding, and/or experience persistent gait and fine motor side effects (e.g. bradykinesia);[107] and c) observational data indicate clinical improvement is greater with STN DBS than GPi DBS. These arguments have been given some further support from a small (twelve-patient) double-blind cross-over RCT of STN and GPi DBS in a mixed CD and generalised dystonia cohort.[114] There are too many limitations to this study to make any firm conclusions, but it does serve to suggest that STN DBS is unlikely to be greatly inferior to GPi DBS, and that there could even be a role for dual STN-GPi DBS. The first application of STN DBS to CD was in 2005 by Baltuch in Pennsylvania,[115] and then explored most extensively by Starr in San Francisco.[108,116] Indeed, comparative observational data from blinded assessors does indicate a greater benefit from STN DBS than GPi DBS. However, such a comparison should be cautious, as STN DBS series

data on CD is currently only available from one group (not including data from a Chinese group reporting on Meige syndrome patients with limited CD, showing a mean of 74% improvement on the Burke-Fahn-Marsden Dystonia Rating Scale at a minimum of 1 year follow-up).[117] In addition, despite favourable results, they represent only level 3 evidence. Therefore, as the clinical alternative (GPi DBS) is supported by level 1 evidence, STN DBS cannot be recommended other than strictly on a research basis or as a second-line surgical therapy following failure or therapeutic inadequacy of GPi DBS. Future robust RCTs to assess STN DBS efficacy in CD would be welcome and timely, but there are open questions on the most appropriate strategy. For example, there are ethical questions about implanting DBS electrodes into CD patients STNs when level 1 evidence for surgery to the GPi is established. Dual implantation RCTs (i.e. an STN versus GPi trial powered for non-inferiority assessment) would be singularly attractive, if it were not for the inability to disambiguate implantation effects from the nucleus not being stimulated (e.g. stun effect, microlesion effect, astrogliosis reaction), and the additional hardware expenses of such a trial. The trial design disposed to the simplest interpretation would be STN DBS versus sham, with a protocol obligation to offer a second operation if a) the trial is negative, b) the trial is positive but with 95% CIs that are less than the 2014 GPi DBS trial,[106] or c) if an individual patient has not benefitted from surgery.

4.2.1 Mechanisms of high frequency deep brain stimulation

4.2.1.1 The role of the globus pallidus interna

The GPi consists mostly of GABA-ergic inhibitory neurons that sources afferents from a range of subcortical structures including the substantia nigra, caudate, putamen, STN, PPN, dorsal raphe, parafasicular nucleus, zona incerta, medial and lateral subthalamic tegmentum,

parabrachial nuclei, and locus coeruleus.[118] Conversely, its' inhibitory output is simpler, focused primarily on the anterior ventrolateral thalamus (ventral oralis anterior and posterior – Voa, Vop).

As previously mentioned, the GPi target was not arrived at from an understanding of dystonia pathophysiology and functional neuroanatomy but instead was largely down to clinical observation. Nonetheless, since instituted, access to the GPi for microelectrode recordings, LFPs, and electrical stimulation in CD patients, has been instrumental in probing its physiology. For example, it appears GPi neurons in dystonia patients have widened somatosensory receptive fields, indicating a form of somatosensory reorganisation[119,120] similar to the somatotopic disorganisation observed in DYT1+ mice.[121] LFP recordings have been extensively utilised with the objective of identifying an electrophysiologic signature of dystonia that may give an insight into the underlying pathology and perhaps improve treatment. Tang et al. found no difference in mean external pallidum (GPe) neuronal firing rate between CD and PD but, conversely, found a lower GPi rate in CD (these differences were limited to ventral GPi).[122] GPi mean neuronal firing rates are 71-72Hz in CD,[122,123] which is similar to healthy non-human primates, much higher than generalised dystonia, and much lower than in PD. Moll et al. suggest that in CD this may be arrived at by hyperactivity of both indirect and direct pathways, the former of which raises GPi activity and the latter of which lowers GPi activity.[123] Conflicting with Tang et al.[122] they observed lower firing rates in the GPi contralateral to the side of head turning, an incongruity which they speculate to be attributed to the relative sampling of the neck-representation neurons of the GPi. If accurate, this could represent greater overactivity of the direct pathway (cortico-striato-pallidal transmission) in the GPi controlling the hypertonic contractions that manifest as head and neck deviations.

Moll et al. also found dominant LFP spectral components in the theta-alpha range, with higher alpha power in the GPe than GPi, and higher theta power in the GPi then GPe, along with GPi single cell recordings of theta-oscilatory cells with unusual bursting characteristics. Silberstein et al. analysed a mixed focal and generalised dystonia cohort, and concluded that greater 4-12 Hz band power (theta-alpha) and less 11-30 Hz band power (beta) is present in the dystonia pallidum than the PD pallidum.[124] This was subsequently replicated by others.[125] This was later assessed further by Liu et al. with the assistance of electromyograms (EMGs) and physical manoeuvres to parse the sensory and motor components of pallidal dystonia LFPs. Initially they demonstrated that EMG relating to phasic dystonic movements, but not sustained hypertonic movements, showed coherence with pallidal LFPs around a burst frequency of 4.8 Hz.[126] Further research revealed increased synchronisation in the 3-20 Hz band (peaking in the 3-8 Hz theta band) associated with hypertonic muscle spasms (preceding them by ~320 ms), and desynchronisation during passive movement, whereas voluntary movement was associated with increased gamma (30-90 Hz) activity.[127] These results led the authors to postulate that theta-alpha activity was responsible for generating rhythmic dystonia symptoms (characteristic of phasic-dominant CD), and that modulation of this band may serve as the basis for the *geste antagoniste*. Investigation specifically of the *geste* supports this. A successful manoeuvre is accompanied by desynchronisation in both 6-8 Hz and the beta band in the pallidum and sensorimotor cortical regions. While desynchronisation of the beta band also accompanies a dummy manoeuvre, synchronisation in the 4-6 Hz band is observed, thereby advancing the case for an important role of pallidal theta.[128] MEG-LFP investigations of dystonia replicate the core finding of sensorimotor cortico-pallidal beta coherence; however, more interestingly, pallido-cerebellar 7-13Hz (theta/alpha) coherence is also observed, which inversely correlates with dystonia severity.[9] Similarly, the normative

resting state functional connectivity of therapeutic GPi DBS locations in CD is negative with respect to S1 and positive with respect to cerebellum.[8]

Overall, this points to two different pathophysiological limbs of a functional network, centred on the pallidum, and both candidates for the therapeutic mechanism of GPi DBS. Clinically, there appears to be some differentiation in the respective response of phasic-dominant and tonic-dominant CD to HF-GPi DBS, with the former perhaps responding more favourably.[105,129] The findings of Liu et al. were extended by Barow et al., who while replicating findings that theta-alpha (4-12 Hz) coherence between EMG and pallidal LFPs is mostly a feature of phasic-dominant rather than tonic-dominant CD, also crucially show that this coherence is suppressed by HF-DBS to the GPi.[130] Their EEG data also suggest that HF-DBS results in pallidal-M1/S1 decoherence in this frequency band (theta-alpha), pointing to a possible mechanistic feature of DBS. Structurally it is likely this would be anatomised in the cortico-basal ganglia loops, but it is unclear whether this would be mediated 'backward' via the putamen or 'forward' via the thalamus.

In summary, research from a range of groups have identified theta-alpha oscillations as of particular relevance to dystonia, and CD specifically. As of writing, this has most recently culminated in the proposal of pallidal theta (4-12 Hz) as a physiomarker (syn. biomarker) in CD, with the possible potential of guiding intraoperative DBS placement, guidance of stimulation parameters, or explicitly in a closed-loop design.[131] In their study of 27 CD patients, Neumann et al. replicated a number of previous findings (such as LFP theta–EMG coherence), but also demonstrated a correlation between pre-operative TWSTRS severity and both theta peak power (r~0.4) and interhemispheric pallidal theta coherence (r~0.5).

Interestingly, the same theta correlations were observed with TWSTRS severity improvement (absolute and relative). These theta power signals were integrated with structural neuroimaging analysis to demonstrate (perhaps unsurprisingly since it correlated with clinical improvement) that peak theta power mapped to the posterior third of the GPi (of note, a region considered to be characterised by M1 connectivity in cortico-basal ganglia-thalamo-cortical loops),[132] in proximity to 'sweet spots' identified by other authors. As such, it is expected that utilisation of GPi-theta will play a prominent role in the next generation of DBS innovation in CD. However, in this aim, it is only in parallel (and not direct) competition with non-invasive imagining techniques that could improve pre-operative targeting and patient selection. In addition, while theta-suppression appears to be a mechanism of HF-DBS in these patients, many questions pertaining to the mechanism of action remain unanswered - not the least whether DBS acts primarily through modulation of the motor system, the sensory system, or both. Sadnicka et al. investigated the effect of GPi HF-DBS on temporal discrimination thresholds (shortest time interval between two stimuli that are distinguished as separate),[104] a metric of sensory processing that is robustly abnormal in CD.[3] This study demonstrated that DBS did not correct these sensory processing abnormalities despite symptomatic improvement in dystonia, which suggests that neuromodulation is likely to be primarily motor. A major mechanistic question that remains disputed is whether the therapeutic effects of GPi DBS are achieved mainly through interaction with the direct or indirect basal ganglia pathways, or pallidothalamic signalling. In other terms, it can be asked whether DBS might work by stimulation of afferents to the GPi (from putamen, STN, or conceivably the PPN), efferents from the GPi to the thalamus, or a more global virtual lesioning effect in the GPi. Disambiguating these possibilities is a key ambition of the experimental research of this chapter. Nambu et al. make the bold claim that reduced pallidal

output causes dystonia.[121] In a DYT1 dystonia mouse model they demonstrate reduced spontaneous activity in the pallidum and that electrical stimulation of M1 results in short latency pallidal excitation following by long lasting inhibition, a phenomenon not observed in normal mice. They then translate these observations to a patient undergoing GPi DBS for CD, with an adjunct subdural M1 electrode strip for the purposes of the experiment. In this patient they observed spontaneous activity in the pallidum, which is lower than that in PD patients (reproducing work of other investigators), and that the pallidal responses to M1 stimulation were very similar to those evoked in the DYT1 mouse. They conclude that increased activity through both M1 cortico-striato-pallidal direct and/or indirect pathways is a fundamental disturbance in dystonia. Antoniades et al. triangulate results of oculomotor neurometrology experiments in PD patients with either GPi DBS, STN DBS, or pallidotomy to construct an argument that, electrophysiologically, HF-DBS in the GPi acts by depressing striato-pallidal signalling and therefore increasing pallido-thalamic signalling.[133] Specifically, they argue that DBS generates antidromic action potentials in striatal medium spiny neurons (MSNs - inhibitory GABAergic projection neurons that comprise about 95% of the cells in the striatum) that project to the GPi, resulting in widespread MSN inhibition via orthodromic potentials along axonal collateral branch points to MSN-MSN inhibitory synapses. They term this process 'striatal dampening'. A case study in generalised dystonia confirms that Vop activity can be modulated by GPi DBS, and while this is complex, it was overall most consistent with increased pallido-thalamic signalling.[134] However, it has been shown that microstimulation of the PD GPi induces inhibition of GPi output, proposed to result from excitation of GABAergic afferents/terminals (e.g. from striatum).[135] Although the authors conclude that GPi DBS is likely to result in a mix of inhibition and excitation of GPi output, it is important to acknowledge there is heterogeneity and nuance to the literature addressing

this aspect of the mechanism of action. Interpretation of many such studies is difficult due to challenges such as binding electrophysiological observations to dystonia improvements, and that effects will probably vary depending on the DBS location in the GPi.[136]

4.2.1.2 The role of the subthalamic nucleus

The role of the STN, and therefore the indirect basal ganglia pathway,[137] in CD has been subject to much less investigation, commensurate with the currently small clinical uptake of STN DBS. Resting state M1 phase-amplitude coupling is reversibly reduced by STN DBS in both dystonia and PD,[138] and both STN and GPi DBS appear to reduce both resting state motor cortex alpha power and movement-related interhemispheric alpha coherence in motor cortex, closer to normal levels.[139] There is a no consensus on pathological STN electrophysiology in dystonia but, similarly to the GPi, there is a suggestion that low frequency theta-alpha may be prominent,[140–142] and that mean STN neuronal firing rates are lower than in PD.[143] In one CD patient, coherence has been demonstrated between motor cortex and STN, specific to the theta band, and which was supressed by therapeutic STN DBS.[144] Indeed, these authors leveraged this for an adaptive stimulation device, driven by motor theta, which appeared to give improved results compared to conventional DBS.

4.2.1.3 The role of the ventral oralis nuclei

Surgery to the ventral lateral thalamus was among the first stereotactic operations attempted for the treatment of dystonia. Intended surgical targets varied between ventral oralis, ventral intermediate, and ventral caudalis nuclei.[145–147] However, morbidity associated with surgery could often be substantial.[145] As the pallidothalamic relay, the Voa/Vop has survived as an infrequent but credible surgical target with some popularity in treating focal dystonias.[148]

More recently, high-frequency focused ultrasound and DBS have both been targeted to Voa/Vop, demonstrating proof-of-concept.[149,150] Nonetheless, little modern research has been performed that illuminates the role of the ventral oralis nuclei in CD and its treatment. Interestingly, similarly to STN and dissimilarly to GPi, symptomatic improvement appears not to be delayed with surgery to Voa/Vop.

4.3 NEUROIMAGING OF THE PALLIDUM

4.3.1 Structural neuroimaging

MRI of the pallidum is challenging due to two features, a) it is a relatively 'pale' nucleus (hence its name) due to traversing axons, creating less contrast with surrounding tissue, and b) it is composed of the GPe laterally and the GPi medially, separated by a thin white matter interface (the lamina medullaris), and accurately disambiguating the two is crucial for meaningful analysis. Older MRI acquisitions have not provided adequate contrast and/or spatial resolution to demarcate GPi and GPe. Therefore, analysis that requires identifying the GPi and that utilises such imaging necessarily relies on registration from anatomical standards (MNI standard space images or AC-PC coordinates) where GPi coordinates are known. However, while this is the best that can be achieved with such suboptimal structural imaging, it should be recognised that this is problematic as the registration can only be driven by standard anatomical relations and cannot generate contrast where there is none. Following from this proviso, optimal electrode location analyses in CD, which ultimately rely on very accurate location identification, should be scrutinised in this regard. Unfortunately, published reports fail this test by not demonstrating plausible acquisition sequences that distinguish GPe from GPi (Table 2), and therefore should be acknowledged as a key limitation.

Table 2. Summary of coordinate studies in pallidal DBS for cervical dystonia

Author (Year)	Patients	Sweet spot	Imaging	Methods
Starr et al. (2006)[151]	23 dystonia with 5 x CD	3.6 mm from pallidocapsular border in intercommisural plane. Lateral part of GPi, i.e. motor territory.	Pre- and post-operative 1.5T 3D Gd-enhanced full brain, IR FSE basal ganglia.	AC-PC coordinates and GPi boundaries (x-y only).
Hamani et al. (2008)[103]	13 x CD	Mean of beneficial active contacts: x=20.3, y=3.0, z=-1,0. Within posterolateral GPi no significant correlation between outcome and location.	T1-w or 3D IR pre-operative and T2-w post-operative	AC-PC coordinates, distance to optic tract, distance to 3rd ventricle, GPi boundaries - did not explore dorso-ventral axis as GPe/i could not be differentiated.
Schönecker et al. (2015)[152]	20 x CD	Left: x=20.6, y=-6.6, z=-4.8, Right: x=-20.1, y=-6.8, z=-5.4. Posterolateroventral GPi abutting lamina medullaris.	1.5T T2-w, 0.5x0.5mm, 2mm thickness	MNI space coordinates
Reich et al. (2019)[153]	43 x CD	Ventral margin of posterior GPi and subpallidal white matter.	T2-w FSE and/or T1-w IR	MNI space VAT. Åstrom et al. (2015) monopolar model.[154]

Schönecker et al. take a classic approach of identifying the centroid of the most (arbitrarily defined as >60% improvement) beneficial contacts, and measure the Euclidian distance from this location to all contacts.[152] Doing so, they find that electrode location explains about 40% of the variance in outcomes. This analysis was however carried out in MNI space based on

scans which are unlikely to demarcate the GPi. The most recent and largest attempt to locate a GPi sweet spot for DBS in CD was carried out by Reich et al.[153] They find that electrode location explains about 10% of the variance in surgical outcomes and that a probabilistic mapping based on a monopolar volume of activated tissue (VAT) model explained about 50% of the variance in outcomes. The use of a monopolar model is open to criticism; there is not a corresponding specification of whether their patients received monopolar or bipolar stimulation, or indeed a mix. In addition, neither MRI acquisition parameters nor example scans are provided to reassure the reader that the GPi was demarcated in their scans. Indeed, there is actually a suggestion that the scans may have been heterogeneous, which has the potential to bias the results. Lastly, it is not clear what a statistically thresholded VAT map offers the surgeon practically above that which coordinates offer, or what insight it gives into the disease and its treatment. Surgically, there is a decision about where to place the electrode (the targeting process), whereas the amplitude/voltage of stimulation (a key driver of VAT sphere size in the monopolar model) is guided by safety standards and patient tolerability of acute and chronic adverse effects. From these studies it is nonetheless clear, unsurprisingly, that electrode location does matter. Indeed, it may well have been underestimated in these studies due to inaccuracies in electrode location identification. However, it is very clear that a) a large amount of variance in clinical outcomes remains unexplained by electrode position, and b) that electrodes ascribed to be (in relative terms) really quite far from the 'sweet spot' can in some cases still be among the most therapeutic electrodes. While analytic inaccuracies may play some role in this, it does perhaps allude to a spatially individualised pathology: different locations may be optimal in different patients. This beckons for an individualised approach to optimise surgery. Theta power assessment

could undoubtedly play such a role, as could feasibly pre-operative advanced MRI analyses that reveal individual differences in brain structure and function.

4.3.2 Diffusion neuroimaging

Diffusion neuroimaging has been applied to the GPi as a non-invasive method of probing its structural connectivity patterns (see Table 3 for summary). The existing literature has sought to examine the anatomical validity of the technique through comparisons with invasive neural tracing, cytological staining experiments etc. in humans and non-human primates. Important observations have been made regarding the connectivity features of the posteroventral region in particular - where therapeutic electrodes are commonly located. Some of this research is limited by low quality of diffusion data, and relevance to clinical outcomes is sparsely studied.

Synthesising the available data, it can be said with confidence that the GPi demonstrates subcortical connectivity gradients across its volume that match plausibly with patterns of known neuronal connections. However, there are some discrepancies in findings. Attempts at connectivity-based parcellation of the GPi have resulted in the thalamic parcel being located anteriorly, posteriorly, and medially. Anatomical descriptions of pallidothalamic tracts (ansa lenticularis - ALent, lenticular fasiculus - LFas, fasiculus thalamicus - FThal) vary.[155,156] Tractographic exploration of this anatomy has identified two tracts: one emerging from the GPi anterolaterally (ALent), and one emerging dorsomedially (LFas), both converging in the field of Forel H1 (FThal) before entering the thalamus.[157] However, low quality diffusion data (3T, b=1000, 20-directions) generates scepticism of this account. Unfortunately, these

results also fail to offer a perspective that might explain the GPi-thalamic connectivity parcel discrepancies, and on their own convey little meaning for interpreting results of GPi DBS.

The majority of direct GPi connections are within the basal ganglia, thalamus, and brainstem (e.g. PPN).[40,118,158] Direct connections of the GPi with the cortex are controversial,[159] with limited direct anatomic evidence[160] that may well represent disynaptic connectivity.[161] Considering the liability for false positive findings with diffusion tractography,[162] it is hubristic to infer such connections are genuine when generated by this non-invasive method. Furthermore, if they do exist, they will be comparatively weak and their function unknown; this stands juxtaposed to the comparatively strong and functionally well-studied connections of established importance in movement disorders within the basal-ganglia and thalamus. Therefore, considering the overall connectivity profile of the GPi, the sense in performing cortical-GPi tractography is marginal. Recognising this explicitly, some authors have pursued other strategies.[132] However, Da Silva et al.[163] and Middlebrooks et al.[164] have nonetheless studied this. Perhaps unsurprisingly, their results are variable and inconsistent. For example, M1 connectivity leads to a large posterior parcel in one study,[164] but none in the other.[163] While both studies identified an anterior prefrontal cortex parcel, this was not replicated in the higher-quality diffusion data from the human connectome project.[163] Patriat et al. unconvinced of the argument for such GPi-cortex connectivity analysis, conceived a novel approach that by design acknowledged the primary inputs/outputs of the GPi[132] as well as recognising the parallel cortical-basal ganglia–thalamo-cortical networks that comprise the major anatomical schema of this region.[63] By conducting their study in this way, their results characterising different regions of the GPi are more germane to characterising electrode positions in the GPi; major theories concerning DBS mechanism of action in dystonia relate to

the indirect and direct basal ganglia pathways. Using high-quality diffusion data (7T, b=1500, 50-directions), they parcellate the thalamus based on its cortical connectivity, then use these thalamic parcels as classifiers for parcellating the GPi. They also parcellate the GPi using the same cortical regions as classifiers but instead with the striatum as a tractography waypoint. The resulting GPi parcellations (i.e. thalamic versus striatal) were remarkably similar, with the M1 parcel found at the mid-posterior GPi, the parieto-occipto-temporal parcel found more posteroventrally, and a premotor and prefrontal associative cortex parcel found more anteriorly. Importantly, 93% of active DBS contacts (14 of 15) were located in the M1 parcel or 1 mm from it. This suggests the GPi component of the M1-basal ganglia-thalamo-M1 loop characterises the therapeutic GPi region for DBS, at least in PD. Somewhat similarly, Rozanski et al. characterise the cortical connectivity of ventral and dorsal contacts of electrodes targeted to the GPi through a thalamic waypoint.[165] Noting that in general the optimal target is considered to be ventral, they found that ventral contacts of implanted arrays had higher S1 connectivity, and lower premotor (possibly also M1) connectivity than dorsal contacts. However, the lack of analysis of more specific variation in electrode positions and their relationship to patient outcomes following stimulation casts doubt on whether this result is of any interest. The same authors intimate in a sequel manuscript that pallidothalamic tracts are a key target structure of GPi DBS for dystonia, due to a perceived close proximity between the ALent in particular and efficacious electrodes. However, this is surely premature as no correlation with clinical outcome is established, and indeed the basis of the suggestion is quite misguided, presumably from a lack of understanding of basic anatomy by the authors. Although AL may well leave the GPi ventrolaterally, the sensorimotor projections from the putamen are also distributed ventrolaterally,[71–73] as are many from the STN,[166,167] and indeed the afferents from the PPN actually 'piggy-back' on the pallidothalamic tracts to arrive at the

GPi.[42] Therefore, this close proximity alluded to does not seriously reduce the number of credible structures, the connectivity with which, could be of prime importance in the therapeutic mechanism of DBS in dystonia.

Excluding the work of this thesis, the only serious study of the clinical outcomes of GPi DBS with diffusion neuroimaging was carried out by Okromelidze et al. in generalised dystonia, albeit using normative (not individualised) structural and functional connectomes. The latter demonstrated that VAT connectivity with primary sensorimotor cortex, motor thalamus, and cerebellum were correlated with improvement, whereas premotor cortex connectivity was inversely correlated. The structural connectivity estimates were less convincing, demonstrating a wide range of small cortical foci that were correlated with outcomes. Again, the problematic nature of GPi-cortex tractography experiments should be recognised and considered in the interpretation of these results. The finding of positive functional connectivity with cerebellum merits emphasis as a feature of CD. In a separate study, also based on a normative connectome, therapeutic GPi DBS locations in CD show negative resting state functional connectivity to the primary somatosensory cortex and positive connectivity to the cerebellum.[8] Supporting this, dual MEG-LFPs demonstrate pallido-cerebellar 7-13Hz coherence, inversely correlating with dystonia severity (in a 78% CD dystonia cohort).[9] However, while cerebellar functional connectivity stands out as a metric of interest, the absence of direct projections between the GPi and cerebellum essentially precludes its reasonable examination by tractography as a metric of structural connectivity.[168,169]

Table 3. Summary of diffusion MRI studies in pallidal DBS for dystonia

Authors (year)	Diffusion scans	Strategy description	Patients	Conclusions
Rozanski et al. (2014)[165]	3T, b = 1000, 20 directions, 2 mm thick	Connectivity patterns of ventral and dorsal DBS electrodes	Dystonia (n=8)	Dorsal electrodes stronger PMv and pre-SMA and weaker S1 connectivity than ventral electrodes.
Rozanski et al. (2017)[157]	3T, b = 1000, 20 directions, 2 mm thick	Pallidothalamic tract reconstruction from DBS electrode locations	Dystonia (n=10)	Delineate pallidothalamic tracts, distinguishing AL and FL. Active electrode in close proximity to tracts.
Da Silva et al. (2017)[163]	3T, b = 1000, directions not specified, 2.4 mm thick	Connectivity-based parcellation of GPi with a) 15 cortical and subcortical classifiers, b) whole brain k-means clustering	Healthy (n=16) + Human Connectome Project (n=25)	Five parcels identified (GPe, putamen, thalamus, brainstem, prefrontal), with thalamus parcel at posteroventral margin. Only two parcels with HCP data (GPe-lateral, thalamus-media). Three clusters with dominant prefrontal (anterior), brainstem (middle), thalamic (posterior) connectivity.
Middlebrooks et al. (2018)[164]	3T, b = 1000, 64 directions, 1.6 mm isotropic	Connectivity-based parcellation of GPi with cortical and subcortical classifiers	PD (n=11)	M1 posteroventral. Thalamus anterior. Increased VAT in M1 parcel correlated with improvement.
Patriat et al. (2018)[132]	7T, b = 1500, 50 directions, 1.5 mm isotropic	Thalamo-cortical connectivity-based parcellation used as classifiers to parcellate the GPi based on thalamo-pallidal. Compared to cortico-striatal connectivity-based parcellation of GPi.	PD (n=15) and dystonia (n=2)	M1 posterior. Frontal associative middle. Limbic anterior. Parieto-occipto-temporal posterior. Good match between thalamic and striatal connectivity parcellations.
Okromelidze et al. (2020)[170]	Normative structural (Human Connectome Project) and functional (3T) connectomes	VAT connectivity with cortex and cerebellum correlated with UDRS outcomes	Generalised dystonia (n=39)	Structural: M1, lateral frontal, inferior parietal and lateral temporo-occipital lobes. Negatively correlated with medial prefrontal region. Functional: M1, S1, motor thalamus, cerebellum. Superior temporal gyrus, lateral occipital lobe. Negatively correlated SMA, lateral occipital, inferior temporal, superior, middle and inferior frontal gyri.

4.4 EXPERIMENTAL WORK WITH PATIENT-SPECIFIC STRUCTURAL CONNECTOMES - see *Brain*, Volume 144, Issue 12, December 2021, Pages 3589-96 for associated published manuscript

Individual (as opposed to normative) connectomes are *a posteriori* muscularly salient to surgery for dystonia. Firstly, the variance in surgical outcomes for cervical dystonia is large (coefficient of variance ≈ 1),[106] mostly unexplained, and therefore indicative of unaccounted heterogeneity in the cohort or matching between cohort and intervention. Secondly, the pathophysiological character of the disorder chimes with plausible patient heterogeneity through an increase in 'anatomical entropy'. Dysfunctional plasticity has increasingly been established as a principal feature of dystonia, as well as profound somatotopic degradation and dedifferentiation. These features are present in cortex, basal ganglia, and thalamus. While the gain in disorder is common, it seems unlikely that this reorganisation will not vary between patients, including at the level of the GPi, thereby rendering patients in different network states. Spatial aspects of network corruption could vary between patients, inviting individualised treatment. Thirdly, similarly to what has been established at the thalamus,[171,172] while the general scheme of connectivity-based parcellations appears to be maintained between healthy individuals, individual differences are nonetheless substantial.[132] This signals topographic differences in connectivity and a substrate for individualised anatomical targeting. Lastly, that stimulation of a completely different location, namely the STN, can be so efficacious in some patients does invite speculation of inter-individual network differences where the relevant node for surgical neuromodulation varies and may be discernible through connectivity analysis. Taken together, the use of individualised connectomes to rationalise and potentially improve stereotactic surgery for CD is particularly germane.

Building on this, exploration is sensibly focused on structural connectivity within key networks: those of highest putative prowess for functional significance in dystonia. As such, my conjecture is that neuromodulation of connectivity within the cortico-basal ganglia loops of the indirect and direct pathways is plausibly an important determinant of the magnitude of clinical benefit derived from GPi HF-DBS. Specifically, input from the putamen (as the relevant striatal unit to sensorimotor loops) in the direct pathway, input from STN in the direct pathway, and the common output from the GPi to thalamus are the prime candidate nodes. Connectivity between GPi and PPN may also be important, but methodological difficulties in locating and segmenting the PPN require more specialist brainstem optimised imaging than available to me, ultimately making examination of this less attractive. Therefore, in this study, I used diffusion-weighted (DW) MRI tractography to derive connectivity estimates between DBS leads and these three nuclei to explore possible relationships with clinical improvement.

4.4.1 Methods

4.4.1.1 Patients

Nineteen patients (age at surgery 54 ± 9 (mean ± SD) years, eight male) with severe, medically refractory isolated cervical dystonia, or cervical dystonia accompanied by dystonia in additional body parts, underwent implantation of bilateral electrodes (Table 1) in the GPi, undergoing surgery as described elsewhere,[101] at the John Radcliffe Hospital. All patients underwent assessment by a consultant neurologist, neurosurgeon, and neuropsychologist, all with expertise in movement disorders, before being offered surgical treatment. Neuroimaging was performed under general anaesthetic as pathological head movement otherwise typically precludes an adequate acquisition.

4.4.1.2 Clinical rating

The patient's pre-operative and post-operative (12 mts [range: 6-18 mts]) clinical state was assessed using the TWSTRS-s (score/35) by a neuromodulation movement disorder specialist nurse or a consultant functional neurosurgeon.

4.4.1.3 Diffusion imaging acquisition and pre-processing

In fifteen patients, pre-operative MRI was performed on a 1.5T Phillips Achieva using a modified spin echo sequence with SENSE parallel imaging. In-plane resolution was 1.818 by 1.818 mm^2, and 64 2 mm thick slices were acquired in an interleaved fashion. Diffusion weighting (b = 1200 s/mm^2) was applied along 32 non-colinear gradient directions, with one non-diffusion weighted volume (b = 0). Correction for distortions and subject movement was carried out using the *FMRIB Software Library* (FSL; Oxford, UK).[173] The susceptibility-induced off-resonance field was estimated using *topup*.[173,174] Instead of using two b=0 spin-echo EPI with opposing PE-direction, the field was estimated from a b=0 volume and a structural T2-weighted scan, without any distortions.

Four additional patients underwent a higher angular resolution acquisition. Pre-operative MRI was performed on a 3T Siemens TrioTim using a modified spin echo sequence with parallel imaging. In-plane resolution was 2 by 2 mm^2, and 64 2 mm thick slices were acquired in an interleaved fashion. Diffusion weighting (b = 1500 s/mm^2) was applied along 60 gradient directions that were chosen to sample the sphere evenly by minimisation of Coulomb forces, with four non-diffusion weighted volumes (b = 0). This was performed twice, with opposing PE-direction (128 volumes in total). The susceptibility-induced off-resonance field was estimated using *topup*, [173,174] with two b=0 spin-echo EPI with opposing PE-direction.

In all nineteen patients, motion and eddy currents were corrected for using *eddy*, with outlier detection and replacement.[175] Single shell ball and stick modelling of local diffusion parameters was carried out using BEDPOSTX, with up to three crossing fibres per voxel. [176]

4.4.1.4 Deep brain stimulation

Patients were programmed to maximise improvements in dystonia. Initially, imaging was reviewed to select an appropriate contact for stimulation, usually the second deepest contact. High frequency stimulation was introduced, and patients typically discharged with two or three programmes for use at patient preference, with the ability to titrate amplitude within an allowed window. For patients with a poor response, alternative contacts were explored, usually at 3-month review.

4.4.1.5 Termination masks

FIRST,[177] a Bayesian model-based segmentation/registration tool in FSL,[173] was applied to same session T1-weighted MRI scans (1 mm isotropic) to extract thalamic and putaminal masks for each patient, with boundary voxels excluded. The Montreal Neurological Institute structural atlas was used to generate masks of the frontal and parietal cortices. The Harvard-Oxford cortical atlas was used to generate masks of the superior frontal gyrus (cropped to the caudal portion, SFGc), middle frontal gyrus (MFG), inferior frontal gyrus pars opercularis (IFGpo), primary motor cortex (M1), and supplementary motor area (SMA), which were then registered to T1-weighted MRI scans using FLIRT and FNIRT.[178–181] SFGc and SMA were combined to approximate the dorsal premotor cortex (PMd), whilst the MFG and IFGpo were combined to approximate the ventral premotor cortex (PMv).

4.4.1.6 Tractography and parcellation

Probabilistic tractography was carried out using PROBTRACX,[176] with modified Euler streaming and distance correction. '<->' is used thereafter to reference connectivity between two regions. Post-operative computed tomography (CT) images were registered to MRI using FLIRT.[173] Lead contacts were identified based on CT artefacts and array dimensions. Stimulation parameters at follow-up were reviewed and the most used cathode contact identified (in patient M, an average between two contacts was taken as two programs with different cathodes were equally used). A 3 mm radius sphere around this contact, for each lead, was used as a tractography seed to thalamus, putamen, and STN. Tracts were visualised for anatomic plausibility. Connectivity-based hard parcellation of the putamen was carried out using the '*find the biggest*' algorithm in FSL,[182] first with frontal and parietal cortex, then second with M1, PMd, and PMv as cortical classifiers.[182] The same tractography was carried out to these putaminal parcellations.

4.4.1.7 Statistical analysis

For each of the streamlines from the cathode generated by PROBTRACX, I counted the number of seeds that reached each region and normalised these by size of the termination mask. Those counts were summed over left and right for each patient and explored for linear relationships with clinical TWSTRS-s improvement by calculating Pearson, Spearman's rho, and Kendall's Tau correlation coefficients (two-tailed).

4.4.1.8 Coordinate-connectivity relationship

Disambiguating the relative contributions of individual's electrode locations and diffusion parameters to the observed improvement-tractography correlation is crucial to its interpretation. To assess this, the anterior commissure – posterior commissure (AC-PC) coordinates were measured (neuroinspire™, Renishaw, UK), and the correlation with clinical improvement calculated using the methodology of Schönecker et al.[152] Then, a forward multiple regression was performed with coordinates and HF-DBS<->M1 putamen connectivity as explanatory variables. In addition, the DBS tractography to the putamen was repeated in a common connectome, thereby removing individual differences in diffusion parameters as a variable. To achieve this, one patient's diffusion scan and all electrode locations were registered to the MNI template and tractography performed in this common space. This was then repeated with a second diffusion scan for confirmation.

While a therapeutic sweet spot is recognised,[131] these are distributions that many patients do not conform to. This strongly supports an individualised approach. In order to probe whether these results might have use in augmenting targeting, and demonstrate how this could be done, an additional four patients were analysed. Preoperative 3T 1 mm isotropic T1-weighted magnetisation prepared rapid acquisition gradient echo (MP-RAGE) gave adequate spatial contrast to confidently demarcate the GPi. Individualised M1-putamen connectivity density maps of each GPi were generated, the region of highest connectivity (hot spot) was identified, and proximity to the lead assessed.

4.4.2 Results

4.4.2.1 Patient demographics

All nineteen patients were successfully implanted with DBS electrodes bilaterally and received bilateral HF (125-130 Hz) DBS. Sixteen patients showed improvement in severity of disease at follow-up (Table 1).

4.4.2.2 DBS connectivity with motor-putamen predicts outcomes

In the 1.5T data set, a significant positive correlation was observed between HF-DBS<->putamen connectivity and clinical improvement (Figure 1A; r_P=0.56, p=0.029, r_S=0.59, p=0.022). No significant correlation was observed between either HF-DBS<->STN or HF-DBS<->thalamus and clinical improvement. In order to examine if the HF-DBS<->putamen relationship was driven by motor or sensory connectivity, a putamen parcellation was subsequently performed (similar to Tziortzi et al.[183]) based on connectivity to frontal (i.e. motor) and parietal (i.e. sensory) cortices (Figure 1B). A significant positive correlation was observed between HF-DBS<->frontal-putamen connectivity and clinical improvement (r_P=0.58, p=0.023, r_S=0.57, p=0.028). No significant correlation was observed between HF-DBS<->parietal-putamen connectivity and clinical improvement. To further characterise the HF-DBS<->putamen relationship, a second parcellation was performed to reveal the motor topography (Figure 1C, similar to Tziortzi et al.; Lehricy et al.; Leh et al.[183–185]). No significant correlations were observed between HF-DBS<->PMv/PMd-putamen and clinical improvement. A significant positive correlation was observed between HF-DBS<->M1-putamen connectivity and clinical improvement (r_P=0.70, p=0.004, r_S=0.65, p=0.009). This result was analysed for robustness: it remained significant after substituting '%' for 'absolute' TWSTRS-s improvement (r_P=0.64, p=0.010, r_S=0.66, p=0.008), and remained significant after

control capping improvement at zero (absolute: r_P=0.68, p=0.005, r_S=0.65, p=0.009, %: r_P=0.63, p=0.013, r_S=0.66, p=0.008). Patient F was an outlier, with a poorer TWSTRS-s improvement than expected from the connectivity. Possibly relevant, the patient's pre-operative severity was low for the cohort, and the surgery was mostly indicated for pain, which decreased by 83%.

4.4.2.3 Connectivity and coordinates are not equivalent

AC-PC coordinates alone explained 44% of the variance in clinical improvement (r=-0.66, p=0.007, Figure 3A), but was not significantly correlated with HF-DBS<->M1-putamen connectivity (r=-0.36, p=0.18, Figure 3B). A forward regression model (F(2,12)=12.8, p=0.001, r=0.83, r^2=0.68), found both coordinates (p=0.02) and HF-DBS<->M1-putamen connectivity (p=0.01) as significant explanatory variables, with the latter entering first as the best fitting variable. The positive correlation of HF-DBS<->putamen connectivity with improvement disappeared when tractography was performed with common diffusion parameters (r_P=-0.30) and confirmed in a second connectome. In the 3T data set, clear variation in the GPi topology of M1-putamen connectivity was observed between patients (see Figure 2A for examples). Stimulation in the middle/posterior GPi, hot spot coverage, and high connectivity were consistent with clinical benefit (Figure 2B).

4.4.3 Discussion

I hypothesised that the structural connectivity between the GPi and one or more of the subcortical nuclei with which it is directly connected might be an important mediator of the clinical effects of DBS in CD. Examining this question using structural connectivity estimates from DW-MRI probabilistic tractography, I found a positive correlation between HF-DBS<-

>putamen connectivity and clinical improvement. I then performed two sequential connectivity-based parcellations of the putamen in order to characterise the region of putamen crucial to this relationship. This revealed that motor-putamen, in particular M1 (middle) putamen, was the essential node of HF stimulation connectivity that explained variance in clinical outcomes. The posterior region of the GPi is characterised as 'M1' based on pallido-thalamo-cortical connectivity, is the most common site of active therapeutic contact in the surgical treatment of dystonia[132], and is the site of local peak theta power: a putative physiomarker for CD.[131] Together with my findings, these neuroimaging results point to intervention in the M1-striato-pallido-thalamo-M1 loop as being mechanistically important in relief of dystonia via HF-DBS.

The research discussed in *4.1.2 Putamen* and *4.1.4 Primary motor and premotor cortex* above advocates for a role for both putamen and M1 in the pathophysiology of CD, and the anatomical context discussed in *4.1.5* establishes these structures as prime putative candidates in the mechanism of GPi HF-DBS. Despite clear implication of sensory cortex in CD, it is notable that therapeutic GPi DBS does not correct sensory abnormalities, consistent with sensory systems not mediating motor improvements.[104] The results presented in this chapter support this understanding. Physiological speculation on the structural connectivity results benefits from reiterating some key literature. Low frequency (LF) coherence within the basal ganglia–cortical network is a putative signature of dystonia; this coherence between motor cortex and GPi is supressed by HF stimulation,[130] a finding also observed in CD following a *geste antagoniste*.[128] Furthermore, LF GPi DBS evokes potentials in primary motor cortex and modulates motor cortex excitability and plasticity.[186] There is a reversible increase in motor cortex excitability (increase in TMS motor thresholds) with HF-DBS, [187] and LTP-like motor

cortex plasticity, known to be abnormal in dystonia,[53,55] is reduced or abolished.[188] In addition, DBS normalises increased M1 LF oscillations and their interhemispheric coherence, as well as decreasing M1 activation.[189] Indeed, in presenting unpublished research at ESSFN (Marseille, 2021) A. Lozano proposed his fMRI work supported decreased M1 activity as a signature of efficacious GPi stimulation for dystonia (principally proposed as a programming technique to circumvent the delay of clinical benefits to emerge from appropriate stimulation). Taken together, a physiological model of GPi DBS reducing thalamocortical inhibition remains coherent. My interpretation of my results, accepting that there are alternative more complex explanations, is that this is achieved via disruption of GABA-ergic inhibitory signalling from the region of putamen receiving dominant input from M1, to the posterior ('M1') GPi. I suggest that the result of this would be increased inhibitory output of the posterior GPi to thalamus, and decreased thalamo-cortical(M1) signalling. This would manifest electrophysiologically as desynchronisation of LF coherence in the M1-basal ganglia loop that is observed, and similarly the decrease in M1 activity.

Clearly, electrode implant location matters and surgically this will vary among patients. While this does account for much statistical variance in clinical outcomes, much remains unexplained, including examples where a primary or secondary anterior/middle GPi lead can be so beneficial.[190] The assumption that pallidal topographic anatomy is essentially the same among CD patients may not be justified, warranting an individualised approach. It should be acknowledged that this is a large claim, with large implications if correct. Nonetheless, in concept, it is supported by tractographic methods in the PD GPi.[132] Even if individual differences between normal subjects were small, the neural reorganisation which takes place in dystonia is a prime candidate generator of heterogeneity. This is the putative substrate for

approaching personalised targeting for this surgery. In our data, I probed this in three different ways, all three of which concurred. Firstly, I demonstrated that specific diffusion parameters encode outcome-predictive information additional to that offered by coordinates. Secondly, showing that the outcome-connectivity relationship broke down when alienated from individual differences in diffusion connectomes, (i.e. by performing tractography in a common connectome) indicates that putamen-GPi tractography patterns do not define a common anatomic region well and that, at least in CD, individual differences are substantial. Thirdly, these implications from the 1.5T data set were confirmed with the 3T GPi mapping (Figure 2A). This demonstrated unequivocal differences in the GPi connectivity topography to the M1-putamen between patients. While this would ideally have been performed with the 1.5T data, the lower spatial contrast structural imaging was not adequate for a high-fidelity segmentation of GPi, and therefore would probably generate maps including substantive numbers of non-GPi voxels and excluding substantive numbers of GPi voxels. Nonetheless, the results of these three approaches were in agreement that inter-individual heterogeneity does exist. Furthermore, it is difficult to conceive how this result, tied as it is to improvement in clinical outcomes, might arise from artefact or bias in our data. Lastly, acknowledging the claim is substantial, further support is given from the observation that in isolation both 'connectivity' and 'coordinates' correlate strongly with outcomes (the latter being generally in line with literature standards), but the correlation *between* connectivity and coordinates was only weak, and not statistically significant (Figure 3). Therefore, it is justifiable to suppose that this study provides a platform where an individualised surgical approach can be pursued using pre-operative diffusion MRI, with connectivity 'hot spots' as a modifier. Initial DBS programming could be guided in the same way. As clinical improvement, particularly the tonic component, takes weeks-to-months to

manifest, stimulation programming is challenging in a way that, for example, programming to treat tremor is not. In treating CD, the initial electrode contact could be selected based on proximity to the connectivity hot spot.

Outwith of an 'optimised' DBS location, strength of connectivity, both from the relevant surgical target and within the dysfunctional network broadly, is a prime putative explanatory factor for variance in outcomes. I suppose that total network dysfunction in CD is both common and heterogenous. Supporting this, lesions (inevitably leading to loss of connectivity) of numerous nodes can produce the same clinical picture.[8] Patients with strong connectivity within the M1-putamen-GPi limb of the network may have more potential to benefit from HF-GPi DBS, whereas others may be better treated with STN DBS or other treatments. Unlike the GPi, the STN has a close relation to the cerebellum,[191] which as detailed in *4.1.6* has an undoubtedly key role in CD. The STN has reciprocal connections with the PPN,[42,192,193] through which it forms this disynaptic connection with the cerebellum.[169] While speculative, in addition to the connectivity between STN and pallidum,[194] this STN-PPN-cerebellum limb is a plausible component of the 'CD network',[8] which when particularly strong, DBS to the STN may be particularly efficacious.

4.4.4 Limitations

Both the data and analyses in this study have important limitations.

4.4.4.1 Clinical scores

While TWSTRS-s ratings were blind to corresponding connectivity values, they were not blinded to pre- or post-operative status. The principal concern with respect to this lack of

blinding is the possibility of inflation of post-operative improvement, or minimisation of post-operative decline, animated by the expectation or wish for the procedure to benefit the patient. However, such bias is likely to be systematic, and therefore as my analyses are correlational, this would not undermine or be materially consequential for any of my findings or conclusions. Supplementary analyses leveraging clinical assessment videos of a sample of the study's patients indeed indicate any bias is trivial or may not even exist (see Figure 4).

4.4.4.2 Diffusion data

The spatial and angular resolution of the diffusion data is at the lower end suitable to perform my analyses. There is no obvious reason why such limitations would generate a false positive result (i.e. the main finding of the study), particularly in light of the analyses that point to an uncoupling of 'connectivity' and 'coordinates', as well as the use of 'distance correction' tractography. However, as the resolution and complexity of the diffusion model is low, this will decrease sensitivity and therefore increase the risk of false negatives. The white matter between the GPi and STN, but particularly between GPi and thalamus, is particularly complex and may not have been adequately modelled for the purposes of tractography in this study. As such, a relationship between GPi<->STN/thalamus and clinical improvement from HF-DBS may well exist and been missed. Therefore, this study should not be interpreted as evidence that connectivity between GPi and these two nuclei is unimportant for the therapeutic mechanisms of HF-DBS. This highlights the appropriateness and importance of acquiring higher resolution diffusion data if replication of this study is attempted.

4.4.4.3 Diffusion tractography

The anatomical robustness of tractography findings can always be doubted. Ultimately, tractography is non-invasive, and both inferential and indirect in the conclusions that can be drawn from its results. Direct validation in specific anatomic cases requires challenging invasive research that is only achievable by post-mortem comparisons, most practicably in non-human primates using neuronal tracer experiments and dissection. Such results have generated a high degree of scepticism in some authors,[195] and a large amount of variability in results between different tractography algorithms has been observed by others, as well as less anatomical accuracy over longer distances.[196] The results of other authors generate more confidence in the use of tractography for connectivity estimates,[197] particularly if tractography algorithms are optimised,[198] and the context for false positives and false negatives are taken into account in the interpretation and study design.[162,199] Considering the experimental work of this chapter specifically, increased anatomical confidence would require histological validation of the specific anatomy investigated, as has been performed in other anatomical cases.[200] It is expected that the streamlines track the highly anisotropic Wilson pencils that traverse between the putamen and GPi.[201,202]

Questions can also be raised regarding the legitimacy and interpretation of the parcellation methodology used in this chapter. The technique has gained broad popularity since its inception, where it was applied to the thalamus in an attempt to demarcate subnuclei.[182] Clearly, the putamen cannot be considered in this way as it is cytoarchitechtonically homogenous and receives cortical input in a distinctly patterned yet more distributed way. As such, the interpretation relies on the concept of characterisation via relative cortical connectivity density, which in principle should carry a functional meaning. Its anatomical

validity can still be questioned but, nonetheless, application of this concept is widely published with typically cogent results that have served to bolster its credibility.[183,203–208]

4.4.4.4 Tractography stimulation seed

Finally, I used a standardised tractography seed instead of seeding an estimated field of 'activation' for each patient. In short, lack of a validated bipolar-DBS model, and changes in impedance and applied voltage over long-term follow-up created uncertainty, which I felt favoured an identical tractography experiment in every patient. There are some tractography studies where the individualised stimulation field modelling is certainly the right approach. Such an example of this is the study by Vanegas-Arroyave et al.[209] Monopolar stimulation was explicitly used in all patients, with impedances, voltage, and clinical/side effects all measured in an experiment on the same day. Therefore, there is a tight connection between parameters and effects, and validated monopolar models of VAT are well established.[154,210–212] This matching/relationship breaks down in studies such as the experimental work of this chapter. In the simplest case, patients are programmed with a given voltage of stimulation, with an upper and lower bound which is patient directed and changes while they are in the community. The electrode impedance also changes over time, as observed at follow-up. The VAT models depend fundamentally on the voltage and impedance values that are inputted and therefore this uncertainty generates error – enough which very plausibly can undermine the project. Furthermore, to my knowledge, there are no validated models for bipolar stimulation in DBS, although technically complicated clinically non-validated models have been developed,[213] and one is available in the LeadDBS open source package. Attempting a very specific, individualised approach to the VAT that makes the approximation of a monopolar model to bipolar stimulation is clearly problematic. Another issue that may arise

in attempting the individualised VAT approach is a 'self-fulfilling prophecy' effect, which could theoretically generate spurious connectivity-outcome correlations. Clinically, general DBS experience indicates some patients who do not receive benefit from stimulation will run their voltage low (perhaps to avoid side-effects) whereas patients receiving good benefit may tend to raise their voltage to the higher bound of what is tolerable/programmed. As larger tractography seeds necessarily generate larger connectivity estimates, it is easy to see how this individualised VAT approach could generate a bias in a correlation, and results that could be misinterpreted. As such, on balance, the elegance and simplicity of performing the same tractography experiment for every patient seemed favourable.

4.4.5 Future work

Despite the apparent robustness of the findings in our dataset, there are a range of future studies that are required to validate and further explore the findings. Firstly, replication in a new patient cohort is a priority. To confirm that my results have indeed not come about simply by chance, or by some unknown systematic bias, the study should be repeated prospectively with a new set of patients. Due to the strength of relationships I observed, the study size need not be larger than mine (fifteen patients) and could indeed reasonably be as low as twelve patients. While the lower quality of the diffusion data would be unlikely to be responsible for a false positive result in my study, it may very well have been responsible for false negative results, i.e. with respect to the STN and thalamus. The mechanisms of DBS are likely to be multiple and complex, and it may well be the case that direct connectivity to multiple regions are important for clinical outcomes. The white matter region between pallidum and thalamus is particularly complex, and tractography performed with our diffusion data may not have adequately navigated it faithful to the anatomy. The clinical practical

limitations on acquiring high quality diffusion data are substantial, therefore compromise is inevitable. A modern plausible proposal could follow parameters such as 3T, b = 1500, 128 directions, 1.5 mm isotropic, and would represent a substantial and relevant improvement in angular and spatial resolution to my study. If such validation was established, and in my view only when, it would be incumbent on surgeons to prospectively, and on a research basis, to apply this individualised metric to personalising GPi DBS surgery. Proving beyond reasonable doubt whether surgical outcomes had or had not then been improved may be statistically difficult, and the assessment will probably rely on case-control analysis, although an RCT format could be attempted. As previously mentioned, the three principal ways in which our results could be used to make practice more sophisticated are a) rejection of 'connectomically poor' surgical candidates, b) guiding electrode targeting within the GPi, and c) guiding selection of the chronically stimulating cathode from the implanted array.

While this study focused on dystonia of the neck (focal or segmental), whether the same results may be found in investigating generalised dystonia, genetic dystonias, or indeed other focal/segmental dystonias remains an open question. As few of our patients had dystonia outwith the neck, that this dystonic body part/s varied, and that the appropriate clinical rating metric to make comparisons across body parts is not clear, my study was not able to give us insights into whether my findings are likely to apply to dystonia other than CD. Furthermore, surgically relevant somatotopy of the 'dystonic' GPi is unclear and controversial,[214,215] with no consensus on whether dystonic body parts, other than the neck, should generally respond in parallel with neck symptoms in a segmental syndrome (in this CD study, patient J did very well but had her blepharospasm worsen notably following surgery; patient D declined slightly following surgery, and also developed a significant blepharospasm at that point; patient N

improved a lot, as did his arm dystonia), or whether focal dystonia in specific body regions are best targeted with specific individualised approaches. In principle, functional neuroimaging may be able to probe this question. Nonetheless, studies like mine in generalised dystonia and another focal dystonia, using the Unified Dystonia Rating Scale (UDRS) or the Burke-Fahn-Marsden Dystonia Rating Scale (BFMDRS), would be a prudent next step in assessing the generalisability of my results to the landscape of dystonia disorders. These two studies would be sufficient to establish whether my findings in CD apply broadly across dystonia, apply to more focal disease, or whether they are genuinely idiosyncratic to CD.

Functional, spectroscopic, or other advanced imaging modalities were not acquired alongside diffusion data in this study. These may well provide further insights into the interpretation of this treatment. For example, pallidal GABA may be an important predictor of surgical outcome. Electrophysiology was not collected either. The relationship between M1-putamen connectivity and pallidal theta is of particular interest, and merits investigation within a prospective validation challenge to this study.

Lastly, as outlined in *4.1.3 Pedunculopontine nucleus*, it is difficult to exclude an important role for the PPN in dystonia and its treatment with GPi DBS. However, exploring this in a study such as mine is highly problematic. The reliability of identifying the PPN and segmenting it appropriately for use as a tractography endpoint is not well established, and to have a high degree of confidence in the segmentation will probably require multi-modal high quality structural MRI data to relate to a specialised atlas.[216] Furthermore, 'brainstem optimised'

diffusion data (see Ezra et al. as example studying the periaqueductal grey)[208] may well be required for further confidence in the results.

4.5 CONCLUSIONS

CD is a sensorimotor network disorder with cortical, subcortical, and cerebellar pathology. HF-DBS to the GPi is proven to improve the motor symptoms of CD, confirming the importance of this nucleus in the disorder. Although both motor and sensory dysfunction are recognised in CD, this study supports a theory of motor-striato-pallidal connectivity, not sensory circuits, as a crucial factor in efficacious DBS. Nonetheless, the importance to clinical response from DBS, of GPi connectivity to other nuclei or between nuclei elsewhere within the network, cannot be excluded. The amount of variance in outcomes explained by M1-putamen-GPi connectivity is of a magnitude that merits material consideration in personalisation of surgical care. There is compelling evidence of uncoupling between coordinates and this connectivity metric, which is in keeping with a concept of dysfunctional plasticity in dystonia, with varying parameters between individuals. Prospective replication (non-interventional) is an essential step required to validate these results before interventional investigation is pursued with the purpose of improving surgical outcomes.

Addendum

Since the original submission of this thesis, two particularly relevant manuscripts have been published that merit note here. First, a normative connectome study suggested that striatopallidal bundles accounted for optimal DBS treatment of CD, whereas pallidothalamic bundles accounted for optimal treatment of generalised dystonia.[217] Secondly, an

electophysiological manuscript detailed that the extent of putamen-GPi LF coherence correlated (r=0.63) with dystonia severity (putamen-GPe and GPi-GPe coherence did not).[218] *Both these papers somewhat buttress the experimental findings I present in this chapter.*

REFERENCES

1. Jankovic J, Tsui J, Bergeron C. Prevalence of cervical dystonia and spasmodic torticollis in the United States general population. Parkinsonism Relat Disord 2007;13(7):411–6.

2. LaHue SC, Albers K, Goldman S, et al. Cervical Dystonia Incidence and Diagnostic Delay in a Multiethnic Population. Mov Disord 2020;35(3):450–6.

3. Bradley D, Whelan R, Kimmich O, et al. Temporal discrimination thresholds in adult-onset primary torsion dystonia: an analysis by task type and by dystonia phenotype. J Neurol 2012;259(1):77–82.

4. Fiorio M, Tinazzi M, Ionta S, et al. Mental rotation of body parts and non-corporeal objects in patients with idiopathic cervical dystonia. Neuropsychologia 2007;45(10):2346–54.

5. Romano R, Bertolino A, Gigante A, Martino D, Livrea P, Defazio G. Impaired cognitive functions in adult-onset primary cranial cervical dystonia. Parkinsonism Relat Disord 2014;20(2):162–5.

6. Walsh R, O'Dwyer JP, Sheikh IH, O'Riordan S, Lynch T, Hutchinson M. Sporadic adult onset dystonia: sensory abnormalities as an endophenotype in unaffected relatives. J Neurol Neurosurg Psychiatry 2007;78(9):980–3.

7. LeDoux MS, Brady KA. Secondary cervical dystonia associated with structural lesions of the central nervous system. Mov Disord 2003;18(1):60–9.

8. Corp DT, Joutsa J, Darby RR, et al. Network localization of cervical dystonia based on causal brain lesions. Brain 2019;142(6):1660–74.

9. Neumann W-J, Jha A, Bock A, et al. Cortico-pallidal oscillatory connectivity in patients with dystonia. Brain 2015;138(7):1894–906.

10. Byl NN, Merzenich MM, Jenkins WM. A primate genesis model of focal dystonia and repetitive strain injury: I. Learning-induced dedifferentiation of the representation of the hand in the primary somatosensory cortex in adult monkeys. Neurology 1996;47(2):508–20.

11. Bara-Jimenez W, Catalan MJ, Hallett M, Gerloff C. Abnormal somatosensory homunculus in dystonia of the hand. Ann Neurol 1998;44(5):828–31.

12. Butterworth S, Francis S, Kelly E, McGlone F, Bowtell R, Sawle GV. Abnormal cortical sensory activation in dystonia: An fMRI study. Mov Disord 2003;18(6):673–82.

13. Delmaire C, Vidailhet M, Elbaz A, et al. Structural abnormalities in the cerebellum and sensorimotor circuit in writer's cramp. Neurology 2007;69(4):376–80.

14. Delmaire C, Vidailhet M, Wassermann D, et al. Diffusion Abnormalities in the Primary Sensorimotor Pathways in Writer's Cramp. Arch Neurol 2009;66(4):502–8.

15. Lenz FA, Byl NN. Reorganization in the Cutaneous Core of the Human Thalamic Principal Somatic Sensory Nucleus (Ventral Caudal) in Patients With Dystonia. J Neurophysiol 1999;82(6):3204–12.

16. Lenz FA, Jaeger CJ, Seike MS, et al. Thalamic Single Neuron Activity in Patients With Dystonia: Dystonia-Related Activity and Somatic Sensory Reorganization. J Neurophysiol 1999;82(5):2372–92.

17. Tamburin S, Manganotti P, Marzi CA, Fiaschi A, Zanette G. Abnormal somatotopic arrangement of sensorimotor interactions in dystonic patients. Brain 2002;125(12):2719–30.

18. Ochudło S, Drzyzga K, Drzyzga ŁR, Opala G. Various patterns of gestes antagonistes in cervical dystonia. Parkinsonism Relat Disord 2007;13(7):417–20.

19. Patel N, Hanfelt J, Marsh L, Jankovic J. Alleviating manoeuvres (sensory tricks) in cervical dystonia. J Neurol Neurosurg Psychiatry 2014;85(8):882–4.

20. Naumann M, Magyar-Lehmann S, Reiners K, Erbguth F, Leenders KL. Sensory tricks in cervical dystonia: Perceptual dysbalance of parietal cortex modulates frontal motor programming. Ann Neurol 2000;47(3):322–8.

21. Burton K, Farrell K, Li D, Calne DB. Lesions of the putamen and dystonia: CT and magnetic resonance imaging. Neurology 1984;34(7):962–5.

22. Marsden CD, Obeso JA, Zarranz JJ, Lang AE. The anatomical basis of symptomatic hemidystonia. Brain 1985;108(2):463–83.

23. Pettigrew LC, Jankovic J. Hemidystonia: a report of 22 patients and a review of the literature. J Neurol Neurosurg Psychiatry 1985;48(7):650–7.

24. Delmaire C, Krainik A, Tezenas du Montcel S, et al. Disorganized somatotopy in the putamen of patients with focal hand dystonia. Neurology 2005;64(8):1391–6.

25. Albin RL, Cross D, Cornblath WT, et al. Diminished striatal [123I]iodobenzovesamicol binding in idiopathic cervical dystonia. Ann Neurol 2003;53(4):528–32.

26. Mente K, Edwards NA, Urbano D, et al. Pedunculopontine Nucleus Cholinergic Deficiency in Cervical Dystonia: Cholinergic Deficiency in Cervical Dystonia. Mov Disord 2018;33(5):827–34.

27. Pappas SS, Darr K, Holley SM, et al. Forebrain deletion of the dystonia protein torsinA causes dystonic-like movements and loss of striatal cholinergic neurons. eLife 2015;4:e08352.

28. Ikeda K, Yanagihashi M, Sawada M, Hanashiro S, Kawabe K, Iwasaki Y. Donepezil-induced Cervical Dystonia in Alzheimer's Disease: A Case Report and Literature Review of Dystonia due to Cholinesterase Inhibitors. Intern Med 2014;53(9):1007–10.

29. Black KJ, Ongiir D, Perlmutter JS. Putamen volume in idiopathic focal dystonia. Neurology 1998;51(3):819–24.

30. Granert O, Peller M, Jabusch H-C, Altenmuller E, Siebner HR. Sensorimotor skills and focal dystonia are linked to putaminal grey-matter volume in pianists. J Neurol Neurosurg Psychiatry 2011;82(11):1225–31.

31. Pantano P, Totaro P, Fabbrini G, et al. A Transverse and Longitudinal MR Imaging Voxel-Based Morphometry Study in Patients with Primary Cervical Dystonia. Am J Neuroradiol 2011;32(1):81–4.

32. Obermann M, Yaldizli O, De Greiff A, et al. Morphometric changes of sensorimotor structures in focal dystonia. Mov Disord 2007;22(8):1117–23.

33. Draganski B, Schneider SA, Fiorio M, et al. Genotype–phenotype interactions in primary dystonias revealed by differential changes in brain structure. NeuroImage 2009;47(4):1141–7.

34. Colosimo C. Diffusion tensor imaging in primary cervical dystonia. J Neurol Neurosurg Psychiatry 2005;76(11):1591–3.

35. Fabbrini G, Pantano P, Totaro P, et al. Diffusion tensor imaging in patients with primary cervical dystonia and in patients with blepharospasm: DTI in patients with cervical dystonia and blepharospasm. Eur J Neurol 2008;15(2):185–9.

36. Magyar-Lehmann S, Antonini A, Roelcke U, et al. Cerebral glucose metabolism in patients with spasmodic torticollis. Mov Disord 1997;12(5):704–8.

37. Galardi G, Perani D, Grassi F, et al. Basal ganglia and thalamo-cortical hypermetabolism in patients with spasmodic torticollis. Acta Neurol Scand 1996;94(3):172–6.

38. Moore RD, Gallea C, Horovitz SG, Hallett M. Individuated finger control in focal hand dystonia: An fMRI study. Neuroimage 2012;61:823–31.

39. Delnooz CCS, Pasman JW, Beckmann CF, van de Warrenburg BPC. Altered striatal and pallidal connectivity in cervical dystonia. Brain Struct Funct 2015;220(1):513–23.

40. Shink E, Sidibe M, Smith Y. Efferent connections of the internal globus pallidus in the squirrel monkey: II. topography and synaptic organization of pallidal efferents to the pedunculopontine nucleus. J Comp Neurol 1997;382(3):348–63.

41. Lavoie B, Parent A. Pedunculopontine nucleus in the squirrel monkey: Cholinergic and glutamatergic projections to the substantia nigra. J Comp Neurol 1994;344(2):232–41.

42. Lavoie B, Parent A. Pedunculopontine nucleus in the squirrel monkey: Projections to the basal ganglia as revealed by anterograde tract-tracing methods. J Comp Neurol 1994;344(2):210–31.

43. Spann BM, Grofova I. Origin of ascending and spinal pathways from the nucleus tegmenti pedunculopontinus in the rat. J Comp Neurol 1989;283(1):13–27.

44. McNaught KStP, Kapustin A, Jackson T, et al. Brainstem pathology in DYT1 primary torsion dystonia. Ann Neurol 2004;56(4):540–7.

45. Zhang J, Wang ZI, Baker KB, Vitek JL. Effect of globus pallidus internus stimulation on neuronal activity in the pedunculopontine tegmental nucleus in the primate model of Parkinson's disease. Exp Neurol 2012;233(1):575–80.

46. Ridding MC, Sheean G, Rothwell JC, Inzelberg R, Kujirai T. Changes in the balance between motor cortical excitation and inhibition in focal, task specific dystonia. J Neurol Neurosurg Psychiatry 1995;59(5):493–8.

47. McCambridge AB, Bradnam LV. Cortical neurophysiology of primary isolated dystonia and non-dystonic adults: A meta-analysis. Eur J Neurosci 2021;53(4):1300–23.

48. Garibotto V, Romito LM, Elia AE, et al. In vivo evidence for GABA $_A$ receptor changes in the sensorimotor system in primary dystonia: GABA $_A$ Receptor Changes in Primary Dystonia. Mov Disord 2011;26(5):852–7.

49. Gallea C, Herath P, Voon V, et al. Loss of inhibition in sensorimotor networks in focal hand dystonia. NeuroImage Clin 2018;17:90–7.

50. Berman BD, Pollard RT, Shelton E, Karki R, Smith-Jones PM, Miao Y. GABAA Receptor Availability Changes Underlie Symptoms in Isolated Cervical Dystonia. Front Neurol 2018;9:188.

51. Gilio F. Abnormalities of motor cortex excitability preceding movement in patients with dystonia. Brain 2003;126(8):1745–54.

52. Quartarone A, Morgante F, Sant'Angelo A, et al. Abnormal plasticity of sensorimotor circuits extends beyond the affected body part in focal dystonia. J Neurol Neurosurg Psychiatry 2008;79(9):985–90.

53. Quartarone A, Bagnato S, Rizzo V, et al. Abnormal associative plasticity of the human motor cortex in writer's cramp. Brain 2003;126(12):2586–96.

54. Quartarone A, Rizzo V, Terranova C, et al. Abnormal sensorimotor plasticity in organic but not in psychogenic dystonia. Brain 2009;132(10):2871–7.

55. Weise D, Schramm A, Stefan K, et al. The two sides of associative plasticity in writer's cramp. Brain 2006;129(10):2709–21.

56. Edwards MJ, Huang Y-Z, Mir P, Rothwell JC, Bhatia KP. Abnormalities in motor cortical plasticity differentiate manifesting and nonmanifesting DYT1 carriers. Mov Disord 2006;21(12):2181–6.

57. Pirio Richardson S, Tinaz S, Chen R. Repetitive Transcranial Magnetic Stimulation in Cervical Dystonia: Effect of Site and Repetition in a Randomized Pilot Trial. PLoS One 2015;10(4):e0124937.

58. Houdayer E, Beck S, Karabanov A, Poston B, Hallett M. The differential modulation of the ventral premotor-motor interaction during movement initiation is deficient in patients with focal hand dystonia: Premotor-motor cortical interactions. Eur J Neurosci 2012;35(3):478–85.

59. Richardson SP. Enhanced dorsal premotor–motor inhibition in cervical dystonia. Clin Neurophysiol 2015;126(7):1387–91.

60. Draganski B, Thun-Hohenstein C, Bogdahn U, Winkler J, May A. "Motor circuit" gray matter changes in idiopathic cervical dystonia. Neurology 2003;61(9):1228–31.

61. Thickbroom GW, Byrnes ML, Stell R, Mastaglia FL. Reversible reorganisation of the motor cortical representation of the hand in cervical dystonia. Mov Disord 2003;18(4):395–402.

62. Parent A, Hazrati L-N. Functional anatomy of the basal ganglia. I. The cortico-basal ganglia-thalamo-cortical loop. Brain Res Rev 1995;20(1):91–127.

63. Alexander GE, DeLong MR, Strick PL. Parallel Organization of Functionally Segregated Circuits Linking Basal Ganglia and Cortex. Annu Rev Neurosci 1986;9:357–81.

64. Künzle H. Bilateral projections from precentral motor cortex to the putamen and other parts of the basal ganglia. An autoradiographic study in Macaca fascicularis. Brain Res 1975;88(2):195–209.

65. Künzle H. Projections from the primary somatosensory cortex to basal ganglia and thalamus in the monkey. Exp Brain Res 1977;30(4):481–92.

66. Jones EG, Coulter JD, Burton H, Porter R. Cells of origin and terminal distrubution of corticostriatal fibers arising in the sensory-motor cortex of monkeys. J Comp Neurol 1977;173(1):53–80.

67. Alexander GE, DeLong MR. Microstimulation of the primate neostriatum. I. Physiological properties of striatal microexcitable zones. J Neurophysiol 1985;53(6):1401–16.

68. Alexander GE, DeLong MR. Microstimulation of the primate neostriatum. II. Somatotopic organization of striatal microexcitable zones and their relation to neuronal response properties. J Neurophysiol 1985;53(6):1417–30.

69. Crutcher MD, DeLong MR. Single cell studies of the primate putamen. I. Functional Organization. Exp Brain Res 1984;53(2):233–43.

70. Johnson TN, Rosvold HE. Topographic projections on the globus pallidus and the substantia nigra of selectively placed lesions in the precommissural caudate nucleus and putamen in the monkey. Exp Neurol 1971;33(3):584–96.

71. Cowan WM, Powell TP. Strio-pallidal projection in the monkey. J Neurol Neurosurg Psychiatry 1966;29(5):426–39.

72. Szabo J. Topical distribution of the striatal efferents in the monkey. Exp Neurol 1962;5(1):21–36.

73. Szabo J. The efferent projections of the putamen in the monkey. Exp Neurol 1967;19(4):463–76.

74. DeLong MR, Crutcher MD, Georgopoulos AP. Primate globus pallidus and subthalamic nucleus: functional organization. J Neurophysiol 1985;53(2):530–43.

75. Hoover JE, Strick PL. The Organization of Cerebellar and Basal Ganglia Outputs to Primary Motor Cortex as Revealed by Retrograde Transneuronal Transport of Herpes Simplex Virus Type 1. J Neurosci 1999;19(4):1446–63.

76. Middleton F. Basal ganglia and cerebellar loops: motor and cognitive circuits. Brain Res Rev 2000;31(2–3):236–50.

77. DeLong M, Wichmann T. Update on models of basal ganglia function and dysfunction. Parkinsonism Relat Disord 2009;15:S237–40.

78. Filip P, Gallea C, Lehéricy S, et al. Disruption in cerebellar and basal ganglia networks during a visuospatial task in cervical dystonia: Cerebellar Disruption in Cervical Dystonia. Mov Disord 2017;32(5):757–68.

79. Neychev VK, Fan X, Mitev VI, Hess EJ, Jinnah HA. The basal ganglia and cerebellum interact in the expression of dystonic movement. Brain 2008;131(9):2499–509.

80. Kaji R, Bhatia K, Graybiel AM. Pathogenesis of dystonia: is it of cerebellar or basal ganglia origin? J Neurol Neurosurg Psychiatry 2018;89(5):488–92.

81. Bologna M, Berardelli A. Cerebellum: An explanation for dystonia? Cerebellum Ataxias 2017;4(1):6.

82. Batten FE. On the diagnostic value of the position of the head in cases of cerebellar disease. Brain 1903;26(1):71–80.

83. Zoons E, Tijssen MAJ. Pathologic changes in the brain in cervical dystonia pre- and post-mortem — a commentary with a special focus on the cerebellum. Exp Neurol 2013;247:130–3.

84. Krauss JK, Seeger W, Jankovic J. Cervical dystonia associated with tumors of the posterior fossa. Mov Disord 1997;12(3):443–7.

85. Batla A, Sánchez MC, Erro R, et al. The role of cerebellum in patients with late onset cervical/segmental dystonia?–Evidence from the clinic. Parkinsonism Relat Disord 2015;21(11):1317–22.

86. Prudente CN, Pardo CA, Xiao J, et al. Neuropathology of cervical dystonia. Exp Neurol 2013;241:95–104.

87. Puglisi F, Vanni V, Ponterio G, et al. Torsin A Localization in the Mouse Cerebellar Synaptic Circuitry. PLoS ONE 2013;8(6):e68063.

88. Vanni V, Puglisi F, Bonsi P, et al. Cerebellar synaptogenesis is compromised in mouse models of DYT1 dystonia. Exp Neurol 2015;271:457–67.

89. Fremont R, Tewari A, Angueyra C, Khodakhah K. A role for cerebellum in the hereditary dystonia DYT1. eLife 2017;6:e22775.

90. Argyelan M, Carbon M, Niethammer M, et al. Cerebellothalamocortical Connectivity Regulates Penetrance in Dystonia. J Neurosci 2009;29(31):9740–7.

91. Carbon M, Argyelan M, Ghilardi MF, et al. Impaired sequence learning in dystonia mutation carriers: a genotypic effect. Brain 2011;134(5):1416–27.

92. Raike RS, Pizoli CE, Weisz C, van den Maagdenberg AMJM, Jinnah HA, Hess EJ. Limited regional cerebellar dysfunction induces focal dystonia in mice. Neurobiol Dis 2013;49:200–10.

93. Prudente CN, Stilla R, Singh S, et al. A Functional Magnetic Resonance Imaging Study of Head Movements in Cervical Dystonia. Front Neurol 2016;7:201.

94. Laitinen LV, Bergenheim AT, Hariz MI. Leksell's posteroventral pallidotomy in the treatment of Parkinson's disease. J Neurosurg 1992;76(1):53–61.

95. Krauss JK, Toups EG, Jankovic J, Grossman RG. Symptomatic and functional outcome of surgical treatment of cervical dystonia. J Neurol Neurosurg Psychiatry 1997;63(5):642–8.

96. Krauss JK, Pohle T, Weber S, Ozdoba C, Burgunder J-M. Bilateral stimulation of globus pallidus internus for treatment of cervical dystonia. Lancet 1999;354(9181):837–8.

97. Parkin S, Aziz T, Gregory R, Bain P. Bilateral internal globus pallidus stimulation for the treatment of spasmodic torticollis. Mov Disord 2001;16(3):489–93.

98. Walsh RA, Sidiropoulos C, Lozano AM, et al. Bilateral pallidal stimulation in cervical dystonia: blinded evidence of benefit beyond 5 years. Brain 2013;136(3):761–9.

99. Vidailhet M, Vercueil L, Houeto J-L, et al. Bilateral Deep-Brain Stimulation of the Globus Pallidus in Primary Generalized Dystonia. N Engl J Med 2005;352(5):459–67.

100. Kupsch A, Trottenberg T, Eisner W, et al. Pallidal Deep-Brain Stimulation in Primary Generalized or Segmental Dystonia. N Engl J Med 2006;355(19):1978–90.

101. FitzGerald JJ, Rosendal F, de Pennington N, et al. Long-term outcome of deep brain stimulation in generalised dystonia: a series of 60 cases. J Neurol Neurosurg Psychiatry 2014;85(12):1371–6.

102. Kiss ZHT, Doig-Beyaert K, Eliasziw M, Tsui J, Haffenden A, Suchowersky O. The Canadian multicentre study of deep brain stimulation for cervical dystonia. Brain 2007;130(11):2879–86.

103. Hamani C, Moro E, Zadikoff C, Poon Y-Y, Lozano AM. Location of Active Contacts in Patients with Primary Dystonia Treated with Globus Pallidus Deep Brain Stimulation. Oper Neurosurg 2008;62(suppl_1):ONS217–25.

104. Sadnicka A, Kimmich O, Pisarek C, et al. Pallidal stimulation for cervical dystonia does not correct abnormal temporal discrimination: GPI-DBS For Cd Does Not Correct Abnormal TDT. Mov Disord 2013;28(13):1874–7.

105. Witt JL, Moro E, Ash RS, et al. Predictive factors of outcome in primary cervical dystonia following pallidal deep brain stimulation: Cervical Dystonia Outcomes for GPI DBS. Mov Disord 2013;28(10):1451–5.

106. Volkmann J, Mueller J, Deuschl G, et al. Pallidal neurostimulation in patients with medication-refractory cervical dystonia: a randomised, sham-controlled trial. Lancet Neurol 2014;13(9):875–84.

107. Huebl J, Brücke C, Schneider G-H, Blahak C, Krauss JK, Kühn AA. Bradykinesia induced by frequency-specific pallidal stimulation in patients with cervical and segmental dystonia. Parkinsonism Relat Disord 2015;21(7):800–3.

108. Ostrem JL, Racine CA, Glass GA, et al. Subthalamic nucleus deep brain stimulation in primary cervical dystonia. Neurology 2011;76(10):870–8.

109. Albanese A, Asmus F, Bhatia KP, et al. EFNS guidelines on diagnosis and treatment of primary dystonias: EFNS dystonia guidelines. Eur J Neurol 2011;18(1):5–18.

110. Krack P. From off-period dystonia to peak-dose chorea: The clinical spectrum of varying subthalamic nucleus activity. Brain 1999;122(6):1133–46.

111. Lyons KE. Effects of bilateral subthalamic nucleus stimulation on sleep, daytime sleepiness, and early morning dystonia in patients with Parkinson disease. J Neurosurg 2006;104(4):502–5.

112. Sun B, Chen S, Zhan S, Le W, Krahl SE. Subthalamic nucleus stimulation for primary dystonia and tardive dystonia. In: Sakas DE, Simpson BA, editors. Operative Neuromodulation: Volume 2: Neural Networks Surgery. Vienna: Springer Vienna; 2007. p. 207–14.

113. Kleiner-Fisman G, Lin Liang GS, Moberg PJ, et al. Subthalamic nucleus deep brain stimulation for severe idiopathic dystonia: impact on severity, neuropsychological status, and quality of life. J Neurosurg 2007;107(1):29–36.

114. Schjerling L, Madsen FF, Jensen SR, Karlsborg M. A randomized double-blind crossover trial comparing subthalamic and pallidal deep brain stimulation for dystonia. J Neurosurg 2013;119(6):1537–45.

115. Chou KL, Hurtig HI, Jaggi JL, Baltuch GH. Bilateral subthalamic nucleus deep brain stimulation in a patient with cervical dystonia and essential tremor. Mov Disord 2005;20(3):377–80.

116. Ostrem JL, San Luciano M, Dodenhoff KA, et al. Subthalamic nucleus deep brain stimulation in isolated dystonia: A 3-year follow-up study. Neurology 2017;88(1):25–35.

117. Zhan S, Sun F, Pan Y, et al. Bilateral deep brain stimulation of the subthalamic nucleus in primary Meige syndrome. J Neurosurg 2018;128(3):897–902.

118. DeVito JL, Anderson ME, Walsh KE. A horseradish peroxidase study of afferent connections of the globus pallidus in Macaca mulatta. Exp Brain Res 1980;38(1):65–73.

119. Vitek JL, Chockkan V, Zhang J-Y, et al. Neuronal activity in the basal ganglia in patients with generalized dystonia and hemiballismus. Ann Neurol 1999;46(1):22–35.

120. Lenz FA, Suarez JI, Metman LV, et al. Pallidal activity during dystonia: somatosensory reorganisation and changes with severity. J Neurol Neurosurg Psychiatry 65(5):767–70.

121. Nambu A, Chiken S, Shashidharan P, et al. Reduced Pallidal Output Causes Dystonia. Front Syst Neurosci 2011;5:89.

122. Tang JKH, Moro E, Mahant N, et al. Neuronal Firing Rates and Patterns in the Globus Pallidus Internus of Patients With Cervical Dystonia Differ From Those With Parkinson's Disease. J Neurophysiol 2007;98(2):720–9.

123. Moll CKE, Galindo-Leon E, Sharott A, et al. Asymmetric pallidal neuronal activity in patients with cervical dystonia. Front Syst Neurosci 2014;8:15.

124. Silberstein P. Patterning of globus pallidus local field potentials differs between Parkinson's disease and dystonia. Brain 2003;126(12):2597–608.

125. Wang DD, de Hemptinne C, Miocinovic S, et al. Pallidal Deep-Brain Stimulation Disrupts Pallidal Beta Oscillations and Coherence with Primary Motor Cortex in Parkinson's Disease. J Neurosci 2018;38(19):4556–68.

126. Liu X, Yianni J, Wang S, Bain PG, Stein JF, Aziz TZ. Different mechanisms may generate sustained hypertonic and rhythmic bursting muscle activity in idiopathic dystonia. Exp Neurol 2006;198(1):204–13.

127. Liu X, Wang S, Yianni J, et al. The sensory and motor representation of synchronized oscillations in the globus pallidus in patients with primary dystonia. Brain 2008;131(6):1562–73.

128. Tang JKH, Mahant N, Cunic D, et al. Changes in cortical and pallidal oscillatory activity during the execution of a sensory trick in patients with cervical dystonia. Exp Neurol 2007;204(2):845–8.

129. Chung M, Huh R. Different clinical course of pallidal deep brain stimulation for phasic- and tonic-type cervical dystonia. Acta Neurochir (Wien) 2016;158(1):171–80.

130. Barow E, Neumann W-J, Brown P, Krauss JK, Schneider G-H. Deep brain stimulation suppresses pallidal low frequency activity in patients with phasic dystonic movements. Brain 2014;137(11):3012–24.

131. Neumann W, Horn A, Ewert S, et al. A localized pallidal physiomarker in cervical dystonia. Ann Neurol 2017;82(6):912–24.

132. Patriat R, Cooper SE, Duchin Y, et al. Individualized tractography-based parcellation of the globus pallidus pars interna using 7T MRI in movement disorder patients prior to DBS surgery. NeuroImage 2018;178:198–209.

133. Antoniades CA, Rebelo P, Kennard C, Aziz TZ, Green AL, FitzGerald JJ. Pallidal Deep Brain Stimulation Improves Higher Control of the Oculomotor System in Parkinson's Disease. J Neurosci 2015;35(38):13043–52.

134. Montgomeryjr E. Effects of GPi stimulation on human thalamic neuronal activity. Clin Neurophysiol 2006;117(12):2691–702.

135. Dostrovsky JO, Levy R, Wu JP, Hutchison WD, Tasker RR, Lozano AM. Microstimulation-Induced Inhibition of Neuronal Firing in Human Globus Pallidus. J Neurophysiol 2000;84(1):570–4.

136. Krack P, Pollak P, Limousin P, et al. Opposite motor effects of pallidal stimulation in Parkinson's disease. Ann Neurol 1998;43(2):180–92.

137. Parent A, Hazrati L-N. Functional anatomy of the basal ganglia. II. The place of subthalamic nucleus and external pallidium in basal ganglia circuitry. Brain Res Rev 1995;20(1):128–54.

138. Miocinovic S, de Hemptinne C, Qasim S, Ostrem JL, Starr PA. Patterns of Cortical Synchronization in Isolated Dystonia Compared With Parkinson Disease. JAMA Neurol 2015;72(11):1244–51.

139. Miocinovic S, Miller A, Swann NC, Ostrem JL, Starr PA. Chronic deep brain stimulation normalizes scalp EEG activity in isolated dystonia. Clin Neurophysiol 2018;129(2):368–76.

140. Geng X, Zhang J, Jiang Y, et al. Comparison of oscillatory activity in subthalamic nucleus in Parkinson's disease and dystonia. Neurobiol Dis 2017;98:100–7.

141. Wang DD, de Hemptinne C, Miocinovic S, et al. Subthalamic local field potentials in Parkinson's disease and isolated dystonia: An evaluation of potential biomarkers. Neurobiol Dis 2016;89:213–22.

142. Neumann W-J, Huebl J, Brücke C, et al. Enhanced low-frequency oscillatory activity of the subthalamic nucleus in a patient with dystonia. Mov Disord 2012;27(8):1063–6.

143. Schrock LE, Ostrem JL, Turner RS, Shimamoto SA, Starr PA. The Subthalamic Nucleus in Primary Dystonia: Single-Unit Discharge Characteristics. J Neurophysiol 2009;102(6):3740–52.

144. Johnson V, Wilt R, Gilron R, et al. Embedded adaptive deep brain stimulation for cervical dystonia controlled by motor cortex theta oscillations. Exp Neurol 2021;345:113825.

145. Andrew J, Fowler CJ, Harrison MJG. Stereotaxic thalamotomy in 55 cases of dystonia. Brain 1983;106(4):981–1000.

146. Cooper IS. 20-year follow-up study on the neurosurgical treatment of dystonia musculorum deformans. Adv Neurol 1976;14:423–52.

147. Riechert T. Long Term Follow-Up of Results of Stereotaxic Treatment in Extrapyramidal Disorders. Confin Neurol 1962;22(3–5):356–63.

148. Horisawa S, Ochiai T, Goto S, et al. Safety and long-term efficacy of ventro-oral thalamotomy for focal hand dystonia: A retrospective study of 171 patients. Neurology 2019;92(4):e371–7.

149. Horisawa S, Yamaguchi T, Abe K, et al. A single case of MRI-guided focused ultrasound ventro-oral thalamotomy for musician's dystonia. J Neurosurg 2019;131(2):384–6.

150. Owen RL, Grewal SS, Thompson JM, Hassan A, Lee KH, Klassen BT. Effectiveness of Thalamic Ventralis Oralis Anterior and Posterior Nuclei Deep Brain Stimulation for Posttraumatic Dystonia. Mayo Clin Proc Innov Qual Outcomes 2022;6(2):137–42.

151. Starr PA, Lindsey N, Jr WJM. Microelectrode-guided implantation of deep brain stimulators into the globus pallidus internus for dystonia: techniques, electrode locations, and outcomes. J Neurosurg 2006;104(4):488–501.

152. Schönecker T, Gruber D, Kivi A, et al. Postoperative MRI localisation of electrodes and clinical efficacy of pallidal deep brain stimulation in cervical dystonia. J Neurol Neurosurg Psychiatry 2015;86(8):833–9.

153. Reich MM, Horn A, Lange F, et al. Probabilistic mapping of the antidystonic effect of pallidal neurostimulation: a multicentre imaging study. Brain 2019;142(5):1386–98.

154. Åstrom M, Diczfalusy E, Martens H, Wardell K. Relationship between Neural Activation and Electric Field Distribution during Deep Brain Stimulation. IEEE Trans Biomed Eng 2015;62(2):664–72.

155. Baron MS, Sidib M, DeLong MR, Smith Y. Course of motor and associative pallidothalamic projections in monkeys. J Comp Neurol 2001;429(3):490–501.

156. Parent M, Parent A. The pallidofugal motor fiber system in primates. Parkinsonism Relat Disord 2004;10(4):203–11.

157. Rozanski VE, da Silva NM, Ahmadi S-A, et al. The role of the pallidothalamic fibre tracts in deep brain stimulation for dystonia: A diffusion MRI tractography study: A Diffusion MRI Tractography Study. Hum Brain Mapp 2017;38(3):1224–32.

158. Sidibe M, Bevan MD, Bolam JP, Smith Y. Efferent connections of the internal globus pallidus in the squirrel monkey: I. topography and synaptic organization of the pallidothalamic projection. J Comp Neurol 1997;382:323–47.

159. Milardi D, Gaeta M, Marino S, et al. Basal ganglia network by constrained spherical deconvolution: A possible cortico-pallidal pathway? Mov Disord 2015;30(3):342–9.

160. Leichnetz GR, Astruc J. The course of some prefrontal corticofugals to the pallidum, substantia innominata, and amygdaloid complex in monkeys. Exp Neurol 1977;54(1):104–9.

161. Akkal D, Dum RP, Strick PL. Supplementary Motor Area and Presupplementary Motor Area: Targets of Basal Ganglia and Cerebellar Output. J Neurosci 2007;27(40):10659–73.

162. Maier-Hein KH, Neher PF, Houde J-C, et al. The challenge of mapping the human connectome based on diffusion tractography. Nat Commun 2017;8(1):1349.

163. da Silva NM, Ahmadi S-A, Tafula SN, et al. A diffusion-based connectivity map of the GPi for optimised stereotactic targeting in DBS. NeuroImage 2017;144:83–91.

164. Middlebrooks EH, Tuna IS, Grewal SS, et al. Segmentation of the Globus Pallidus Internus Using Probabilistic Diffusion Tractography for Deep Brain Stimulation Targeting in Parkinson Disease. Am J Neuroradiol 2018;39(6):1127–34.

165. Rozanski VE, Vollmar C, Cunha JP, et al. Connectivity patterns of pallidal DBS electrodes in focal dystonia: A diffusion tensor tractography study. NeuroImage 2014;84:435–42.

166. Carpenter MB, Strominger NL. Efferent fibers of the subthalamic nucleus in the monkey. A comparison of the efferent projections of the subthalamic nucleus, substantia nigra and globus pallidus. Am J Anat 1967;121(1):41–71.

167. Smith Y, Hazrati L-N, Parent A. Efferent projections of the subthalamic nucleus in the squirrel monkey as studied by the PHA-L anterograde tracing method. J Comp Neurol 1990;294(2):306–23.

168. Hoshi E, Tremblay L, Féger J, Carras PL, Strick PL. The cerebellum communicates with the basal ganglia. Nat Neurosci 2005;8(11):1491–3.

169. Bostan AC, Strick PL. The basal ganglia and the cerebellum: nodes in an integrated network. Nat Rev Neurosci 2018;19(6):338–50.

170. Okromelidze L, Tsuboi T, Eisinger RS, et al. Functional and Structural Connectivity Patterns Associated with Clinical Outcomes in Deep Brain Stimulation of the Globus Pallidus Internus for Generalized Dystonia. Am J Neuroradiol 2020;41(3):508–14.

171. Traynor C, Heckemann RA, Hammers A, et al. Reproducibility of thalamic segmentation based on probabilistic tractography. NeuroImage 2010;52(1):69–85.

172. Lambert C, Simon H, Colman J, Barrick TR. Defining thalamic nuclei and topographic connectivity gradients in vivo. NeuroImage 2017;158:466–79.

173. Smith SM, Jenkinson M, Woolrich MW, et al. Advances in functional and structural MR image analysis and implementation as FSL. NeuroImage 2004;23:S208–19.

174. Andersson JLR, Skare S, Ashburner J. How to correct susceptibility distortions in spin-echo echo-planar images: application to diffusion tensor imaging. NeuroImage 2003;20(2):870–88.

175. Andersson JLR, Sotiropoulos SN. An integrated approach to correction for off-resonance effects and subject movement in diffusion MR imaging. NeuroImage 2016;125:1063–78.

176. Behrens TEJ, Woolrich MW, Jenkinson M, et al. Characterization and propagation of uncertainty in diffusion-weighted MR imaging. Magn Reson Med 2003;50(5):1077–88.

177. Patenaude B, Smith SM, Kennedy DN, Jenkinson M. A Bayesian model of shape and appearance for subcortical brain segmentation. NeuroImage 2011;56(3):907–22.

178. Jenkinson M, Smith S. A global optimisation method for robust affine registration of brain images. Med Image Anal 2001;5(2):143–56.

179. Jenkinson M, Bannister P, Brady M, Smith S. Improved Optimization for the Robust and Accurate Linear Registration and Motion Correction of Brain Images. NeuroImage 2002;17(2):825–41.

180. Greve DN, Fischl B. Accurate and robust brain image alignment using boundary-based registration. NeuroImage 2009;48(1):63–72.

181. Andersson JL, Jenkinson M, Smith S. Non-linear registration aka Spatial normalisation FMRIB Technical Report TR07JA2. FMRIB Anal Group Univ Oxf 2007;1–22.

182. Behrens TEJ, Johansen-Berg H, Woolrich MW, et al. Non-invasive mapping of connections between human thalamus and cortex using diffusion imaging. Nat Neurosci 2003;6(7):750–7.

183. Tziortzi AC, Haber SN, Searle GE, et al. Connectivity-Based Functional Analysis of Dopamine Release in the Striatum Using Diffusion-Weighted MRI and Positron Emission Tomography. Cereb Cortex 2014;24(5):1165–77.

184. Lehericy S. 3-D Diffusion Tensor Axonal Tracking shows Distinct SMA and Pre-SMA Projections to the Human Striatum. Cereb Cortex 2004;14(12):1302–9.

185. Leh SE, Ptito A, Chakravarty MM, Strafella AP. Fronto-striatal connections in the human brain: A probabilistic diffusion tractography study. Neurosci Lett 2007;419(2):113–8.

186. Ni Z, Kim SJ, Phielipp N, et al. Pallidal deep brain stimulation modulates cortical excitability and plasticity: Pallidal DBS. Ann Neurol 2018;83(2):352–62.

187. Kuhn AA, Meyer B-U, Trottenberg T, Brandt SA, Schneider GH, Kupsch A. Modulation of motor cortex excitability by pallidal stimulation in patients with severe dystonia. Neurology 2003;60(5):768–74.

188. Tisch S, Rothwell JC, Bhatia KP, et al. Pallidal stimulation modifies after-effects of paired associative stimulation on motor cortex excitability in primary generalised dystonia. Exp Neurol 2007;206(1):80–5.

189. Detante O, Vercueil L, Thobois S, et al. Globus pallidus internus stimulation in primary generalized dystonia: a H215O PET study. Brain 2004;127(8):1899–908.

190. Joint C, Thevathasan W, Green AL, Aziz T. Pallidal somatotopy suggested by deep brain stimulation in a patient with dystonia. Neurology 2013;80(7):685–6.

191. Bostan AC, Dum RP, Strick PL. The basal ganglia communicate with the cerebellum. Proc Natl Acad Sci 2010;107(18):8452–6.

192. Giolli RA, Gregory KM, Suzuki DA, Blanks RHI, Lui F, Betelak KF. Cortical and subcortical afferents to the nucleus reticularis tegmenti pontis and basal pontine nuclei in the macaque monkey. Vis Neurosci 2001;18(5):725–40.

193. Carpenter MB, Carleton SC, Keller JT, Conte P. Connections of the subthalamic nucleus in the monkey. Brain Res 1981;224(1):1–29.

194. Hazrati L-N, Parent A. Convergence of subthalamic and striatal efferents at pallidal level in primates: an anterograde double-labeling study with biocytin and PHA-L. Brain Res 1992;569(2):336–40.

195. Thomas C, Ye FQ, Irfanoglu MO, et al. Anatomical accuracy of brain connections derived from diffusion MRI tractography is inherently limited. Proc Natl Acad Sci 2014;111(46):16574–9.

196. Schilling KG, Gao Y, Stepniewska I, Janve V, Landman BA, Anderson AW. Anatomical accuracy of standard-practice tractography algorithms in the motor system - A histological validation in the squirrel monkey brain. Magn Reson Imaging 2019;55:7–25.

197. Girard G, Caminiti R, Battaglia-Mayer A, et al. On the cortical connectivity in the macaque brain: A comparison of diffusion tractography and histological tracing data. NeuroImage 2020;221:117201.

198. Girard G, Whittingstall K, Deriche R, Descoteaux M. Towards quantitative connectivity analysis: reducing tractography biases. NeuroImage 2014;98:266–78.

199. Schilling KG, Petit L, Rheault F, et al. Brain connections derived from diffusion MRI tractography can be highly anatomically accurate—if we know where white matter pathways start, where they end, and where they do not go. Brain Struct Funct 2020;225(8):2387–402.

200. Gao Y, Choe AS, Stepniewska I, Li X, Avison MJ, Anderson AW. Validation of DTI Tractography-Based Measures of Primary Motor Area Connectivity in the Squirrel Monkey Brain. PLoS ONE 2013;8(10):e75065.

201. Horn A, Ewert S, Alho EJL, et al. Teaching NeuroImages: In vivo visualization of Edinger comb and Wilson pencils. Neurology 2019;92(14):e1663–4.

202. Wilson SAK. An experimental research into the anatomy and physiology of the corpus striatum. Brain 1914;36(3–4):427–92.

203. Mars RB, Jbabdi S, Sallet J, et al. Diffusion-Weighted Imaging Tractography-Based Parcellation of the Human Parietal Cortex and Comparison with Human and Macaque Resting-State Functional Connectivity. J Neurosci 2011;31(11):4087–100.

204. Mars RB, Sallet J, Schuffelgen U, Jbabdi S, Toni I, Rushworth MFS. Connectivity-Based Subdivisions of the Human Right "Temporoparietal Junction Area": Evidence for Different Areas Participating in Different Cortical Networks. Cereb Cortex 2012;22(8):1894–903.

205. Neubert F-X, Mars RB, Sallet J, Rushworth MFS. Connectivity reveals relationship of brain areas for reward-guided learning and decision making in human and monkey frontal cortex. Proc Natl Acad Sci 2015;112(20):E2695–704.

206. Neubert F-X, Mars RB, Thomas AG, Sallet J, Rushworth MFS. Comparison of Human Ventral Frontal Cortex Areas for Cognitive Control and Language with Areas in Monkey Frontal Cortex. Neuron 2014;81(3):700–13.

207. Johansen-Berg H, Behrens TEJ, Robson MD, et al. Changes in connectivity profiles define functionally distinct regions in human medial frontal cortex. Proc Natl Acad Sci 2004;101(36):13335–40.

208. Ezra M, Faull OK, Jbabdi S, Pattinson KT. Connectivity-based segmentation of the periaqueductal gray matter in human with brainstem optimized diffusion MRI: Segmentation of the PAG with Diffusion MRI. Hum Brain Mapp 2015;36(9):3459–71.

209. Vanegas-Arroyave N, Lauro PM, Huang L, et al. Tractography patterns of subthalamic nucleus deep brain stimulation. Brain 2016;139(4):1200–10.

210. Butson CR, Cooper SE, Henderson JM, McIntyre CC. Patient-specific analysis of the volume of tissue activated during deep brain stimulation. NeuroImage 2007;34(2):661–70.

211. Mädler B, Coenen VA. Explaining Clinical Effects of Deep Brain Stimulation through Simplified Target-Specific Modeling of the Volume of Activated Tissue. Am J Neuroradiol 2012;33(6):1072–80.

212. Maks CB, Butson CR, Walter BL, Vitek JL, McIntyre CC. Deep brain stimulation activation volumes and their association with neurophysiological mapping and therapeutic outcomes. J Neurol Neurosurg Psychiatry 2009;80(6):659–66.

213. Chaturvedi A, Luján JL, McIntyre CC. Artificial neural network based characterization of the volume of tissue activated during deep brain stimulation. J Neural Eng 2013;10(5):056023.

214. Burchiel KJ. Dystonia and deep brain stimulation. J Neurosurg 2004;101(2):179–80.

215. Vayssiere N, van der Gaag N, Cif L, et al. Deep brain stimulation for dystonia confirming a somatotopic organization in the globus pallidus internus. J Neurosurg 2004;101(2):181–8.

216. Bianciardi M, Strong C, Toschi N, et al. A probabilistic template of human mesopontine tegmental nuclei from in vivo 7 T MRI. NeuroImage 2018;170:222–30.

217. Horn A, Reich MM, Ewert S, et al. Optimal deep brain stimulation sites and networks for cervical vs. generalized dystonia. Proc Natl Acad Sci 2022;119(14):e2114985119.

218. Lofredi R, Scheller U, Feldmann L, et al. FV 5 Striato-pallidal connectivity in oscillatory activity of patients with dystonia. Clin Neurophysiol 2022;137:e3–4.

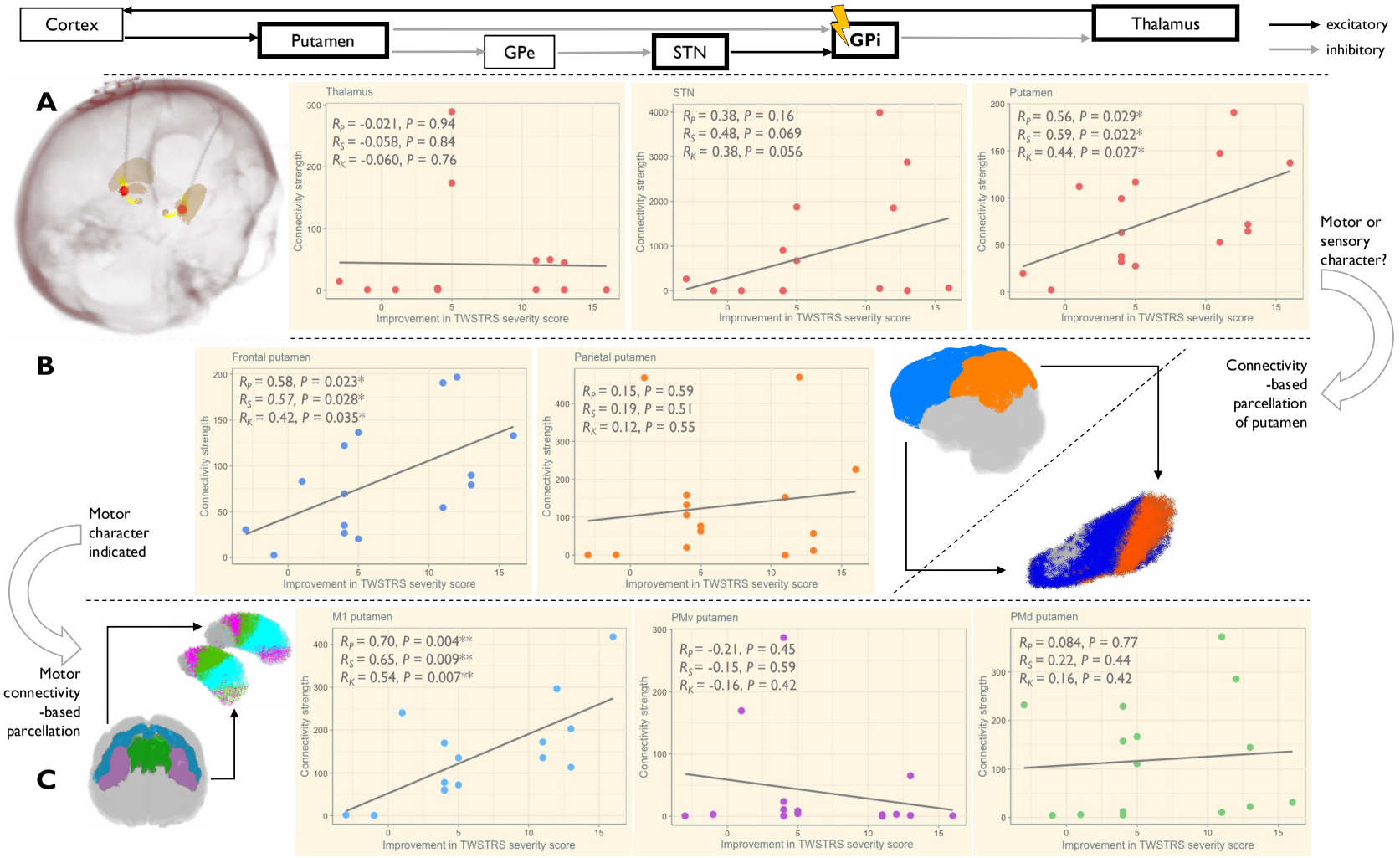

Figure 1. **Tractography**. Top: Diagram of cortico-basal ganglia-thalamo-cortical loop. (A) Left: 3D fused MR-CT (red) with stimulation (red) and streamlines (yellow) to putamen and STN in 3D view. Right: Initial tractography to STN and putamen with correlation between normalized streamlines and clinical improvement. (B) Right: Frontal and parietal cortical classifiers with example of hard parcellation of the putamen, dividing into regions with high motor and high sensory input. Left: Tractography to frontal and parietal putaminal parcels with correlation between normalised streamlines and clinical improvement. (C) Left: Motor cortical classifiers with bilateral example of hard parcellation of putamina, dividing into regions with high primary motor (M1), high dorsal premotor (PMd) and high ventral premotor (PMv) connectivity. Right: Tractography to M1, PMd and PMv putaminal parcels with correlation between normalised streamlines and clinical improvement. R_P = Pearson's; R_S = Spearman's; R_K = Kendall's coefficients.

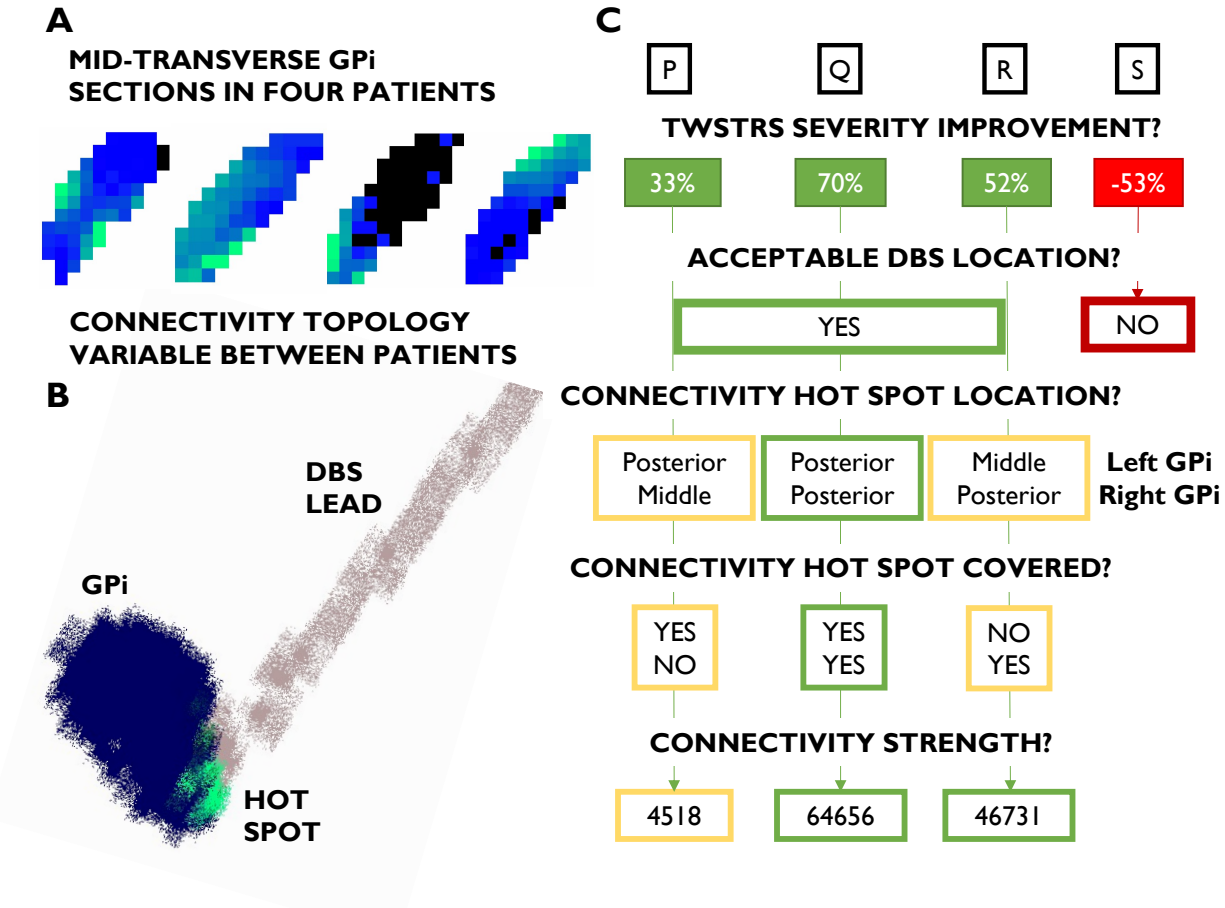

Figure 2. **Targeting assessment**. Exploration of GPi connectivity in the 3-T cohort as a possible strategy to individualize DBS targeting. A: Example GPi maps of M1 putamen connectivity density (green = high, blue = low, black = none) demonstrating spatial between patient differences, presenting a putative substrate for individualised targeting. B: Example rendering (FSLeyes) of a DBS lead penetrating a connectivity hotspot (Patient Q). C: 3-T cohort outcomes rationalised through both electrode location and connectivity, demonstrates congruency with 1.5-T cohort results. Patient S scheduled for lead revision, but delayed due to pandemic. Hotspot is spatial peak M1-putamino-pallidal connectivity. Connectivity strength given as streamlines.

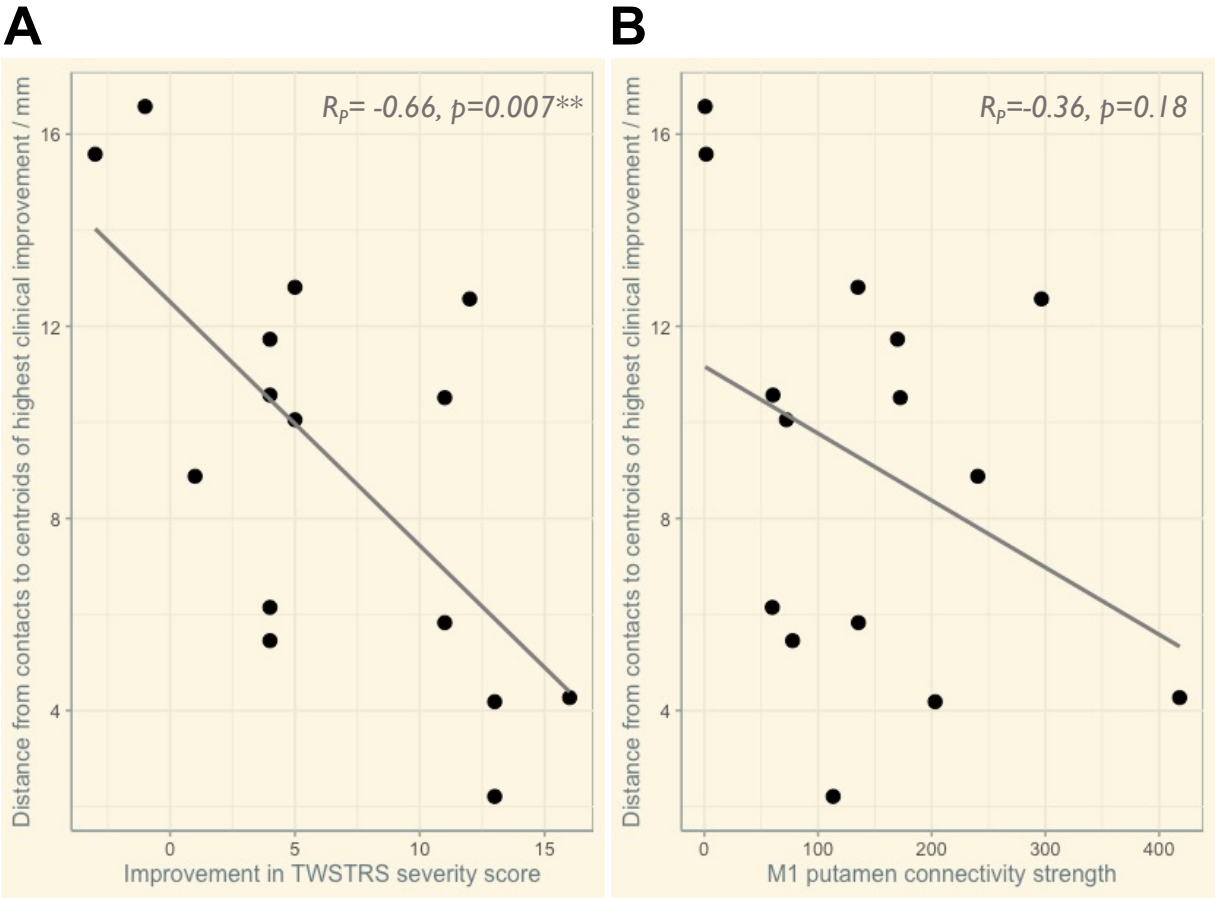

Figure 3. **Stimulation coordinates.** Anterior commissure – posterior commissure (AC-PC) coordinates assessed with a centroid of highest clinical improvement 'sweet spot' analysis. A: Significant correlation with clinical improvement present and of similar magnitude to literature standards. B: Correlation with GPi-DBS<->M1 putamen not significant. In principle, a weak correlation is likely to be present, therefore statistical insignificance is presumably due to low power.

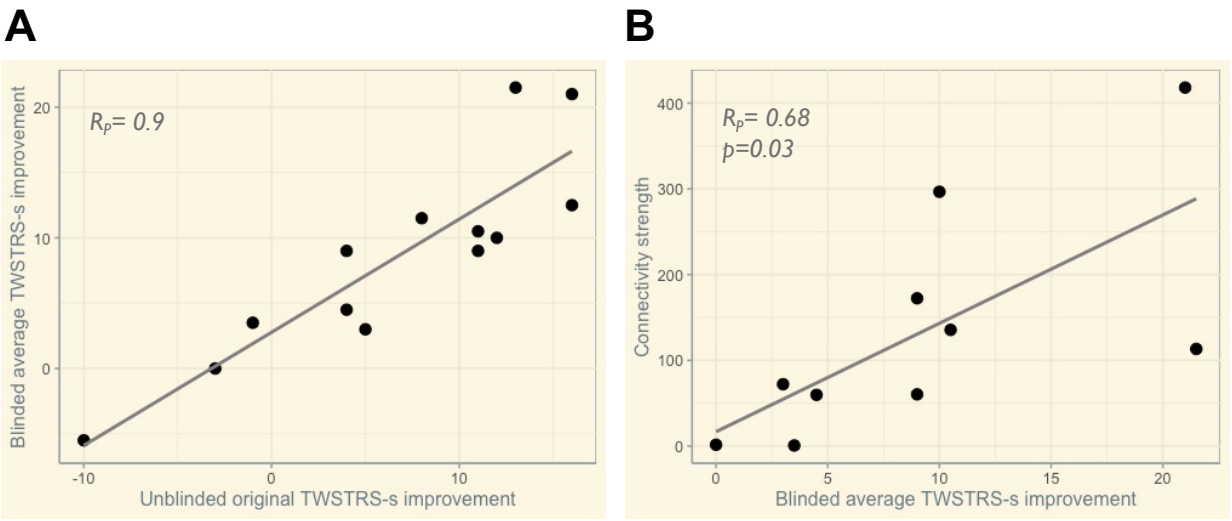

Figure 4. **Assessment of non-blinding.** A: 13-patient sample (1.5T cohort, *n*=10, 3T cohort *n*=3) of pre-operative and post-operative follow-up clinical assessment video pairs, anonymised, randomised, TWSTRS severity rated by two clinicians blind, and improvement averaged across raters. Plot shows very strong correlation between this blinded metric and the unblinded clinical assessment. The intra-class correlation coefficient was 0.94 (95% CI: 0.80-0.98), and was 0.95 (95% CI: 0.84-0.99) between the two blinded raters, indicating that lack of blinding in our original data had little or no effect. B: Plot shows relationship between video-based blind-assessed clinical improvement (1.5T cohort, *n*=10) and the HF-DBS<->M1 putamen connectivity strength. The statistically significant correlation is maintained, despite the smaller cohort.

Luck is what happens when preparation meets opportunity.

~

Lucius A. Seneca